



HAL
open science

Intérêt du traitement par UV-C des communautés bactériennes, fongiques et des protistes autotrophes des biofilms colonisant la pierre patrimoniale: structure des peuplements, effets des UV-C sur la physiologie algale et innocuité du traitement vis à vis du support pictural.

Stéphane Pfendler

► **To cite this version:**

Stéphane Pfendler. Intérêt du traitement par UV-C des communautés bactériennes, fongiques et des protistes autotrophes des biofilms colonisant la pierre patrimoniale: structure des peuplements, effets des UV-C sur la physiologie algale et innocuité du traitement vis à vis du support pictural.. Sciences agricoles. Université Bourgogne Franche-Comté, 2017. Français. NNT : 2017UBFCD030 . tel-01905921

HAL Id: tel-01905921

<https://theses.hal.science/tel-01905921v1>

Submitted on 26 Oct 2018

HAL is a multi-disciplinary open access archive for the deposit and dissemination of scientific research documents, whether they are published or not. The documents may come from teaching and research institutions in France or abroad, or from public or private research centers.

L'archive ouverte pluridisciplinaire **HAL**, est destinée au dépôt et à la diffusion de documents scientifiques de niveau recherche, publiés ou non, émanant des établissements d'enseignement et de recherche français ou étrangers, des laboratoires publics ou privés.



**THESE DE DOCTORAT DE L'ETABLISSEMENT UNIVERSITE BOURGOGNE
FRANCHE-COMTE
PREPAREE AU LABORATOIRE CHRONO-ENVIRONNEMENT**

Ecole doctorale n°554
Environnement Santé

Doctorat de Biologie des organismes

Par
PFENDLER Stéphane

**Intérêt du traitement par UV-C des communautés bactériennes, fongiques et des
protistes autotrophes des biofilms colonisant la pierre patrimoniale : structure des
peuplements, effets des UV-C sur la physiologie algale et innocuité du traitement vis à
vis du support pictural.**

Thèse présentée et soutenue à Besançon, le jeudi 16 novembre 2017

Composition du Jury :

| | |
|---|---------------|
| Vincent Gloaguen (Pr, Université de Limoges) | Président |
| Patrick Di Martino (Pr, Université de Cergy Pontoise) | Rapporteur |
| Didier Cailhol (Ingénieur, Université Savoie Mont Blanc) | Examineur |
| Aline Magnien (Dr, CRC- LRMH-USR3224, Champs sur Marne) | Membre invité |
| Lotfi Aleya (Pr, Université Bourgogne Franche-Comté) | Directeur |
| Badr Alaoui-Sossé (MCF, Université Bourgogne Franche-Comté) | Co-directeur |
| Faisl Boustia (Dr, CRC- LRMH-USR3224, Champs sur Marne) | Co-directeur |

Remerciements

Pour commencer, je remercie les membres du jury Vincent Gloaguen, Patrick Di Martino, Aline Magnien et Didier Cailhol pour avoir accepté d'évaluer mon travail. Je remercie également les membres du comité de thèse Faisl Bousta, Stéphanie Touron, Lise Leroux, Michel Denis, Laurence Alaoui Sosse, Badr Alaoui Sosse et Lotfi Aleya pour m'avoir suivi et évalué mon travail durant ces trois années de thèse.

Merci à Badr Alaoui Sossé et Faisl Bousta d'avoir porté ce projet depuis plusieurs années et de m'y avoir intégré. Merci à vous deux de m'avoir permis d'effectuer ce travail dans les meilleures conditions.

Je tiens tout particulièrement à remercier Lotfi Aleya pour son aide si précieuse. Merci à toi d'avoir été présent dans les moments les plus difficiles et d'avoir su trouver les mots qui motivent. Merci à toi de m'avoir tant appris dans la rédaction d'article scientifique et d'avoir consacré tant de temps aux corrections. Je retiendrai toujours ta passion pour la recherche, ton efficacité et ta diplomatie. Merci beaucoup de m'avoir porté jusqu'à la soutenance.

Ce travail de thèse a été possible grâce à la contribution de nombreuses autres personnes :

- Tout d'abord, je tiens à remercier toutes les personnes qui ont apporté leur aide lors des sessions terrains. Un grand merci à Didier Cailhol, pour son aide dans la grotte de la Glacière ainsi que pour les travaux d'écritures. Merci à Christophe Gauchon, Battle, Olympe, Thomas pour votre aide à la Glacière ! Je remercie également Alex, Fabien, Dom et Lisa pour leur participation lors des sessions de prélèvements.
- Un grand merci à Nadia Crini, Caroline Amiot, Abderrahim Khatyr et Stéphanie Touron pour votre contribution dans les analyses physiques et chimiques tout au long de cette thèse.

- Je remercie également mes stagiaires, Alex, Olympe et Thomas pour leur contribution non négligeable dans l'avancée de ma thèse.
- Michel Chalot, Pierre-Alain Maron, Benoît Valot, Eve Afonso et Nicolas Capelli ont tous contribué financièrement ou par leurs précieux conseils à toutes les manipes concernant le barcoding et le métabarcoding ; Je vous en remercie !
- Je tiens à exprimer un immense MERCI aux propriétaires des grottes qui m'ont accueilli lors des sessions de prélèvements ou de traitements ; en premier lieu, je remercie Michel et Romain Roland de m'avoir si gentiment accueilli et nourri !! Merci également à tous les autres propriétaires ou gestionnaires des grottes d'Arcy sur Cure, de Cravanche, des Moidons, d'Osselle, de la Cocallière, des Demoiselles, de Clamouse, de Soyons, de Saint Marcel, de Blanot, d'Azé et de Réclère. Un merci tout particulier à toi, Lionel Barriquand, pour ton aide et ta disponibilité ! Enfin, je remercie Christian France, Maire de Vicherey, de nous avoir ouvert les portes de l'église.

Merci aux membres du bureau pour les très bons moments passés en votre compagnie ! Je n'oublierai jamais cette exceptionnelle première année ! Merci à vous Quentin, Bien-Aimé et Shinji pour votre bonne humeur ☺

Battle !! Je ne savais pas dans quel paragraphe te remercier, alors en voici un spécialement pour toi ! Tu as été ma voisine de bureau, mon souffre douleur, ma confidente, mon amie, ma statisticienne personnelle, ma secrétaire, et j'en passe. Que de souvenirs ! Un grand merci à toi !

Merci à toi Lisa de m'avoir toujours soutenu et d'avoir été là pour moi ; merci aussi pour ton aide dans les corrections d'articles et du manuscrit ainsi que pour le travail sur le terrain.

Merci à tous les collègues et amis du laboratoire pour tous les bons moments passés ensemble !

Enfin, merci à ma famille de m'avoir soutenu durant ces trois ans.

Table des matières

| | |
|--|-----------|
| REMERCIEMENTS | 3 |
| TABLE DES MATIERES | 5 |
| TABLE DES FIGURES | 9 |
| TABLE DES TABLEAUX | 15 |
| PRODUCTIONS ET COMMUNICATIONS SCIENTIFIQUES | 17 |
| PUBLICATIONS | 18 |
| INTRODUCTION GENERALE | 21 |
| SYNTHESE BIBLIOGRAPHIQUE | 23 |
| I. LES GROTTES : GEOLOGIE ET BIODIVERSITE..... | 23 |
| 1. <i>Formations des grottes et paramètres physico-chimiques</i> | 23 |
| 2. <i>La biodiversité : Flore, faune et micro-organismes des grottes</i> | 25 |
| II. LE TOURISME DANS LES GROTTES ET SES CONSEQUENCES | 31 |
| 1. <i>Historique du tourisme cavernicole</i> | 31 |
| 2. <i>L'éclairage des grottes</i> | 31 |
| 3. <i>Conséquence de l'activité touristique</i> | 32 |
| III. LES BIOFILMS PHOTOSYNTHETIQUES..... | 35 |
| 1. <i>La formation d'un biofilm</i> | 35 |
| 2. <i>Les micro-organismes formant les biofilms</i> | 37 |
| IV. BIODETERIORATION DU SUPPORT PAR LES BIOFILMS..... | 40 |
| 1. <i>La biodétérioration</i> | 40 |
| 2. <i>Conséquences de la biodétérioration</i> | 41 |
| V. LA PREVENTION ET LE TRAITEMENT CONTRE LES LAMPENFLORA..... | 42 |
| 1. <i>Les méthodes de détection préventive</i> | 42 |
| 2. <i>Les traitements curatifs</i> | 43 |
| 3. <i>Le traitement à la lumière UV-C</i> | 48 |
| VI. EFFET DES UV-C AU NIVEAU CELLULAIRE ET MOLECULAIRE | 52 |
| 1. <i>Introduction</i> | 52 |
| 2. <i>Les effets des UV-C sur les paramètres physiologiques</i> | 52 |
| VII. CONSEQUENCE DES UV-C SUR LA MATIERE PICTURALE..... | 57 |
| 1. <i>Composition des peintures</i> | 57 |
| 2. <i>Altération des peintures</i> | 58 |
| 3. <i>L'effet des UV-C sur les peintures</i> | 59 |

| | |
|---|------------|
| OBJECTIFS DE LA THESE..... | 63 |
| MATERIEL ET METHODES..... | 69 |
| I. BIODIVERSITE DES MICRO-ORGANISMES FORMANT LES BIOFILMS | 69 |
| 1. <i>Prélèvements et identification</i> | 70 |
| 2. <i>Méthode classique</i> | 70 |
| 3. <i>Séquençage haut débit (Illumina MiSeq)</i> | 71 |
| II. LES TRAITEMENTS UV-C MENES SUR LE TERRAIN | 76 |
| 1. <i>Mesures colorimétriques des biofilms</i> | 79 |
| 2. <i>Le fonctionnement du PSII</i> | 80 |
| 3. <i>Mesure des caractéristiques physico-chimiques</i> | 80 |
| III. LES EXPERIMENTATIONS MENEES EN LABORATOIRE..... | 81 |
| <i>Partie A: Effets physiologiques des UV-C sur les algues</i> | |
| 1. <i>Origine de la souche étudiée</i> | 81 |
| 2. <i>Traitement des suspensions algues aux UV-C</i> | 81 |
| 3. <i>Les mesures du rendement quantique et des quenchings</i> | 82 |
| 4. <i>Mesure du spectre de la chlorophylle a et b</i> | 82 |
| 5. <i>Mesure de l'évolution de la concentration en dioxygène</i> | 82 |
| 6. <i>Test de survie cellulaire</i> | 83 |
| 7. <i>Dosage de la chlorophylle</i> | 83 |
| <i>Partie B: Les champignons</i> | |
| 1. <i>Prélèvement et culture</i> | 84 |
| 2. <i>Irradiation des champignons</i> | 84 |
| <i>Partie C: Effets des UV-C sur les pigments et les liants</i> | |
| 1. <i>Les effets des UV-C sur les pigments et les liants</i> | 87 |
| 2. <i>Technique d'infrarouge à transformée de Fourier</i> | 87 |
| 3. <i>Technique de diffraction aux rayons X</i> | 87 |
| 4. <i>Microscopie Electronique à Balayage (MEB)</i> | 88 |
| 5. <i>Inductively Coupled Plasma (ICP)</i> | 88 |
| <i>Partie D: Croissance microbienne sur les pigments</i> | |
| CHAPITRE 1 : ANALYSE DE LA BIODIVERSITE MICROBIENNES FORMANT LES BIOFILMS DANS LES GROTTES TOURISTIQUES..... | 93 |
| CHAPITRE 2 : EFFET DES UV-C SUR LES MICRO-ALGUES ET LES CHAMPIGNONS FORMANT LES BIOFILMS | 129 |
| EFFET DES UV-C SUR LES CHAMPIGNONS..... | 161 |
| CHAPITRE 3 : ETUDE EN LABORATOIRE DE L'UTILISATION DES UV-C COMME MOYEN DE TRAITEMENT DES BIOFILMS COLONISANT LES PEINTURES PREHISTORIQUES | 197 |
| CHAPITRE 4 : TRAITEMENT <i>IN SITU</i> DES BIOFILMS COLONISANT LA PIERRE PATRIMONIALE | 221 |
| DISCUSSION GENERALE ET PERSPECTIVES..... | 279 |

| | |
|---|------------|
| I. LA BIODIVERSITE DES BIOFILMS | 280 |
| II. LES REPONSES PHYSIOLOGIQUES DES MICRO-ORGANISMES..... | 280 |
| III. L'EFFET DES UV-C SUR LA MATIERE PICTURALE..... | 281 |
| IV. LE TRAITEMENT <i>IN SITU</i> DES BIOFILMS | 282 |
| CONCLUSION GENERALE | 287 |
| RÉFÉRENCES..... | 295 |
| ANNEXES..... | 319 |

Table des figures

SYNTHESE BIBLIOGRAPHIQUE.....25

Figure 1 : Dissolution de la roche calcaire (Palmer, 2007)

Figure 2 : Photographies (A) de la reconstitution du squelette d'un ours préhistorique (grotte de Blanot) (*Ursus deningeri* datant du Pléistocène moyen récent) ainsi que de nombreux autres ossements (B) d'animaux actuellement disparus (ours, lion, etc.). Des cloportes cavernicoles (*Androniscus dentiger*, grotte de Soyons) (C) et des chauves souris (D) (grotte de Blanot) ont été observés.

Figure 3 : Disponibilité de la lumière à l'intérieur d'une grotte (Azua, 2010).

Figure 4 : Entrée de la grotte de Réclère (Suisse). La flore est composée de plantes supérieures (flèche bleue), de bryophytes (flèche rouge) et de micro-algues/cyanobactéries (flèche jaune). Les micro-organismes provoquent une biodétérioration du support colonisé (flèche orange).

Figure 5 : Certaines bactéries peuvent former une couche calcaire (A) à la surface de l'eau (Grotte d'Arcy-sur-Cure). Le développement de bactéries (Actinomycètes) peut former des colonies dorées, blanches et vertes à la surface de la roche (B). Différentes sortes de champignons sont visibles sur du guano de chauves-souris dans les grottes de Blanot (C) et des Moidons (D).

Figure 6 : Différents types d'éclairage sont présents dans les grottes touristiques (LED, projecteur allogène et spot) (<http://www.cavelighting.com>).

Figure 7 : (A) Taux de CO₂ mesuré dans la « Imperial Cave » à trois endroits différents (« Site 1, 2 et 3 ») en fonction du nombre de visiteurs. (B) Moyenne des concentrations en CO₂ avant les visites de la grotte, après les visites et le lendemain matin (avant la reprise des visites).

Figure 8 : Suivi de la température intérieure de l'air (« Lepe Jame air temperature ») et de l'eau (« Rimstone pool »), de la température extérieure, des précipitations, et du nombre de touristes dans la Grotte Postojna (Stanka et Turk, 2014).

Figure 9 : Schéma synthétique montrant la colonisation d'une surface par les algues et les cyanobactéries ainsi que le développement d'un biofilm avec production d'exopolysaccharide, sa maturation et sa dissémination.

Figure 10 : Le mur de l'église de Vicherey est colonisé et détérioré par des cyanobactéries.

Figure 11 : Schéma d'une grotte représentant les différents facteurs permettant le développement des biofilms ainsi que leur traitement par voie chimique et les conséquences sur l'environnement karstique.

Figure 12 : Schéma représentant le rayonnement électromagnétique partant des rayons gamma jusqu'aux ondes radio.

Figure 13 : Efficacité de la décontamination en fonction de la distance de la source d'UV-C (Champlot *et al.*, 2010).

Figure 14 : Schéma d'une grotte représentant les différents facteurs permettant le développement des biofilms ainsi que leur traitement par l'utilisation de la lumière UV-C.

Figure 15 : Peinture préhistorique de la grotte de Lascaux (Oriol *et al.*, 2011)

Figure 16 : Prolifération de champignon noir (*Ulocladium sp.* et *Gliocladium sp.*) sur l'une des fresques de la grotte de Lascaux (Oriol *et al.*, 2011).

Figure 17 : Schéma représentant les quatre objectifs de la thèse.

MATERIEL ET METHODES.....71

Figure 1 : Représentation des lieux de prélèvements à travers en France et en Suisse.

Figure 2 : Isolement de la souche *Chlorella sp.* à partir d'un échantillonnage d'un biofilm photosynthétique se développant sur les parois de la grotte des Moidons.

Figure 3 : Photographies de tous les biofilms échantillonnés puis séquencés par la technique de séquençage haut débit de type Illumina par l'entreprise MicroSynth (Suisse). Les biofilms proviennent de la grotte de Blanot (1 à 5), des grottes d'Azé (6 à 12), de la grotte de Réclère (13 à 17), des grottes de Soyons (18 à 22) et de la grotte de Saint-Marcel (23 et 24).

Figure 4: Plan d'une des grottes de Soyons : le Trou du Renard.

Figure 5 : Plan de la grotte de Réclère.

Figure 6 : Plan de la grotte de Blanot.

Figure 7 : Plans des deux grottes d'Azé.

Figure 8 : Plan de la grotte de la Glacière (Dessin : Didier Cailhol et Christophe Gauchon).

Figure 9 : Illustration de l'Église de Vicherey.

Figure 10 : Illustration de l'intérieur de l'Église de Vicherey. Les biofilms algaux et cyanobactériens sont visibles sur le mur de droite.

Figure 11 : (A) Illustration d'une UV-C box en bois comprenant 4 lampes UV-C (Borderie et al, 2011). Les box ont été modifiées de manière à considérablement les alléger (utilisation de plexiglass) et de quadrupler la surface traitée. L'ensemble du système a ensuite été mis sur « échasse » ainsi que sur un échafaudage, afin d'atteindre des zones jusqu'à une hauteur de 4 mètres.

Figure 12 : Illustration du patron utilisé pour les suivis colorimétriques dans la grotte de la Glacière et dans l'Église de Vicherey.

Figure 13 : Protocole expérimental des différentes irradiations effectuées sur les six souches de champignons.

Figure 14 : Photographie du diffractomètre à rayon X (LRMH, Paris).

Figure 15 : Illustration de la contamination de la peinture par les algues, les champignons, les cyanobactéries et les mousses. Tous ces organismes provoquent une biodétérioration de la peinture.

CHAPITRE 1.....95

Figure 1 : Illustration of all the sampled biofilms in the five caves. Cave localizations are shown with colored triangles, rounds and squares.

Figure 2 : Principal Component Analyses (PCA) of environmental parameters reported in the five caves ("Temp": Temperature; "light.int": Light intensity; "treat": Treatment; "alt": Altitude; "lat": Latitude; "light.dis": Distance of biofilm from light source; "visit": number of visitors per year; "dist": Distance of biofilm from cave entrance; "quant": Quantum yield, $F'v/F'm$; "moist": Moisture).

Figure 3 : Microbial community composition at the phylum and class (*Proteobacteria*) level based on 16S rRNA gene sequencing.

Figure 4 : Microbial community composition at the phylum level based on ITSrRNA gene sequencing.

Figure 5: Microbial community composition at the phylum level based on 23S rRNA gene sequencing.

Figure 6 : Comparison of organism communities (bacteria, fungi, autotrophic organisms) in Azé-prehistoric ("Azé-pre"), Azé-river, Blanot, Réclère and Soyons Caves and in biofilms of Azé-prehistoric, Réclère and Soyons Caves using Venn diagram.

Figure 7 : Non-metric multidimensional scaling of bacterial communities in the five sampled show caves.

Figure 8 : Non-metric multidimensional scaling of photosynthetic communities in the five sampled show caves.

CHAPITRE 2.....131

Figure 1 : FDA survival test was performed on untreated algae and on UV-C exposed suspensions (2, 4, 6, 8, 10, 20 and 30 kJ m⁻²).

Figure 2 : Absorbance spectra of *Chlorella* sp. following (a) 0, (b) 2, (c) 10 and (d) 30 kJ m⁻² UV-C irradiations. Alga suspensions were maintained under culture condition.

Figure 3 : Absorbance spectra of *Chlorella* sp. following (a) 0, (b) 2, (c) 10 and (d) 30 kJ m⁻² UV-C irradiations. Alga suspensions were maintained in the darkness.

Figure 4 : Evolution of *Chlorella* sp. photosynthesis (a) and respiration (b), before and after 2.5, 5, 7.5 and 10 kJ m⁻² UV-C exposition.

Figure 5 : Quantum yield (Fv/Fm) (a), photochemical quenching (qP) (c) and non-photochemical quenching (NPQ) (d) were monitored before and after UV-C irradiations (0, 2, 4, 6, 8, 10, 20 and 30 kJ m⁻²). Graphic (b) represents the quantum yield of *Chlorella* sp., which was measured directly after the treatment and represented in logarithmic scale.

CHAPITRE 3.....165

Figure 1 : Growth of algae, fungi and mosses on a limestone block previously painted with red ochre.

Figure 2 : Infra-red analysis of treated and untreated lard (a) and beeswax (c). Graphics (b) (lard) and (d) (beeswax) show results of colorimetric measurements of both treatments.

Figure 3 : (a) SEM picture of red ochre before (A) and after (B) UV-C radiations. The red powder (C) has been used by prehistoric human (D). Colorimetric measurements (b), DRX analysis (c), and infrared spectrometry (d) has been carried out before and after UV-C treatment.

Figure 4 : X-Ray microanalysis on red ochre (A) before and (B) after UV-C radiations.

CHAPITRE 4.....189

UV-C as an efficient means to combat biofilm formation in show caves: evidence from the La Glacière Cave (France) and laboratory experiments

Figure 1 : Sections and plan of the Glacière cave (Doubs, France). The green triangles represent the location of both treated “Bio.int” and “Bio.ext” biofilms.

Figure 2 : Temperature inside La Glaciere show cave has been monitored during 7 months close to both “Bio.ext” and “Bio.int” biofilms with the temperature sensors: Niphargus (from May to August 2016) and Reefnet (from August to December 2016). Change of temperature device is shown with the red symbol “Δ”.

Figure 3 : For 20 years ago, La Glacière show cave produced huge quantity of ice (A). Since global warming, positive temperatures were measured and no more ice was produced during the winter (B). In summer, plants (C) are able to growth between C-C section and cave entrance. “Bio.ext” (D) and “bio.int” (E) biofilms were eradicated by UV-C treatment and showed no proliferation (E), (G) after 21 months. “Bio.ext” showed a variety of color corresponding to different algae, cyanobacteria and mosses strains (F). After UV-C irradiation, all photosynthetic microorganisms showed a loss of their green color and an important amount of organic matter stayed on the treated cave wall (G).

Figure 4 : Illustration of the cave showing (i) environmental parameters influencing biofilm proliferation and (ii) UV-C treatment on “Bio.ext.” with the measurement pattern.

Figure 5 : Biofilm (“Bio.ext.” and “Bio.int.”) colorimetric measurement (green-red scale a^* (a) (c), and dark-light scale L^* (b) (d)) after 4 treatments of 12 hours. Statistical significant differences are represented with the letters “a” to “i”.

Figure 6 : Green colorimetric parameter (a^*) (a) and (b) quantum yield (Fv/Fm) of biofilms growing on limestone and treated with UV-C (30 kJ m^{-2}) maintained under light conditions throughout the experiment or in the dark. Green colorimetric parameter (a^*) (c) and (d) quantum yield of biofilm maintained in the dark for 21 days and previously treated with UV-C (30 kJ m^{-2}). They were then cultivated under light conditions.

Figure 7 : Algal suspensions were irradiated with UV-C (30 kJ m^{-2}) and then cultivated under light conditions (a) or in the dark (b). Suspensions were monitored with a spectrometer before treatment and every day for 5 days.

Figure 8 : Colorimetric measurements (a), infra-red analysis (b) and DRX analysis (c) has been carried out before and after UV-C treatment on manganese dioxide powder.

Comparison of biocides, allelopathic substances and UV-C as treatments for biofilm proliferation on heritage monuments

Figure 1 : Illustration of Vicherey church (a) and its biodeterioration (b) due to biofilm proliferation. Wall with southern exposure and floor othe church were affected by micro-algae and cyanobacteria (c), while north exposed wall was less invaded (d).

Figure 2 : (a) Biofilms on the floor of the Vicherey church: (a) before treatment, and (b) at 1 and 6 months after biocide treatments.

Figure 3 : Green (a) and black (c) biofilms growing on the floor and wall of Vicherey church, respectively. Both biofilms were treated with UV-C light (b, d). Pictures were taken one month after UV-C exposition.

Figure 4 : Colorimetric parameters were monitored on all biofilms treated with biocides, allelopathic solution and UV-C. x-axis: time of day; y-axis: green–red scale and dark–light scale. The values *a*, *b*, *c*, *d* and *ns* correspond to statistically significant or non-significant differences.

Figure 5 : Quantum yield was measured on all biofilms treated with biocides, allelopathic solution and UV-C. x-axis: time of day; y-axis: Quantum yield ($F'v/F'm$). The values *a*, *b*, *c*, *d* and *ns* correspond to statistically significant or non-significant differences.

Figure 6 : Illustration (a) shows remaining green spot six months after Devor'mousse (D), Biotine T (B) and Net Toit (N) application. Black UV-C irradiated biofilm shows fungi colonization.

Table des tableaux

| | |
|--|------------|
| SYNTHESE BIBLIOGRAPHIQUE..... | 25 |
| Tableau 1 : Méthodologie utilisées lors des identifications des micro-organismes formant des biofilms dans les grottes touristiques à travers le monde. | |
| Tableau 2 : Récapitulatif des méthodologies utilisées pour nettoyer les supports rocheux des agents biologiques les contaminant (modifié, Navdeep Kaur Dhami <i>et al.</i> , 2014). | |
| CHAPITRE 1..... | 95 |
| Tableau 1 : Environmental parameters of the five sampled caves. Physical, chemical and physiological parameters were measured for 21 biofilms. | |
| Tableau 2 : Shannon and Pielou indices are reported for all biofilms sampled and sequenced with 16S, 23S and ITS primers. | |
| Tableau 3 : Comparison of biofilm composition between untreated and treated caves. | |
| CHAPITRE 2..... | 131 |
| Tableau 1 : Statistical results (p-value) of colorimetric measurements. | |
| Tableau 2 : Mineral composition of the five studied pigments. | |
| Tableau 3 : ICP results of red ochre pigment. | |
| CHAPITRE 3..... | 165 |
| Tableau 1 : Characteristics of the two biofilms and statistical results of colorimetric measurements. | |
| Tableau 2 : List of algae, cyanobacteria and mosses sampled on both biofilms and growing on Petri dishes. | |
| Tableau 3 : Statistical results of colorimetric and quantum yield measurements. | |
| CHAPITRE 4..... | 189 |
| Tableau 1 : Statistical results of colorimetric parameters and quantum yield measurements of black and green biofilms. | |

Productions et communications scientifiques

Vulgarisation et animations scientifiques

- Nuit des chercheurs, Besançon (Septembre 2015)
- Fabrica Sciences, Besançon (Mars 2016)
- Radio Campus, Besançon (Mars 2016)

Communications orales

- Journée des doctorants, Besançon (Décembre 2014)
- Congrès « Rencontre d'Octobre », Chalain (Octobre 2015)
- Journée des doctorants, Besançon (Décembre 2015)
- XIIIème Forum de Biodétérioration des Matériaux, CEFRAFOR, Toulouse (Mars 2016)
- Concours de communication scientifique de la Société de Biologie de Besançon (SBB), Besançon (Décembre 2016)
- 10th International Symposium on the Conservation of Monuments in the Mediterranean Basin Athens, Grèce (Septembre 2017)

Posters

- Journées Portes Ouvertes de la Faculté de Franche Comté, Besançon (2014)
- Forum des Jeunes Chercheurs, Dijon (2^{ème} prix de vulgarisation) (2015)
- Journées Portes Ouvertes de la Faculté de Franche Comté, Besançon (2015)
- XIIIème Forum Biodétérioration des Matériaux, CEFRAFOR, Toulouse (2016)
- 6th International Conference on Algal Biomass, Biofuels and Bioproducts, San Diego, United States (2016)

Publications

Stéphane Pfendler, Olympe Einhorn, Faisl Bousta, Abderrahim Khatir, Laurence Alaoui-Sossé, Lotfi Aleya, Badr Alaoui-Sossé (2017) **UV-C as a means to combat biofilm proliferation on prehistoric paintings: evidence from laboratory experiments. Environmental Science Pollution Research.**

Stéphane Pfendler, Olympe Einhorn, Battle Karimi, Faisl Bousta, Didier Cailhol, Laurence Alaoui-Sosse, Badr Alaoui-Sosse, Lotfi Aleya - **UV-C as an efficient means to combat biofilm formation in show caves: evidence from *in situ* and laboratory experiments. Environmental Science Pollution Research.**

Stéphane Pfendler, Badr Alaoui-Sossé, Laurence Alaoui-Sosse, Faisl Bousta, Lotfi Aleya - **UV-C radiation on *Chlorella* sp., a biofilm-forming algal strain. Journal of applied Phycology.**

Stéphane Pfendler, Battle Karimi, Pierre-Alain Maron, Lisa Ciadamidaro, Benoît Valot, Faisl Bousta, Laurence Alaoui-Sosse, Badr Alaoui-Sossé and Lotfi Aleya - **Biofilm biodiversity in French and Swiss show caves using the metabarcoding approach: first data. Science of the Total Environment.**

Stéphane Pfendler, Fabien Borderie, Faisl Bousta, Laurence Alaoui-Sosse, Badr Alaoui-Sosse and Lotfi Aleya - **A comparison of different methods commonly used for treating biofilm proliferation on heritage monument.**

→ Soumis, *Journal of Cultural Heritage*, *Major revision*.

Stéphane Pfendler, Thomas Munch, Laurence Alaoui-Sossé, Faisl Bousta, Badr Alaoui-Sossé and Lotfi Aleya - **Optimizing UV-C treatment of biofilms in heritage monuments: Use of UV-C irradiation as a substitute for chemical treatments.**

→ *Environmentale Science and Pollution research*, *Under review*.

Introduction générale

De nombreuses grottes ou monuments historiques sont confrontés à la prolifération de micro-organismes provoquant une gêne esthétique ainsi que des problèmes d'érosion et d'altération des supports par voie chimique et/ou physique. Afin d'y remédier l'utilisation de produits chimiques est une pratique très répandue, avec de nombreuses conséquences négatives sur l'environnement. L'objectif de cette thèse est de traiter les biofilms de manière écologique, en utilisant la lumière ultra-violette. Cette technique se doit d'être efficace contre les micro-organismes formant les biofilms, tout en préservant le support sur lequel les bactéries, les micro-algues et les moisissures se développent. À contrario des produits chimiques, la lumière UV-C est une méthode efficace, non destructive et qui ne laisse aucun résidu sur la surface traitée.

La prolifération de biofilms est un problème récurrent sur toutes les façades extérieures des bâtiments. De tels développements microbiens ont été observés à l'intérieur de monuments, mais également sur les parois et les spéléothèmes des grottes touristiques. Au cours de ce travail de recherche, les études ont été essentiellement menées sur les problématiques d'encrassement biologique des grottes touristiques, un problème récurrent depuis de nombreuses années et appelé « la maladie verte ». Dans ce travail de recherche, quatorze grottes françaises et suisses ont fait l'objet de prélèvements et/ou d'irradiations *in situ* de biofilms. Afin de connaître la composition microbienne des biofilms, des prélèvements ont été effectués et les échantillons ont été séquencés par une technique de séquençage nouvelle génération (NGS). Les réponses physiologiques des micro-algues vertes suite à une exposition à la lumière UV-C ont permis d'optimiser la méthode de traitement. Afin de mettre en évidence l'innocuité du rayonnement UV-C, des analyses minéralogiques de la roche calcaire des grottes, ainsi que des pigments et liants utilisés comme peinture par les Hommes Préhistoriques, ont été réalisées. Enfin, dans le but d'évaluer l'efficacité des UV-C en condition *in situ* et de les comparer par rapport aux produits chimiques actuellement utilisés dans la lutte contre le développement des microorganismes, plusieurs tests ont été effectués dans la grotte de la Glacière (25) mais également dans l'Église de Vicherey (88), classée Monument Historique de France.

Synthèse bibliographique

I. Les grottes : géologie et biodiversité

1. Formations des grottes et paramètres physico-chimiques

Les grottes sont des cavités souterraines issues de la dissolution de roches plus ou moins solubles tels que les carbonates ou les évaporites (voie chimique) ou par la fracturation et les éboulements (voie mécanique). Dans la majorité des cas, il s'agit du résultat de l'attaque chimique du calcaire par l'eau de pluie contenant du gaz carbonique atmosphérique. L'eau s'infiltré ensuite dans le sol et dans les fissures des massifs calcaires puis commence à dissoudre le calcaire (Fig. 1). Les phénomènes de spéléogénèse peuvent également se produire du fait de la présence d'acide sulfurique dans un contexte de remontée de flux thermaux ou hydrothermaux, de la présence d'eau salée en contexte marin, ou biogénique du fait de la décomposition des guanos. Dans ce cas, il est associé aussi à des processus liés à l'acide nitrique, processus observés à la grotte de la Glacière dans le Doubs ou la grotte de Saint-Marcel en Ardèche. Ces phénomènes vont se dérouler pendant plusieurs milliers d'années jusqu'à la formation de galeries et de drains interconnectés.

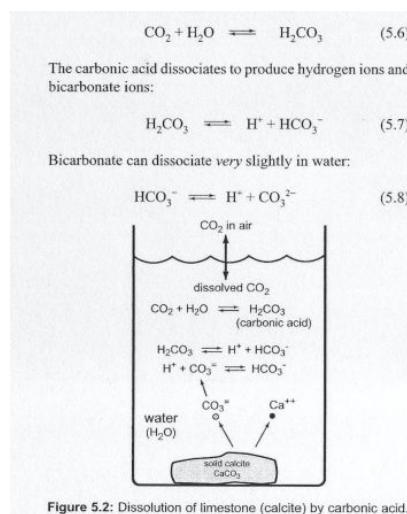
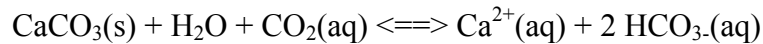


Figure 5.2: Dissolution of limestone (calcite) by carbonic acid.

Figure 3 : Dissolution de la roche calcaire (Palmer, 2007)

Equation générale de dissolution de la roche calcaire :



Les grottes peuvent avoir une taille comprise entre quelques mètres à plusieurs centaines de kilomètres comme la Mammoth Cave aux Etats Unis d'Amérique (580 km). De plus, ce sont des milieux oligotrophes dans lesquels, malgré des variations saisonnières, la température et l'humidité sont relativement constantes au cours de l'année (Czerwik-Marcinkowska et Mrozinska, 2011; Borderie *et al.*, 2014; Popovic *et al.*, 2015; Piano *et al.*, 2015).

Les grottes présentent une forte stabilité climatique (Bourges *et al.*, 2014) ce qui permet dans certaines conditions de confinement, la conservation d'art rupestre ancien. La température y est stable, mais on observe une augmentation depuis plusieurs décennies du fait du réchauffement climatique ($\pm 0,3$ °C). Dans les grottes d'Europe Centrale, la température est comprise entre 5 et 8°C et l'humidité entre 85 et 95 % (Popovic *et al.*, 2015); elle est le reflet de la température moyenne annuelle du lieu (Badino, 1992). Suivant les conditions aérologiques, la composition de l'air peut être différente du milieu extérieur ; en effet, la concentration en CO₂ dans l'atmosphère libre est de 0,035 %, et atteint en grotte des valeurs comprises entre 0,035 % et 6 % (Lismonde, 2002).

La lumière ne pénètre pas ou peu dans les grottes ; c'est un milieu essentiellement obscur où les organismes strictement photosynthétiques ne peuvent pas s'y développer (Lismonde, 2002) sans l'intervention de l'Homme. Toutes ces conditions physico-chimiques font des grottes des milieux extrêmes, obligeant les organismes vivants à s'adapter. De plus, les grottes sont généralement caractérisées par un faible apport en nutriments (Mulec, 2008) et donc une faible abondance et diversité d'organismes (Holsinger, 1998).

2. *La biodiversité : Flore, faune et micro-organismes des grottes*

a. *La faune cavernicole*

La faune du milieu souterrain qu'on appelait autrefois la faune cavernicole se subdivise en trois types de faunes (Ginet, 1977; Juberthie, 1994; Culver, 2005):

- Faune trogloxène : espèces qui fréquentent occasionnellement le milieu souterrain ;
- Faune troglophile : des espèces qui effectuent certaines parties de leur cycle de vie dans le milieu souterrain ou qui le partagent également avec le milieu souterrain superficiel et les milieux endogés ;
- Faune Troglobie : espèces qui se sont complètement adaptées au milieu souterrain et effectuent l'ensemble de cycle de vie dans le milieu hypogé. Il s'agit d'invertébrés et de poissons.

La richesse spécifique est fonction de l'influence de la climatologie (température moyenne, amplitude thermique) et de la distance à l'entrée. La proportion d'espèces troglophile/troglobies permet de mesurer l'influence de la distance à l'entrée et de la profondeur ; Ce sont des variables judicieuses pour déterminer la zonation (Montreux, 2013). De nombreux fossiles d'animaux (Fig.2), de la faune Pléistocène, datant pour certains de 160 000 à 180 000 ans ont été retrouvés dans les grottes : ours, lion des cavernes, hyène, panthère, jaguar européen, rhinocéros, éléphantidé, etc. (Argant, 1981; Guerin, 2009; Barriquand *et al.*, 2011). Une partie de ces fossiles confirment l'utilisation des grottes comme refuges ou lieux de vie pour ces animaux. Cependant, une autre partie des fossiles provient de restes alimentaires d'humains ou d'animaux, comme par exemple des os présentant des stries faites à l'aide d'un outil en silex (Barriquand *et al.*, 2011).

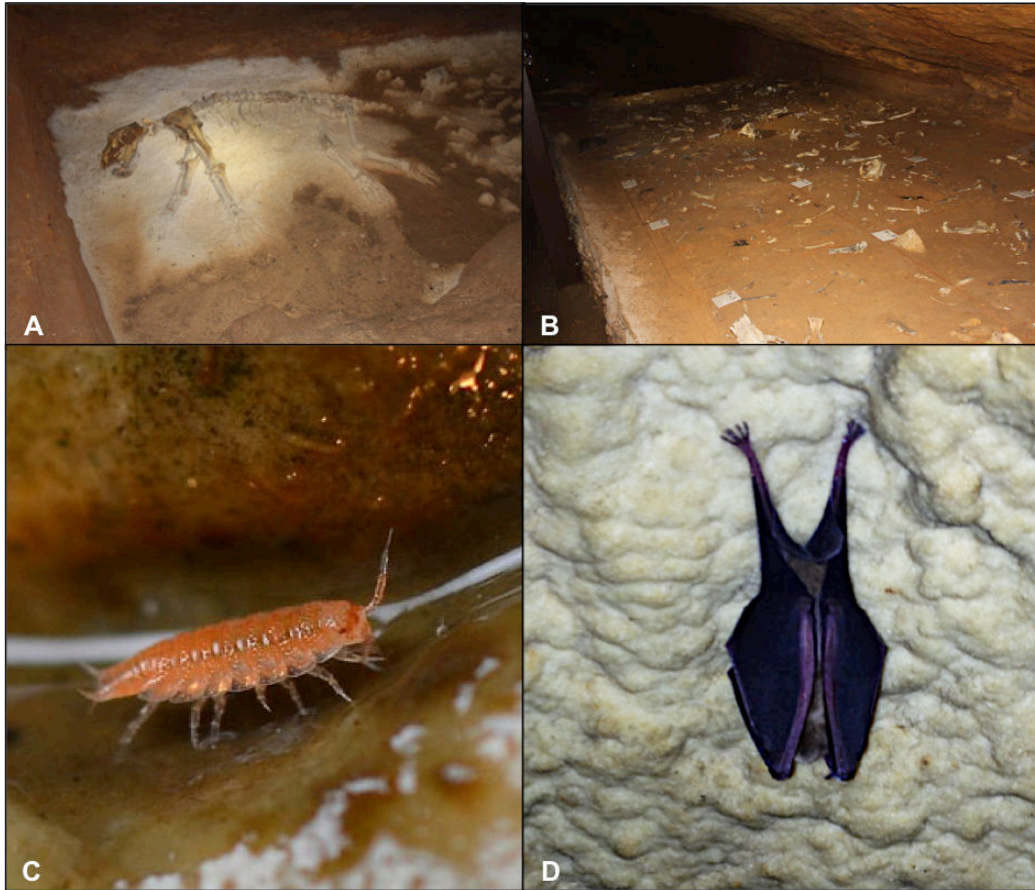


Figure 4 : Photographies (A) de la reconstitution du squelette d'un ours préhistorique (grotte de Blanot) (*Ursus deningeri* datant du Pléistocène moyen récent) ainsi que de nombreux autres ossements (B) d'animaux actuellement disparus (ours, lion, etc.). Des cloportes cavernicoles (*Androniscus dentiger*, grotte de Soyons) (C) et des chauves souris (D) (grotte de Blanot) ont été observés.

De nos jours, les grottes sont souvent considérées comme un milieu faible en biodiversité. Cependant, plusieurs études ont montré la présence de nombreuses espèces animales. Culver *et al.* (2000) ont recensé 973 espèces cavernicoles dans 48 états des États Unis d'Amérique dont 673 terrestres et 300 aquatiques. Parmi ces animaux, on y retrouve des insectes, des amphibiens des mollusques, des crustacés, des poissons, des mammifères, etc. (Culver *et al.*, 2000). Ces espèces vivent dans un milieu dit oligotrophe, qui peut être considéré comme environnement extrême, et sont par conséquent une niche écologique adaptée aux organismes hautement spécialisés (Jurado *et al.*, 2008).

b. La flore cavernicole

La plus part du temps les grottes ne reçoivent pas de lumière naturelle (Piano *et al.*, 2015) (Fig.3).

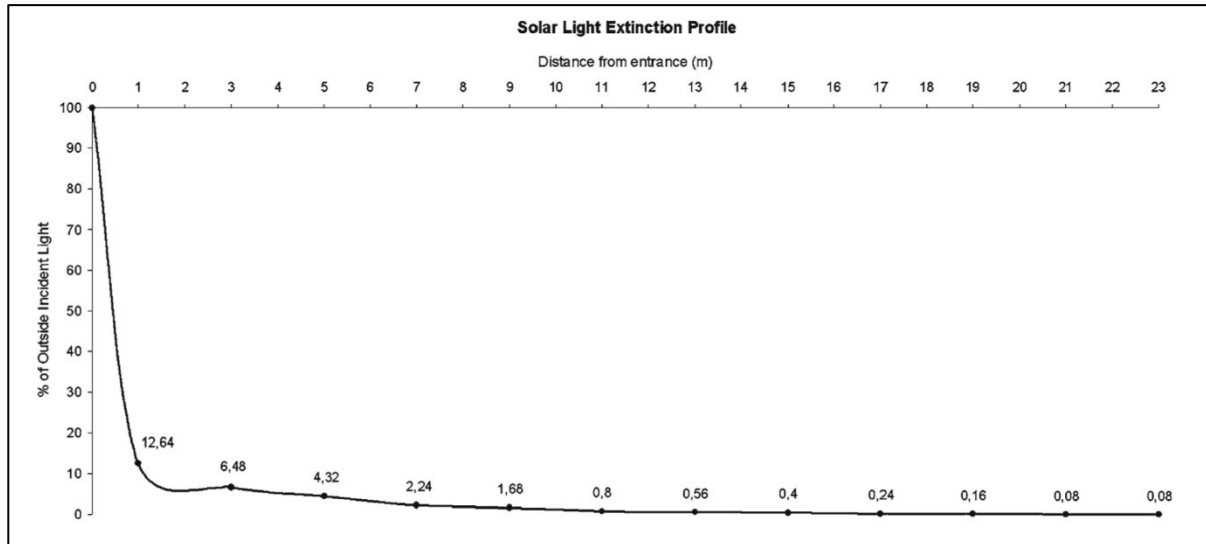


Figure 3 : Disponibilité de la lumière à l'intérieur d'une grotte (Azua, 2010).

La flore cavernicole se concentre à l'entrée des grottes (Piano *et al.*, 2015) ou dans des zones comprenant une lumière atténuée (zone disphotique), avec un développement d'algues, de mousses, et de fougères (Fig. 4). C'est une flore généralement adaptée aux faibles luminosités. Les aménagements pour les visites touristiques effectués dans des grottes apportent des niveaux de lumière qui peuvent être importants dans les zones aphotiques. Suite à ces modifications, des biofilms photosynthétiques composés principalement de cyanobactéries et de micro-algues s'y développent alors rapidement.



Figure 4 : Entrée de la grotte de Réclère (Suisse). La flore est composée de plantes supérieures (flèche bleue), de bryophytes (flèche rouge) et de micro-algues/cyanobactéries (flèche jaune). Les micro-organismes provoquent une biodétérioration du support colonisé (flèche orange).

c. Les micro-organismes

Les micro-organismes sont présents sur toute la surface de la Terre, dans des conditions favorables ou extrêmes comme dans les grottes. Certains d'entre eux comme les bactéries, contribuent à la formation de certaine curiosité géologique telles que des spéléothèmes croissant en direction d'une source lumineuse (Mulec *et al.*, 2007), la formation de couches de calcaire à la surface de certain point d'eau (Fig. 5), la croissance de spéléothèmes spécifiques et la formation d'oxyde de manganèse sur les parois des grottes (Canaveras *et al.*, 2001). Les bactéries peuvent également proliférer sous forme de colonies aux couleurs variées (Fig. 5).

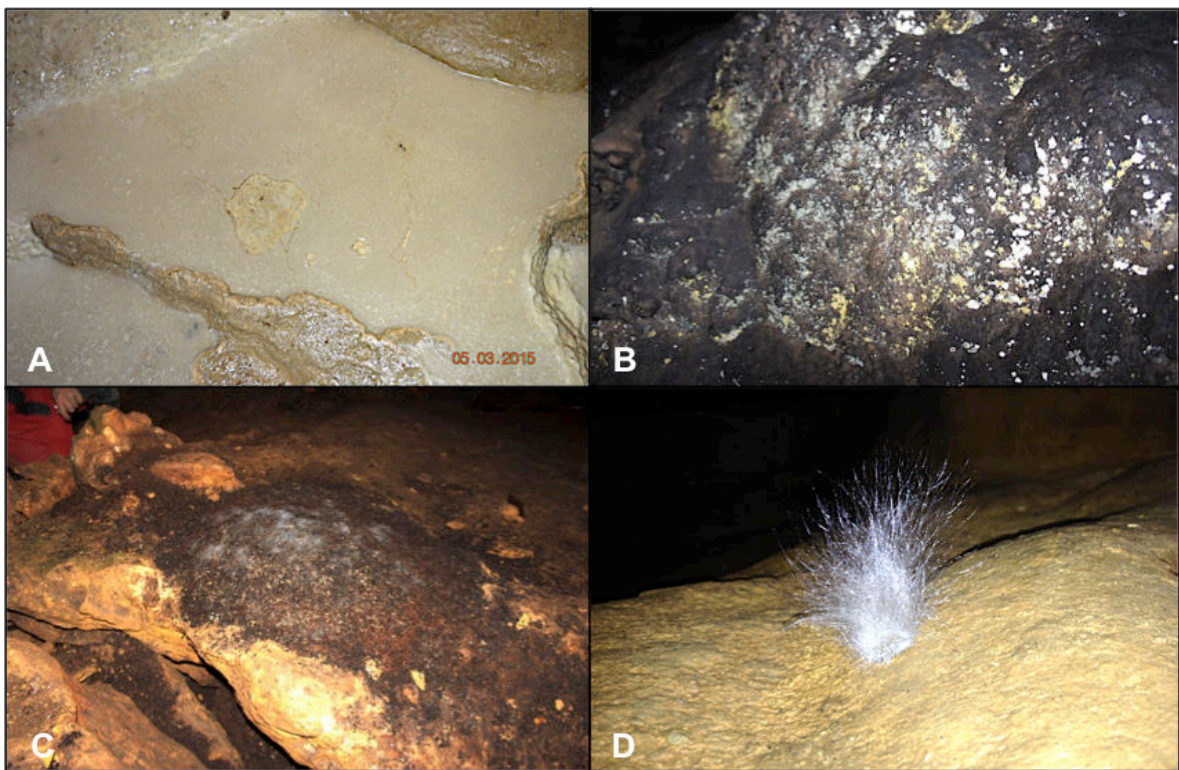


Figure 5 : Certaines bactéries peuvent former une couche calcaire (A) à la surface de l'eau (Grotte d'Arcy-sur-Cure). Le développement de bactéries (Actinomycètes) peut former des colonies dorées, blanches et vertes à la surface de la roche (B). Différentes sortes de champignons sont visibles sur du guano de chauves-souris dans les grottes de Blanot (C) et des Moidons (D).

Les champignons microscopiques sont quant à eux dépendants d'apports nutritifs extérieurs (Popovic *et al.*, 2015) ou alors peuvent profiter de la présence de la matière organique nécrotique provenant d'autres organismes. Plus généralement, ils se développent également grâce aux déchets organiques laissés par les touristes et aux excréments la faune cavernicole tel que les guanos de chauve-souris (Fig. 5), jouant ainsi leur rôle de décomposeur. D'autres espèces de champignons sont connues comme étant des parasites d'invertébrés (Vanderwolf *et al.*, 2013) ou des pathogènes de chauve-souris (*Geomyces* sp.).

II. Le tourisme dans les grottes et ses conséquences

1. *Historique du tourisme cavernicole*

Les grottes ont de tous temps suscité un intérêt particulier pour l'Homme. Utilisées par les Hommes préhistoriques comme lieu de refuge, elles ont été décorées de peintures pariétales dont les plus anciennes remontent à 40 000 ans (Aubert *et al.*, 2014). Cependant, la plus vieille présence humaine (Homme de Néandertal) a été découverte dans la Grotte de Bruniquel en France et daterait de 176 500 ans (Jaubert *et al.*, 2016). Les grottes sont actuellement un lieu d'émerveillement où le tourisme se développe rapidement.

L'intérêt pour les grottes débuta très tôt. En 1213, la grotte slovaque Postojna accueillait ses premiers visiteurs qui y laissèrent un autographe (Cigna, 2012). En France, la première grotte touristique ouverte aux touristes est celle de Balme qui fut exploitée dès 1807. De nos jours, plus de 2,5 millions de personnes visitent les grottes françaises chaque année (source ANECAT). Zhang et Jin (1996) estiment qu'il y a 800 grottes touristiques dans le monde, visitées par 250 millions de touristes par an (Cigna, 2016), ce qui engendrerait 2,3 milliards de dollars (US dollars) de recettes (Cigna et Burri, 2000). Afin d'accueillir les touristes, des aménagements ont été réalisés dans les grottes tels que l'illumination et la création de chemins d'accès (Gillieson, 2011). Cependant, les visites touristiques ainsi que les nombreux aménagements ont modifié l'écosystème des grottes, les mettant en péril (Baker et Genty, 1998).

2. *L'éclairage des grottes*

Les premiers éclairages artificiels ont été installés en 1880 dans la grotte Chifley en Australie. Dans les grottes françaises, différents types de lumière ont été installés : les anciens éclairages sont composés essentiellement de projecteurs de très forte puissance (jusqu'à 2000W). Les installations se modernisent avec le temps (Fig. 6) et on voit à présent apparaître dans une très grande majorité des grottes des éclairages de type LED. Les avantages sont nombreux : (i) les LED consomment beaucoup moins d'énergie avec une efficacité d'éclairage qui peut être supérieure ou égale aux lampes classiques, (ii) elles permettent pour certaines un ralentissement de la croissance des micro-algues (en choisissant les longueurs

d'ondes les moins favorables à la photosynthèse) et enfin (iii) ne produisent pas ou très peu de chaleur (Agostino *et al.*, 2015). Outre l'apport en lumière, l'éclairage favorise la croissance des micro-organismes chlorophylliens par son apport en chaleur. Cette pollution thermique (Caumartin, 1993) peut augmenter la température jusqu'à 10°C à une distance de 10 cm de la lampe (Cigna, 2011). Cet apport de chaleur est non négligeable dans des grottes où la température est généralement basse.



Figure 6 : Différents types d'éclairage sont présents dans les grottes touristiques (LED, projecteur allogène et spot) (<http://www.cavelighting.com>).

3. Conséquence de l'activité touristique

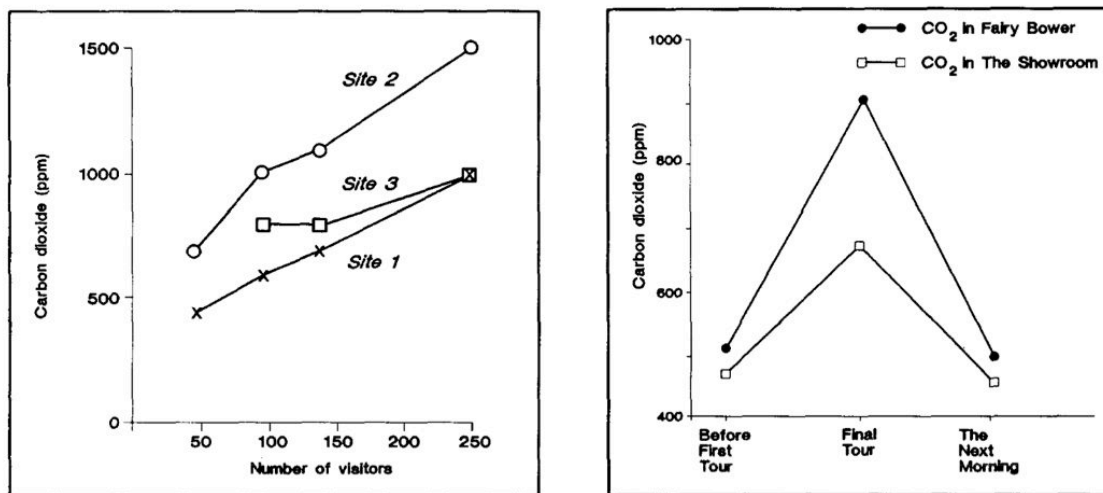
Les conséquences de l'activité touristique sont nombreuses :

- Lors des visites, les touristesensemencent involontairement les grottes avec de nombreux micro-organismes, tels que des algues, des champignons ou des bactéries. De plus, ils apportent de la matière organique en grande quantité (Lamprinou *et al.*, 2014), servant de source de carbone aux organismes hétérotrophes. Cependant, l'apport en micro-organismes se fait également par la faune cavernicole où les courants d'air (Dobat, 1970; Mulec *et al.*, 2008; Palmer *et al.*, 1991; Keswick *et al.*, 1982; Cunningham *et al.*, 1993; Northup *et al.*, 1994; Rusterholtz et Mallory, 1994).

Synthèse bibliographique

- L'éclairage artificiel des grottes (jusqu'à 10 heures par jour en continu) a conduit à la prolifération de micro-organismes photosynthétiques (cyanobactéries, algues) sous forme de biofilms (Cigna, 2011 ; Cennamo, 2012). Ce phénomène est connu depuis très longtemps et a été étudié pour la première fois par Kyrle en 1923 et Morton et Gams en 1925 (cité dans Cigna, 2011; Lamprinou, 2014). Depuis, de nombreuses études s'y sont intéressées (Abdelahad, 1989; Bahls, 1981; Claus, 1962; Couté, 1984; Davis et Rands, 1982; St. Clair et Rushforth, 1976). Les espèces composant les biofilms ont été nommées Lampenflora en 1963 par Dobson. Elles sont capables de se développer avec une très faible intensité lumineuse : $1 \mu\text{mol photon m}^{-2} \text{s}^{-1}$ (Grobbelaar, 2000).

- Une augmentation des concentrations en CO_2 a été mesurée (Baker et Genty, 1998; Dragovich et Grose, 1990) favorisant d'autant plus la prolifération des Lampenflora. Cette augmentation a été corrélée avec l'affluence touristique (Fig. 7).



Dragovich et Grose, 1990

Figure 7 : (A) Taux de CO_2 mesuré dans la « Imperial Cave » à trois endroits différents (« Site 1, 2 et 3 ») en fonction du nombre de visiteurs. (B) Moyenne des concentrations en CO_2 avant les visites de la grotte, après les visites et le lendemain matin (avant la reprise des visites).

- L'augmentation de la température en lien direct avec le flux touristique (Fig. 8) est bien connue et démontrée notamment par Stanka et Turk (2014). En effet, avec un apport énergétique compris entre 82 et 170 W par personne et par visite (Villar *et al.*, 1984), les touristes engendrent une augmentation non négligeable de la température de l'eau et de l'air, impactant le taux d'humidité (Cigna, 1993; Cigna et Burri, 2000; Mulec et Kosi, 2009).

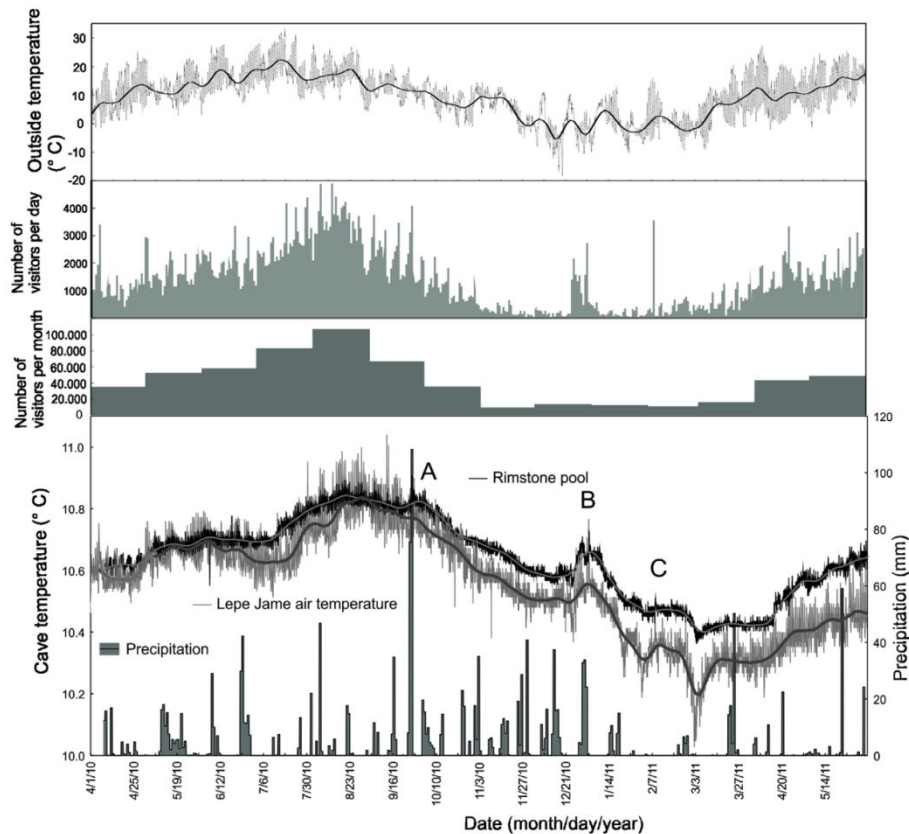


Figure 8 : Suivi de la température intérieure de l'air (« Lepe Jame air temperature ») et de l'eau (« Rimstone pool »), de la température extérieure, des précipitations, et du nombre de touristes dans la Grotte Postojna (Stanka et Turk, 2014).

L'ensemencement des grottes, l'éclairage artificiel, l'augmentation de la concentration en dioxyde de carbone et des températures, engendrent et favorisent la formation des biofilms photosynthétiques. Cependant, l'éclairage artificiel est de loin le premier facteur influençant la croissance des autotrophes (Piano *et al.*, 2015).

III. Les biofilms photosynthétiques

1. La formation d'un biofilm

Les bactéries sont la plupart du temps les premiers colonisateurs d'un support et favorisent l'établissement d'autres micro-organismes (Barberousse, 2006). Dans les grottes, leur biomasse est faible car ce sont des milieux oligotrophes.

Suite à l'établissement des biofilms bactériens, l'éclairage artificiel permet la croissance et le développement d'organismes photosynthétiques. Parmi ces organismes, on retrouve les cyanobactéries, les micro-algues, les lichens (Zuconni *et al.*, 2012), les bryophytes et les plantes dites supérieures. Grâce à une source de lumière artificielle, les cyanobactéries et les micro-algues vont être les premiers organismes microscopiques photosynthétiques à se développer (Mulec et Kosi, 2009). Les cyanobactéries sont des organismes clés dans la genèse des biofilms ; en effet, elles sont capables de produire des exopolysaccharides (EPS) permettant l'installation de communautés microbiennes complexes (bactéries, champignons, algues, diatomées, etc.) ainsi que leur adhésion à la surface rocheuse (Cennamo, 2012). Les biofilms assurent à ces micro-organismes une protection physique et permettant des échanges de nutriments (Gorbushina, 2007). C'est également un réservoir d'eau durant les périodes sèches (Macedo *et al.*, 2009; Keshari et Adhikary, 2013). Les organismes qui y vivent, s'y développent rapidement, puis se disséminent dans l'environnement. Les biofilms peuvent être denses et former une couche importante de matière organique pouvant servir de substrat à des organismes multicellulaires tels que les champignons, les mousses ou les plantes (Barberousse, 2006) permettant ainsi une succession écologique (Fig. 9). Les hépatiques utilisent la matière organique produite par les unicellulaires comme substrat pour se développer. Tout comme les bactéries et les micro-algues, les mousses vont produire de la matière organique en grande quantité. Cette dernière pourra être utilisée par des plantes supérieures comme les fougères (Perrichet, 1991), plantes fréquemment retrouvées dans les grottes. Tous ces organismes vont conduire à la biodétérioration du support qu'ils colonisent.

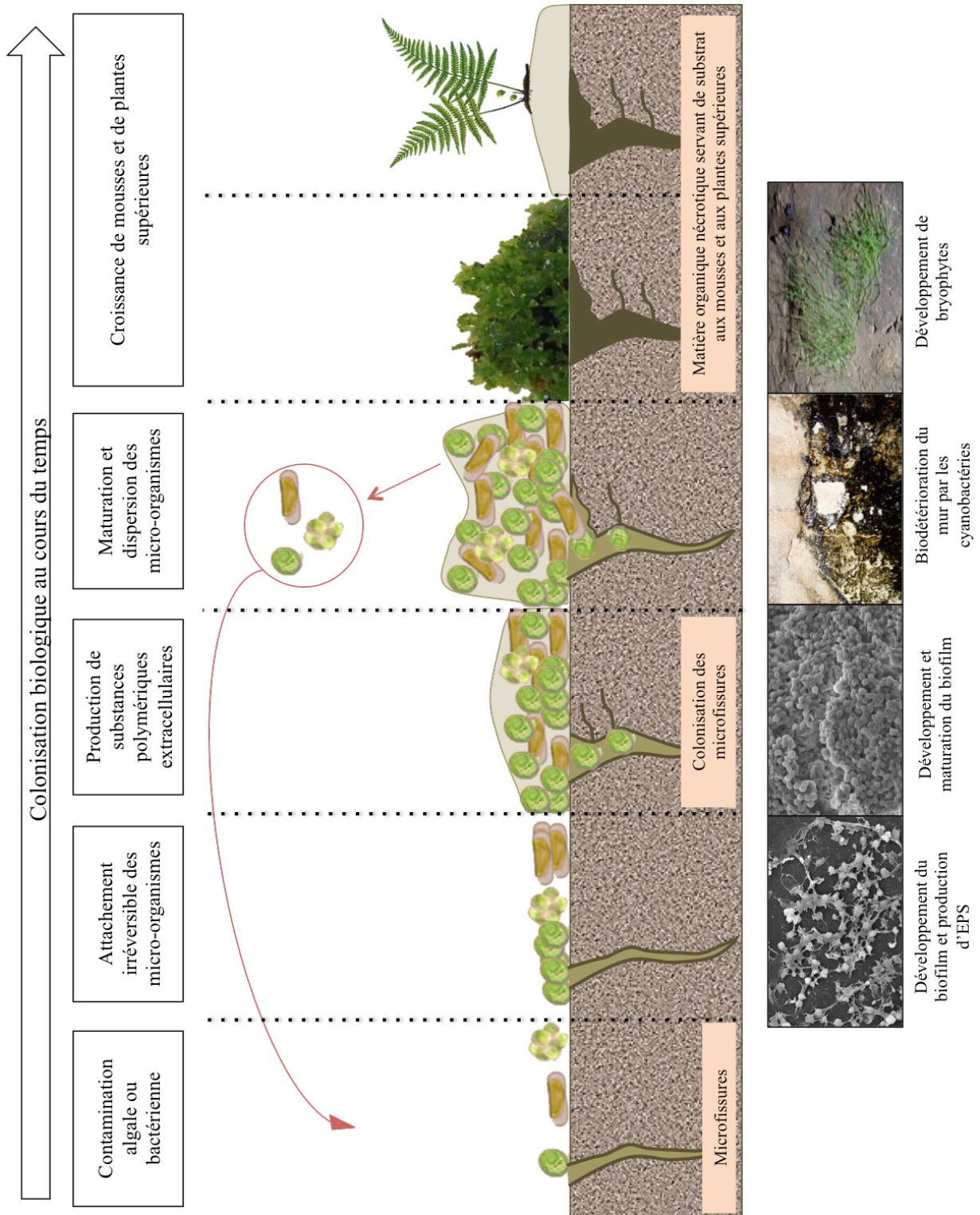


Figure 9 : Schéma synthétique montrant la colonisation d'une surface par les algues et les cyanobactéries ainsi que le développement d'un biofilm avec production d'exopolysaccharide, sa maturation et sa dissémination.

2. Les micro-organismes formant les biofilms

a. Identification des micro-organismes

Différentes techniques peuvent être mise en œuvre (Tableau 1) afin d'évaluer la diversité des micro-organismes formant les biofilms et de les identifier. La technique d'identification des micro-organismes la plus couramment répertoriée dans la bibliographie est la culture sur boîte de Pétri. Les échantillons sont prélevés avec un ruban adhésif, un écouvillon stérile ou un scalpel, puis ensemencés sur un milieu de culture spécifique aux organismes étudiés, additionné d'agarose. Après leur croissance sous forme de colonies, les micro-organismes sont identifiés par microscopie ou par séquençage de type Sanger. Il est également possible d'étudier la diversité microbienne grâce à des techniques de « fingerprinting » comme la TTGE/DDGE, le RISA (Urzi, 2010) ou alors la cytométrie en flux (Borderie *et al.*, 2016). Cependant, ces techniques ne permettent pas d'identifier les taxons présents dans les biofilms mais uniquement d'estimer la richesse spécifique. Durant ces dernières années, des techniques de biologie moléculaire (clonage puis séquençage Sanger) ont été couramment utilisées (Mihajlovski *et al.*, 2017) et ont l'avantage de permettre l'identification des espèces.

Des listes non exhaustives de micro-organismes formant les biofilms ont été publiées. En effet, une partie de ces techniques permettent de mettre en évidence les algues, les cyanobactéries et les champignons cultivables sur milieu gélosé. Or, il est bien connu que seule une petite fraction des micro-organismes est cultivable (Bartosch *et al.*, 2003; Prieto *et al.*, 2004; de los Ríos et Ascaso 2005; Berdoulay et Salvado 2009; Qi-Wang *et al.*, 2011; Cutler *et al.*, 2012).

Le séquençage nouvelle génération (NGS) permet d'étudier avec une bien meilleure précision les communautés microbiennes. Cette technique apporte en plus des techniques classiques une information semi-quantitative sur les communautés et sur la biodiversité des biofilms. Cependant, aucune étude ne rapporte l'utilisation de cette technique dans les grottes touristiques pour les algues, les cyanobactéries et les diatomées.

Tableau 1 : Méthodologies utilisées lors des identifications des micro-organismes formant des biofilms dans les grottes touristiques à travers le monde.

| Méthodes | Milieus de culture | Prélèvements | Pays | Auteurs |
|--------------------|--------------------------------|------------------------------|------------|------------------------------------|
| Microscopie | / | Brosse à dent | Etats Unis | <i>Smith et Olson (2007)</i> |
| Microscopie | / | Scalpel | Grèce | <i>Lamprinou (2012, 2014)</i> |
| Microscopie | Bischoff and Bold Medium (BBM) | Fragment de roche | Israël | <i>Vinogradova (2011)</i> |
| Microscopie | Blue Green Medium (BG11) | Scalpel | Espagne | <i>Martinez (2010)</i> |
| Microscopie | Bristol | Scalpel et fragment de roche | Pologne | <i>Czerwik-Marcinkowska (2011)</i> |
| Microscopie | Bristol | Scalpel | Pologne | <i>Czerwik-Marcinkowska (2013)</i> |
| Microscopie | / | Ruban adhésif | Italie | <i>Urzi (2001)</i> |
| Microscopie | / | Ruban adhésif et écouvillon | Serbie | <i>Popovic (2015)</i> |
| RISA | BG11 | Scalpel | Espagne | <i>Urzi (2010)</i> |
| Clonage | BG11, BBM | Scalpel | Italie | <i>Cennamo (2012)</i> |
| Clonage, ARISA | / | Scalpel | Italie | <i>Cennamo (2016)</i> |
| MALDI TOF | Gélose au sang | Scalpel | Slovénie | <i>Mulec (2015)</i> |
| Cytométrie en flux | / | Écouvillon | France | <i>Borderie (2016)</i> |

b. Communauté microbienne

Les biofilms photosynthétiques sont la plupart du temps formés d'une majorité de cyanobactéries (Mulec, 2008; Smith et Olson, 2007; Czerwik-Marcinkowska et Mrozinska, 2011; Vinogradova *et al.*, 2009; Lamprinou *et al.*, 2014; Popovic *et al.*, 2015), puis de chlorophycées et de diatomées. Les trois facteurs essentiels au développement d'une telle communauté microbienne dans une grotte sont la température, l'humidité et l'éclairage (Popovic *et al.*, 2015). D'autres facteurs de la grotte peuvent entrer en ligne de compte : la dimension de l'entrée, la morphologie, l'orientation, les propriétés du substrat et les paramètres microclimatiques (circulation de l'air, condition hydrogéologique, etc.) (Martinez et Asencio, 2010; Czerwik-Marcinkowska, 2013).

Le développement des algues et des cyanobactéries peuvent être ralenti par des animaux qui les utilisent comme source de nourriture (Grobbelaar, 2000; Czerwik-Marcinkowska et Mrozińska, 2009) comme certains collemboles. Ces derniers peuvent également se nourrir de champignons noirs (Bastian *et al.*, 2010). Cependant, cela n'est pas suffisant pour stopper le développement des biofilms, et ces derniers vont causer des problèmes de biodétérioration du support.

IV. Biodétérioration du support par les biofilms

1. La biodétérioration

La biodétérioration peut être définie comme des changements indésirables de la propriété d'un matériau, causée par l'activité biologique d'organismes vivants (Hueck 2001). Dans le cas des grottes, il s'agit de l'activité microbienne (algues, bactéries/cyanobactérie et champignons) sur la pierre calcaire.

Outre l'aspect inesthétique dû à la présence de tâches vertes, brunes ou noires (Mihajlovski, 2014 ; Hoffmann et Darienko, 2005; Bruno *et al.*, 2006, 2008; Lamprinou *et al.*, 2012), les micro-organismes jouent un rôle important dans la biodétérioration de la pierre calcaire (Aley, 1972; Aley *et al.*, 1985; Elliott, 1997; Olson, 2002; Cennamo, 2012; Piano *et al.*, 2015), mais également de la matière picturale composant les fresques préhistoriques (Canaveras *et al.*, 2001). En se développant, ils peuvent modifier le support colonisé et la structure minérale de la roche (Asencio et Aboal, 2001; Mihajlovski, 2014). Les cyanobactéries et les algues produisent de l'acide carbonique durant la respiration (Shields et Durell, 1964) ce qui a pour conséquence de dissoudre la pierre calcaire. De plus, ces derniers produisent des acides organiques (Perrichet, 1991; Aley, 2004; Smith et Olson, 2007) qui peuvent dégrader la roche, les formations calcaires (Aley, 2004) ainsi que les peintures préhistoriques (Canaveras *et al.*, 2001). Dans certains cas, les algues et cyanobactéries se font encalcifier dans la pierre calcaire, rendant leur nettoyage impossible (Smith et Olson, 2007).

Les micro-organismes colonisent les moindres porosités et fissures du support (Ortega-Calvo *et al.*, 1991). En croissant, ces organismes prennent du volume et dégradent (Fig. 10) de manière physique le support minéral (Ortega-Calvo *et al.*, 1991; Mihajlovski 2014). Une fois les plantes installées, leurs racines vont également s'introduire dans les porosités du support provoquant une érosion mécanique (Perrichet, 1991; Canaveras *et al.*, 2001).



Figure 10 : Le mur de l'église de Vicherey est colonisé et détérioré par des cyanobactéries.

2. Conséquences de la biodétérioration

Les conséquences de la biodétérioration dans les grottes touristiques sont particulièrement évidentes en prenant l'exemple de la célèbre grotte de Lascaux. Elle fut la première grotte française à avoir fermée définitivement ses portes au public en 1963, soit 23 ans après sa découverte et 13 années après le début de son exploitation touristique. Les détériorations sur le site ont été provoquées, entre autres, par la prolifération des algues (dont *Bracteacoccus* sp.). Plusieurs répliques de section de la grotte ont vu le jour, mais également une réplique exacte ouverte à la fin de l'année 2016 pour un coût total de 57 millions d'euros. Outre les perturbations occasionnées par le tourisme, la grotte a également connu une prolifération de champignons microscopiques dans les années 2000. Des traitements chimiques ont été appliqués durant de nombreuses années avant leur suspension définitive; certains biocides se sont avérés inefficaces et ont servi de source de carbone aux champignons. Bastian *et al.* (2010) ont montré que la pression de sélection exercée par les biocides a provoqué un changement de la communauté de bactéries et champignons présents dans la grotte de Lascaux est maintenant composée de micro-organismes pathogènes pour l'Homme (comme par exemple *Pseudomonas*, *Ralstonia* ou *Escherichia*).

V. La prévention et le traitement contre les Lampenflora

1. Les méthodes de détection préventive

a. La gestion de la grotte

Suite aux proliférations de biofilms dans les grottes, plusieurs propositions de changement de management sont évoquées dans la littérature avec notamment une réduction de la période d'éclairage (Gurnee, 1994), l'utilisation d'éclairage moins puissant et une limitation du nombre de visiteurs (Cigna, 1993; Cigna et Burri, 2000). Dans les faits, les gérants de grotte changent peu à peu leur éclairage, passant d'un éclairage puissant à des lampes LED, qui ont le double avantage de ne pas ou très peu produire de chaleur et d'être très économiques. De plus, la plupart des grottes sont à présent illuminées uniquement lors des visites touristiques, permettant ainsi de réduire la vitesse de prolifération des algues. Cependant, il est à noter que les Lampenflora peuvent survivre durant de longues périodes dans l'obscurité totale (Nugari *et al.*, 2009; Aley, 2004; Mulec et Kosi, 2009; Cigna, 2011) et sont également résistantes à la dessiccation (Grobbelaar, 2000; Lüttge and Büdel, 2009).

b. Mode d'éclairage

Les Lampenflora peuvent se développer grâce aux longueurs d'ondes favorables que produit l'éclairage artificiel. En changeant ce système d'éclairage par les lampes produisant des longueurs moins favorables à la photosynthèse, il est possible de réduire significativement le développement des Lampenflora (Olson, 2006; Mulec et Kosi 2009; Lamprinou *et al.*, 2014). En effet, Smith et Olson (2007) affirment que l'utilisation de lampes à longueur d'onde 595 nm a permis d'inhiber le développement des biofilms. Cependant, en changeant de longueur d'onde, la couleur de la lumière est également changée; par conséquent, l'éclairage de la grotte pourra causer une gêne esthétique. De plus, les auteurs ont rapporté que certaines souches de cyanobactéries se sont adaptées au changement de longueur d'onde, en augmentant la concentration de pigments spécifiques capables d'absorber la nouvelle longueur d'onde. Cet éclairage exercera donc une pression de sélection en favorisant ces espèces capables de s'adapter, mais ne conduira pas à long terme à une inhibition de la prolifération des biofilms (Smith et Olson, 2007).

c. *Le suivi préventif des micro-organismes*

À l'aide de l'instrument « *BenthoTorch*[®] », des mesures *in situ* de la concentration en chlorophylle *a* permettent de détecter préventivement le développement des Lampenflora (Piano *et al.*, 2015). Quant aux champignons, il est possible de les quantifier directement dans l'air de la grotte à l'aide d'un bio-collecteur. Saiz-Jimenez (2011) a proposé 5 seuils de vigilance arbitraire de la présence fongique allant de 50 UFC/m³ correspondant à une valeur normale (absence de problème) à > 1000 UFC/m³, une valeur signalant l'urgence d'intervenir. D'autres seuils de vigilance ont été proposés, notamment par les scientifiques travaillant dans la grotte de Lascaux. La quantification des micro-organismes présents dans l'air de la grotte peut également se faire pour les bactéries et les algues. Les bio-collecteurs aspirent les particules présentes dans l'air et les concentrent sur une boîte de Pétri contenant un milieu de culture adapté aux organismes que l'on souhaite quantifier. Après incubation, les colonies se développant sur le milieu de culture sont dénombrées. D'autres méthodes préventives sont utilisées comme la « Real-Time PCR » afin de détecter et de quantifier la présence et la concentration de champignons, comme par exemple *Ochroconis lascauxensis*, un champignon responsable des taches noirs sur les parois de la grotte de Lascaux (Martin-Sanchez *et al.*, 2013). Cette méthode est également utilisée dans la Mammoth Cave aux États Unis (Fowler, 2011) pour le suivi de la micro-algue *Chlorella*.

2. *Les traitements curatifs*

a. *Les biocides*

L'utilisation des biocides est aussi controversée car leur efficacité peut être variable (Faimon *et al.*, 2003), surtout en extérieur en raison de certains paramètres météorologiques, comme l'exposition aux ultra-violets, le rinçage par la pluie, etc. D'autre part, ces produits chimiques peuvent être utilisés comme source de carbone et d'azote par des champignons microscopiques et des bactéries Gram négatives (Urzi *et al.*, 2016), permettant ainsi leur prolifération (Bastian *et al.*, 2009). Bastian *et al.* (2009) rapportent que les microflore, les bactéries et les moisissures s'y développant deviennent résistantes à certain biocide. Par exemple, Urzi *et al.* (2000) montrent que certains micro-organismes deviennent résistant à l'Algophase[®]. De plus, les produits chimiques ont un impact négatif (Fig. 11) sur la biodiversité des grottes (Boston, 2006; Elliot, 2006; Hildreth-Werker et Werker, 2006). Urzi *et al.* (2016) ont montré que suite à un traitement chimique, la biodiversité microbienne

change de manière drastique en tuant une population microbienne mais en permettant l'installation d'une autre. En effet, la matière morte sert de substrat à des bactéries qui prolifèrent à leur tour (Urzi *et al.*, 2016).

Des effets négatifs sur la pierre ou sur l'environnement ont également été rapportées. En effet, certains produits chimiques peuvent entre en réaction avec certains composés de la pierre et former, suite à la cristallisation des sels, un voile blanc pouvant engendrer des phénomènes de dissolution de la pierre (Borderie, 2014, Faimon *et al.*, 2003). De plus certains biocides sont facilement lessivables et peuvent contaminer l'environnement karstique ainsi que les aquifères. Ces derniers ont été ciblés en Février 1998 par une directive Européenne concernant la mise sur le marché des produits biocides (Directive du 16 février 1998) dans le but de réguler leur utilisation et leur présence sur le marché (Borderie, 2014, Caneva *et al.*, 2008).

b. L'hypochlorite de sodium

Face à la prolifération des algues, les gérants des grottes luttent généralement avec des produits chimiques tels que l'hypochlorite de sodium (Smith et Olson, 2007) et des produits anti-algues commercialisés dans la plupart des grandes surfaces (grotte des Moidons). L'eau de javel est souvent utilisée de manière peu diluée (grotte de Saint Marcel); son efficacité, presque instantanée, sa rapidité d'application (quelques minutes à quelques heures suivant la taille de la grotte) et son faible coût sont des avantages majeurs pour les gérants. Cependant, le traitement affecte drastiquement la biodiversité de la grotte et installe une dynamique biologique dont on ne mesure pas actuellement les changements. De plus, la formation de sel d'hypochlorite est dangereuse pour l'environnement. Enfin, c'est un produit d'application dangereuse en milieu confiné.

c. Le peroxyde d'hydrogène (H₂O₂)

Des traitements moins néfastes pour l'écosystème des grottes sont envisagés comme l'utilisation de l'oxydant H₂O₂ (Grobbelaar, 2000; Faimon *et al.*, 2003; Mulec, 2014), qui a l'avantage d'être rapidement dissocié en eau et en oxygène. Son utilisation a été optimisée en tamponnant la solution à un pH de 7-7,5 (versus pH = 4) le rendant moins néfaste sur les formations calcaires (dissolution de la calcite). L'avantage de la méthode est l'absence de produits résiduels (vapeurs gazeuses nocives) ainsi que la facilité de l'emploi. Cependant,

l'acquisition du produit est contraignante (demandes d'autorisations d'achat) et son stockage nécessite de nombreuses précautions (produit explosif). De plus, une étape de retrait de la matière organique résiduelle doit être effectuée pour empêcher toute prolifération microbienne.

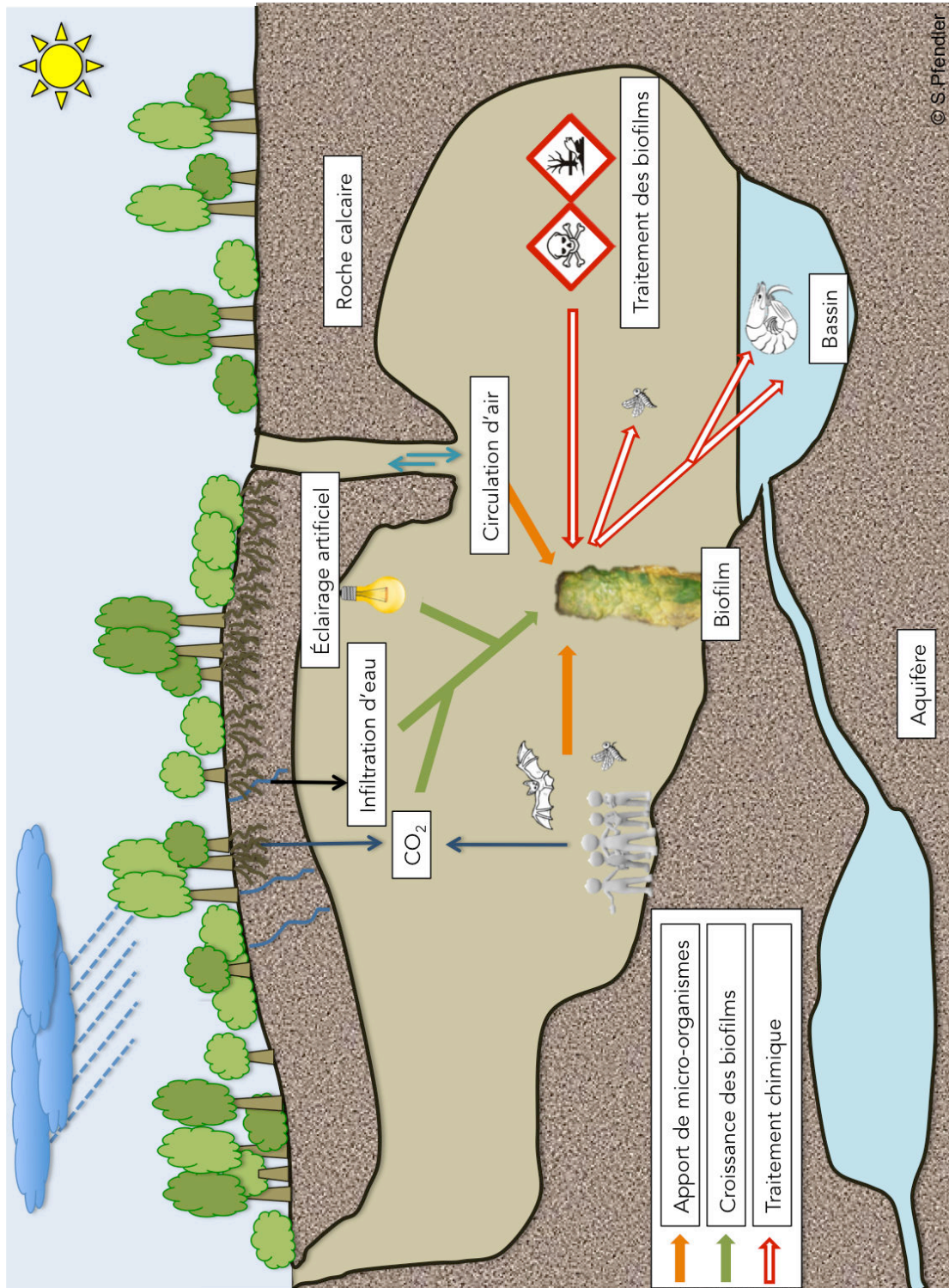


Figure 11 : Schéma d'une grotte représentant les différents facteurs permettant le développement des biofilms ainsi que leur traitement par voie chimique et les conséquences sur l'environnement karstique.

d. Les produits allelopathiques

Les molécules dites allélopathiques sont connues pour leur effets négatives sur les espèces autotrophes (Zuo *et al.*, 2016), mais peuvent également agir en tant que fongicide ou insecticide. Ces molécules peuvent être des acides phénolique, des flavonoïdes, des terpénoïdes ou des alcaloïdes (Leflaive et Ten-Hage, 2007) et la plus part d'entre elles sont des métabolites secondaires (Fistarol *et al.*, 2004). Elles peuvent affecter les fonctions permettant la photosynthèse, comme par exemple le photosystème II (Wang *et al.*, 2016). Une de ces molécules, la juglone, est synthétisée par le noyer afin d'inhiber la croissance des plantes aux alentours de l'arbre (Hejl *et al.*, 1993). Elle est également capable de tuer certaines souches de micro-algues comme *Micrasterias* and *Eudorina* (Kessler, 1989). Les molécules allélopathiques peuvent également être sécrétées par le phytoplancton lui même, entraînant une compétition entre les espèces (Wang *et al.*, 2016).

e. Les huiles essentielles

Les huiles essentielles sont utilisées comme un moyen de lutte biologique contre une grande variété de micro-organismes comme les bactéries, les champignons ou les levures (Vetas *et al.*, 2017), mais très peu d'études ont été réalisées sur les micro-algues. En 2009, Yang *et al.* ont montré l'effet délétère de l'huile essentielle de pin sur la croissance d'*Alexandrium tamarense*. Cependant, il est à noter que le coût des huiles essentielles peut être un frein important dans leur utilisation.

f. Les traitements mécaniques

Les brosses dures peuvent être utilisées comme traitement mécaniques et après cette étape, un lessivage à l'eau ou aux détergents est appliqué (Gibeaux *et al.*, 2014). Cependant cette technique est déconseillée à cause des risques de dégradation du support (Warscheid et Braams, 2000 ; Lisci *et al.*, 2003).

g. Le nettoyage à la vapeur

Gibeaux *et al.* (2014) rapportent que la vapeur permet de tuer les microorganismes et de diminuer leur encrage au support. Puis, les résidus sont enlevés à l'aide d'une brosse douce. Cette technique est préconisée sur les surfaces dures et en extérieur.

h. Les nettoyeurs haute pression

Les nettoyeurs haute pression est la deuxième solution privilégiée par les gérants de grotte. Ils nécessitent des moyens beaucoup plus importants et plus coûteux. Ils permettent le traitement de surfaces qui sont très souvent inaccessibles (Grotte des Moidons). Cependant, leur utilisation ne résout pas le problème de la prolifération des algues. Au contraire, les algues ne sont pas tuées et une partie est disséminée dans l'air sous forme d'aérosol, conduisant à leur dissémination dans toute la grotte. De plus, les techniques de nettoyage à la vapeur et haute pression posent d'énormes problèmes de destruction des surfaces (abrasion des microcristaux et des films argileux du concrétionnement). Des techniques de nettoyage par l'utilisation de lance à eau à faible pression pour des traitements locaux est à privilégier.

i. Les chlorovirus

En matière de lutte biologique, une des solutions proposées dans la bibliographie est l'utilisation de chlorovirus (May *et al.*, 2011). L'intérêt de la méthode est son coût peu élevé et le fait que ce soit un moyen totalement écologique. Cependant, il est très important d'envisager l'éventualité de la dispersion des virus dans l'environnement ; c'est entre autre pour cela que cette méthode n'est pas appliquée à l'heure actuelle.

Finalement, quelque soit le traitement appliqué, une recolonisation apparaît après quelques mois et le traitement se doit d'être renouvelé. Ceci montre bien leur faible efficacité dans le temps, car selon les gérants des grottes, une recolonisation est observée aux mêmes endroits où les biofilms avaient été traités l'année précédente.

3. Le traitement à la lumière UV-C

Des méthodes plus respectueuses de l'environnement peuvent être utilisées comme l'irradiation à la lumière ultra-violette de type C. La lumière UV est subdivisée en trois parties, l'UV-A (400-315 nm), UV-B (315-280 nm) et UV-C (280-100 nm) (Fig. 12).

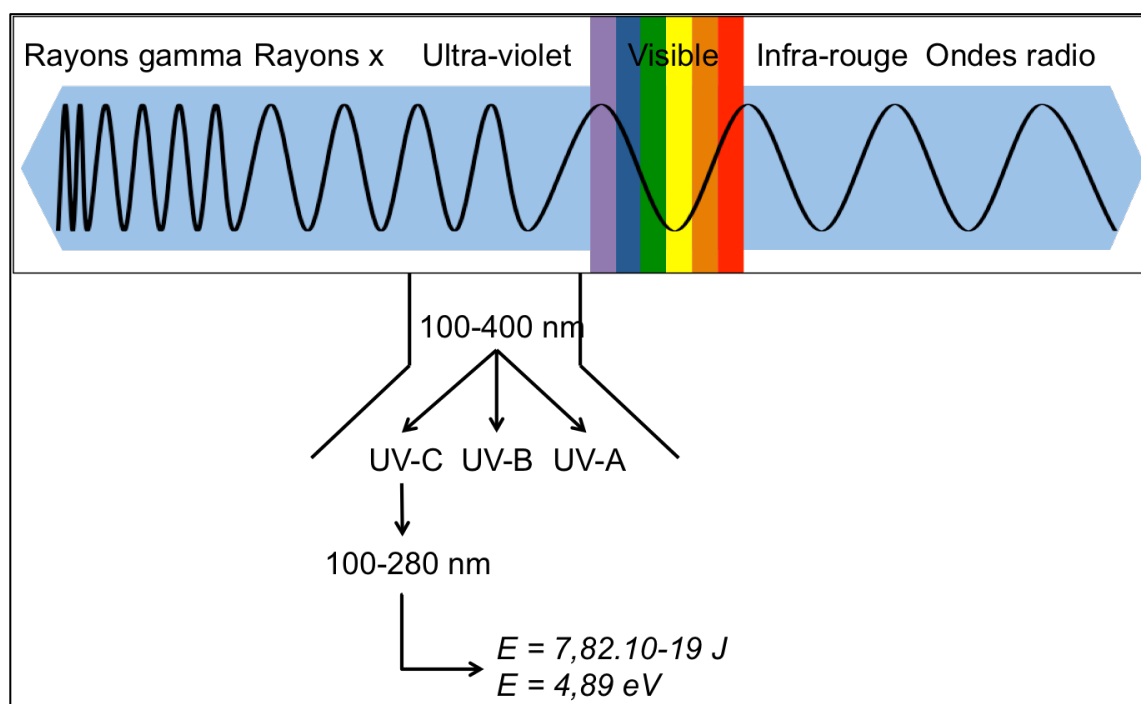


Figure 12 : Schéma représentant le rayonnement électromagnétique partant des rayons gamma jusqu'aux ondes radio.

L'UV-A représente 95% de la lumière ultra-violette atteignant la surface de la Terre ; l'UV-B les 5% restant. L'UV-C est une lumière dont les longueurs d'ondes sont faibles et donc très énergétiques. La couche d'ozone de l'atmosphère terrestre empêche ces longueurs d'ondes de traverser, permettant la vie sur la Terre (Kulandaivelu and Noorudeen, 1983; Gao *et al.*, 2009). L'utilisation de la lumière UV-C contre les algues proliférant dans les grottes a été suggérée par Grobbelaar *et al.* (2000) et la première convention pour l'étude sur l'utilisation des UV-C fut signée en 2007 entre le Laboratoire de Recherche des Monuments Historiques (Paris) et le Laboratoire Chrono-Environnement (Besançon). L'efficacité de la méthode a été démontrée dans plusieurs études par Borderie *et al.* (2010, 2011, 2014). D'autres groupes (Wang *et al.*, 2015) ont proposé l'utilisation des UV-C sur les blooms algaux principalement composés de cyanobactéries. Les radiations sont extrêmement néfastes pour les algues et les cyanobactéries. En effet, elles sont responsables de la dégradation de

macromolécules telles que l'ADN (Bolige *et al.*, 2005), les protéines (Kreslavski *et al.*, 2011) ou les lipides (Borderie *et al.*, 2014). De manière générale, les UV-C sont délétères sur la matière organique mais sans effet observé sur la matière inorganique, ce qui pourrait permettre de traiter des biofilms colonisant des peintures préhistoriques sans risque de dommages collatéraux. À ce jour, seule une étude sur le traitement des biofilms photosynthétiques (Borderie *et al.*, 2014) a été menée avec l'aide des UV-C dans les grottes touristiques. Dans cette étude, la couleur de quatre biofilms (traités aux UV-C ou non), a été suivie à l'aide d'un spectrocromimètre. Les résultats montrent que le traitement est plus efficace sur les biofilms de faible épaisseur que sur les biofilms épais. Pour ces derniers, la couleur verte ne disparaît pas entièrement, et une recolonisation a pu être observée 16 mois après le traitement (8 heures d'irradiation, soit 300 kJ m^{-2}). Enfin, le traitement UV est d'autant plus efficace que la source ultra-violette est proche (Champlot *et al.*, 2010) (Fig. 13).

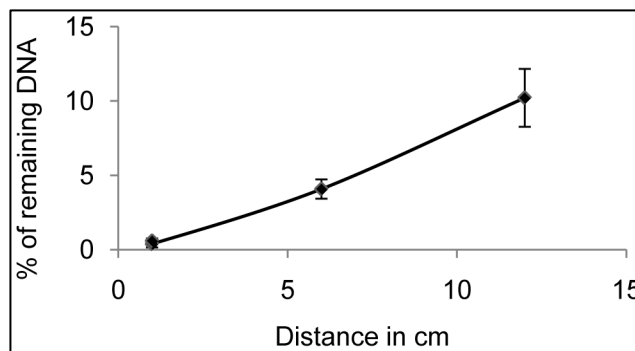


Figure 13 : Efficacité de la décontamination en fonction de la distance de la source d'UV-C (Champlot *et al.*, 2010).

En comparant tous les traitements, on s'aperçoit que l'utilisation des UV-C semble être la méthode la plus écologique à ce jour (Fig. 14, Tableau 2). Cependant, avant d'utiliser ce procédé, il est important de connaître ces effets sur les micro-organismes ainsi que sur leur support pictural ou rocheux.

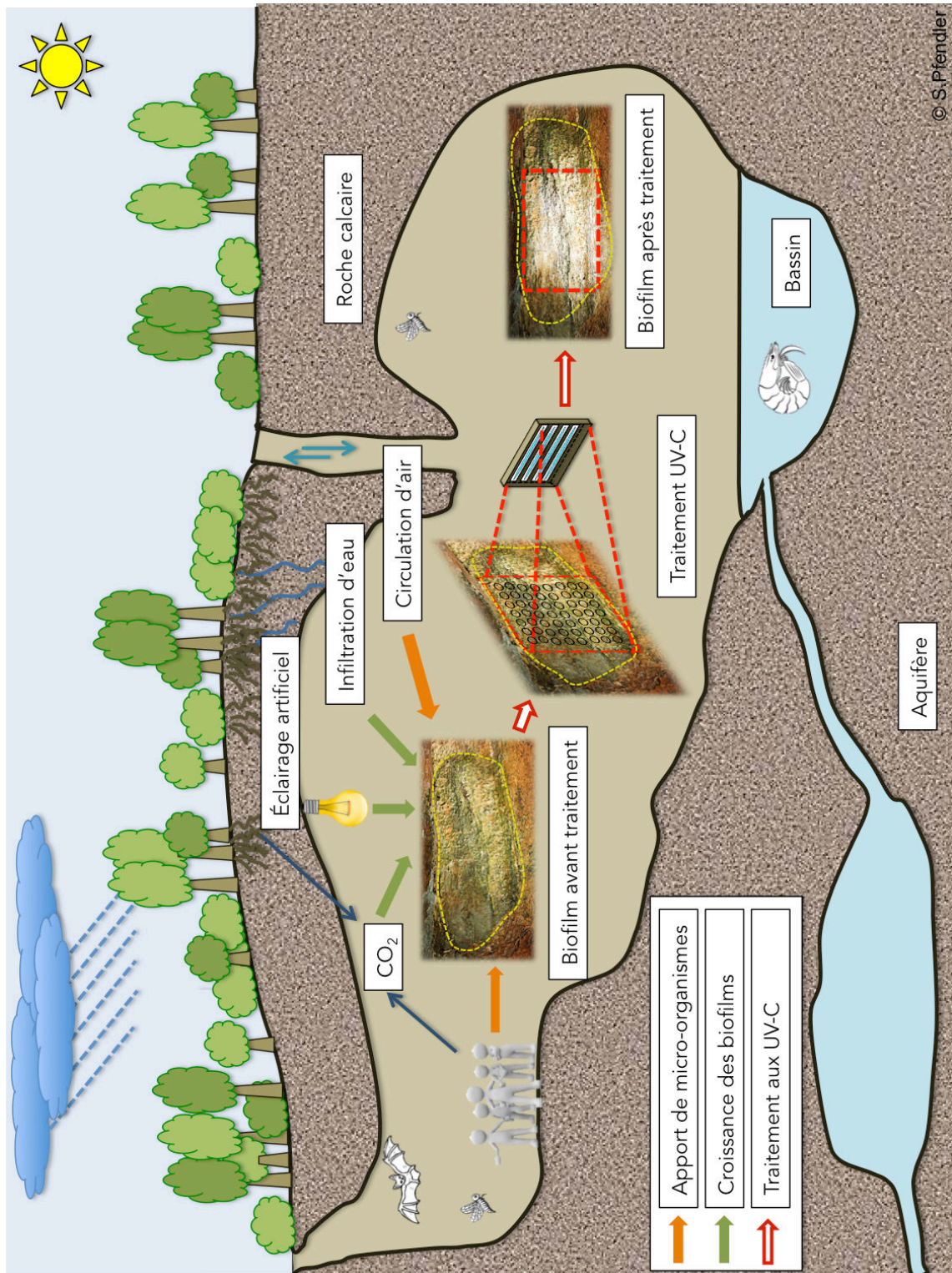


Figure 14 : Schéma d'une grotte représentant les différents facteurs permettant le développement des biofilms ainsi que leur traitement par l'utilisation de la lumière UV-C.

Tableau 2 : Récapitulatif des méthodologies utilisées pour nettoyer les supports rocheux des agents biologiques les contaminant (modifié, Navdeep Kaur Dhani *et al.*, 2014).

| Type de méthodes | Avantages | Inconvénients | Références |
|--|---|--|---|
| Physique | | | |
| Gamma, Rayon X | Simple, haute pénétration (gammas, X) Efficace contre les insectes | Applicable pour des objets de petites tailles | <i>Warscheid et Braams, 2000; Salvadori, 2003</i> |
| UV-C | Efficace contre les micro-organismes Écologique | Faible pénétration | <i>Borderie, 2014; Grobbelaar, 2000; Mulec et Kosi, 2009</i> |
| Mécanique | Méthode classique, très répandue | Résultats peu efficaces sur le long terme. Dommages sur le support. Les micro-organismes ne sont pas tués. | <i>Dakal et Cameotra, 2012</i> |
| Nettoyeur à haute ou basse pression | Efficace contre les mousses, algues et lichens | L'eau est retenue dans les pores favorisant la recolonisation. | <i>Kumar et Kumar, 1999</i> |
| Chimique | | | |
| Biocides | Spectre large | Toxique, corosif, inflammable, rémanent, efficacité variable, explosif | <i>Kumar et Kumar, 1999; Salvadori, 2003; Cappitelli et Sorlini, 2005</i> |
| Fumigation | Efficace contre les champignons, insectes | Très toxique | <i>Kumar et Kumar, 1999; Warscheid et Braams, 2000; Salvadori, 2003</i> |
| Atmosphère anoxique | Les champignons sont sensibles à la baisse d'oxygène | Période d'exposition longue, très coûteux | <i>Gu, 2003; Salvadori, 2003</i> |
| Biologique | | | |
| Virus | Rapidité d'application | Potentiellement dangereux pour l'environnement | <i>May, 2011</i> |

VI. Effet des UV-C au niveau cellulaire et moléculaire

1. Introduction

Il y a plusieurs millions d'années, les UV-C irradiaient la Terre de manière continue, empêchant le développement de la vie. Progressivement, la concentration en oxygène dans l'atmosphère a augmenté grâce aux algues procaryotes jusqu'à la formation de la couche d'ozone qui filtre les rayons UV-C et a conduit au développement des micro-algues eucaryotes. Cette théorie est confirmée par les études sur les fossiles algaux de cette époque (Gao et al., 2009). De nos jours la lumière ultra-violette de type C est un moyen de désinfection d'instruments ou de locaux dans les hôpitaux, les laboratoires (stérilisation de l'air, de l'eau ou de surface) ou utilisée pour optimiser la conservation des légumes dans l'industrie alimentaire. De plus, les UV-C sont utilisés pour lutter contre les blooms et biofilms algaux. De nombreuses études (Borderie *et al.*, 2011 ; Wang *et al.*, 2015) ont mis en avant le potentiel antimicrobien des UV-C dû à sa faible longueur d'onde qui lui confère un pouvoir énergétique important, permettant ainsi d'inhiber la croissance des bactéries, des champignons et la germination des spores. Cependant, à contrario des UV-A et des UV-B, les effets physiologiques des UV-C sur ces micro-organismes ont été très peu étudiés (Kulandaivelu et Nooruden, 1983 ; Gao *et al.*, 2009), probablement dû au fait que les UV-C ne traversent pas l'atmosphère terrestre. Dans les années 1990, l'effet de serre et la formation du trou d'ozone ont menés à de nombreux travaux de recherche sur les effets des UV-C sur les plantes. Cependant, les études sur les algues et cyanobactéries restent peu nombreuses (Goa *et al.*, 2009).

2. Les effets des UV-C sur les paramètres physiologiques

a. Effet visible sur les biofilms

Le premier effet visible d'une forte intensité d'UV-C sur un biofilm algale, est le « bleaching » ou blanchiment des cellules. Cela est dû à la dégradation progressive des pigments présents dans les cellules. Cette dégradation a été observée dans de nombreuses

études sur les algues vertes, diatomées, algues rouges et cyanobactéries (Gao *et al.*, 2009 ; Borderie *et al.*, 2011, 2014).

b. Effet des UV-C sur le métabolisme des algues

À de faibles intensités, la dégradation de la chlorophylle entraîne une baisse de la photosynthèse (Kulandaivelu et Nooruden, 1983) qui peut entre autre être mise en évidence par une baisse du rendement quantique et une augmentation du quenching non photochimique. Cependant, même si la photosynthèse baisse, il est possible, grâce à une forte exposition à la lumière visible, de l'augmenter significativement. Il est connu que la photosynthèse est une cible importante des UV (Gao *et al.*, 2009), entraînant une photoinhibition et donc une diminution de la production de dioxygène qui est entre autres dû à la destruction du complexe d'oxydation de l'eau (Wang *et al.*, 2015) ainsi qu'à la destruction de la protéine D1 associée au PSII. Ce dernier est très sensible aux UV-C car les protéines peuvent absorber les UV-C contribuant à des modifications et des dégradations moléculaires (Tyystjarvi, 2008). Alors que la photosynthèse baisse, la respiration des micro-algues, suite à un traitement aux UV-A et B, augmente (Aguilera *et al.*, 1999; Mulley *et al.*, 2001). Cependant, peu d'études sont disponibles pour les UV-C. La maintenance de la respiration est expliquée par le fait que les organismes tentent de maintenir leur métabolisme de base. Afin de lutter contre les UV-C, des mécanismes de réduction de l'efficacité de la photosynthèse peuvent être mis en place pour éviter les photo-dommages causés lors d'une exposition à un rayonnement UV. D'autres mécanismes permettent de dissiper l'énergie absorbée par PSII en chaleur par le cycle des xanthophylles (Osmond, 1994).

c. Effet des UV-C sur la chlorophylle

Suite à une faible irradiation, la teneur en chlorophylle des micro-algues augmente légèrement et directement après l'irradiation, avant de baisser en suivant une cinétique de dégradation dépendante de l'exposition des cellules à la lumière visible (Sztatelman *et al.*, 2015). Cette propriété est utilisée en industrie alimentaire afin de conserver les légumes et de donner une meilleure coloration aux produits en les maintenant à l'obscurité. L'augmentation de la teneur en pigment est expliquée par l'inhibition des enzymes de dégradation de la chlorophylle par les UV-C (chlorophyllase, Mg-dechelatase, chlorophylle peroxidase, etc) (Costa *et al.*, 2006; Jiang *et al.*, 2010; Aiamaor *et al.*, 2010). De plus,

l'obscurité permet de retarder l'apparition des symptômes de sénescence chez *Arabidopsis* tandis que la lumière induit la dégradation de la chlorophylle. La cinétique de dégradation de la chlorophylle est également dépendante de l'intensité en UV-C appliquée sur les cellules (Zvezdanović *et al.*, 2009).

d. Les effets indirects des UV-C

Outre les dommages directs de l'UV-C, des effets indirects ont été décrits, notamment la production d'espèces réactives de l'oxygène (ROS, Reactive oxygen species) conduisant à de multiples dommages dans la cellule. Les ROS sont générées naturellement dans les cellules dans le cadre de leur métabolisme (Slesak *et al.*, 2007), mais peuvent aussi être produites en excès dans le cas de stress oxydatif provoqué par une exposition aux rayons UV (Sjöberg, 2014). En faibles quantités, les ROS sont utiles pour plusieurs mécanismes cellulaires (Höhn *et al.*, 2013) comme dans l'expression des gènes, la lutte contre certains pathogènes (Dickinson et Chang, 2011) et dans des voies de signalisation cellulaires (Ray *et al.*, 2012 ; Jain *et al.*, 2013). Cependant, lorsqu'elles sont en trop fortes quantités, leurs effets deviennent délétères. Les principales cibles des ROS sont :

- Les acides gras polyinsaturés par la peroxydation des lipides (Wang *et al.*, 2015; Borderie *et al.*, 2014), la formation de malondialdéhyde (MDA), des déformations et des destructions des membranes lipidiques (Xu *et al.*, 2006), la déformation des vacuoles, la dilatation, le plissement et la désintégration des membranes des thylakoïdes chez les cyanobactéries, les algues vertes, les algues rouges et les diatomées (Wang *et al.*, 2015; Buma *et al.*, 1995; Meindl et Lütz, 1996; Holzinger *et al.*, 2004). Enfin, Tao *et al.*, (2010) ont montré que les UV-C causent la lyse cellulaire chez *M. aeruginosa*.

- L'ADN est la cible prédominante de l'irradiation UV pour certains micro-organismes comme les cyanobactéries (Xue *et al.*, 2005) entraînant la formation de la deoxyguanosine et de la deoxyadenosine (Marnett, 1999) qui sont mutagènes pour les cellules. Il a également été démontré que les irradiations aux UV-C peuvent entraîner un blocage de la transcription et de la synthèse des protéines dans les bactéries (Sinha et Hader, 2002). De plus, Borderie *et al.* (2014) ont démontré que les UV-C entraînent une fragmentation de l'ADN sur la micro-algue *Chlorella minutissima*.

- Les protéines sont présentes dans tous les systèmes biologiques et à des concentrations particulièrement élevées, ce qui en font des cibles privilégiées de l'oxygène singulet (Davies et Truscott, 2001; Davies, 2003; Davies, 2004; Gracanin *et al.*, 2009). De plus, les constantes de réaction de certaines ROS oxydent les chaînes latérales des protéines (Baraibar *et al.*, 2013) et fragmentent le squelette protéique (Baraibar *et al.*, 2013) car elles sont plus élevées qu'avec la plupart des autres cibles cellulaires (Wilkinson *et al.*, 1995). Tous ces dégâts entraînent la dimérisation/agrégation, le déploiement ou des changements de conformation, l'inactivation enzymatique et des altérations dans l'entretien et le turnover cellulaire (Gracanin *et al.*, 2009; Davies, 2003; Wright, 2003).

e. La mort cellulaire programmée

L'hypothèse de la mort cellulaire programmée est évoquée dans plusieurs publications dont notamment Danon (2000). Des études récentes ont montré que les UV-C provoquent la formation de ROS dans les chloroplastes et les mitochondries (Nawkar *et al.*, 2013) ce qui permet d'induire les caspases des plantes. Ces dernières vont agir sur des gènes provoquant la mort cellulaire programmée (Nawkar *et al.*, 2013).

f. Les mécanismes de protections

Si la plupart des micro-organismes sont sensibles aux UV, la plupart tentent de se protéger via différents mécanismes. Un des mécanismes de protection le plus connu est celui de la synthèse de Mycosporine-like amino acids (MAAs) qui permettent d'absorber et de dissiper le rayonnement UV (Karsten *et al.*, 2007; Karsten, 2008; Lee et Shiu, 2009). De plus, des molécules telles que les xanthophylles et les composés phénoliques sont connus pour leur action antioxydante (Duval *et al.*, 2000; Stahl et Sies, 2003). Les caroténoïdes, par exemple, peuvent agir comme des écrans aux UV-B dans de nombreuses espèces d'algues (Gao *et al.*, 2009). De plus, ils peuvent avoir à la fois une fonction de protection et une fonction antioxydante. Cette dernière a été démontrée pour de nombreuses structures de caroténoïdes (Woodall *et al.*, 1997). D'autres pigments comme la zéaxanthine sont également des protecteurs efficaces contre les UV-B (Sandmann *et al.*, 1998).

Afin de se prémunir d'un excès de ROS, plusieurs mécanismes antioxydants sont mis en place par les cellules comme celui de la synthèse d'enzymes ayant un rôle antioxydant (superoxyde dismutase, glutathion réductase, catalase...) capables d'inactiver et de capturer les intermédiaires réactifs de l'oxygène (Sjöberg, 2014). Ces enzymes et espèces antioxydants ne

sont cependant pas capables d'éviter les dommages oxydatifs (Höhn *et al.*, 2013). Ainsi, d'autres enzymes sont produits afin de réparer les dégâts dus aux oxydants (thiorédoxine réductase, méthionine sulfoxyde réductase...) (Sjöberg, 2014).

En conclusion, les irradiations UV sont efficaces sur une large gamme de molécules (protéines, lipides, ADN) et de métabolismes cellulaires. De plus, il a été montré que les radiations UV les plus efficaces sont les UV-C. En effet, Bolige *et al.* (2005) ont démontré que l'EC50 sur *Euglenia gracilis* due aux UV-C est 13 fois plus élevée qu'avec les UV-B. L'utilisation de la lumière UV-C est donc un outil prometteur dans le traitement des biofilms à condition de démontrer son innocuité sur la matière picturale.

VII. Conséquence des UV-C sur la matière picturale

Depuis la préhistoire, les Hommes ont toujours laissé des traces de leur passage sous forme de peintures, que ce soit de simples empreintes de main, des œuvres d'art, ou des graffitis (Barnett *et al.*, 2006). Les peintures préhistoriques qui ont survécu au temps se localisent principalement dans les grottes, des endroits où le climat était tel, qu'elles n'ont pas ou peu été altérées (Barnett *et al.*, 2006). Après les découvertes des grottes et de leurs peintures, le tourisme a contribué de manière très rapide à leur détérioration, qui pour certaines comme à Lascaux, sont considérées comme des chef d'œuvres de l'art pariétal (Fig. 15) et classées ainsi au patrimoine mondial de l'UNESCO (Oriol *et al.*, 2011).



Figure 15 : Peinture préhistorique de la grotte de Lascaux (Oriol *et al.*, 2011)

1. Composition des peintures

Les peintures sont principalement composées de pigments inorganiques. Ces derniers ont certainement été mélangés avec de l'eau ou des liants organiques comme la salive, le sang, la cire d'abeille ou des matières grasses. Les premiers pigments utilisés ont été prélevés aux abords des habitations et étaient composés d'ocres rouges, jaunes et noires (Barnett *et al.*, 2006) ou d'os d'animaux calcinés (noir d'os). La palette de couleur était restreinte mais a évolué dans le temps avec l'amélioration de la technologie pour la préparation des pigments.

De nombreuses techniques sont actuellement utilisées en laboratoire ou directement sur le terrain afin de déterminer la composition des peintures :

- Diffraction des rayons X (XRD) : permet de connaître la composition cristalline ;
- Infra-rouge à transformée de Fourier (FTIR): permet d'identifier les vibrations caractéristiques d'une molécule organique ;
- X-ray fluorescence (XRF) : permet d'étudier la fluorescence de rayons X de la matière qui sera différent selon la composition de l'échantillon ;
- Microscopie électronique à balayage (SEM): permet d'obtenir des images haute résolution de la surface d'un matériau ;
- Spectrométrie de Raman : permet d'observer et de caractériser la composition moléculaire et de la composition externe d'un échantillon ;
- Émission de photons X induite par particules (PIXE) : permet de déterminer la composition élémentaire des éléments chimiques ;

Toutes ces techniques, pour la plupart non-destructives, sont largement utilisées dans l'étude des peintures préhistoriques des grottes (Edwards *et al.*, 2000; Mortimore *et al.*, 2004; Chalmin, 2006; Beck, 2011; Jezequel *et al.*, 2011; Zucconi *et al.*, 2012; Gomes *et al.*, 2013).

2. Altération des peintures

L'altération des peintures provient principalement de la prolifération des micro-organismes chlorophylliens ou non (Fig. 16) les colonisant. Les algues, cyanobactéries, champignons, lichens, mousses ou encore plantes supérieurs altèrent de manière mécanique ou chimiques les peintures. Le traitement des peintures pariétales peut être effectué par des méthodes chimiques, mécanique (enlèvement manuel des bio-contaminants) ou par laser UV-C. Toutes ces méthodes présentent des risques pour l'intégrité des peintures.

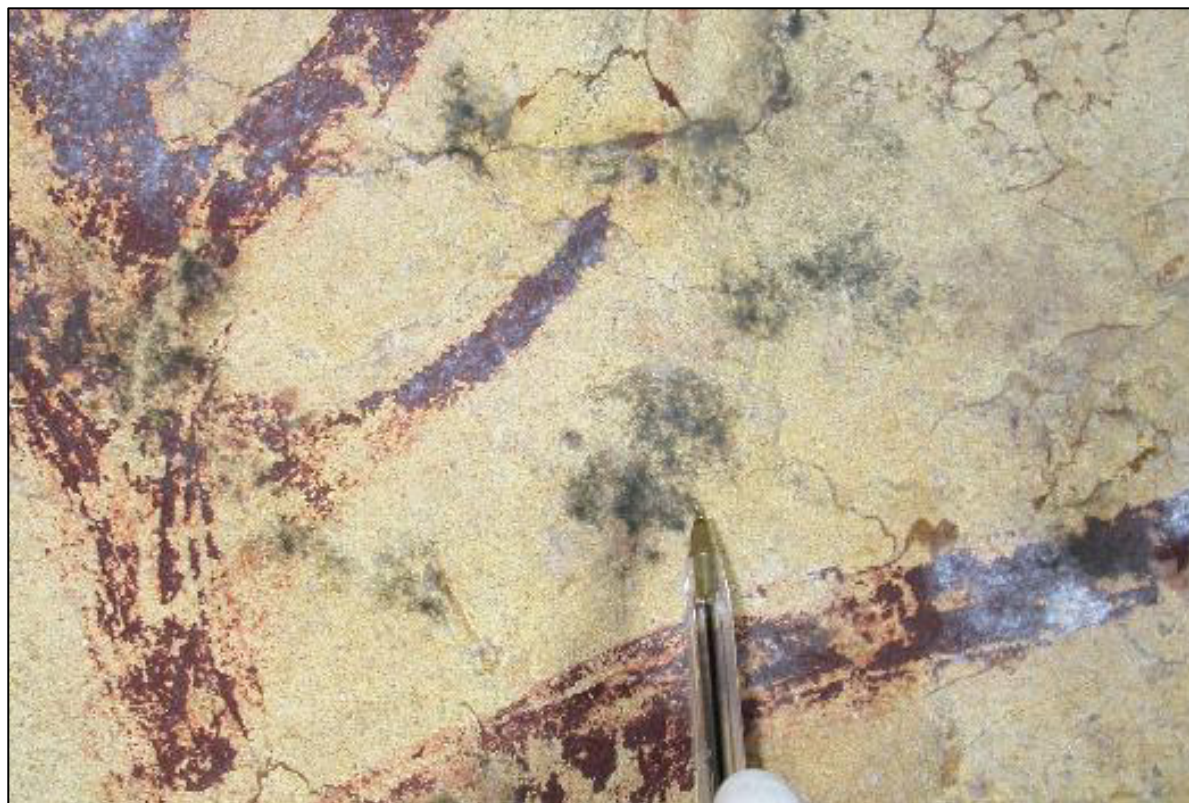


Figure 16 : Prolifération de champignon noir (*Ulocladium* sp. et *Gliocladium* sp.) sur l'une des fresques de la grotte de Lascaux (Oriol *et al.*, 2011).

3. L'effet des UV-C sur les peintures

Dans la littérature, peu d'études sont disponibles concernant l'effet des UV-C sur la matière picturale. Athanassiou *et al.*, (2000) ainsi que Chappée *et al.*, (2003) rapportent un effet négatif de l'utilisation des lasers UV-C sur certains pigments provoquant leur assombrissement. Ceci n'est pas surprenant connaissant l'intensité énergétique d'un laser qui provoque une surchauffe au point d'impact et un réarrangement de la structure cristalline.

Dans l'étude de Borderie (2014), des lampes UV-C (25 W) ont été utilisées. Les résultats obtenus à la DRX montrent que les UV-C (13 heures, 655 kJ m^{-2}) n'ont aucun effet sur les pigments irradiés (noir d'os, ocre jaune, oxyde de manganèse, oxyde de fer rouge et oxyde de fer jaune). Des mesures colorimétriques ont été effectuées sur l'oxyde de fer rouge et l'oxyde de fer jaune après 185 heures d'exposition (9200 kJ m^{-2}), et là non plus aucune différence entre les témoins et les échantillons irradiés n'a pu être mise en évidence.

Schaeffer (2001) a rapporté que « *Seule l'énergie lumineuse absorbée par un matériau peut provoquer un changement photochimique dans ce matériau. Mais l'absorption de la lumière ne garantit pas qu'un changement chimique suivra. Pour considérer l'absorption de l'énergie lumineuse par les substances, la description quantique de la lumière en tant que photons est appropriée. Une molécule absorbe un photon si l'énergie de ce photon est exactement ou très près égale à la différence entre deux états d'énergie de la molécule. Lorsque le photon est absorbé, on dit que la molécule est dans un état électronique excité. Dans cette condition, plusieurs choses différentes peuvent se produire: la molécule peut réémettre l'énergie en fluorescence. L'énergie peut être dissipée sous forme de chaleur. L'énergie peut être transférée à une autre molécule. La molécule peut perdre une fraction particulière de l'énergie et se transformer en un état excité légèrement plus bas, qui émet ensuite l'excès d'énergie restante sous forme de phosphorescence ou dissipe l'énergie restante sous forme de chaleur ; Ou une liaison entre les atomes dans la molécule excitée peut casser. Seule cette dernière possibilité entraîne une modification chimique de la molécule.* »

Si les UV-C n'ont aucun effet sur les pigments, il n'en est pas de même pour les liants utilisés dans la composition des peintures. En effet, la matière organique est sensible aux faibles longueurs d'ondes de la lumière UV-C. Caneva *et al.* (2008) a démontré que des molécules organiques comme la kératine, le collagène et la cellulose sont altérés par les UV-C. Cependant, Gibeau *et al.* (2014) ont montré que les UV-C (15 et 45 W pendant 8 ou 16 heures) n'altèrent pas les liants utilisés dans leur étude (salive synthétique, hémoglobine bovine lyophilisée et cire d'abeille naturelle). Ces résultats sont néanmoins surprenants et ne sont pas en accord avec ceux obtenus dans ce travail de thèse (Chapitre III).

L'utilisation des UV-C comme traitement des biofilms colonisant les peintures semble donc conditionnée à la présence de liants organiques. Or, la présence de liants dans les peintures préhistoriques est controversée (Chalmin, 2003). En effet, les liants organiques ne sont pas stables sur une durée de plusieurs dizaines de milliers d'années notamment les liants composés de graisse animale (Pallipurath *et al.*, 2015). De plus, dans ces milieux oligotrophes les bactéries et champignons hétérotrophes peuvent utiliser cette source de carbone comme nutriment (Cennamo *et al.*, 2016).

Objectifs de la thèse

Ce travail de thèse est la continuité d'une première thèse menée par Fabien Borderie et soutenue en 2014. Cette étude se veut également pluridisciplinaire afin de pouvoir couvrir les principales thématiques de recherche qui sont la biodiversité des biofilms, la physiologie végétale, l'impact des UV-C sur les pigments et les liants, et l'optimisation de l'utilisation des UV-C au laboratoire puis leur application sur le terrain. Ces quatre objectifs ont été abordés au cours de ces trois ans de thèse et sont décrits ci-après.

Objectif 1 : Biodiversité des biofilms

Le premier objectif de cette thèse est de connaître la biodiversité microbienne colonisant la pierre patrimoniale, et en particulier celle des grottes touristiques. Cet objectif permet une meilleure compréhension des organismes s'étant adaptés à des conditions environnementales particulières (faible lumière et température basse). De plus, il permettra également de savoir si la biodiversité des biofilms change suite à une recolonisation après un traitement chimique. L'analyse des communautés bactériennes, autotrophes (algues, cyanobactéries, diatomées et mousses) et fongiques donnera également des informations semi-quantitatives sur la composition du biofilm.

Objectif 2 : Effets des UV-C sur les micro-algues

Le second objectif a pour but la compréhension des réponses physiologiques des micro-algues vertes suite à un traitement aux UV-C (viabilité cellulaire, rendement quantique, dégradation de la chlorophylle, suivi de la photosynthèse, etc), en utilisant comme algue modèle *Chlorella* sp., une espèce dominante composant les biofilms (Grobbelaar, 2000). Les objectifs sont d'apporter des connaissances fondamentales sur les effets des UV-C ainsi que d'optimiser l'irradiation UV-C en déterminant la dose efficace la plus faible applicable lors d'un traitement en condition *in situ*. Une dernière partie sera consacrée à l'étude, en condition de laboratoire, des effets des UV-C sur des champignons microscopiques prélevés sur les sites d'étude.

Objectif 3 : Innocuité des UV-C sur le support rocheux et les peintures rupestres

Dans ce chapitre de thèse, les effets des UV-C seront analysés sur des pigments et des liants utilisés dans la réalisation des peintures à la préhistoire. L'objectif est de démontrer l'innocuité des UV-C vis à vis des parois calcaires de la grotte ainsi que des peintures rupestres. Cet objectif permettra de valider l'utilisation des UV-C comme outil contre la prolifération algale dans les grottes touristiques ornées ou non.

Objectif 4 : Traitement *in situ* des biofilms

Le dernier objectif aura pour but d'appliquer le traitement UV-C sur des biofilms se développant dans les grottes. Ainsi, ce chapitre donnera une réponse claire quant à l'applicabilité et de l'efficacité dans le temps du traitement UV-C en condition *in situ* (grotte de la Glacière). De plus, les UV-C ont été comparées en condition *in situ* (église de Vicherey) aux produits chimiques actuellement conseillés par le Laboratoire de Recherche des Monuments Historiques (LRMH) ainsi qu'à une molécule allélopathique. Enfin, ce chapitre traitera également des champignons microscopiques opportunistes se développant sur la matière organique nécrotique suite aux irradiations UV-C.

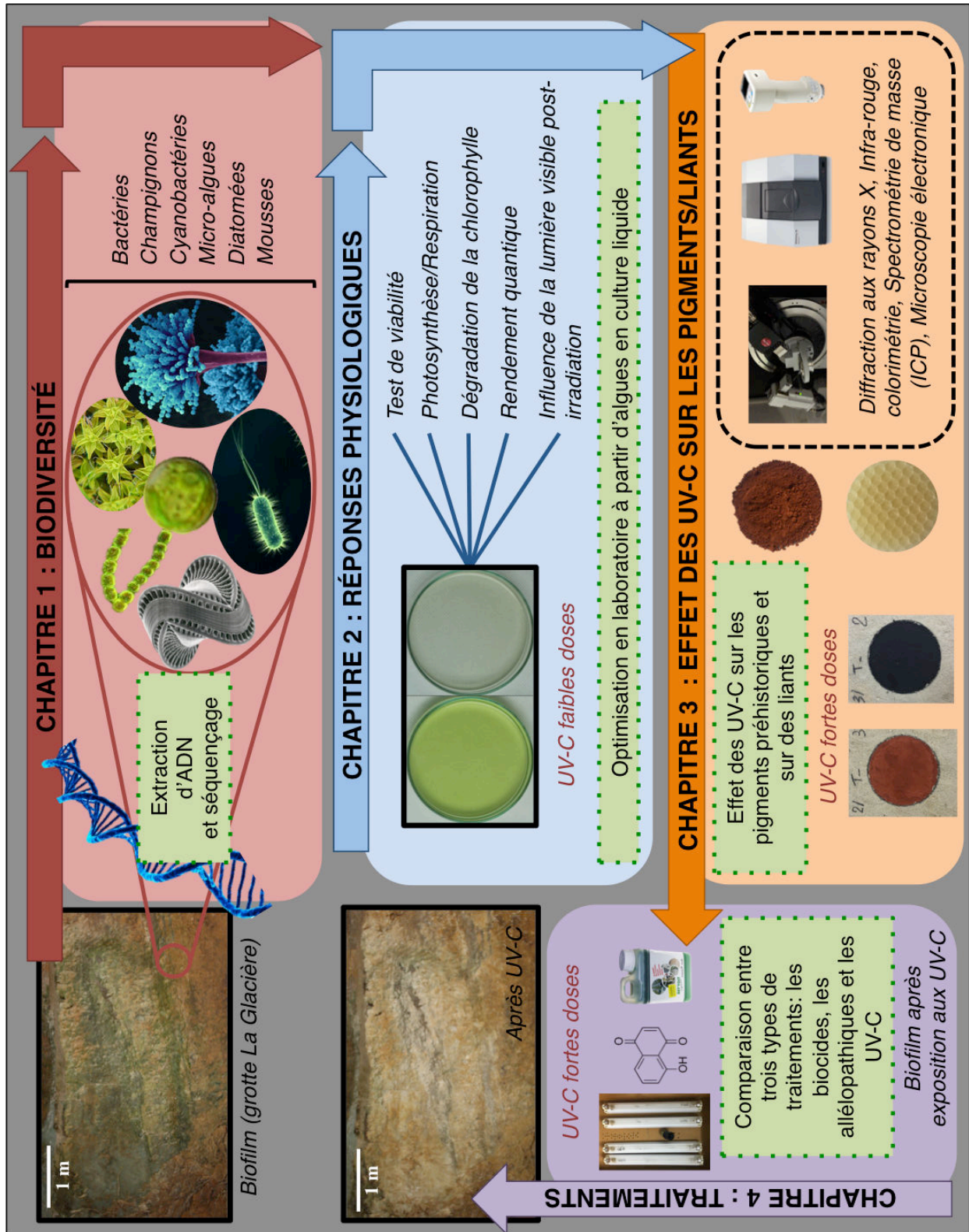


Figure 17 : Schéma représentant les quatre objectifs de la thèse.

Matériel et méthodes

I. Biodiversité des micro-organismes formant les biofilms

Au cours de la thèse, quatorze grottes ont été échantillonnées à travers toute la France et une grotte en Suisse (Fig. 1). Le but de tous ces prélèvements est de répertorier toutes les espèces de micro-algues, de cyanobactéries, de bactéries, de diatomées, de bryophytes et de champignons formant les biofilms. Pour cela, des techniques de cultures en boîte de Pétri et de biologie moléculaire ont été utilisées.



Figure 1 : Représentation des lieux de prélèvements à travers en France et en Suisse.

1. Prélèvements et identification

Lors de cette thèse, deux séries d'échantillonnage ont été menées ; l'une utilisant des techniques classiques pour l'identification des micro-organismes et l'autre une technique de métabarcoding (séquençage haut débit). La première série concerne les grottes de Cravanche, de la Glacière, d'Osselle, des Moidons, d'Arcy-sur-Cure, de la Cocalière, de Clamouse et des Demoiselles, et la seconde les grottes de Réclère, de Blanot, d'Azé (Rivière, Préhistorique), de Soyons (Trou du Renard, Grotte de Néron) et de Saint Marcel.

2. Méthode classique

Les échantillonnages des biofilms ont été effectués à l'aide d'un écouvillon stérile. Directement après le prélèvement, les échantillons sont étalés sur un milieu Blue Green Medium (BG11, Sigma) (additionné par 15 % d'agarose) et Malt Extract Agar (MEA) en boîte de Pétri. Les milieux gélosés BG11 ont ensuite été mis en culture à 20°C et 150 $\mu\text{mol m}^{-2} \text{s}^{-1}$ durant trois semaines. Les cultures, sur le milieu MEA, ont été incubées à 20°C pendant 1 semaine. Les colonies algales et fongiques ainsi obtenues ont été isolées jusqu'à obtention de cultures pures (mono-spécifiques) (Fig. 2).

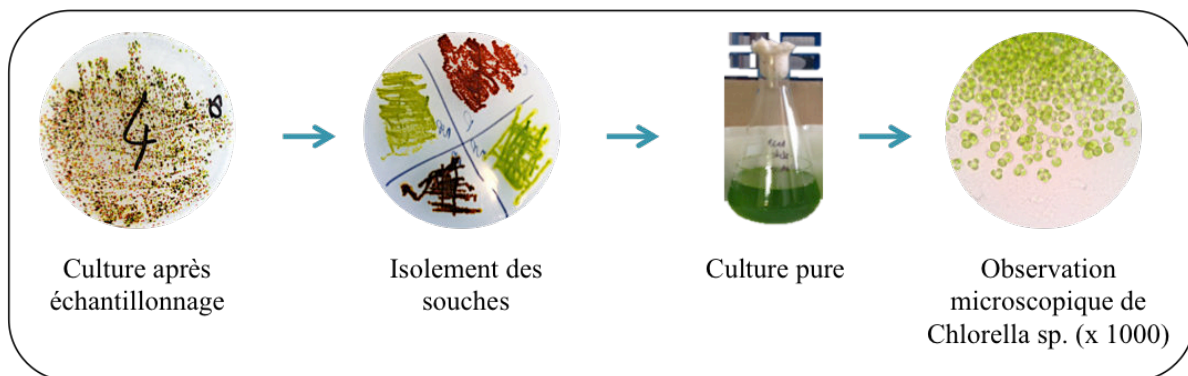


Figure 2 : Isolement de la souche *Chlorella* sp. à partir d'un échantillonnage d'un biofilm photosynthétique se développant sur les parois de la grotte des Moidons.

L'identification des souches algales a été réalisée par microscopie optique. Concernant les 6 souches de champignon, des méthodes de biologie moléculaire (PCR, Séquençage Sanger) ont été utilisées: à partir des cultures fongiques pures, l'ADN a été extrait dans 100 µl d'une solution de Prepman (Thermofisher) chauffé durant 10 min à 95 °C. Après homogénéisation au vortex puis centrifugation à 8000 rpm, 2.5 µl du surnageant a été ajouté à 250 µl d'eau ultra pure. Les échantillons ont alors été stockés à -20 °C. La PCR a été réalisée suivant le protocole ci-après: 25 µl de Mastermix (Thermofisher), 12.5 µl de l'échantillon, 2 µl de primer ITS 1f et 2 µl de primer ITS2, et 8.5 µl d'eau ultra pure (volume total: 50 µl). Les températures de PCR ont été les suivantes: dénaturation initiale à 95°C pendant 5 min, puis 35 cycles de dénaturation (95°C, 30 sec), d'hybridation (61°C, 30 sec), d'extension (72°C, 1 min) et enfin l'extension finale à 72°C pendant 10 min. La PCR a été suivie d'une étape de purification des produits PCR utilisant 2 µl d'exoSAP-IT® (Thermofisher) à 37°C pendant 15 min puis à 80 °C durant 15 min. Le témoin négatif a été réalisé suivant les conditions décrites précédemment en remplaçant l'ADN par de l'eau ultra pure. Le séquençage a été effectué par un séquenceur Sanger 3130 à la plateforme de séquençage. Les séquences d'ADN obtenus ont été comparées à la base de données GenBank.

3. Séquençage haut débit (*Illumina MiSeq*)

Les biofilms (Fig. 3) (entre 100 et 200 mg de matière fraîche) ont été prélevés directement dans un tube de 2,5 ml contenant un réactif de lyse cellulaire. Suite au prélèvement, les tubes ont été congelés dans de la carboglace (-78°C) afin de fixer l'échantillon et de conserver l'ADN. Les échantillons ont ensuite été envoyés à la plateforme de séquençage MicroSynth AG (Suisse) pour un Séquençage Nouvel Génération (NGS) de type Illumina, MiSeq. La plateforme a effectué les manipulations suivantes : *Extraction de l'ADN total, 1^{ère} PCR, 2^{ème} PCR, purification des produits PCR et répartition équimolaire, séquençage*. Le protocole détaillé est joint en Annexe. Suite au séquençage, une analyse bio-informatique des données du séquençage a été effectuée au sein du laboratoire Chrono-environnement et de l'INRA de Dijon (pour les résultats du primer 23S).

Liste des primers utilisés pour le séquençage Illumina:

- Primer bactérien : cible uniquement les bactéries en excluant la plupart des organismes chloroplastiques
 - 16S 799 *f*: 5' -AACMGGATTAGATACCCKG- 3'
 - 16S 1115 *r*: 5' -AGGGTTGCGCTCGTTG- 3'

- Primer fongique : cible uniquement les champignons en excluant les organismes chloroplastiques
 - ITS1 *f*: 5' -CTTGGTCATTTAGAGGAAGTAA- 3'
 - ITS2 *r*: 5' -GCTGCGTTCTTCATCGATGC- 3'

- Primer « chlorophyllien » : cible les organismes autotrophes (algues, cyanobactéries, diatomées, bryophytes)
 - 23S *f*: 5' -GGACAGAAAGACCCTATGAA- 3'
 - 23S *r*: 5' -TCAGCCTGTTATCCCTAGAG- 3'

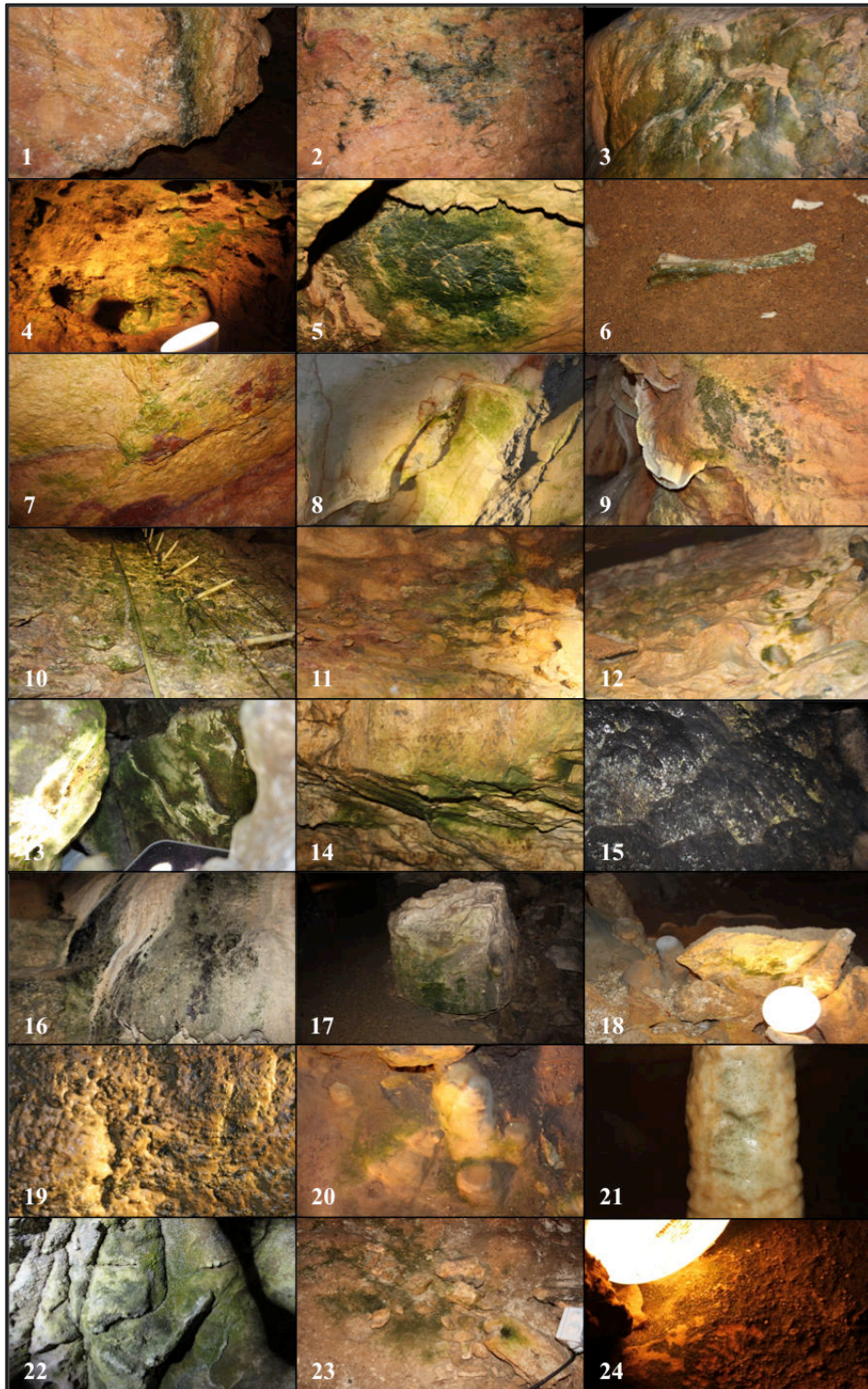


Figure 3 : Photographies de tous les biofilms échantillonnés puis séquencés par la technique de séquençage haut débit de type Illumina par l'entreprise MicroSynth (Suisse). Les biofilms proviennent de la grotte de Blanot (1 à 5), des grottes d'Azé (6 à 12), de la grotte de Réclère (13 à 17), des grottes de Soyons (18 à 22) et de la grotte de Saint-Marcel (23 et 24).

Les prélèvements pour le séquençage ont été effectués dans les grottes suivantes :

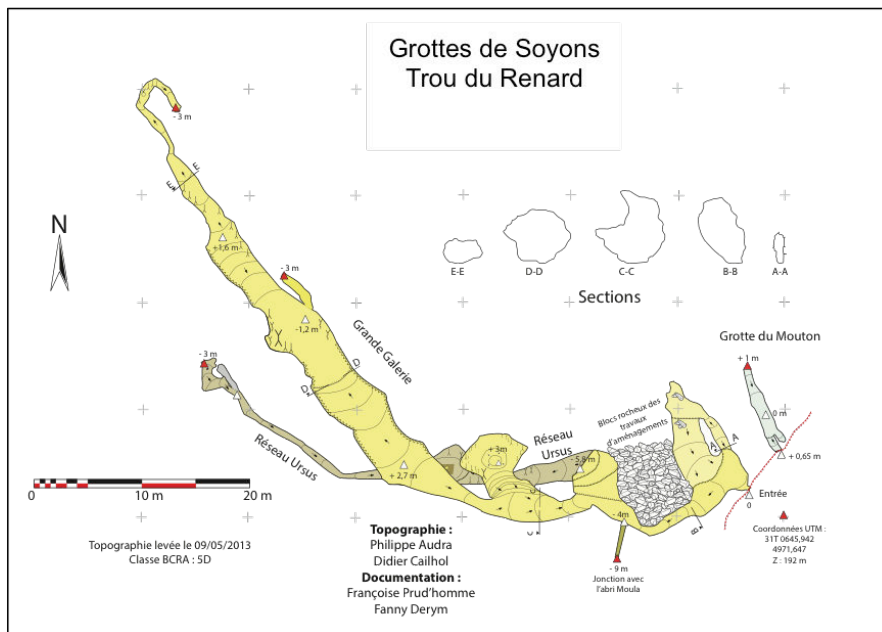


Figure 4: Plan d'une des grottes de Soyons : le Trou du Renard.

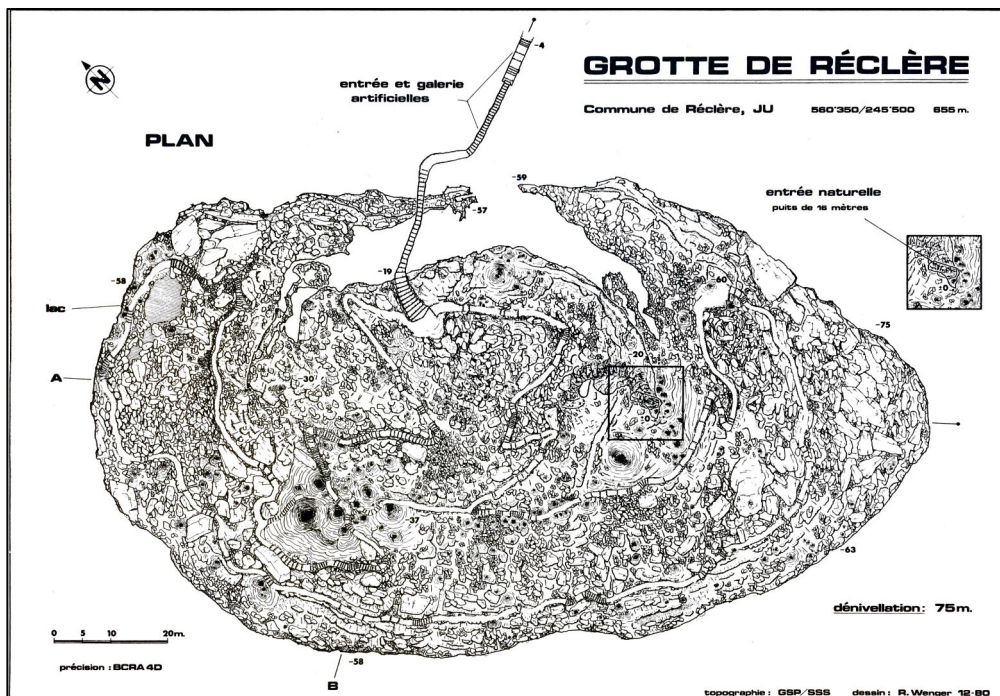


Figure 5 : Plan de la grotte de Réclère.

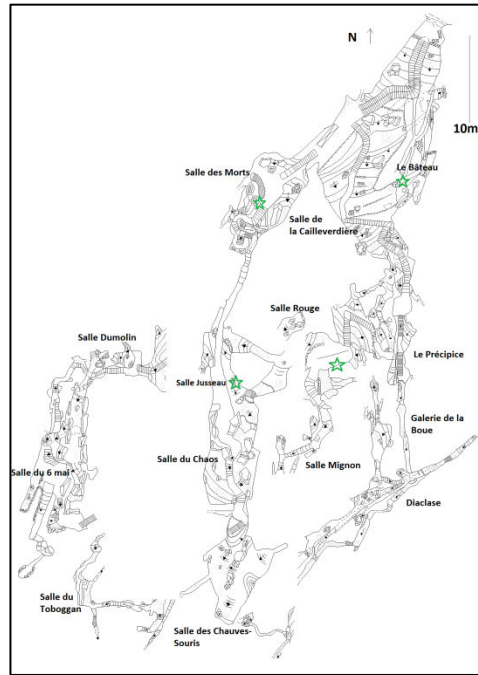


Figure 6 : Plan de la grotte de Blanot.

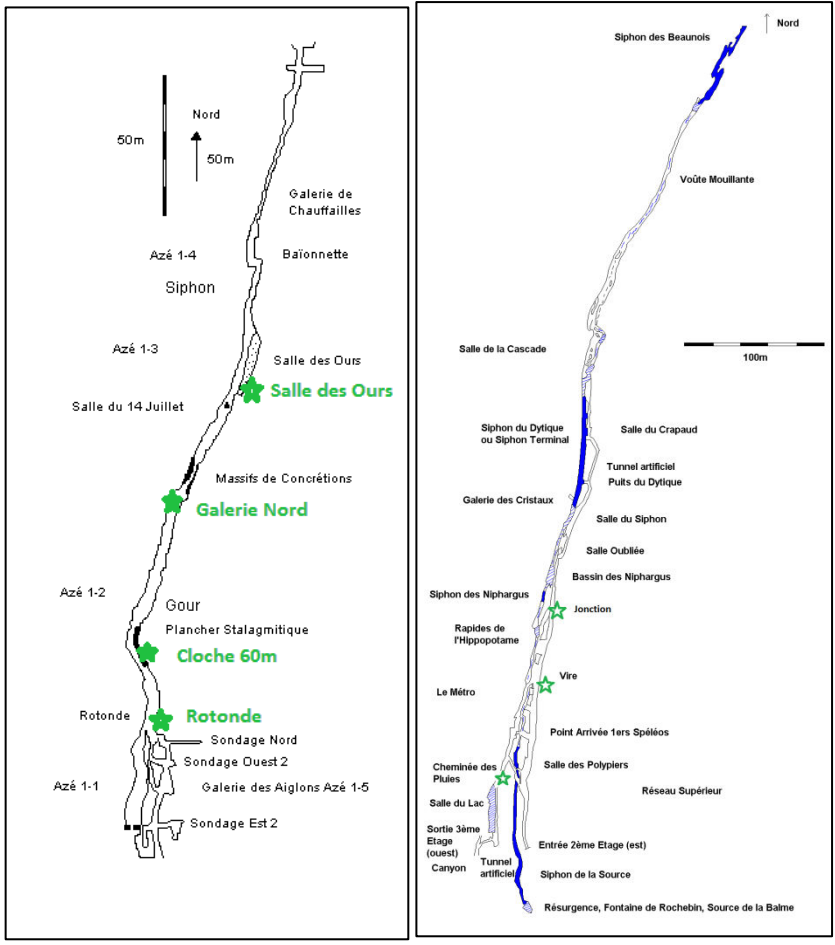


Figure 7 : Plans des deux grottes d'Azé.

II. Les traitements UV-C menés sur le terrain

Deux campagnes de traitements de biofilms ont été menées durant cette thèse. La première s'est déroulée à la Grotte de la Glacière (Chaux-lès-Passavant, 25) (Fig. 8) et la seconde à l'Eglise de Vicherey (Vosges, 88) (Fig. 9 et 10).

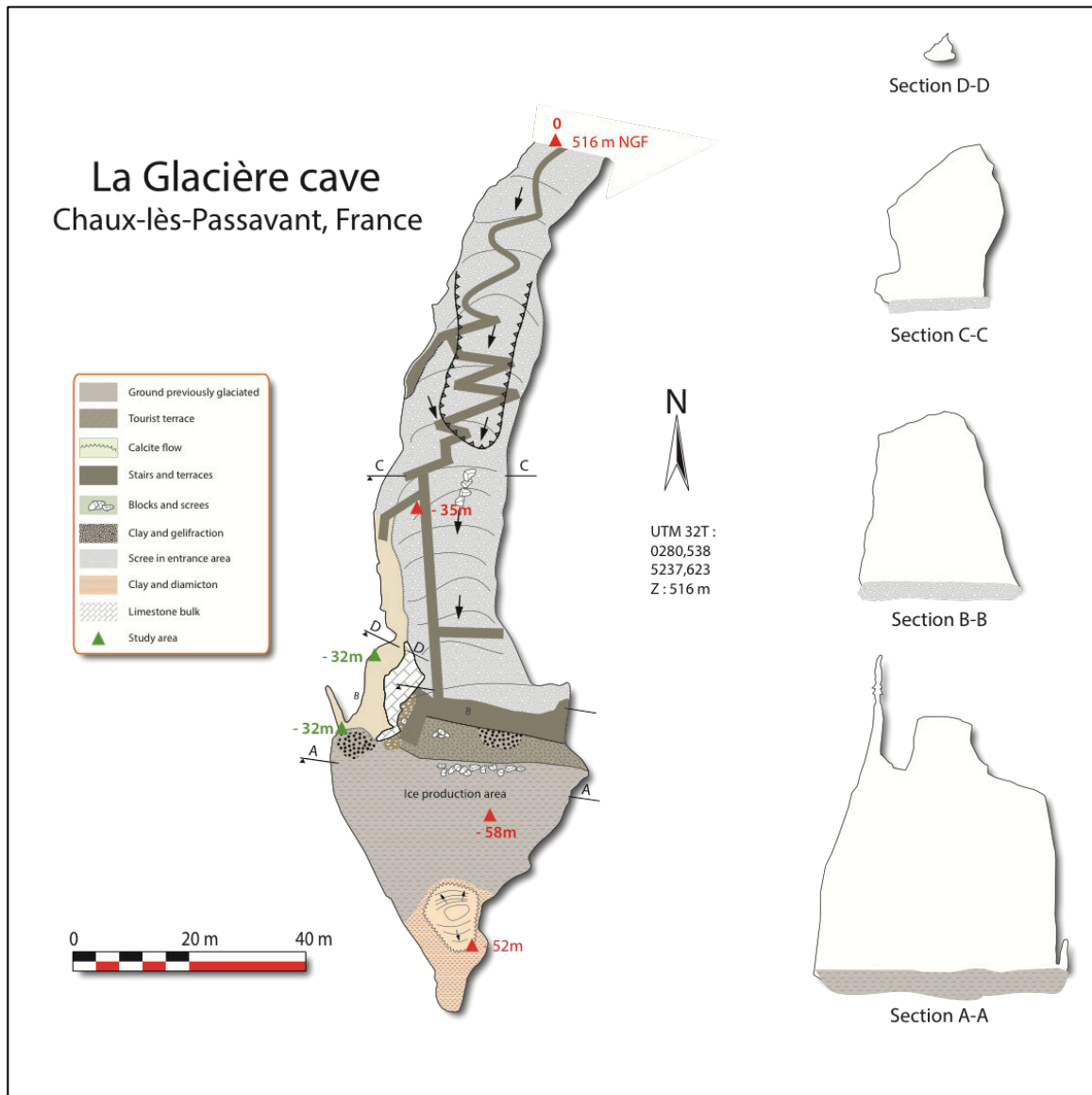


Figure 8 : Plan de la grotte de la Glacière (Dessin : Didier Cailhol et Christophe Gauchon).



Figure 9 : Illustration de l'Église de Vicherey.



Figure 10 : Illustration de l'intérieur de l'Église de Vicherey. Les biofilms algaux et cyanobactériens sont visibles sur le mur de droite.

Matériel et Méthodes

Quatre biofilms ont été irradiés quatre fois pendant 12 heures dans la grotte de la Glacière. D'une taille variable entre 0,7 m² à plus de 12 m², ils se trouvaient à une hauteur comprise entre 2,5 mètres et 4 mètres du sol. Pour cette raison, l'utilisation d'UV-C box (Borderie, 2014) modifiées a été nécessaire. Les box utilisées comprenaient 8 lampes UV-C de 25 W chacune. Elles ont été montées sur une plaque en plexi-glace, elles même fixée à deux poutres de bois de 2,40 mètres de haut. Le tout a été placé sur un échafaudage afin d'irradier les différents biofilms. Les box étaient à 20 cm de distance des biofilms et ont été mises en fonctionnement durant la nuit. Afin de cibler uniquement les zones recouvertes de biofilms, les box ont été recouvertes d'une bâche permettant d'empêcher les fuites de la lumière ultra-violette.

Dans l'église de Vicherey, les biofilms ont été traitées durant 14 heures (646 kJ m⁻²) avec les UV-C box modifiées (Fig. 11) ainsi que celles utilisées par Borderie (2014). De plus, une comparaison avec des produits biocides (Biotin T (3%), Devor'mousse (10%) et Net'toit (3%)) et un produit allélopathique (Juglone, 100 µM) a été effectué sur le mur et le sol de l'église.



Figure 11 : (A) Illustration d'une UV-C box en bois contenant 4 lampes UV-C (Borderie *et al*, 2011). Les box ont été modifiées de manière à considérablement les alléger (utilisation de plexiglass) et de quadrupler la surface traitée. L'ensemble du système a ensuite été mis sur « échasse » ainsi que sur un échafaudage, afin d'atteindre des zones jusqu'à une hauteur de 4 mètres.

1. Mesures colorimétriques des biofilms

La mesure de la couleur des biofilms donne une indication sur la concentration en cellule algale présente au sein du biofilm ainsi que sur le type de micro-algues (cyanobactéries, algues vertes, bactéries, moisissures). CIE $L^*a^*b^*$, souvent abrégé CIE LAB, est un espace de couleur pour la caractérisation des couleurs de surface. Trois grandeurs caractérisent les couleurs. La clarté L^* dérive de la luminance de la surface. Les deux paramètres a^* et b^* expriment l'écart de la couleur par rapport à celle d'une surface grise de même clarté. La composante L^* est la clarté, qui va de 0 (noir) à 100 (blanc). La composante a^* représente une gamme de 600 niveaux sur un axe vert (-300) → rouge (+299). La composante b^* représente une gamme de 600 niveaux sur un axe bleu (-300) → jaune (+299). (Borderie, 2014)



Figure 12 : Illustration du patron utilisé pour les suivis colorimétriques dans la grotte de la Glacière et dans l'Église de Vicherey.

2. Le fonctionnement du PSII

Le fluorimètre (PAM, WALZ, Allemagne) permet de donner des indications sur l'état physiologique des organismes photosynthétiques. Les mesures du rendement quantique (F_v'/F_m') ont été réalisées sur les biofilms (1 mesure par trou en utilisant le patron (Fig. 12)) dans l'église de Vicherey.

3. Mesure des caractéristiques physico-chimiques

D'autres paramètres comme le type d'éclairage, la distance entre le biofilm et les lampes, l'énergie lumineuse reçue par les biofilms, le pH, la température, l'humidité, la distance entre l'entrée de la grotte et le biofilm, le type de traitement, ainsi que le nombre de visiteurs ont été relevés. Une photographie de chaque biofilm permet d'illustrer les résultats obtenus.

III. Les expérimentations menées en laboratoire

Partie A : Effet physiologique des UV-C sur les algues

1. Origine de la souche étudiée

À l'aide d'un écouvillon stérile, un biofilm a été prélevé à la Grotte des Moidons (05° 48' 21.5'' E 46° 50' 20.7'' N). Directement après le prélèvement, une boîte de Pétri contenant un milieu de culture BG11 + agarose (15 %) a étéensemencée. Après trois semaines de culture à 20 °C avec 150 $\mu\text{mol photons m}^{-2} \text{s}^{-1}$ avec une photopériode de 16 heures, les colonies isolées ont été repiquées dans un milieu de culture liquide (BG11). C'est à partir de cette souche, choisie pour ses capacités à se développer rapidement, que toutes les expériences sur les effets physiologiques des UV-C sur les algues ont été réalisées. Des mesures en microscopie optique ont permis de déterminer sa taille (6,7 μm de diamètre). Visuellement, cette micro-algue semble être *Chlorella vulgaris* ; cependant, des analyses ADN (séquençage Sanger) devraient confirmer avec une plus grande précision le nom de l'espèce.

Avant d'être utilisée comme modèle dans le cadre de cette thèse, la souche a été cultivée en milieu liquide, son absorbance a été mesurée, sa masse fraîche pesée et la concentration de la suspension a été mesurée par cytométrie en flux couplée à un comptage à la cellule de Malassez. Les trois paramètres ont ensuite été corrélés afin d'avoir une estimation rapide de la concentration (nombre de cellules par ml) et de la masse de la matière fraîche (mg) grâce la densité optique.

2. Traitement des suspensions algues aux UV-C

Les cellules en phase de croissance exponentielle ont été placées dans des boîtes de Pétri en verre de diamètre 5 cm et agitées avec un agitateur magnétique. Chaque suspension algale est ajustée de manière à avoir une densité optique de 0,3 correspondant à une masse fraîche de 1,88 mg. Tous les traitements ont été effectués à des doses de 0, 2, 4, 6, 8, 10, 20, 30 kJ.m^{-2} à l'aide d'une UV-C box (Philips, 4 x 25 W = 100 W, $\lambda_{\text{max}} = 254 \text{ nm}$). L'énergie

lumineuse des UV-C est contrôlée par un UV-C mètre. Les échantillons ont été placés à 20 cm des lampes et la température a été stabilisée à 20°C (+/- 1°C) grâce à un climatiseur.

3. *Les mesures du rendement quantique et des quenchings*

Une suspension de *Chlorella* sp. a été irradiée à différentes doses d'UV-C (0, 2, 4, 6, 8, 10, 20, 30 kJ.m⁻²). Les répliques (n = 5) ont ensuite été filtrés avec une pompe à vide sur du papier filtre (diamètre 1 cm). Les algues ont été filtrées afin de pouvoir effectuer les différentes mesures qui ne sont pas adaptées en milieu liquide. Après avoir acclimaté les algues durant 30 minutes à l'obscurité, les mesures ont été effectuées. Les algues ont ensuite été placées à la lumière (condition de culture), puis des mesures ont été réalisées toutes les heures. Les mesures ont été effectuées avec le fluorimètre mini-PAM (WALZ, Allemagne).

$$\text{Rendement quantique : } Fv/Fm = (Fm - Fo) / Fm$$

$$\text{Quenching photochimique : } qP = (Fm' - F) / (Fm' - Fo)$$

$$\text{Quenching non photochimique : } qN = (Fm - Fm') / (Fm - Fo)$$

4. *Mesure du spectre de la chlorophylle a et b*

Une suspension de la souche d'algue *Chlorella* sp. a été placée dans des micro-cuves de 1 ml puis leur absorbance été mesurée à l'aide du spectromètre Analytikjena specord 205 sur la gamme de longueur d'onde entre 350 et 750 nm. Après traitement aux UV-C, chaque suspension a été divisée en deux : une première moitié a été placée dans des conditions de culture et l'autre moitié à l'obscurité totale. Chaque jour et pendant 5 jours, les mesures d'absorbance ont été mesurées sur les suspensions dans les deux conditions de culture.

5. *Mesure de l'évolution de la concentration en dioxygène*

L'évolution de la concentration en oxygène a été suivie grâce à un oxygraphe (DW2/2 Electrode Chamber) équipé d'une électrode à oxygène de Clark (S1 oxygen electrode disc, Hansatech Instruments). La calibration de l'électrode a été effectuée avec du sodium métabisulfite de sodium. Ensuite, 2 ml de suspension d'algues (traitées ou non) ont été introduits dans l'oxygraphe sous agitation constante. Durant les 5 premières minutes, la concentration en oxygène a été mesurée à l'obscurité, puis avec de la lumière faible (340

$\mu\text{mol m}^{-2} \text{ s}^{-1}$) pendant les 5 minutes suivantes, et enfin avec de la lumière forte ($980 \mu\text{mol m}^{-2} \text{ s}^{-1}$) durant les 5 dernières minutes. Le logiciel Hansatch a permis de calculer l'évolution de la concentration en oxygène en $\text{nmol O}_2 \text{ min}^{-1} \text{ ml}^{-1}$. Pour cette expérience, les doses d'UV-C utilisées ont été de 0, 2,5, 5, 7,5 et 10 kJ.m^{-2} .

6. *Test de survie cellulaire*

Après avoir irradié les algues, 300 μl de diacetate de fluorescéine (FDA, $\text{C}_{24}\text{H}_{11}\text{O}_7$, 97% pur, ACROS Organics) ont été ajoutés à 400 μl de suspension algale. Un temps de 15 minutes d'incubation a été respecté afin de pouvoir avoir une fluorescence suffisante pour pouvoir être mesurée par le cytomètre de flux ACCURY C6. La poudre de FDA a été diluée dans de l'acétone (99 %) et conservée à -20°C . Lors de l'utilisation du FDA, 40 μl de la solution stock ont été dilués dans 10 ml d'eau distillée. En parallèle du test de survie, les algues témoins et irradiées ont été cultivées sur boîte de Pétri contenant un milieu de culture BG11 + agarose (15 %).

7. *Dosage de la chlorophylle*

Les échantillons ont été centrifugés à 5900 G pendant 5 minutes à 4°C (centrifuge 5415R, EppendorfTM). Les culots de cellules ont alors été repris dans 5 mL de méthanol et ont ensuite été placés à l'obscurité à 4°C pendant 12 heures de façon à optimiser l'extraction. Puis, ceux-ci ont été broyés 5 minutes dans un mortier avec 4 pointes de spatule de sable de Fontainebleau. Les broyats ont été placés à l'obscurité à 4°C durant 1 heure puis ont été centrifugés à 5900 G pendant 5 minutes à 4°C afin de récupérer le surnageant ; tandis que le culot a été lavé une fois en utilisant 4 ml de méthanol. Après lavage, les surnageants obtenus ont été regroupés avec les extraits précédents puis le volume total de solvant dans tous les extraits a été ajusté afin de normaliser les concentrations. Entre chaque utilisation, les extraits ont été stockés à l'obscurité à 4°C afin d'éviter la formation de produits de dégradation. Par la suite, les extraits de pigments ont été analysés par mesure de l'absorbance UV-VIS par balayage spectral de 350 à 750 nm. Les calculs des concentrations en chlorophylle *a* et *b* ont été effectués en utilisant la formule de Lichtenthaler et Wellburn (1983) :

$$[\text{Chl } a] = 15,65 \times A_{666} - 7,34 \times A_{653}$$

$$[\text{Chl } b] = 27,05 \times A_{653} - 11,21 \times A_{666}$$

Partie B : Les champignons

Dans cette partie de la thèse, six souches de champignons microscopiques ont été irradiées de manière à connaître leur sensibilité au rayonnement ultra-violet. Les six souches fongiques ont précédemment été identifiées par séquençage Sanger (Fig. 13).

1. Prélèvement et culture

Deux souches de champignons ont été prélevées dans la grotte de Lascaux par le Laboratoire de Recherche des Monuments Historiques (Paris): *Ochroconis lascauxensis* et *Penicillium* sp.. Dans la grotte de la Glacière, des prélèvements ont été effectués sur les deux plus gros biofilms (« Bio.int » et « Bio.ext ») un an après leur première irradiation aux UV-C. Deux souches ont été identifiées comme étant *Geomyces* sp. et *Rhizomucor* sp.. À l'église de Vicherey des prélèvements ont été effectués sur un biofilm principalement formé de cyanobactéries six mois après une irradiation aux UV-C. Les deux souches isolées correspondent à *Penicillium bilaiae* et *Engyodontium album*.

Dans les deux grottes et l'église, les prélèvements, les isolements et le séquençage des souches ont été effectués selon le protocole décrit dans la section du Matériel et Méthodes intitulé « Biodiversité des micro-organismes formant les biofilms ».

2. Irradiation des champignons

a. Sur une suspension fongique

Afin de déterminer la sensibilité des cellules fongiques aux UV-C, les 6 souches précédemment prélevées et ont été diluées afin d'obtenir +/- 30 UFC par boîte de Pétri, puis les suspensions ont été irradiées à des doses de 2, 10, 20 et 30 kJ m⁻². Directement après irradiation aux UV-C, 100 µl de suspension ont été étalés sur le milieu Malt Extract Agar (MEA) et maintenus à 20°C durant une semaine. La capacité des champignons à croître sur un milieu irradié aux UV-C a également été évaluée sur un milieu de culture préalablement irradié à une dose 100 kJ m⁻², puisensemencé avec les 6 souches de champignons utilisées dans cette étude.

b. Sur des spores

Les spores ont été prélevées à l'aide d'un ruban adhésif sur une colonie en sporulation (présentant des spores), déposées sur une gélose MEA, irradiées à 30 kJ m^{-2} et incubées durant 2 semaines.

c. Sur des colonies fongiques

Le milieu MEA a étéensemencé avec chaque souche provenant d'une culture jeune de 4 jours afin d'obtenir 30 UFC par boîte de Pétri. Les colonies isolées ont été repiquées sur un milieu frais puis irradiées à 30 kJ m^{-2} . La taille des colonies exposées aux UV-C a été suivie durant une semaine et comparée aux cultures témoins. Afin de mieux mettre en évidence les effets des UV-C sur la structure de la colonie de *Rhizomucor* sp., un nouveau lot de cette souche a été irradié à 2 reprises et à 2 jours d'intervalle.

d. Sur un tapis fongique

Afin de reproduire une prolifération fongique qui se rapproche le plus des conditions de grotte, en termes de structure colonie, 2 ml du milieu MEA ont été étalés sur des blocs de tuf (25 cm^2) et ces derniers ont étéensemencés avec les 6 souches de champignons. Les blocs sont placés dans des boîtes de Pétri et sont régulièrement humidifiés avec de l'eau distillée stérile. Après une semaine de culture à température ambiante, les tapis fongiques ainsi obtenus ont été irradiés 4 fois à une dose de 555 kJ m^{-2} en respectant une semaine d'intervalle entre chaque irradiation. Des cultures témoins ont été préparées dans les conditions précédemment décrites.

Toutes les quatre manipulations ont été réalisées en 3 répliques chacune.

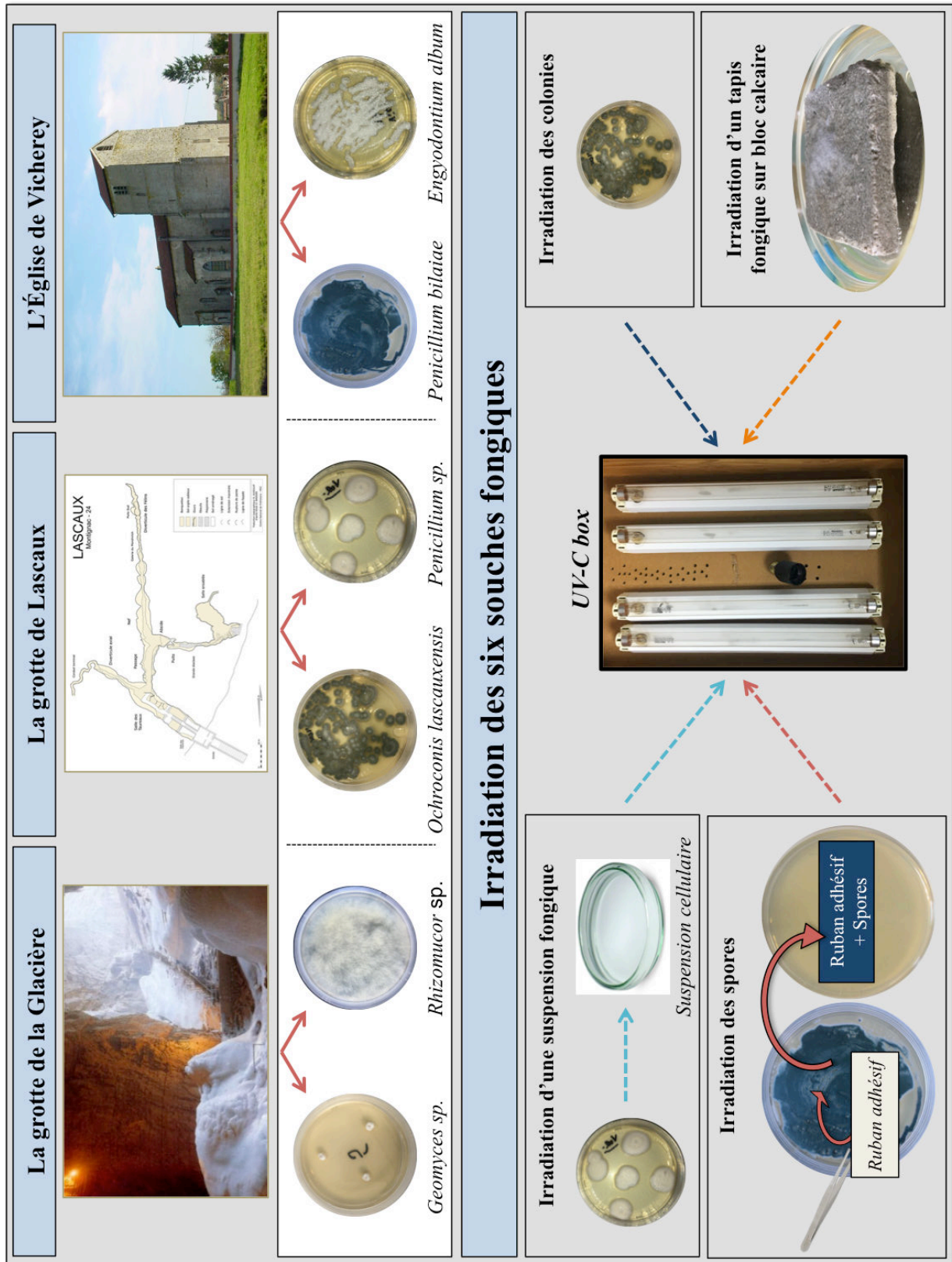


Figure 13 : Protocole expérimental des différentes irradiations effectuées sur les six souches de champignons.

Partie C : Effet des UV-C sur les pigments et liants

1. Les effets des UV-C sur les pigments et les liants

Durant ce travail de thèse, cinq pigments et deux liants utilisés par les Hommes préhistoriques ont été analysés afin de connaître les éventuels effets d'une irradiation aux UV-C sur leur structure chimique. Six techniques ont été utilisées : (i) la spectrométrie infra-rouge, (ii) la diffraction des rayons X, (iii) la colorimétrie, (iv) l'ICP, (v) la microscopie électronique à balayage et (vi) X-ray microanalysis .

2. Technique d'infra-rouge à transformée de Fourier

Les cinq pigments ont été broyés en une fine poudre puis mélangés équitablement avec de la poudre de KBr préalablement déshumidifiée. Le mélange a ensuite été pastillé à l'aide d'une presse mécanique. L'échantillon a été placé sur la platine diamant du banc ATR (Single Reflexion Attenuated Total Reflectance) et analysé par un spectromètre à transformée de Fourier (IRAffinity-1, Shimadzu) et 30 lectures ont permis d'obtenir les résultats bruts. Les liants ont été analysés avec le spectromètre Perkin-Elmer Spectrum 100-400 du Laboratoire de Recherche des Monuments Historiques. Les échantillons ont été pressés par une presse préalablement nettoyée avec de l'éthanol ultra-pur. Comme les pigments, 30 lectures de l'appareil ont fourni les résultats bruts.

3. Technique de diffraction aux rayons X

Les 5 pigments ont été répartis dans des boîtes de Pétri. La moitié des échantillons a été exposée aux UV-C (8 x 25W soit 200W) pendant 62 heures. Les pigments ont ensuite été broyés avec l'aide d'un mortier et d'un pilon en agate, puis placés sur une lame en verre creuse placée dans le diffractomètre Bruker D8 Advance Lynx Eye Detector (Tube au cobalt $\lambda_{K\alpha 1} \approx 1,789 \text{ \AA}$) automatisé (Fig. 14). Le balayage va de 0 à $70^\circ 2\theta$ à la vitesse de $0,005^\circ$ par seconde. Les diffractogrammes obtenus sont tracés sur le logiciel Diffrac Plus Measure puis interprétés sur le logiciel Diffrac Plus Eva.

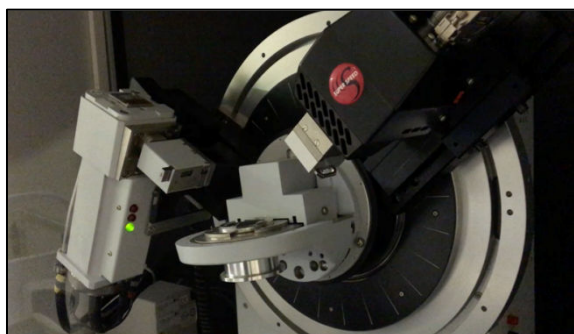


Figure 14 : Photographie du diffractomètre à rayon X (LRMH, Paris).

4. Microscopie Electronique à Balayage (MEB)

Les photos et les analyses EDS ont été effectuées avec le microscope JEOL 5510 couplé à un module SamX 30 mm² EDX. Les mesures ont été effectuées sous vide (24 kV) et à une distance de travail de 21 mm. Les échantillons ont été fixés avec un scotch carbone et ensuite recouvert avec 20 nm de carbone par sublimation thermique.

5. Inductively Coupled Plasma (ICP)

Les pigments ont été analysés avant et après exposition aux UV-C. Les éléments chimiques présent dans la composition de 0.25 mg de chaque pigment (AL, As, B, Ca, Cd, Co, Cr, Cu, Fe, Hg, K, Mg, Mn, Na, Ni, P, Pb, S, Sb, Se, Si, Sn, Sr, Ti et Zn) ont été dosés par ICP-AES après minéralisation dans 1 ml HNO₃ et 2.5 ml de HCl dans un minéralisateur Digiprep. Les échantillons ont été dilués dans de l'eau ultra-pure (qsp 25 ml) et ont été ensuite filtrés avec un filtre de 1 µm. Le « Loamy Clay » est l'échantillon référence qui a été utilisé dans ce protocole.

Partie D : Croissance microbienne sur les pigments

Mise en place du dispositif

Une expérience en laboratoire a permis de démontrer la croissance des micro-organismes et des bryophytes sur les peintures rupestres (Fig. 15) suivant le protocole suivant : des blocs de tuf ont été peints avec un mélange composé de 2 g de pigment et de 20 ml d'eau (n=3). Les blocs ont ensuite été déposés sur de la vermiculite afin de garder une humidité constante. L'expérience a été menée dans une salle de culture à 15°C, 100% d'humidité et avec une photopériode de 16 heures. Aucun ensemencement des blocs n'a été effectué ; la colonisation des blocs provient uniquement des spores/bactéries/algues provenant de l'air (climatisation ou courant d'air). Après 73 jours, les blocs n'ont plus été humidifiés afin de simuler une période sèche. L'humidification des blocs a été reprise une semaine plus tard et jusqu'à la fin de l'expérience qui aura duré 10 mois. Les paramètres (température, humidité et éclairage) ne correspondent pas à ceux des grottes, mais permettent d'observer la croissance des micro-organismes et des bryophytes de manière plus rapide.

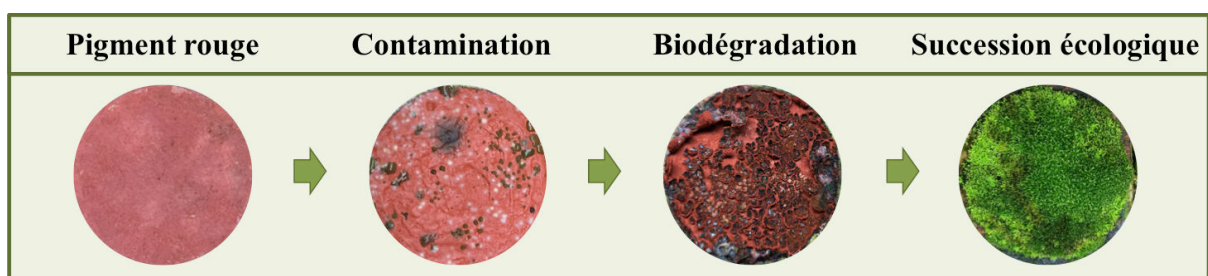


Figure 15 : Illustration de la contamination de la peinture par les algues, les champignons, les cyanobactéries et les mousses. Tous ces organismes provoquent une biodétérioration de la peinture.

Chapitre 1 : Analyse de la biodiversité microbiennes formant les biofilms dans les grottes touristiques.

Ce premier chapitre présente les premiers résultats obtenus suite à la campagne de prélèvements de biofilms effectuée dans cinq grottes en France et en Suisse (les grottes d'Azé [2 grottes], la grotte de Blanot, la grotte de Réclère (Suisse), la grotte de Soyons). L'analyse des communautés de bactéries, de cyanobactéries, de micro-algues, de diatomées, de champignons ainsi que les mousses composant les biofilms photosynthétiques y sont décrites. Les communautés sont ensuite analysées en fonction des paramètres environnementaux des grottes.

Ce chapitre est rédigé sous la forme d'un article scientifique et soumis dans *Science of the Total Environment*.

Biofilm biodiversity in French and Swiss show caves using the metabarcoding approach: first data

Stéphane Pfendler ^{a*}, Battle Karimi ^b, Pierre-Alain Maron ^b, Lisa Ciadamidaro ^a, Benoît Valot ^a, Faisal Boustia ^c, Laurence Alaoui-Sosse ^a, Badr Alaoui-Sossé ^a and Lotfi Aleya ^a

^a Laboratoire Chrono-Environnement – UMR CNRS 6249, Université de Bourgogne Franche-Comté Besançon

^b Institut National de Recherche Agronomique (INRA), UMR1347 Agroécologie, BP 86510, F-21000 Dijon, France

^c Laboratoire de Recherche des Monuments Historiques (LRMH)– CRC-USR 3224, Champs-Sur-Marne.

Abstract

In recent decades, show caves have begun to suffer from Lampenflora proliferation due artificial lighting installations for touristic activity. In addition to the aesthetic problem, light encourages microorganisms that are responsible for physical and chemical degradation of limestone walls, speleothems and prehistoric paintings of cultural value. Lampenflora have previously been described by microscopy or culture-dependent methods, but data provided by new generation sequencing are very scarce. The authors identified for the first time Lampenflora proliferating in one Swiss and four French show caves using three different primers. The results showed that both photosynthetic and non-photosynthetic bacteria were the dominant taxa present in biofilms. Microalgae were heavily represented by the *Trebouxiophyceae*, *Eustigmatophyceae* and *Chlorophyceae* groups. Twelve diatoms were also recorded with dominance of *Syntrichia* sp. (96.1%). Fungi were predominantly represented by *Ascomycota*, *Zygomycota*, *Basidiomycota*, half of the sampled biofilms where Fungi were detected. Comparing microbial communities in bleach-treated to untreated caves showed no significant difference except for a low change in the abundance of certain taxa. These findings provided by Illumina sequencing reveal a complex community structure in the 5 caves based on the assembly of bacteria, cyanobacteria, algae, diatoms, fungi and mosses.

Key words: Metabarcoding, Caves, Conservation, Biodiversity, Biofilm

I. Introduction

Caves have always commanded a special interest for human beings. Already used by prehistoric humans, some of them were decorated with parietal paintings, the oldest dating back 40,000 years [1]. The oldest human presence (Neanderthal Man), however, was discovered in Bruniquel Cave (France) and dates back 176,500 years [2]. Caves are currently places of both paleo-anthropological and archaeological discoveries, but also of tourism. Natural caves were first opened to tourists over 400 years ago [3]. Nowadays, there are 800 tourist caves in the world [4] visited by 250 million tourists per year [3] and generating 2.3 billion US dollars per year [5].

In order to accommodate tourists, improvements have been made in caves, such as lighting and access ways [6] which deeply alter cave ecosystems [7]. For instance, the increase in carbon dioxide, temperature and lighting [8,9] has allowed the proliferation of unwanted photosynthetic microorganisms, also called Lampenflora [10,11], which assemble in structurally complex biofilms [12]. These microorganisms are highly competitive and can proliferate at very low light intensity: $1 \mu\text{mol photon m}^{-2} \text{ s}^{-1}$ [13]. Besides the esthetic appearance due to the presence of green, brown or black spots [14,15,16,17], Lampenflora lead to biodeterioration of limestone [11,18,19,20] and thus damage prehistoric paintings [21] by altering the mineral structure of the rock [17,22]. For example, cyanobacteria and microalgae exhibit a capacity to produce carbonic acid during respiration [23], inducing limestone dissolution. In addition, they produce organic acids [24,25] that may degrade rock, speleothems [24] and prehistoric paintings [21] as observed in the Lascaux Cave [26]. In some cases, biofilm cleaning becomes impossible since Lampenflora are trapped within the limestone [25].

Therefore, and in an effort to diagnose the biodeterioration processes and to implement control strategies and appropriate treatments [17,27], it is important to study the diversity and structure of biological communities that colonize stone formations. Many authors have investigated the diversity of epilithic organisms by means of microscopic observations inside caves [25,28,29,30]. However, some microalgae cannot be clearly distinguished due to similar morphology, simple ultra-structure, similar pigment composition and cell wall structure [31]. Other researchers have taken samples of biofilms by scalpel [32], toothbrush or tape [25], and then cultured them on agar plates for identification. Community fingerprinting methods such as Ribosomal Intergenic Spacer Analysis (RISA) [33], Random Amplified Polymorphic DNA (RAPD) [34] or Denaturing Gradient Gel

Electrophoresis (DGGE) [35] have also been used. More recently, cloning followed by Sanger sequencing [36,37,38], has proven to be a more reliable method to approach Lampenflora diversity. Most of these techniques are culture-dependent methods, useful in understanding the physiological and biochemical potential of isolated organisms, yet they exhibit a weakness since it is well known that only a few microorganisms can grow in a synthetic medium [38,39,40,41,42,43]. Consequently, they do not provide accurate information as to the diversity of complex microbial communities [44].

New generation sequencing (NGS) appears to fill the gap since it can detect a large spectrum of prokaryotes and eukaryotes including bacteria, fungi and bloom-forming phytoplankton, both in freshwater [45,46,47] and marine [48] ecosystems. However, only limited NGS data are available concerning show caves, and those that do exist: 1) never include the simultaneous identification of bacteria, fungi, cyanobacteria, micro-algae, diatoms and mosses, and 2) have not investigated the many show caves having different characteristics and locations. In addition, up to now, no reports have appeared on the molecular characterization of microorganism-form biofilms by applying metabarcoding via high-throughput sequencing.

We thus investigated the biofilm community structure in 4 show caves in France and 1 in Switzerland using the metabarcoding approach. We also used, for the first time, three primers to study the community structure of Eubacteria (16S), Fungi (ITS), Cyanobacteria (23S), Chlorophyta (23S), Bacillariophyta (23S) and Bryophyta (23S). For each of the 5 caves, biofilm composition and diversity were described and compared to each of the other caves. In addition, biofilm diversity was compared between bleach-treated and untreated caves.

II. Materials and methods

1. Site description

Twenty-one biofilm samples were collected in October 2016 in 1 Swiss and 4 French show caves (Fig. 1). The first, Réclère Cave (Switzerland), was discovered in 1890. Located in western Switzerland, 655 m a.s.l., it is app. 145 m long, 83 m deep and 75 m high, and receives 25–30,000 tourists each year. Biofilms have been treated almost every year with diluted sodium hypochlorite. Five biofilm samples were taken here.

In Blanot Cave, 5 biofilm samples were taken. Located in eastern France (395 m a.s.l., 75 m long, 45 m wide), it is visited by approximately 5,500 visitors each year. Blanot Cave has never been treated against biofilms. This was not the case of the two caves at Azé which are visited annually by 28,000 visitors. The first (Azé-prehistoric) is 300 m long and 20 m wide at its widest. The second (Azé-river) is 633 m long and 26 m wide. Both are located 275 m a.s.l. Twelve biofilm samples were taken in the 3 caves; 5 in Blanot Cave and 4 and 3 for Azé-prehistoric and Azé-river, respectively.

The Soyons Caves, discovered at the end of the 19th century, are famous for their pre-history and are visited by 13,000 tourists every year. Like Réclère Cave, the Soyons Caves have been treated with sodium hypochlorite. The “Trou du Renard” is one of the Soyons caves, where we collected 4 samples.

It is noteworthy that 20 of the 21 studied biofilms from these caves combined were taken from limestone rock. In fact, the 21st was taken from a 160,000-year-old *Ursus deningeroides* bones found in Azé-prehistoric.

2. Sampling

Samples were collected in different parts of each cave (Table 1). In accordance with the sequencing platform (Microsynth AG, Balgach, Switzerland), 100 to 200 mg of fresh matter was taken from each biofilm. In order to avoid unwanted contamination, samples were directly collected in 2-ml tubes (MicroSynth AG) containing balls for mechanical lysis and subsequently kept on dry ice (-78°C) for the three days of sampling. Samples were then conserved by MicroSynthAG at -20°C until total DNA extraction, amplification steps and sequencing.

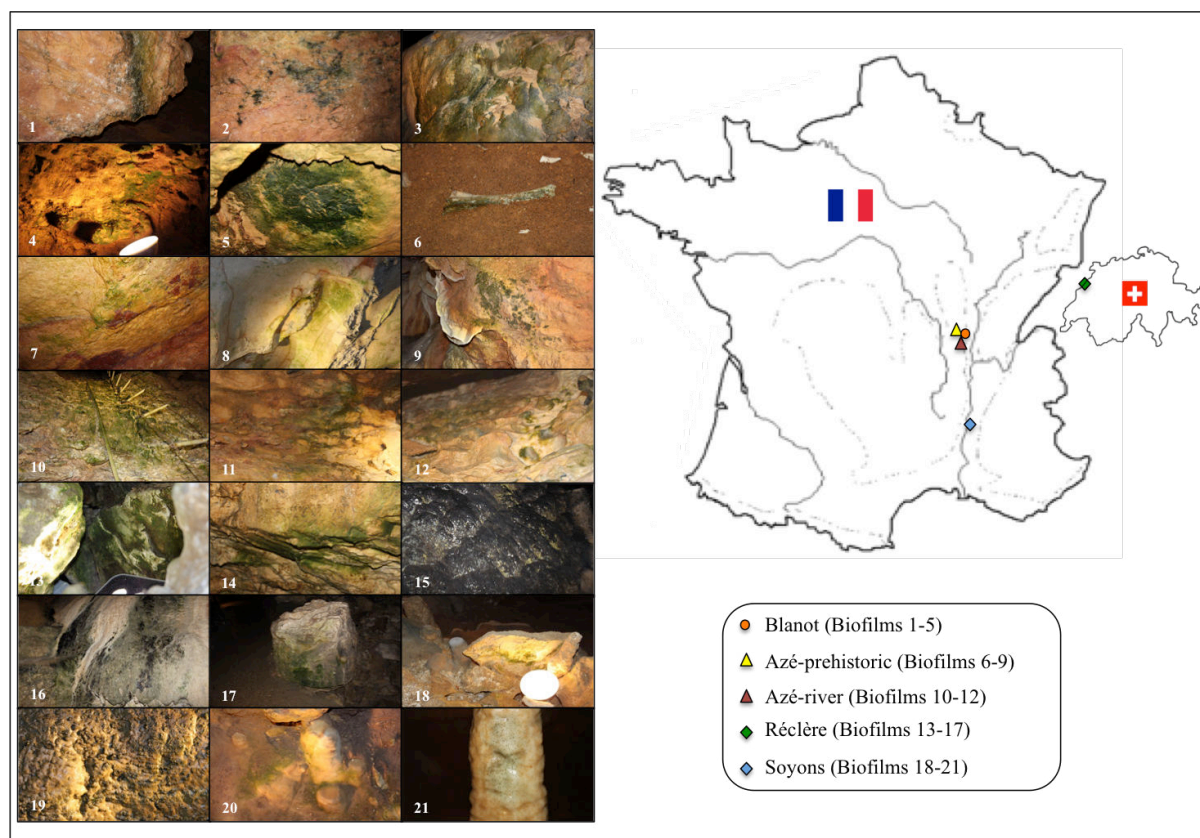


Fig. 1: Illustration of all the sampled biofilms in the five caves. Cave localizations are shown with colored triangles, rounds and squares.

3. *Environmental parameters*

Eleven environmental parameters were measured in each cave and are reported in Table 1. Temperature and moisture were measured with a HOBO® data logger. Light intensities were measured with a light meter (Li-250A, Licor, Lincoln, Nebraska), as well as the distance between biofilm and lamp type. Also reported were the distance between the cave entrance and the biofilms, the number of tourists per year, biofilm treatment type and altitude/latitude.

Biofilm colorimetric parameters were measured with a spectrophotometer (CM-600d KONICA MINOLTA, illuminant D65, SCI mode and 8 mm diameter target mask). Color measurements were analyzed according to the CIELAB color system. The dark-light scale (L^*) is associated with the lightness of the color and ranges from bottom (value: 0, black) to top (value: 100, white). The a^* and b^* scales are associated with changes in redness-greenness (positive a^* is red and negative a^* is green) while changes in yellowness-blueness

(positive b* is yellow and negative b* is blue) [49]. Finally, biofilm quantum yield (F_v/F_m) was measured using a fluorimeter Mini-PAM (Walz[®], Germany).

4. Sequencing

DNA sequencing was performed on an Illumina MiSeq device according to standard protocols. Polymerase chain reaction (PCR) amplifications were performed with the primers p23SrV_f1 (5'-GGACAGAAA- GACCCTATGAA-3'), p23SrV_r1 (5'-TCAGCCTGT-TATCCCTAGAG-3') (Sherwood and Presting, 2007; Marcelino and Verbruggen, 2016), ITS1 f (5' -CTTGGTCATTTAGAGGAAGTAA- 3'), ITS2 r (5' -GCTGCGTTCTTCATCGATGC- 3') [50], 16S 799 f (5' -AACMGGATTAGATACCKG- 3') and 16S 1115 r (5' -AGGGTTGCGCTCGTTG- 3').

5. Data analysis

Reads were assigned to each sample according to a unique barcode. Paired reads were grouped on a contig using the Mothur pipeline [51]. An *in silico* PCR kept only reads containing the used forward and reverse primer, except for the reverse primer for fungi, whereas the 18S motifs sequence was sought on contigs using HMMER software. Reads were then filtered by length, quality, homopolymer and unknown base. For ITS and 23S generated sequences, the contigs were pre-clustered at 100% identity; 99% for bacteria (16S). Rare sequences represented by less than 10 reads for 16S and 23S, and less than 5 reads for ITS primer, were removed from the analysis. The 16S, ITS and 23S taxonomic assignments were performed using Silva Seed v123, UNITE v6 and the database of the *Institut National de Recherche Agronomique* (INRA) (Dijon, France) (data unpublished), respectively. Operational taxonomic units (OTUs) were then constructed using the Needleman-Whunch distance and average neighbor clustering (UPGMA) at a distance of 0.03, 0.03 and 0.05 for 16S, ITS and 23S primer sequences, respectively. The number of reads per sample was calculated after a random sub-sampling of 10,000 reads.

Reads were assigned to each sample according to a unique barcode, and contigs were then assigned using the Mothur pipeline [51]. An *in silico* PCR kept only reads containing the used forward and reverse primer. Adaptors were later removed to maintain amplified region. However, for fungi reads, no PCR took place on the reverse primer, whereas forward sequences were compared to the end of 18S sequences database using HMMER software. Reads were then filtered by length and quality; artifactual sequences, such as photopolymers, were removed. For ITS and 23S generated sequences, the reads were pre-clustered at 100%

identity; 99% for bacteria (16S). Rare sequences represented by less than 10 reads for 16S and 23S and less than 5 reads for ITS primer were removed from the analysis. The 16S, ITS and 23S taxonomic assignments were performed with Silva Seed v123, UNITE v6 and using the INRA database (Dijon, France) (data unpublished), respectively. The OTUs were constructed using the Needleman distance and average neighbor clustering (UPGMA) at a distance of 0.03, 0.03 and 0.05 for 16S, ITS and 23S primer sequences, respectively. The number of reads per sample was calculated after a random sub-sampling of 10,000 reads.

6. *Species diversity*

Specific diversity was expressed with the Shannon and Weaver [53] index.

$$H = - \sum_{i=1}^s ni/N \log_2 ni/N.$$

ni/N : frequency of species i in the sample

s : number of species of the community.

The evenness J was proposed by Pielou [54] to prevent weighting of H index by rare species and is expressed as.

$$J = H/H_{\max}$$

Where

$$H_{\max} = \log_2 s$$

s : number of species of the community.

7. *Statistical analysis*

All statistical analyses were performed using R software v. 1.0.136 (R Development Core Team, 2016) at the significant level of 0.05. Environmental parameters were analyzed using Principal Component Analyses (PCA). An ANOVA test was performed to compare total species diversity difference between the caves. Finally, an analysis of similarity (ANOSIM) test was performed on the non-metric multidimensional scaling (NMDs) analysis.

III. Results

1. Cave environmental parameters

Table 1 summarizes the environmental parameters in the five sampled caves. The PCA (Fig. 2), illustrates that the cave environments were statistically different from each other by 71% ($p\text{-value} < 0.001$). In fact, both temperature and light intensity were correlated in the Soyons Cave, while moisture, quantum yield and distance from the entrance to the biofilm were highly correlated in both caves at Azé. Finally, Réclère Cave was correlated with the altitude. None of the other parameters showed any clear differences among the five caves.

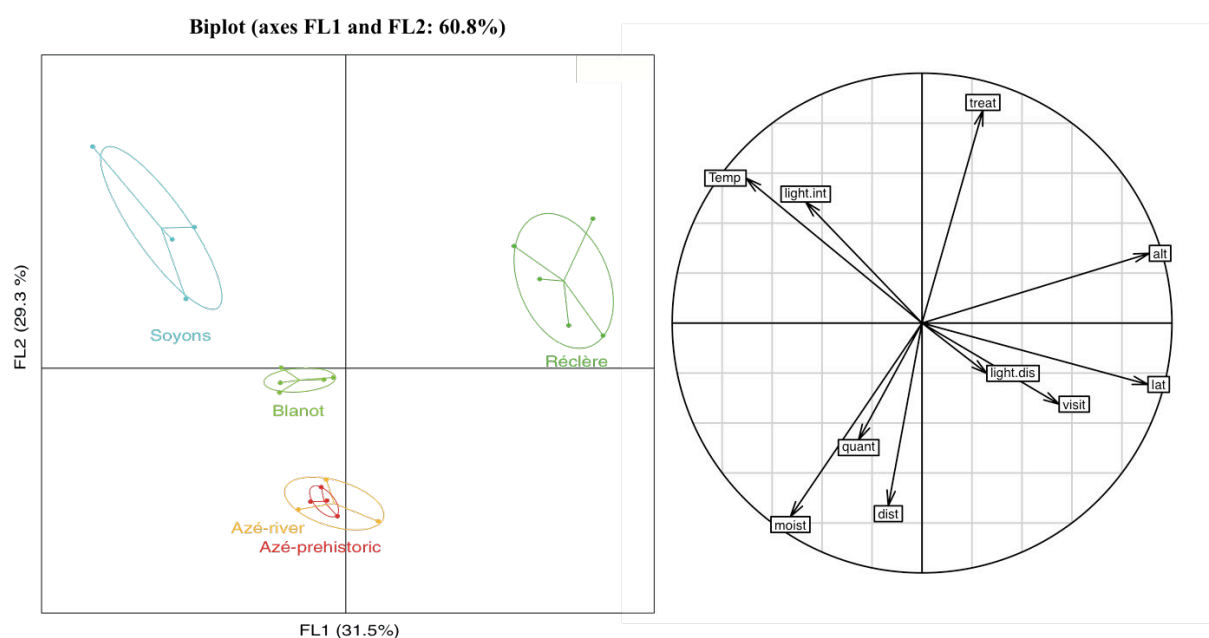


Fig. 2: Principal Component Analyses (PCA) of environmental parameters reported in the five caves (“Temp”: Temperature; “light.int”: Light intensity; “treat”: Treatment; “alt”: Altitude; “lat”: Latitude; “light.dis”: Distance of biofilm from light source; “visit”: number of visitors per year; “dist”: Distance of biofilm from cave entrance; “quant”: Quantum yield, $F'v/F'm$; “moist”: Moisture).

2. Taxonomic composition of biofilms

The biofilm taxonomic composition was explored in terms of abundance of reads (number of DNA fragments read by the sequencer) from samples taken in the 5 caves. The results showed that unicellular microorganisms were dominant. In fact, paired end reads of bacteria (242,550), fungi (78,802), cyanobacteria (65,507), eukaryote algae (50,831) and diatoms (34,030) represented 88.5% of total reads while multi-cellular mosses (63,726 paired end reads) represented only 11.5%.

Bacterial community (Fig. 3) was represented by the groups Alpha-Proteobacteria, Actinobacteria, Beta-, and Gamma-Proteobacteria, *Bacteroidetes*, and to a lesser extent by Delta-Proteobacteria, Chloroflexi, Gemmatimonadetes, Chlorobi, Acidobacteria, Firmicutes and Chlamydiae. Proteobacteria was the major bacterial group accounting for 57.3% of the entire community. Actinobacteria and *Bacteroidetes* were the second and third largest of contributors in terms of sequences number with 20.2 and 8.1%, respectively. The remaining Bacteria group accounted for 14.3%, with 3.1% *Chloroflexi*, 1.2% *Gemmatimonadetes*, 5.7% of unclassified bacteria and 4.3% of 19 other bacteria groups, which accounted for less than 1% of the total.

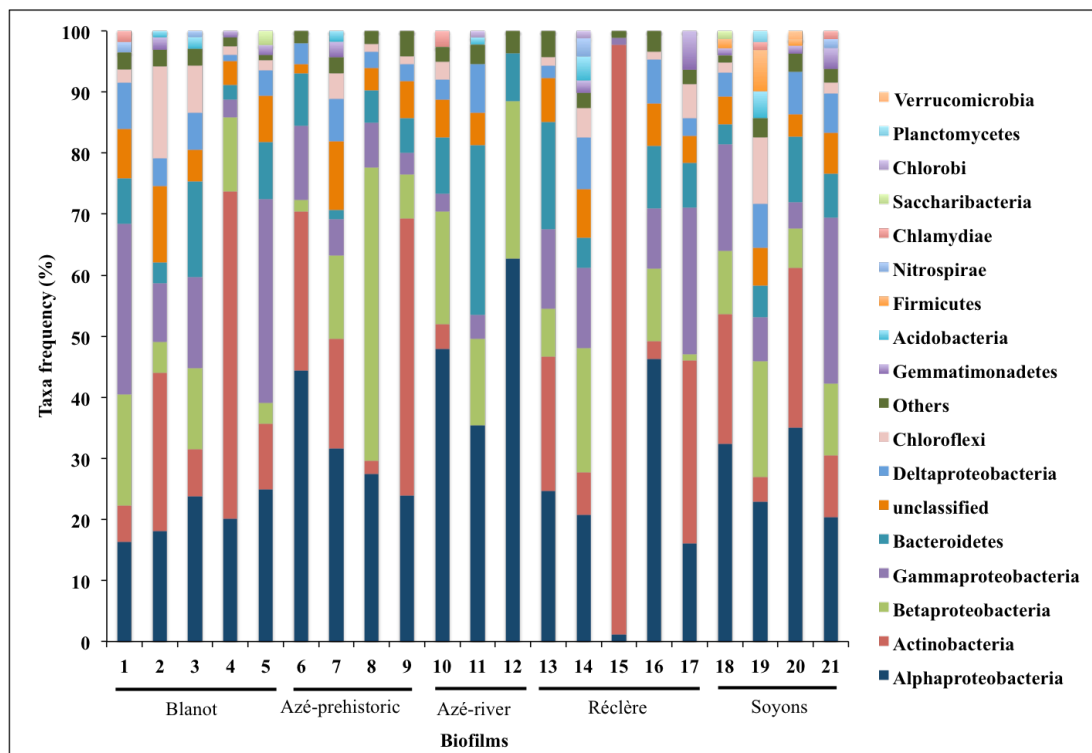


Fig. 3. Microbial community composition at the phylum and class (*Proteobacteria*) level based on 16S rRNA gene sequencing.

Concerning the fungal community (Fig. 4), results showed that fungi were less present in biofilms, especially within 11 biofilms in which too few sequences appeared. These results are in accordance with the absence of amplification of DNA during the PCR. In this case, DNA reads were not taken into consideration. For the 10 other samples, fungal diversity was represented by Ascomycota (71.3%), Zygomycota (21.6%), Basidiomycota (7.1%) and Rozellomycota (<0.01%).

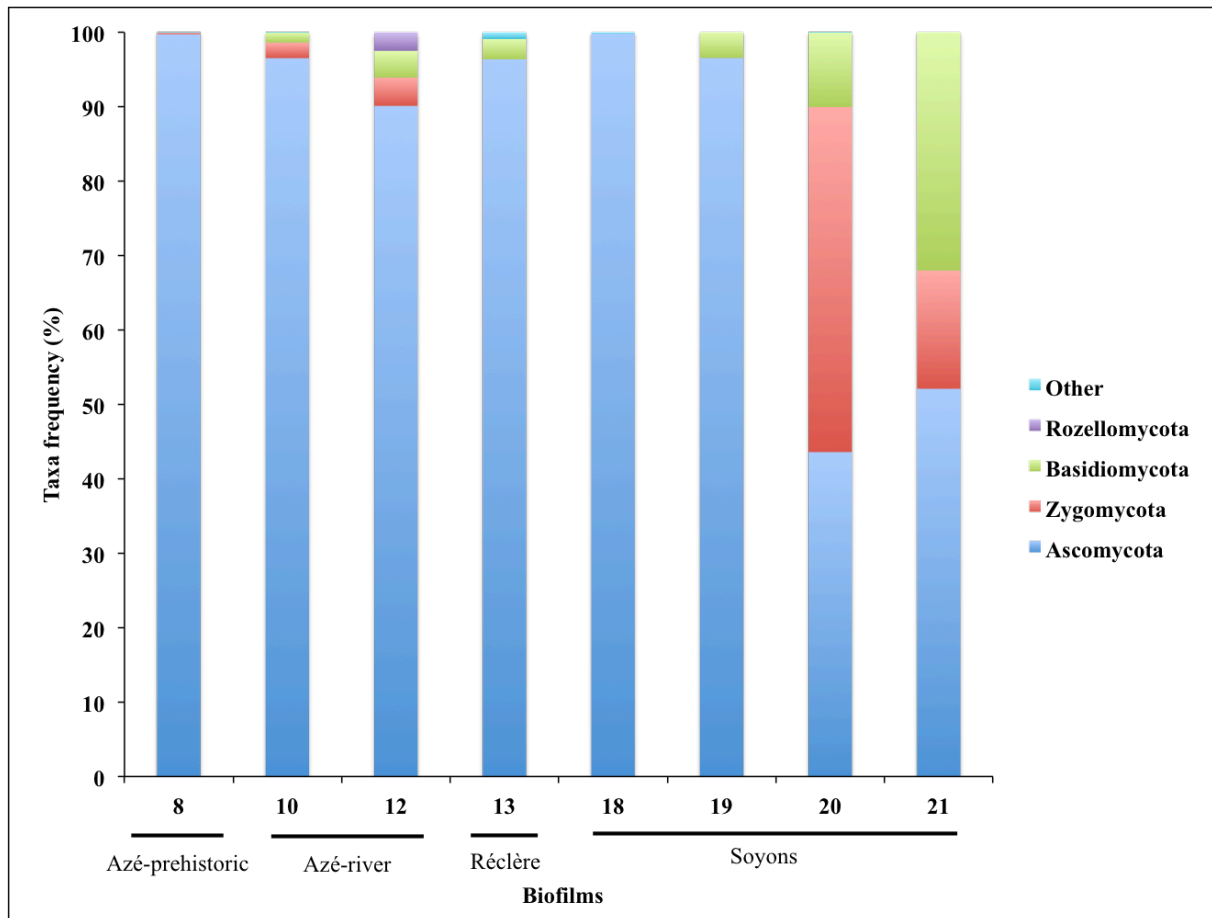


Fig. 4. Microbial community composition at the phylum level based on ITSrRNA gene sequencing.

Table 1. Environmental parameters of the five sampled caves. Physical, chemical and physiological parameters were measured for 21 biofilms.

| Caves | Biofilms | Tourists per year | Altitude (m) | Temperature (°C) | Moisture | Distance from cave entrance (m) | Lamp type | PAR ($\mu\text{mol m}^{-2} \text{s}^{-1}$) | Distance biofilm-light source (m) | Treatment | L* | a* | b* | Quantum yield |
|-------------------------|----------|-------------------|--------------|------------------|----------|---------------------------------|-----------|--|-----------------------------------|--------------|-------|-------|-------|---------------|
| Blancot | 1 | | | 14.14 | 74.11 | 20 | P | 0.29 | 4.98 | | 11.73 | 0.3 | 2.79 | 526 |
| | 2 | | | 14.21 | 73.16 | 20 | P | 0.42 | 4.35 | | 13.42 | 0.72 | 5.01 | 599 |
| | 3 | 5 500 | 395 | 14.45 | 77.04 | 30 | P | 5.17 | 1.00 | No treatment | 20.94 | -1.00 | 7.84 | 671 |
| | 4 | | | 14.26 | 73.34 | 40 | S | 30.21 | 0.24 | | 10.06 | 0.96 | 10.18 | 653 |
| | 5 | | | 14.88 | 76.48 | 60 | P | 2.10 | 1.63 | | 5.68 | -1.15 | 2.11 | 679 |
| | 6 | | | 12.89 | 80.98 | 125 | L | 0.63 | 2.46 | | 20.63 | 0.54 | 11.80 | 688 |
| Azé-pre-historic | 7 | 28 000 | | 13.49 | 79.77 | 165 | L | 0.82 | 1.61 | | 14.90 | 1.716 | 11.52 | 686 |
| | 8 | | | 13.49 | 74.04 | 224 | L | 10.09 | 0.91 | Bleach | 17.55 | 3.984 | 12.01 | 556 |
| | 9 | | 275 | 12.67 | 71.61 | 250 | L | 5.42 | 1.59 | | 13.3 | -0.05 | 12.85 | 651 |
| Azé-river | 10 | | | 10.00 | 81.94 | 75 | L | 2.63 | 2.45 | | 10.72 | -1.17 | 9.27 | 706 |
| | 11 | 28 000 | | 12.89 | 82.56 | 117 | L | 5.68 | 1.39 | Bleach | 12.88 | 0.61 | 8.89 | 551 |
| | 12 | | | 13.37 | 85.08 | 175 | L | 8.36 | 1.01 | | 1.71 | -0.11 | 2.16 | 617 |
| | 13 | | | 14.55 | 52.43 | 8 | L | 13.72 | 0.10 | | 3.92 | -0.14 | 4.03 | 632 |
| | 14 | | | 13.64 | 54.04 | 11 | L | 0.49 | 1.72 | | 15.36 | -1.03 | 11.80 | 661 |
| Réclère | 15 | 27 250 | 655 | 12.48 | 55.05 | 37 | L | 3.28 | 0.03 | Bleach | 21.86 | 0.72 | 11.23 | 0 |
| | 16 | | | 11.88 | 56.64 | 44 | P | 0.62 | 7.46 | | 6.34 | 0.64 | 0.93 | 576 |
| | 17 | | | 11.44 | 57.44 | 56 | L | 0.03 | 1.24 | | 19.04 | -3.05 | 12.07 | 599 |
| Soyons | 18 | | | 16.39 | 60.52 | 24 | S | 25 | 0.10 | | 9.96 | -1.62 | 11.71 | 584 |
| | 19 | 13 000 | 191 | 16.89 | 67.10 | 36 | S | 313 | 0.38 | Bleach | 14.72 | 0.58 | 5.97 | 433 |
| | 20 | | | 16.82 | 66.94 | 47 | L | 38.28 | 0.23 | | 14.99 | 2.52 | 14.89 | 519 |
| | 21 | | | 16.67 | 68.17 | 65 | P | 0.74 | 3.37 | | 29.09 | 0.74 | 12.81 | 714 |

P: Projector; S: Spot light; L: LED.

Six cyanobacteria orders were recorded in the 5 caves (Fig. 5): Chroococcales (40.7%), Nostocales (38.8%), Pleurocapsales (15%), Oscillatoriales (1.6%) and Prochlorales (0.1%); one unclassified order accounted for 3.5%. In the three dominant orders previously mentioned, 3 genera were always overwhelmingly dominant: *Cyanothece* (96.3%), *Nostoc* (98.6%) and *Pleurocapsa* (87.8%) respectively.

Among eukaryote algae, DNA reads comprised seven groups: the most abundant were Trebouxiophyceae (51.2%), followed by Eustigmatophyceae (24.6%) and Chlorophyceae (23.8%). All Xanthophyceae, Ulvophyceae, Klebsormidiophyceae and Phaeophyceae groups represented a total of only 0.4%. Additionally, Chlorophyceae was divided into 23 genera with *Pseudochloris* (33.7%), *Jenufa* (26.3%) and *Marvania* (20.5%) the most abundant and representing 80.5% of all sequences.

Biofilms also included 12 diatom genera with 2 unclassified (33.6 and 23.9%), while *Fistulifera* (17.4%), *Didymosphenia* (12.8%) and *Phaeodactylum* (11.3%) accounted for 41.5% of the reads while the seven other genera accounted for only 1.1%.

Finally, the 23S primer allowed a taxonomic overview of mosses, which, interestingly, were not visible during the sampling. The results showed that *Syntrichia* sp. was by far the largest genus present in biofilms with 96.1% of all the moss sequences.

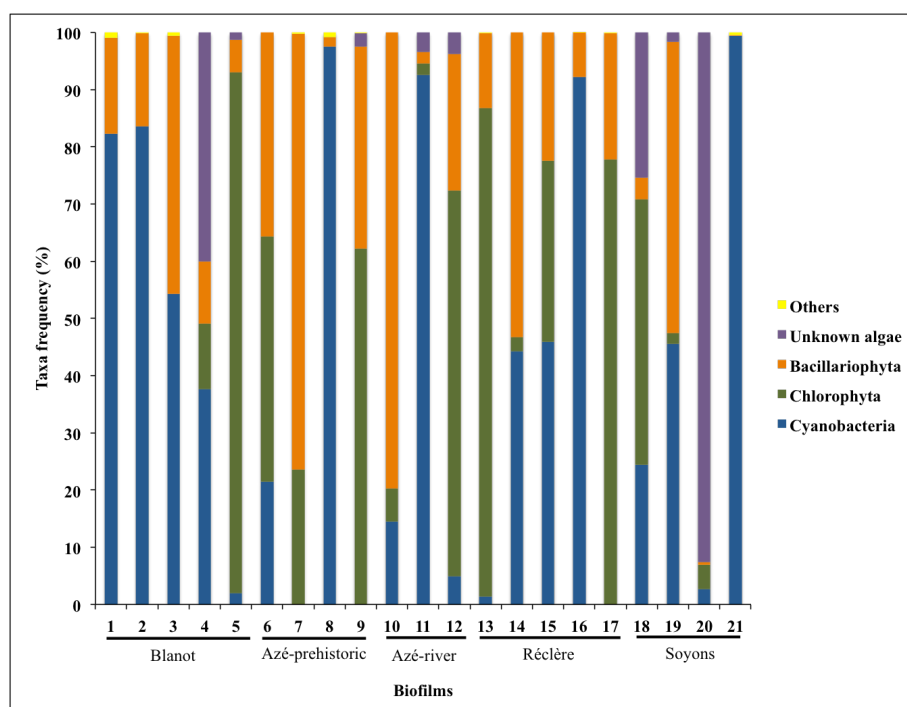


Fig. 5. Microbial community composition at the phylum level based on 23S rRNA gene sequencing.

3. *Biological diversity in the 5 caves*

The results (Fig. 6) indicate that the microbial diversity of the five caves (Fig. 6) comprised 75 genera of autotrophic organisms sequenced with the 23S primer with an average of 46 genera per cave. The total number of genera was compared among the caves themselves and results showed no significant difference (p -value = 0.77). Altogether, the five caves showed 18 genera not shared by another cave. While Azé-prehistoric Cave showed no specific strain, 10 genera were recorded in Réclère Cave, while only 2, 3 and 3 genera were recorded in Azé-river, Blanot and Soyons Caves, respectively. Finally, 20 of the 75 genera (27%) were present in all caves.

For bacteria, 442 genera were recorded with an average of 290 for each cave. Like autotrophic organisms, no difference between the caves, in terms of number of genera, was observed (p -value = 0.58). Altogether, the 5 caves showed 20.5% of genera not shared by another cave (average = 4% per cave) and 147 of the 442 genera (33%) were shared by all the caves.

Finally, 215 Fungi genera were recorded in 4 caves (Azé-prehistoric, Azé-River, Réclère and Soyons). Due to the low number of samples in which fungi were present, no statistical analysis, in terms of number of genera in each cave could be conducted. However, it is noteworthy that 53.5% of the total genera were of a specific strain, with an average of 29 genera (13.5%) per cave. Finally, the 4 caves shared only 9.3% of genera.

4. *Comparison of biofilm diversity in the same cave*

Autotrophic organisms, sequenced by the 23S primer, and bacteria (16S primer) appeared to be specific within each biofilm of the same cave (Fig. 6). In fact, results showed that an average of 40.2% and 35.8% of autotrophs and bacteria, respectively, were specific. However, only 15% of autotrophs and 21.2% of bacteria were shared by all the biofilms of the same cave. All other genera were shared at least by 2 biofilms of the same cave.

The Shannon index (Table 2), based on 23S reads from the same cave, was variable. For example, the lowest value was recorded in Azé-prehistoric Cave (0.04 bits/cell) and the highest (2.38 bits/cell) in Réclère Cave with biofilm number 14. Finally, the average difference between the lowest and the highest Shannon index in the 5th cave was 1.39 bits/cell. As for phototrophs, the Shannon index for Fungi was variable between each biofilm, ranging from 0.47 to 2.96 bits/cell. The Shannon index for Bacteria was much higher than for phototrophs, with an average of 3.67 bits/cell. No significant difference (p -value < 0.05) in the

Shannon index was observed among the different caves. It is noteworthy that biofilm number 15, composed of 95.6% of Actinobacteria, showed a low value (0.39 bits/cell).

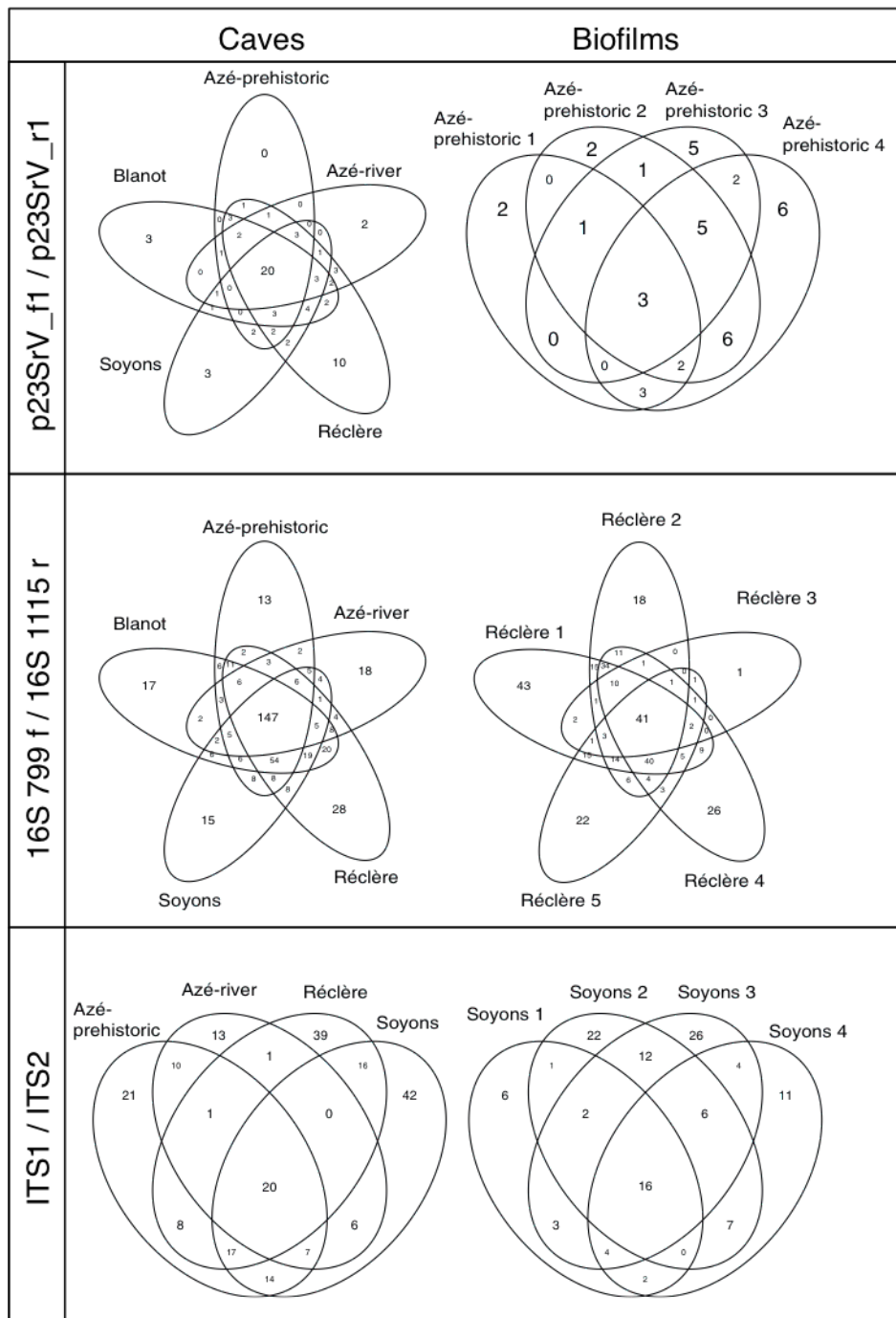


Fig. 6. Comparison of organism communities (bacteria, fungi, autotrophic organisms) in Azé-prehistoric (“Azé-pre”), Azé-river, Blanot, Réclère and Soyons Caves and in biofilms of Azé-prehistoric, Réclère and Soyons Caves using Venn diagram.

Table 2. Shannon and Pielou indices are reported for all biofilms sampled and sequenced with 16S, 23S and ITS primers.

| Cave | Biofilm | Shannon | | | Pielou | | |
|-------------------|---------|---------|------|------|--------|------|------|
| | | 16S | 23S | ITS1 | 16S | 23S | ITS1 |
| Blanot | 1 | 3.53 | 0.85 | n.a. | 0.71 | 0.07 | n.a. |
| Blanot | 2 | 3.71 | 0.95 | n.a. | 0.73 | 0.08 | n.a. |
| Blanot | 3 | 4.17 | 1.50 | n.a. | 0.78 | 0.14 | n.a. |
| Blanot | 4 | 3.45 | 0.22 | n.a. | 0.68 | 0.05 | n.a. |
| Blanot | 5 | 3.61 | 1.79 | n.a. | 0.7 | 0.14 | n.a. |
| Azé- pre-historic | 6 | 3.77 | 0.04 | 2.29 | 0.75 | 0.09 | 0.50 |
| Azé- pre-historic | 7 | 4.07 | 1.13 | n.a. | 0.79 | 0.09 | n.a. |
| Azé- pre-historic | 8 | 3.48 | 0.33 | 1.04 | 0.69 | 0.06 | 0.40 |
| Azé- pre-historic | 9 | 3.82 | 1.81 | n.a. | 0.74 | 0.16 | n.a. |
| Azé- river | 10 | 3.64 | 0.25 | 1.12 | 0.72 | 0.04 | 0.28 |
| Azé- river | 11 | 3.94 | 0.60 | 0.57 | 0.78 | 0.05 | 0.22 |
| Azé- river | 12 | 3.26 | 0.25 | n.a. | 0.71 | 0.04 | n.a. |
| Réclère | 13 | 4.12 | 1.24 | n.a. | 0.76 | 0.07 | n.a. |
| Réclère | 14 | 4.01 | 2.38 | n.a. | 0.76 | 0.16 | n.a. |
| Réclère | 15 | 0.39 | 1.87 | n.a. | 0.09 | 0.16 | n.a. |
| Réclère | 16 | 3.95 | 0.85 | 0.47 | 0.75 | 0.05 | 0.11 |
| Réclère | 17 | 3.61 | 1.44 | 1.79 | 0.71 | 0.14 | 0.40 |
| Soyons | 18 | 4.25 | 0.96 | 1.06 | 0.8 | 0.07 | 0.30 |
| Soyons | 19 | 3.87 | 1.78 | 1.56 | 0.75 | 0.11 | 0.37 |
| Soyons | 20 | 4.50 | 0.44 | 2.04 | 0.83 | 0.07 | 0.47 |
| Soyons | 21 | 3.84 | 0.07 | 2.96 | 0.75 | 0.07 | 0.75 |

"n.a." corresponds to samples without fungal DNA.

5. NMDs analysis

NMDs analysis was performed on both bacteria (Fig. 7) and chlorophyll organisms (Fig. 8) excepting “sample 15”, which was not a biofilm but rather *Actinobacteria* colonies. The results showed no significant difference among the biofilm organism communities in any of the caves. In fact, NMDs graphs showed that communities overlapped each other except for the bacterial community of Azé-river Cave. However, an ANOSIM test demonstrated a non-significant difference for both bacterial ($p\text{-value} = 0.16$) and autotrophic-microorganisms ($p\text{-value} = 0.15$).

It is noteworthy that different bacteria and autotrophic-microorganisms comprised the biofilms of the same cave. For example, both “Blanot 1” and “Blanot 4” samples were completely different as to their bacterial composition. Also the Soyons samples showed strong differences in their autotrophic microorganism structure.

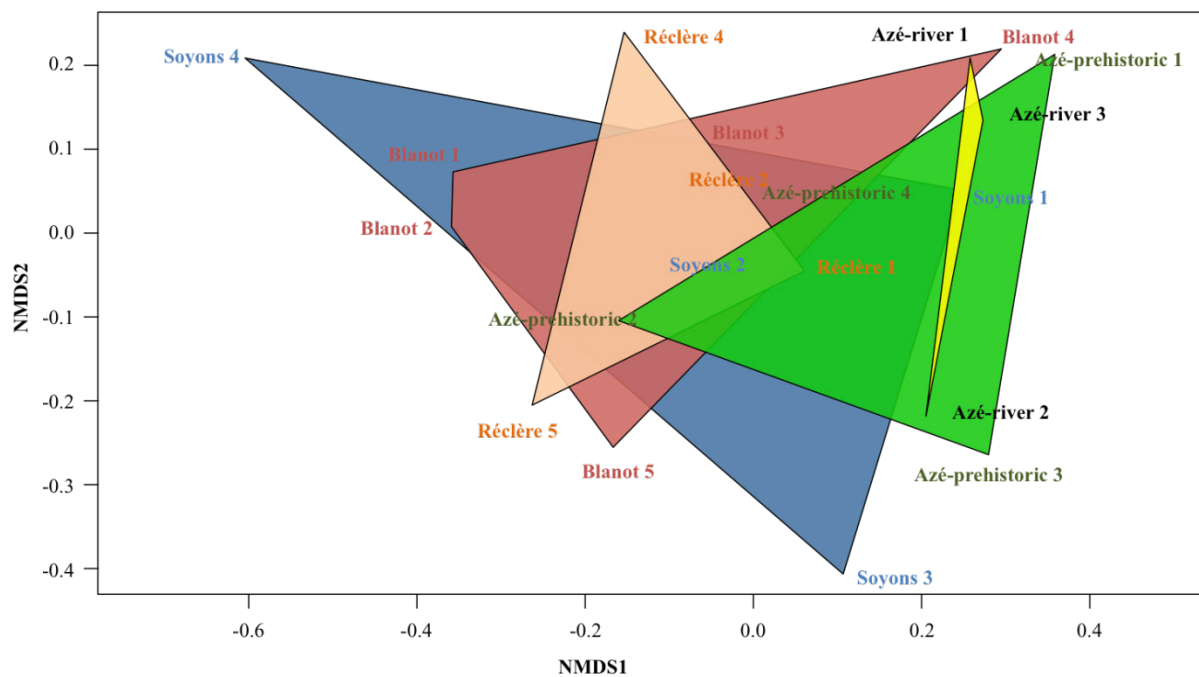


Fig. 7. Non-metric multidimensional scaling of bacterial communities in the five sampled show caves.

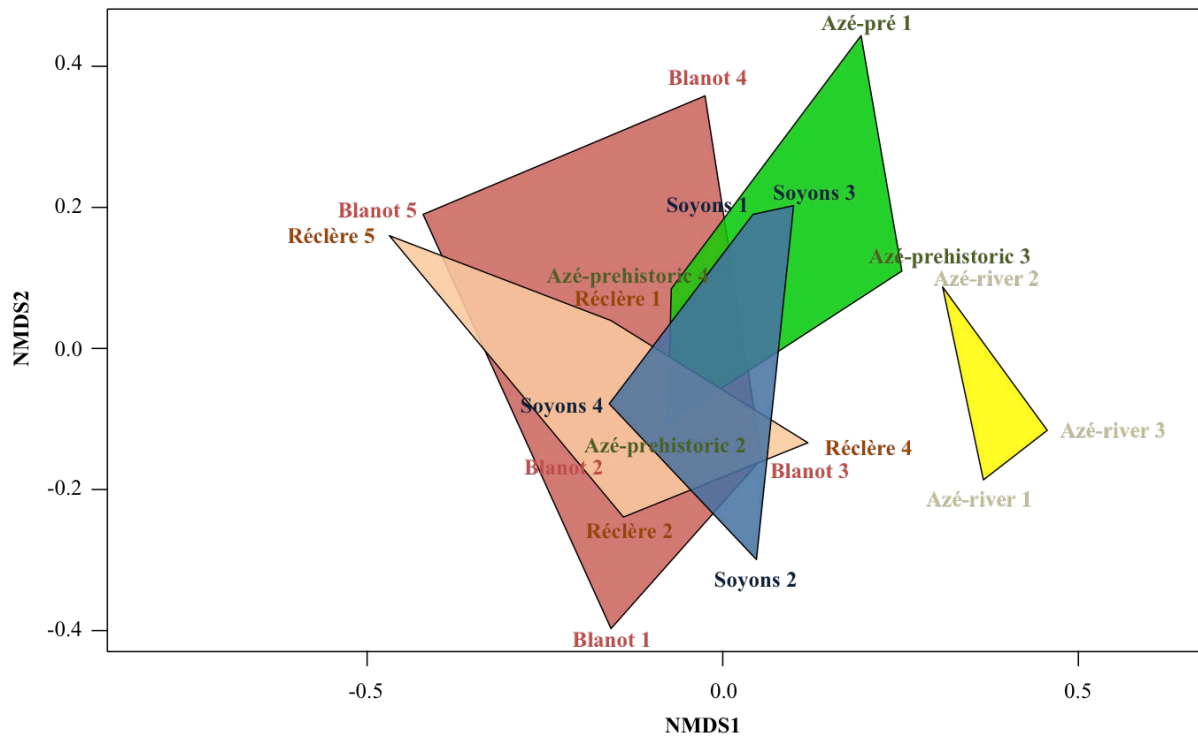


Fig. 8. Non-metric multidimensional scaling of photosynthetic communities in the five sampled show caves.

6. Effects of bleach treatment on the biological community

The proportion of each group of bacteria present in biofilms treated annually, appeared close to those biofilms never having been sprayed with bleach (Table 3). For organisms sequenced with the 23S primer, results of Cyanobacteria and Chlorophyta showed no difference. However, 11.6% more *Cyanobacteria* and 6.4% fewer unknown algae were observed in untreated caves. Finally, no fungus was observed in untreated caves compared to treated ones.

Table 3. Comparison of biofilm composition between untreated and treated caves.

| | Untreated (%) | Treated (%) |
|--|---------------|-------------|
| <i>Bacteria</i> | | |
| Alphaproteobacteria | 31,4 | 27,3 |
| Actinobacteria | 16,6 | 15,4 |
| Betaproteobacteria | 15,1 | 11,1 |
| Gammaproteobacteria | 10,4 | 14,5 |
| Bacteroidetes | 8,7 | 8,3 |
| Unclassified | 5,9 | 6,0 |
| Deltaproteobacteria | 4,2 | 5,6 |
| Chloroflexi | 3,1 | 3,4 |
| Others | 2,6 | 2,8 |
| Gemmatimonadetes | 0,6 | 1,8 |
| Acidobacteria | 0,5 | 1,0 |
| Firmicutes | 0,0 | 1,2 |
| Nitrospirae | 0,2 | 0,6 |
| Chlamydiae | 0,4 | 0,3 |
| Saccharibacteria | 0,2 | 0,2 |
| Chlorobi | 0,1 | 0,1 |
| Planctomycetes | 0,0 | 0,2 |
| Verrucomicrobia | 0,0 | 0,2 |
| <i>Cyanobacteria/Eukaryotic algae/Diatoms</i> | | |
| Cyanobacteria | 40,9 | 38,7 |
| Chlorophyta | 25,5 | 27,3 |
| Bacillariophyta | 29,0 | 19,0 |
| Unknown eukaryotic algae | 4,2 | 14,9 |
| Others | 0,3 | 0,1 |
| <i>Fungi</i> | | |
| Ascomycota | 95,5 | 77,7 |
| Zygomycota | 2,0 | 12,5 |
| Basidiomycota | 1,6 | 9,6 |
| Rozellomycota | 0,8 | 0,0 |
| Other | 0,0 | 0,2 |

IV. Discussion

This study furnished the first quantitative data from biofilms of 5 different caves concerning the simultaneous identification of bacteria, fungi, cyanobacteria, micro-algae, diatoms and mosses along with their structural assembly.

- *Species diversity of biofilms in caves*

Our results showed that the caves under study included a wide range of bacterial groups corroborating findings from other caves [55]. For instance, Proteobacteria were the most important group contributing 57% of the entire community. Most Proteobacteria were closely related to a-Proteobacteria, b-Proteobacteria and g-Proteobacteria, which are found in a wide variety of habitats including extreme karstic environments [56]. Mihajlovski et al. [38] found the same abundance of *Proteobacteria* on the rock surface of a historic monument (Chaalis Abbey, France). It is noteworthy that a-Proteobacteria may interact with some phytoplankton species improving their production and biomass [57], a situation that presumably occurs in biofilms. Actinobacteria were the second largest group with 20.2% of paired end reads. The most important proportion of this phylum was found in sample number 15 (96.6%). This result was expected since grey, white or yellow colonies (Fig. 1), proliferating in caves had already been described by other authors [58,59]. We infer that these colonies are heterotrophs since no photosynthetic activity has been detected with the MINI-PAM fluorimeter. *Actinomycetes* are of special interest because they play a crucial role in the decomposition of organic compounds and environmental pollutants. These bacteria are also capable of deterioration of paintings in hypogean environments [60,61]. However, they also produce a great variety of bioactive chemical compounds, the most important of which are antibiotics [62].

Concerning phototrophs, our results indicate that Cyanobacteria are the most abundant group confirming other findings in caves [25,28,63,64]. The dominant genera found in our caves are *Cyanothece*, *Nostoc* and *Pleurocapsa* accounting for 89.5% of all reads. *Cyanothece* is commonly involved in bloom formation in freshwater ecosystems [65] with the ability to secrete exo-polysaccharides [66] to form biofilm structure. *Nostoc* is considered the most dominant aero-terrestrial cyanobacteria [67] and is prominent in terrestrial limestone environments [68]. Furthermore, its presence in show caves has already been recorded by many authors [16,32,30]. In nutrient-poor environments such as caves, the presence of

nitrogen-fixing cyanobacteria such as *Nostoc* allowed the induction of the establishment and development of other organisms (other cyanobacteria, algae, mosses, etc.) [16,69]. *Pleurocapsa* are endoliths and possess the remarkable property of penetrating into calcareous substrates, where they develop in microscopic tunnels formed through dissolution of calcite [70]. More generally, when cyanobacteria were dominant in a biofilm, eukaryotic microalgae were the ultra minority and *vice versa*. Cennamo et al. [11] have already reported the same results for some samples in Italian caves.

Concerning eukaryotic algae, *Pseudochloris*, *Nannochloropsis*, *Jenufa*, *Marvania*, *Prasiolopsis* and *Chromochloris* were the most abundant genera in the sampled biofilms. *Pseudochloris*, a freshwater alga, has spherical to oval cells and a simple ultra-structure characteristic of small green algae [31]. As far as we know, this strain was not considered a stone monument colonizer. However, *Nannochloropsis*, a yellow-green microalga, was recently reported by Zhang et al. [71] and described as a bloom forming algae. Furthermore, the genus *Jenufa* has previously been found in biofilms in Europe on the surfaces of stone buildings [72] and likewise the EPS secretor *Prasiolopsis* sp. [73].

The diatom community was mainly represented by 4 genera, *Fistulifera*, *Didymosphenia*, *Phaeodactylum* and *Eunotia*, and by 2 unclassified ones. However, just twelve of the twenty-one studied biofilms were composed of a large concentration of diatoms (> 100 paired end reads). To our knowledge, the recorded genus *Fistulifera* has never been reported in biofilms whereas certain recorded species of the genus *Didymosphenia* have been previously reported and considered as invasive in streams [74]. *Eunotia* can be found in acid seeps [75]. In some caves low diatom diversity and abundance may both be related to the lack of silica [76]. It has also been demonstrated that the composition and diversity of diatom communities are influenced by light, moisture, chemical composition and pH of the rock substrate [74].

In this study, the 23S primer provided an overview of the mosses present in biofilms. Since no mosses were observed during the sampling, it was surprising to find 63,726 paired end reads of Bryophyta. We infer that mosses present in cave biofilms were in their first stage of development that cannot be observed, for example spores. Results showed that mosses were as abundant as cyanobacteria. However, it is necessary to consider that mosses are multicellular organisms and that only one moss branch can deeply prevaricate semi-quantitative information (number of paired end reads) provided by the sequencing. In any case, 99.4% of *Bryopsida* and 0.55% of *Tetraphidospida* composed the Bryophyta community. Moreover, the *Syntrichia* genus appeared to be the pioneer and probably the most

adapted moss growing in the biofilms with 96.1% of all sequenced DNA fragments. Some of its species are remarkable by their adaptation to extreme environments [77] such as caves. In fact, it has been reported that they are able to regenerate even after twenty years desiccation, or to remain viable under a Canadian glacier for 400 years [78]. Our results showed a low diversity of Bryophyta (9 taxa in 5 caves) in comparison to Mulec and Kubešová [79]. In fact, these authors identified a maximum of 16 taxa in one cave and 37 taxa in 9 caves and mines. However, some of these taxa were reported in caves or mines where lamps are continuously functioning, which is not the case in our caves. Influence of light on moss development may thus explain the observed discrepancies between our results and theirs.

Cave mycobiota was recorded in eight biofilms from four caves but as completely absent in Blanot Cave. *Ascomycota* dominated the fungal community, while both *Zygomycota* and *Basidiomycota* were less present. These results are in accordance with those of Popovic et al. [30] using culture-dependent and microscopic methods. However, these authors reported other dominant genera, e.g., *Alternaria*, *Aspergillus*, *Cladosporium*, *Epicoccum*, *Penicillium*, and *Trichoderma*. In our study, *Mortierella* and *Plectosphaerella* were highly dominant but were not found in Popovic's. Both *Verticillium* and *Lecanicillium* were also present in the studied biofilms. *Lecanicillium* is a parasite of insects, which has also been found in the air and on biofilms in Roman catacombs [80].

- Tracking changes in biofilm community structure

The five caves studied here differed statistically (71%) from each other according to environmental parameters. However, this difference was not correlated with biofilm community structure. Even if results showed drastic differences when biofilms in the same cave were compared to each other, the community present in all the caves seemed to be relatively similar with only 5.8 and 4% of autotrophs and bacteria per cave, respectively. Differences observed in biofilm diversity and community composition were probably due to the influence of mineralogy, porosity, surface roughness, and the capacity to take up water, the organic substances of a material and to the lighting regime [81,82]. Further analyses should address the role of environmental parameters on organism growth as well as an organism's co-occurrence network. Conversely, results reported a common base of organisms in each cave, representing 27% of autotrophs and 33% of Bacteria. All other organisms (67.2 and 63% for autotrophs and bacteria) were recorded in at least two caves. In some cases, the Shannon index showed poor diversity (0 biofilms reported high biodiversity (e.g. biofilms 20 or 14, with > 4). However, the average of 3.9 bits/cell in bacteria (e.g. biofilm 15) or in

autotrophic organisms (e.g. biofilm 6, 0.04 bits/cell) while other Shannon indices in each cave remain high, showing mature biofilms, even in caves annually treated with bleach.

- Effect of bleach treatment on the biofilm community

Finally, this study demonstrates that bacteria and autotroph communities present in treated biofilms were the same as those in untreated caves. Due to the fact that the studied biofilms were sampled at the end of the year, corresponding to the end of touristic activity, we assumed that the biofilms had already completed their maturation. The only difference was the proportion of Cyanobacteria and unknown algae. We thus hypothesized that treated biofilms may need more time to stabilize their communities.

The use of highly toxic bleach (NaClO) may effectively eradicate Lampenflora but, without efficient changes in cave management (e.g. lighting regime), it has only a transitory effect in preventing growth [79]. Moreover, as reported in this study, bleach treatment led to fungi proliferation only on treated biofilms. We infer that these heterotrophs used necrotic organic matter from the treated biofilm in their development.

V. Conclusion

Caves are mainly composed of carbonate stones such as limestone, which over time undergoes significant deterioration phenomena via *Lampenflora*. Also, prehistoric paintings, such as in the Lascaux Cave, are affected by microorganism proliferation (e.g. *Bracteacoccus* sp.). In this context, descriptions of biofilm communities are critical in understanding the bio-deterioration process and in choosing the most suitable treatment for long-term preservation. In this study, it was reported that biofilm communities showed wide diversity. Photosynthetic and non-photosynthetic bacteria were the most abundant organisms present in the biofilms. To a lesser extent, algae, fungi, diatoms and mosses complete the list of organisms colonizing the biofilms. Moreover, this study reported few differences in the microorganism communities between the treated and untreated caves, suggesting that biofilms were able to grow and mature one year after treatment. These results also highlight the low efficiency of chemical treatment over time (e.g. bleach) and the importance of finding more efficient and environmentally friendly treatments. Further studies should examine how these organisms interact with each other and how environmental parameters influence biofilm proliferation.

VI. Acknowledgments

We are first and foremost grateful to the owners and managers of the five caves, who kindly granted us access. We also thank the *Ministère de la Culture et de la Communication* (France) and the *Laboratoire de Recherche des Monuments Historiques* (LRMH, Paris) for their financial contribution. In addition we are indebted to S. Terrat of INRA for his precious help in providing us with bio-computer analysis.

VII. References

- [1] Aubert M, Brumm A, Ramli M, Sutikna T, Saptomo EW, Hakim B, Morwood MJ, Bergh GD, Van Den, Kinsley L, Dosseto A (2014) Pleistocene cave art from Sulawesi, Indonesia. *Nature* 514:223–227
- [2] Jaubert J, Verheyden S, Genty D, Soulier M, Cheng H, Blamart D, Burette C, Camus H, Delaby S, Deldicque D, Edwards RL, Ferrier C (2016) Early Neanderthal constructions deep in Bruniquel Cave in southwestern France. *Nature* 1–17
- [3] Cigna AA (2016) Tourism and show caves. *Zeitschrift für Geomorphologie*, Vol. 60 (2016), Suppl. 2, pp217-233
- [4] Zhang S, Jin Y (1996) Tourism resources on karst and caves in China. *Acta II Congress ISCA*, Malaga, p. 111-119
- [5] Cigna AA, Burri E (2000) Development management and ‘Lampenflora’ and economy of show caves. *Int. J. Speleol.* 29:1-27
- [6] Gillieson DS (2011) Management of caves. In: Van Beyen P (ed.) *Karst Management*, Springer, pp 141-158
- [7] Baker A, Genty D (1998) Environmental pressures on conserving cave speleothems: Effects of changing surface land use and increased cave tourism. *J. Environ. Manag.* 53:165–175
- [8] Dragovich D, Grose J (1990) Impact of Tourists on Carbon Dioxide Levels at Jenolan Caves, Australia: an Examination of Microclimatic Constraints on Tourist Cave Management. *Geoforum*, Vol. 21, No. 1, pp 111-120
- [9] Sebela S, Turk J (2014) Natural and anthropogenic influences on the year-round temperature dynamics of air and water in Postojna show cave, Slovenia. *Tourism Manage.* 40:233-243
- [10] Cigna AA (2011) The problem of Lampenflora in show caves. In: Bella P, Gazik P (Eds.), *Proceedings of the 6th ISCA Congress*. SNC of Slovak Republic, Slovak Caves Administration, pp 201–205

- [11] Cennamo P, Marzano C, Ciniglia C, Pinto G, Cappelletti P, Caputo P, Studies K (2012) A Survey of the algal flora of anthropogenic caves of CampiFlegrei (Naples, Italy) archeological district. *J. Cave Karst Stud.* 74:243–250
- [12] Borderie F, Denis M, Barani A, Alaoui-Sossé B, Aleya L (2016) Microbial composition and ecological features of phototrophic biofilms proliferating in the Moidons Caves (France): investigation at the single-cell level. *Environ. Sci. Pollut. Res.* 23:12039–49
- [13] Grobbelaar JU (2000) Lithophytic algae: a major threat to the karst formation of show caves. *J. Appl. Phycol.* 12:309-315
- [14] Hoffmann L, Darienko T (2005) Algal biodiversity on sandstone in Luxembourg. *Ferrantia* 44:99–101
- [15] Bruno L, Billi D, Bellezza S, Albertano P (2008) Cytomorphological and genetic characterization of troglobitic *Leptolyngbya* strains isolated from Roman hypogea. *Appl. Environ. Microbiol.* 73:608–617
- [16] Lamprinou V, Danielidis DB, Economouamilli A (2012) Distribution survey of Cyanobacteria in three Greek caves of Peloponnese. *Int. J. Speleol.* 41:267–272
- [17] Mihajlovski A, Seyer D, Benamara H., Bousta F, Di Martino P, (2014) An overview of techniques for the characterization and quantification of microbial colonization on stone monuments. *Microbiol.* 65:1243-1255
- [18] Aley T, Aley C, Rhodes R (1986) Control of exotic plant growth in Carlsbad Caverns, New Mexico. *Proc. Sixth National Cave Management Symposium*, pp. 159-171
- [19] Olson R (2002) Control of lamp flora in Mammoth Cave National Park. In: Hazslinsky, T., (Ed.), *International Conference on Cave Lighting*, November 15-17, 2000. Budapest: Hungarian Speleological Society, 131-133
- [20] Piano E, Bona F, Falasco E, La Morgia V, Badino G, Isaia M (2015) Environmental drivers of phototrophic biofilms in an Alpine show cave (SW-Italian Alps). *Sci. Total Environ.* 536:1007-18
- [21] Cañaveras JC, Sanchez-Moral S, Soler V, Saiz-Jimenez C (2001) Microorganisms and microbially induced fabrics in cave walls. *Geomicrobiol. J.* 18:223-240

- [22] Asencio AD, Aboal M (2001) Biodeterioration of wall paintings in caves of Murcia (SE Spain) by epilithic and chasmoendolithic microalgae. *Algol. Stud.* 103:131-142
- [23] Shields LM, Durell LW (1964) Algae in relation to soil fertility. *Bot. Rev.* 30:92–128
- [24] Aley T (2004) Tourist caves: algae and Lampenflora. In: Gunn J (ed.) *Encyclopedia of Caves and Karst tropical Science*, New York: Fitzroy Dearborn, 1568-1570
- [25] Smith T, Olson R (2007) A taxonomic survey of lamp flora (Algae and Cyanobacteria) in electrically lit passages within Mammoth Cave National Park, Kentucky. *Int. J. Speleol.* 36:105–114
- [26] Ruspoli, M. (1986) *Lascaux: Un nouveau regard*. Paris: Bordas
- [27] Pfendler S, Einhorn O, Bousta F, Khatyr A, Alaoui-Sossé L, Aleya L, Alaoui-Sossé B (2017) UV-C as a means to combat biofilm proliferation on prehistoric paintings: evidence from laboratory experiments. *Environ. Sci. Pollut. Res.* doi: 10.1007/s11356-017-9791-x
- [28] Czerwik-Marcinkowska J, Mrozińska T (2011) Algae and cyanobacteria in caves of the Polish jura. *Pol. Bot. J.* 56:203-243
- [29] Lamprinou V, Danielidis DB, Pantazidou A, Oikonomou A, Economouamilli A (2014) The show cave of Diros vs wild caves of Peloponnese, Greece - distribution patterns of Cyanobacteria. *Int. J. Speleol.* 43:335–342
- [30] Popović S, Simić GS, Stupar M, Unković N, Jovanović J, Grbić ML (2015) Cyanobacteria, algae and microfungi present in biofilm from Božana Cave (Serbia). *Int. J. Speleol.* 44:141–149
- [31] Somogyi B, Felföldi T, Solymosi K, Flieger K, Márialigeti K, Böddi B, Vörös L (2013) One step closer to eliminating the nomenclatural problems of minute coccoid green algae: *Pseudochloris wilhelmii*, gen. n. sp. nov. (Trebouxiophyceae, Chlorophyta). *Eur. J. Phycol.* 48:427–436
- [32] Czerwik-Marcinkowska (2013) Observations on aerophytic cyanobacteria and algae from ten caves in the Ojców National Park. *Acta Agrobot.* 66:39- 52
- [33] Urzì C, De Leo F, Bruno L, Albertano P (2010) Microbial Diversity in Paleolithic Caves:

A Study Case on the Phototrophic Biofilms of the Cave of Bats (Zuheros, Spain). *Microb. Ecol.* 60:116–129

[34] Suihko ML, Alakomi HL, Gorbushina A, Fortune I, Marquardt J, Saarela M (2007) Characterization of aerobic bacterial and fungal microbiota on surfaces of historic Scottish monuments. *Syst. Appl. Microbiol.* 30:494–508

[35] Piñar G, Ripka K, Weber J, Sterflinger K (2009) The micro-biota of a sub-surface monument the medieval chapel of St. Virgil (Vienna, Austria). *Int. Biodeterior. Biodegrad.* 63:851–859

[36] Hallmann C, Stannek L, Fritzlar D, Hause-Reitner D, Friedl T, Hoppert M (2013) Molecular diversity of phototrophic biofilms on building stone. *FEMS Microbiol. Ecol.* 84:355–372

[37] Cennamo P, Montuori N, Trojsi G, Fatigati G, Moretti A (2016) Bio films in churches built in grottoes. *Sci. Total Environ.* 543:727–738

[38] Mihajlovski A, Gabarre A, Seyer D, Bousta F, Di P (2017) Bacterial diversity on rock surface of the ruined part of a French historic monument : The Chaalis abbey. *Int. Biodeterior. Biodegrad.* 120:161–169

[39] Bartosch S, Mansch R, Knötzsch K, Bock E (2003) CTC staining and counting of actively respiring bacteria in natural stone using confocal laser scanning microscopy. *J. Microbiol. Meth.* 52:75–84

[40] Prieto B, Silva B, Lantes O (2004) Biofilm quantification on stone surfaces: comparison comparison of various methods. *Sci. Total Environ.* 333:1–7

[41] Ríos De Los A, Ascaso C (2005) Contributions of in situ microscopy to the current understanding of stone biodeterioration. *Int. Microbiol.* 8:181–188

[42] Berdoulay M, Salvado JC (2009) Genetic characterization of microbial communities living at the surface of building stones. *Lett. Appl. Microbiol.* 49:311–316

[43] Qi-Wang MGY, He LY, Sheng XF (2011) Characterization of bacterial community inhabiting the surfaces of weathered bricks of Nanjing Ming city walls. *Sci. Total Environ.* 409:756–762

- [44] Cutler NA, Oliver AE, Viles HA, Whiteley AS (2012) Non-destructive sampling of rock-dwelling microbial communities using sterile adhesive tape. *J. Microbiol. Meth.* 91:391–398
- [45] Otlewska A, Adamiak J, Gutarowska B (2014) Application of molecular techniques for the assessment of microorganism diversity on cultural heritage objects. *Acta Biochim. Pol.* 61:217–225
- [46] Liu X, Hou W, Dong H, Wang S, Jiang H, Wu G, Yang J, Li G (2015) Distribution and Diversity of Cyanobacteria and Eukaryotic Algae in Qinghai–Tibetan Lakes. *Geomicrobiol. J.* 33:860-869
- [47] Vaughan MJ, Nelson W, Soderlund C, Maier RM, Pryor BM (2015) Assessing Fungal Community Structure from Mineral Surfaces in Kartchner Caverns Using Multiplexed 454 Pyrosequencing. *Environ. Microbiol.* 70:175-87
- [48] Parulekar NN, Kolekar P, Jenkins A, Kleiven S, Utkilen H, Johansen A, Sawant S, Kulkarni-Kale U, Kale M, Sæbø M (2017) Characterization of bacterial community associated with phytoplankton bloom in a eutrophic lake in South Norway using 16S rRNA gene amplicon sequence analysis. *PLoS ONE* doi:10.1371/journal.pone.0173408
- [49] Needham DM, Sachdeva R, Fuhrman JA (2017) Ecological dynamics and co-occurrence among marine phytoplankton, bacteria and myoviruses shows microdiversity matters. *ISME J* 11:1614-1629
- [50] Borderie F, Tête N, Cailhol D, Alaoui-Sehmer L, Bousta F, Rieffel D, Aleya L, Alaoui-Sossé B (2014) Factors driving epilithic algal colonization in show caves and new insights into combating biofilm development with UV-C treatments. *Sci. Tot. Environ.* 484:43-52
- [51] Durand A, Maillard F, Foulon J, Gweon HS, Valot B, Chalot M (2017) Environmental Metabarcoding Reveals Contrasting Belowground and Aboveground Fungal Communities from Poplar at a Hg Phytomanagement Site. *Microb. Ecol.* doi :10.1007/s00248-017-0984-0
- [52] Schloss PD, Westcott SL, Ryabin T, Hall JR, Hartmann M, Hollister EB, Lesniewski RA, Oakley BB, Parks DH, Robinson CJ, Sahl JW, Stres B, Thallinger GG, Horn DJ, Van Weber CF (2009) Introducing mothur: open-source, platform-independent, community-supported software for describing and comparing microbial communities. *Appl. Environ. Microbiol.* 75:7537-7541

- [53] Shannon CE, Weaver W (1949) The mathematical theory of communication. Urbana, IL: University of Illinois Press.
- [54] Pielou, EC (1975) Ecological diversity. Wiley, New York - 1977. Mathematical ecology. Wiley, New York
- [55] Barton HA, Taylor NM, Kreate MP, Springer AC, Oehrle SA, Bertog JL (2007) The impact of host rock geochemistry on bacterial community structure in oligotrophic cave environments. *Int. J. Speleol.* 36:93–104
- [56] Mandal de S, Chatterjee R, Kumar NS (2017) Dominant bacterial phyla in caves and their predicted functional roles in C and N cycle. *BMC Microbiol.* 11:17-90
- [57] Jardillier L, Basset M, Domaizon I, Belan A, Amblard C, Richardot M, Debroas D (2004) Bottom-up and top-down control of the bacterial community composition in the euphotic zone of a reservoir. *Aquat. Microb. Ecol.* 35:259-273
- [58] Pasic L, Kovce B, Sket B, Herzog-Velikonja B (2009) Diversity of microbial communities colonizing the walls of a karstic cave in Slovenia. *FEMS Microbiol. Ecol.* 71:50–60.
- [59] Cuezva S, Fernandez-Cortes A, Porca E, Pašić L, Jurado V, Hernandez-Marine M, Serrano-Ortiz P, Hermosin B, Can˜averas JC, Sanchez-Moral S, Saiz-Jimenez C (2012) The biogeochemical role of Actinobacteria in Altamira Cave, Spain. *FEMS Microbiol. Ecol.* 81, 281–290
- [60] Monte M, Ferrari R (1993) Biodeterioration in subterranean environments. *Aerobiologia* 9:141–148
- [61] Groth I, Saiz-Jimenez C (1999) Actinomycetes in hypogean environments. *Geomicrobiol. J.* 16:1–8
- [62] Groth, I., Vetterman, R., Schuetze, B., Schumann, P., Saiz-Jimenez, C., 1999. Actinomycetes in Karstic caves of northern Spain (Altamira and Tito Bustillo). *J. Microbiol. Meth.* 36:115-122
- [63] Mulec J, Kosi G, Vrhovsek D (2008) Characterization of cave aerophytic algal communities and effects of irradiance levels on production of pigments. *J. Cave Karst Stud.*

70:3–12

[64] Vinogradova ON, Nevo E, Wasser SP (2009) Algae of the Sefunim Cave (Israel): Species diversity affected by light, humidity and rock stresses. *Int. J. Algae*, 11:99-116.

[65] Plooy SJ, Perissinotto R, Smit AJ, Muir DG (2015) Role of salinity, nitrogen fixation and nutrient assimilation in prolonged bloom persistence of *Cyanothece* sp. In Lake St Lucia, South Africa, *Aquat. Microb. Ecol.* 74:73–83

[66] Mota R, Rossi F, Andrenelli L, Pereira SB, Philippis De R, Tamagnini P (2016) Released polysaccharides (RPS) from *Cyanothece* sp. CCY 0110 as biosorbent for heavy metals bioremediation: interactions between metals and RPS binding sites. *Appl. Microbiol. Biotechnol.* 7765–7775

[67] Pattanaik B, Schumann R, Karsten U (2007) Effects of ultraviolet radiation on Cyanobacteria and their protective mechanisms. In: Seckbach J. (ed.) - *Algae and Cyanobacteria in extreme environments*. Springer, pp 29-45

[68] Deli J, Gonda S, Nagy LZS, Szabó I, Gulyás-Fekete G, Agócs A, Marton K, Vasas G (2014) Carotenoid composition of three bloom-forming algae species. *Food Res. Int.* 65:215–223

[69] Ortega-Calvo JJ, Ariño X, Hernandez-Marine M, Saiz-Jimenez C (1995) Factors affecting the weathering and colonization of monuments by phototrophic microorganisms. *Sci. Total Environ.* 167:329–341

[70] Golubic S, Perkins RD, Lukas KJ (1975) Boring microorganisms and microborings in carbonate substrates. In: FreyRW(ed.) *The Study of Trace Fossils*. Springer Verl, New York, pp 229–259

[71] Zhang X, Kan J, Wang J, Gu H, Hu J, Zhao Y, Sun J (2015) First record of a large-scale bloom-causing species *Nannochloropsis granulata* (Monodopsidaceae, Eustigmatophyceae) in China Sea waters. *Ecotoxicology* 24:1430-41

[72] Procházková K, Němcová Y, Neustupa J (2015) A new species *Jenufaaeroterrestrica* (Chlorophyceae incertae sedis, Viridiplantae), described from Europe. *Preslia* 87:403–416

[73] Hallmann C, Rüdlich J, Enseleit M, Friedl T, Hoppert M (2011) Microbial diversity on a

marble monument : a case study. *Environ. Earth Sci.* 63:1701–1711

[74] Falasco, E., Ector, L., Isaia, M., Wetzel, C.E., Hoffmann, L., Bona, F. (2014) Diatom flora in subterranean ecosystems: A review. *Int. J. Speleol.* 43:231–251

[75] Pouličková A, Hašler P (2007) Aerophytic diatoms from caves in central Moravia (Czech Republic). *Preslia* 79:185-204

[76] Selvi B, Altuner Z (2007) Algae of Ballica Cave (Tokat-Turkey). *Int. J. Nat. Eng. Sci.* 1: 99-103

[77] Stark LR, Greenwood JL, Brinda JC (2017) Desiccated *Syntrichiaruralis* shoots regenerate after 20 years in the herbarium Desiccated *Syntrichiaruralis* shoots regenerate after 20 years in the herbarium 6687. *J. Bryol.* 39:85-93

[78] La Farge C, Williams KH, England JH(2013) Regeneration of Little Ice Age bryophytes emerging from a polar glacier with implications of totipotency in extreme environments. *Proc. Natl. Acad. Sci.* 110:9839–44

[79] Mulec J, Kubešová S (2010) Diversity of bryophytes in show caves in Slovenia and relation to light intensities. *Acta Carsologica* 39:587–596

[80] Saarela M, Alakomi H, Suihko M, Maunuksela L, Raaska L, Mattila-Sandholm T (2004) Heterotrophic microorganisms in air and biofilm samples from Roman catacombs , with special emphasis on actinobacteria and fungi. *Int. Biodeter. Biodegrad.* 54:27–37

[81] Adetutu EM, Thorpe K, Bourne S, Cao X, Shahsavari E, Kirby G, Ball AS(2011) Phylogenetic diversity of fungal communities in areas accessible and not accessible to tourists in Naracoorte Caves. *Mycologia* 103:959-968

[82] Krumbein WE, Gorbushina A (1995) Organic pollution and rock decay. In: Morton LHG (ed.) *Biodeterioration of constructional materials*, pp 277–284

Synthèse du chapitre 1

L'étude sur la biodiversité, présentée dans ce premier chapitre, a permis pour la première fois d'analyser aussi précisément les communautés de bactéries, de diatomées, de champignons, de micro-algues ainsi que les mousses. Les résultats essentiels de cette étude sont listés ci-après.

En résumé :

- ✓ L'utilisation du primer 23S a permis l'identification des cyanobactéries, des micro-algues, des diatomées et des mousses.
- ✓ L'analyse de métabarcoding a permis d'apporter une information semi-quantitative quant à la proportion des taxons présents.
- ✓ Les bactéries et les cyanobactéries sont majoritaires dans les biofilms.
- ✓ Les mousses sont présentes, même si elles ne sont pas visibles à l'œil nu.
- ✓ Peu de différences ont été constatées dans les communautés de biofilms traités de ceux non traités.
- ✓ Une très grande différence de communauté a été mise en évidence entre les biofilms d'une même grotte.
- ✓ Les communautés composant les biofilms ne sont pas significativement différentes d'une grotte à une autre.

L'analyse des données obtenues peut être poursuivie notamment en corrélant les paramètres environnementaux aux populations formant dans les biofilms. De plus, des réseaux de co-occurrences pourraient apporter des informations sur les interactions positives ou négatives entre les différents types de populations.

Ces travaux menés dans cinq grottes pourraient être améliorés dans une future étude :

- En augmentant le nombre de réplicats afin d'augmenter la puissance statistique ;
- En choisissant des primers plus spécifiques à chaque type de taxon afin de pouvoir aller plus loin dans la taxonomie ;
- En utilisant des primers ciblant l'ADN viral afin d'avoir une vue globale sur le fonctionnement du biofilm ;

- En effectuant des prélèvements d'un biofilm tout au long d'une année afin de comprendre la dynamique de colonisation (espèces pionnière, apparition de nouvelles espèces, etc).

Afin de remédier à la prolifération des bactéries, des cyanobactéries, des micro-algues, des diatomées, des champignons et des mousses, l'utilisation d'un traitement à large spectre, tel que l'irradiation aux UV-C, doit être testée en laboratoire afin de prouver son efficacité, de comprendre les réponses physiologiques des organismes et d'optimiser le traitement.

Chapitre 2 : Effet des UV-C sur les micro-algues et les champignons formant les biofilms

Ce deuxième chapitre présente les résultats de l'effet des UV-C sur la micro-algue verte *Chlorella* sp. préalablement échantillonnée à la grotte des Moidons. Cette première partie est rédigée sous la forme d'un article scientifique publié dans *Journal of Applied Phycology* et d'un article scientifique soumis dans *Environmental science and Pollution Research*. Le chapitre présente également les effets des UV-C sur six champignons colonisant les biofilms dans les grottes.

Dans la première partie, les effets des UV-C seront étudiés au niveau de la chlorophylle, de la photosynthèse (photosynthèse et respiration), du rendement quantique (Fv/Fm) et de la viabilité cellulaire. L'effet de la lumière visible post-traitement est analysée à des fins d'optimisation du traitement aux UV-C.

La seconde partie concerne les champignons et apportera un premier éclairage sur les effets des UV-C sur la mortalité fongique suite à une irradiation.

Effects of UV-C radiation on *Chlorella vulgaris*, a biofilm-forming alga

Stéphane Pfendler ^{a*}, Badr Alaoui-Sossé ^a, Laurence Alaoui-Sossé ^a, Faisl Bousta ^b and Lotfi Aleya ^a

^a Laboratoire Chrono-Environnement – UMR 6249, Université de Bourgogne Franche-Comté Besançon.

^b Centre de Recherche sur la Conservation - Laboratoire de recherche des monuments historiques – USR 3224, Champs-Sur-Marne, Paris.

* email: stephane.pfendler@univ-fcomte.fr;

16, route de Gray, BESANCON, France

Telephone: + 33 (0) 3 81 66 65 98

Fax: + 33 (0) 3 81 66 57 97

Journal of Applied Phycology
<https://doi.org/10.1007/s10811-017-1380-3>



Effects of UV-C radiation on *Chlorella vulgaris*, a biofilm-forming alga

Stéphane Pfendler ¹ · Badr Alaoui-Sossé ¹ · Laurence Alaoui-Sossé ¹ · Faisl Bousta ² · Lotfi Aleya ¹

Received: 24 July 2017 / Revised and accepted: 21 December 2017
© Springer Science+Business Media B.V., part of Springer Nature 2018

Abstract

Photosynthetic biofilms proliferating on heritage monuments represent a major threat for curators leading to biodegradation and aesthetic issues. Previous studies demonstrated that UV-C, used as a tool for biofilms eradication, is a promising avenue to combat microbial proliferation. In this study, this environmentally friendly method was tested on biofilm-forming *Chlorella vulgaris* suspension. Algal physiological response to UV-C was then assessed. Results showed that $>10 \text{ kJ m}^{-2}$ UV-C exposure was enough to directly kill cells whereas low UV-C exposition reduced quantum yield of photosystem II and inhibited both respiration and photosynthesis. Clear relationships between UV-C exposure times and physiological responses were found. In addition, the use of VIS-light after UV-C treatment enhances chlorophyll bleaching. Our findings contribute to a better understanding of the physiological responses of *Chlorella vulgaris* to UV-C radiations allowing thus an optimization of the UV-C treatment reported in our previous studies.

Key words: UV-C, *Chlorella*, Photosystem II, Bleaching, Biofilm

1. Introduction

Show caves suffer from the “green disease” due to touristic exploitation with the proliferation of photosynthetic biofilms mainly formed by cyanobacteria and microalgae (Smith et Olson 2007; Mulec and Kosi 2009; Lamprinou et al. 2014; Popovic et al. 2015). Microorganism development is mainly due to artificial lighting, carbon dioxide and temperature increase (Faimon et al. 2006; Mulec et al. 2008; Piano et al. 2015; Popovic et al. 2015) which represents a major issue for cave curators. For example, biofilms lead to aesthetic aspects on cave walls, speleothems or parietal paintings (Canaveras et al. 2001) due to unwanted presence of black or green color (Mihajlovski 2014) and to biochemical and/or biophysical erosion (Aley 1972; Elliott 1997; Olson 2002; Cennamo 2012).

In order to combat biofilm formation, cave managers usually use chemicals or biocides (Smith and Olson 2007) which endanger the cave’s fauna. The remaining by-products can infiltrate the karst network leading to environmental issues (Boston 2006; Elliot 2006; Hildreth-Werker and Werker 2006). In addition, these treatments are ineffective and contribute to the selection and proliferation of human pathogens (Urzi et al. 2000) along with inducing fungi resistance (Bastian et al. 2009). Finally, chemicals might be used as carbon and nitrogen source for many heterotroph microorganisms. Thus, it becomes urgent to apply environmentally friendly treatments.

UV-C treatment is commonly used as germicide in surgery (Menetrez et al. 2010), laboratories and industries. Grobbelaar (2000) and Mulec and Kosi (2009) suggested the use of this treatment in show caves and Borderie et al. (2011; 2014) demonstrated its efficiency in the French show cave “Les Moidons” since UV-radiations induced a strong bleaching of biofilms with no recolonization observed during sixteen months. To optimize this bleaching, VIS-light exposition can be applied to increase chlorophyll degradation (Sztatelman et al. 2015).

As far as we know, there are only a few reports detailing UV-C effects on algae and cyanobacteria (Gao et al. 2009) according to UV-A and UV-B light, which reach the surface of the earth (Kulandaivelu and Noorudeen 1983). Short UV-C wavelengths are highly energetic and drastically affect algae metabolic functions such as photosynthesis leading to cell death (Gao et al. 2009). Moreover, DNA is a major target of UV-C radiation which breaks the DNA double strand structure (Bolige et al. 2005) or induces several types of mutation, for example thymine dimers. UV-radiation can oxidize proteins along with inducing conformational changes resulting in enzyme dysfunction (Kreslavski et al. 2012). Wang et al. (2015) and Borderie et al. (2014) reported both lipid and membrane damages after UV-C treatment of the bloom forming cyanobacteria and algae, probably due to an increase in reactive oxygen species (ROS) levels.

The objective of this work is to identify the UV-C effects on *Chlorella* sp., a biofilm-forming microalgae widely present in touristic caves (Grobbelaar 2000; Borderie et al., 2011; 2015). We thus 1) analyzed after different UV-C expositions different physiological parameters such as cell viability, chlorophyll degradation, quantum yield, as well as dioxygen exchange rates, 2) monitored chlorophyll degradation during several days and 3) to understand the role of VIS-light after treatments the microalgae cultured under either normal experimental conditions or maintained in darkness were exposed to UV-C.

2. Materials and methods

2.1. Sampling and grow method culture

Phototrophic biofilms were collected from several wall sections of the Moidons Caves in France (05° 48' 21.5'' E and 46° 50' 20.7'' N). Biofilm sampling was performed with sterile swab and subsequently cultivated in modified BG11 growth medium (added with 15 g l⁻¹ pure agar). Then, *Chlorella* sp. strain was isolated and identified using a Sanger sequencing. The pure algal culture was cultured in 400 ml sterile bottles using liquid BG11 medium with permanent aeration. Algae cultures were maintained at 20°C under 16 hours light per day (about 150 μmol photons m⁻² s⁻¹, 8 lamps T5 54W 6500K).

2.2. Sanger sequencing

DNA was extracted by dissolving a colony in 100 μl Prepman Ultra solution (Applied Biosystems). The suspensions were then heated at 95°C for 10 min. After centrifugation, 2.5 μl of supernatant from each sample were added to 250 μl ultrapure water. PCR reaction solutions were mixed as follows: 12.5 μl of DNA, 2 μl of forwards p23SrV_f1 (5'-GGACAGAAA- GACCCTATGAA-3') and reverse primers p23SrV_r1 (5'-TCAGCCTGT-TATCCCTAGAG-3') (Sherwood and Presting, 2007), 25 μl of mastermix and 8.5 μl of ultrapure water. Then, DNA was amplified using following PCR steps: denaturation at 94°C/2 min, 20 cycles of 94°C/20 sec, 55°C/30 sec, 72°C/30 sec and final elongation 72°C/5 min. Two μl of ExoSAP[®] solution were added to 5 μl of amplified DNA (37°C/15 min and 80°C/15 min). Afterwards, samples were amplified with fluorescent ddNTP (Big Dye Terminator 3.1, Applied Biosystems) and purified with Big Dye X Terminator (Applied Biosystems). Sequencing was finally done with a 3130 DNA sequencer.

2.3. UV-C treatments

Cells in the exponential growth phase were treated with UV-C light (0, 2, 4, 6, 8, 10, 20, 30 kJ m⁻², corresponding to 2.6, 5.2, 7.8, 10.4, 13, 26 and 39 min respectively). Fifteen mL of algal suspension (10⁶ cells ml) were used for each treatment. Irradiations were performed in the bottom half of glass Petri dishes and under constant agitation. Treatments were performed with UV-C Box (Borderie et al. 2014) that contains 4 UV-C lamps (Philips, 25 W each = 100 W, λ max = 254 nm). In order to avoid the heat generated by the lamp, an air-conditioner was used to maintain the temperature at 20 °C \pm 1 °C during all experiments.

2.4. Survival tests

FDA stock solution (C₂₄H₁₁O₇, 97% pure, ACROS Organics) was prepared by dissolving FDA powder in acetone (99%) to a concentration of 10 mg mL⁻¹ and then stored at -20°C. A working solution was prepared by adding 40 μ L of stock solution to 10 ml deionized water. After exposure to UV-C radiation, cells were harvested by centrifugation at 6 000 g for 5 min and washed with Phosphate-Buffered Saline (PBS). 400 μ l of each washed cells in suspension were incubated with 300 μ l of FDA solution for 15 min in the dark at room temperature. The fluorescence measurement was then carried out at 535 nm by flow cytometry (flow cytometer Accuri™ C6, $\lambda_{\text{excitation}}$ = 475 nm).

A second experimentation was carried out to confirm *Chlorella vulgaris* viability by culturing it on solid BG11 medium in Petri dishes. After each treatment, 100 μ l of irradiated and non-irradiated suspensions were sub-cultured and plates were maintained under the previously described culture conditions (150 μ mol photons m⁻² s⁻¹).

2.5. Absorbance spectroscopy

Chlorella vulgaris suspensions were exposed to several UV-C expositions (0, 2, 4, 6, 8, 10, 20, 30 kJ m⁻²). Subsequently, spectrum of algal suspensions was measured using a spectrometer Analytikjena specord 205 (wavelengths between 350 nm and 750 nm). Then, irradiated suspensions were divided in two suspensions and cultivated under culture conditions or in the darkness. Both culture spectra were measured daily during 5 days.

2.6. Oxygen measurement

O₂ evolution rate was followed with an oxygraph (DW2/2 Electrode Chamber) equipped with a Clark oxygen electrode (S1 oxygen electrode disc, Hansatech Instruments). Electrode calibration was carried out with sodium metabisulfite powder. Then, oxygen concentration rate of 2 mL treated (2.5, 5, 7.5 and 10 kJ m⁻²) and untreated algal suspensions was measured every 5 min during 15 min in dark-adapted chamber at 25 °C (5 min in darkness: 0 μmol m⁻² s⁻¹), 5 min with low light intensity: 340 μmol m⁻² s⁻¹) and 5 min with high light: 980 μmol m⁻² s⁻¹) (1 halogen lamp, OSRAM[®], GU5.3, 50W, 12V). The samples were continuously stirred to prevent algal sedimentation. The Hansatech Software calculated the O₂ evolution rate in nmol O₂ min⁻¹ mL⁻¹.

2.7. Kinetics of chlorophyll degradation

Following UV-C irradiation (30 kJ m⁻²), microalgae were cultivated under the 8 previously described lamps until total chlorophyll degradation. A fraction of each culture was isolated before irradiation (control), and then every hour after 14 hours of irradiation.

To measure pigment absorption spectra for spectral scanning 350 to 750 nm samples were centrifuged at 6000 g for 5 minutes at 4°C (centrifuge 5415R Eppendorf™). To optimize extraction the obtained pellets were incubated overnight in 5 mL of methanol at 4°C

in the dark. The samples were then milled for 5 minutes in a grinder with Fontainebleau sand and placed in the dark at 4°C for 1 hour. Supernatants were collected after centrifugation at 6000 g at 4°C for 5 min. Normalized sample concentration was obtained by adjusting the volume with methanol to 10 ml. Pigment extract absorption was analyzed with the spectrometer Analytikjena specord 205.

Chlorophyll *a* and *b* concentrations were then calculated according to Lichtenthaler and Wellburn (1983):

$$\text{Chl } a = 15,65 \times A_{666} - 7,34 \times A_{653}$$

$$\text{Chl } b = 27,05 \times A_{653} - 11,21 \times A_{666}$$

2.8. Quantum yield and chlorophyll fluorescence measurements

Treated and non-treated (0, 2, 4, 6, 8, 10, 20, 30 kJ m⁻²) *Chlorella vulgaris* suspensions (10 ml) were filtered through a cotton disk (1 cm diameter) with a vacuum pump. The discs were then placed for 30 min at room temperature in the dark. Fluorescence parameters (quantum yield (Fv/Fm), photochemical quenching (qP), non-photochemical quenching (NPQ)) were then monitored using the photosynthesis yield analyser mini-PAM (WALZ, Germany) as follows:

$$Fv/Fm = \phi_{PSII} / qP$$

$$qP = (Fm' - F) / (Fm' - Fo)$$

$$NPQ = Fm - Fm' / Fm'$$

2.9. Statistical analysis

All statistical analyses were conducted using R.2.14 software (R Development Core Team, 2011) at a significant level of 0.05. Parametric statistics (ANOVA) were used after

checking normality (Shapiro test) and homogeneity of variances (Bartlett test of equality of variances). All treatments were carried out in 5 replicates.

Half maximal effective concentrations (EC50) were calculated using the Dose Response Curve (DRC) library (Ritz et al., 2015) with R 3.4.2 software and a 4 parameters Weibull model.

3. Results

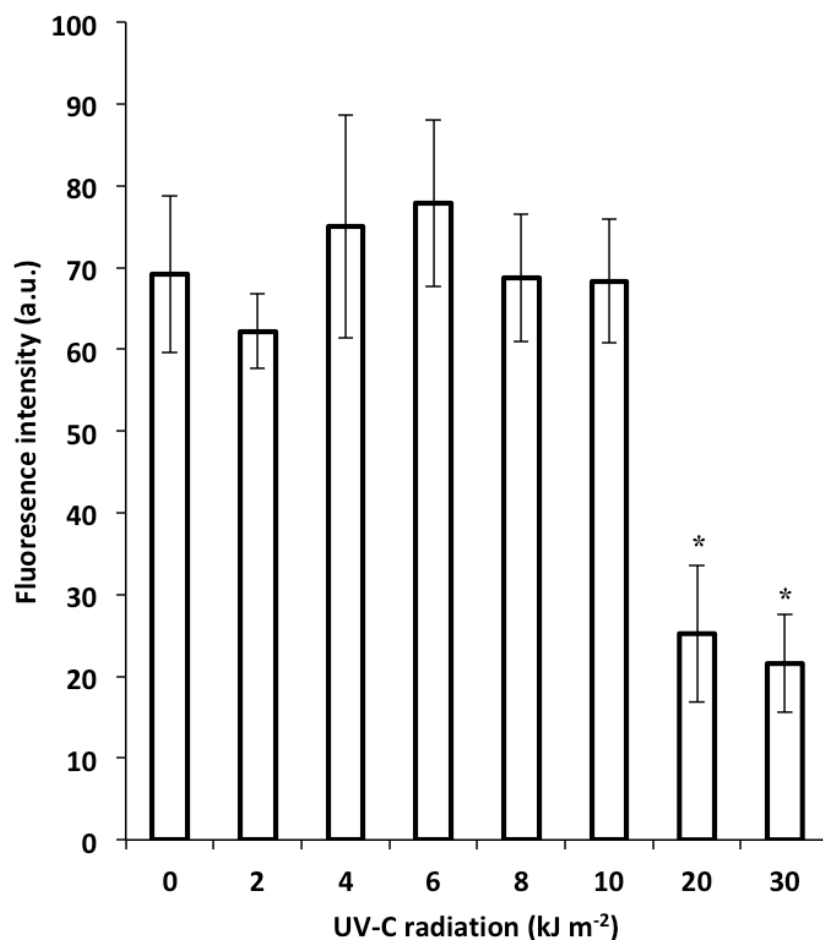
3.1. Algal strain identification

The previously isolated algal strain was identified by microscopic observation as *Chlorella vulgaris* (Chlorophyta). This result was confirmed through comparison of sequencing data to Genbank (identification at 99%).

3.2. Cell viability test

Results of cell viability showed no significant difference in comparison to the control when samples were treated with $\leq 10 \text{ kJ m}^{-2}$ UV-C ($p\text{-value} > 0.05$) (Fig. 1). Furthermore, UV-C doses $> 10 \text{ kJ m}^{-2}$ led to direct cell death ($p\text{-value} < 0.05$). Then, treated and untreated algae were put in Petri dishes and cultivated during three weeks. With the exception of the control, no cells were able to build new assemblages (data not shown).

EC50 have been calculated using “ED” function. Results showed that EC20 (20% inhibition), EC50 (50% inhibition) and EC90 (90% inhibition) corresponded to 11.18, 13.25 and 19.36 kJ m^{-2} respectively.



* : P-value < 0.05 (comparison to the control), n = 5 ; Error bars correspond to the standard error.

Fig. 1. FDA survival test was performed on untreated algae and on UV-C exposed suspensions (2, 4, 6, 8, 10, 20 and 30 kJ m⁻²).

3.3. Optical density of irradiated algae suspension

Chlorophyll degradation kinetics was daily monitored with a spectrometer until total bleaching. Results of light-maintained samples exposed to ≤ 10 kJ m⁻² showed a complete degradation of chlorophylls *a* and *b* after two days of UV-radiation (Fig. 2) while ≤ 20 kJ m⁻² irradiated sample needed only one day. The control showed an increase in chlorophyll intensity whereas the samples maintained in darkness (Fig. 3) showed a lower degradation kinetics with no complete degradation. It is noteworthy that the control also started to decrease.

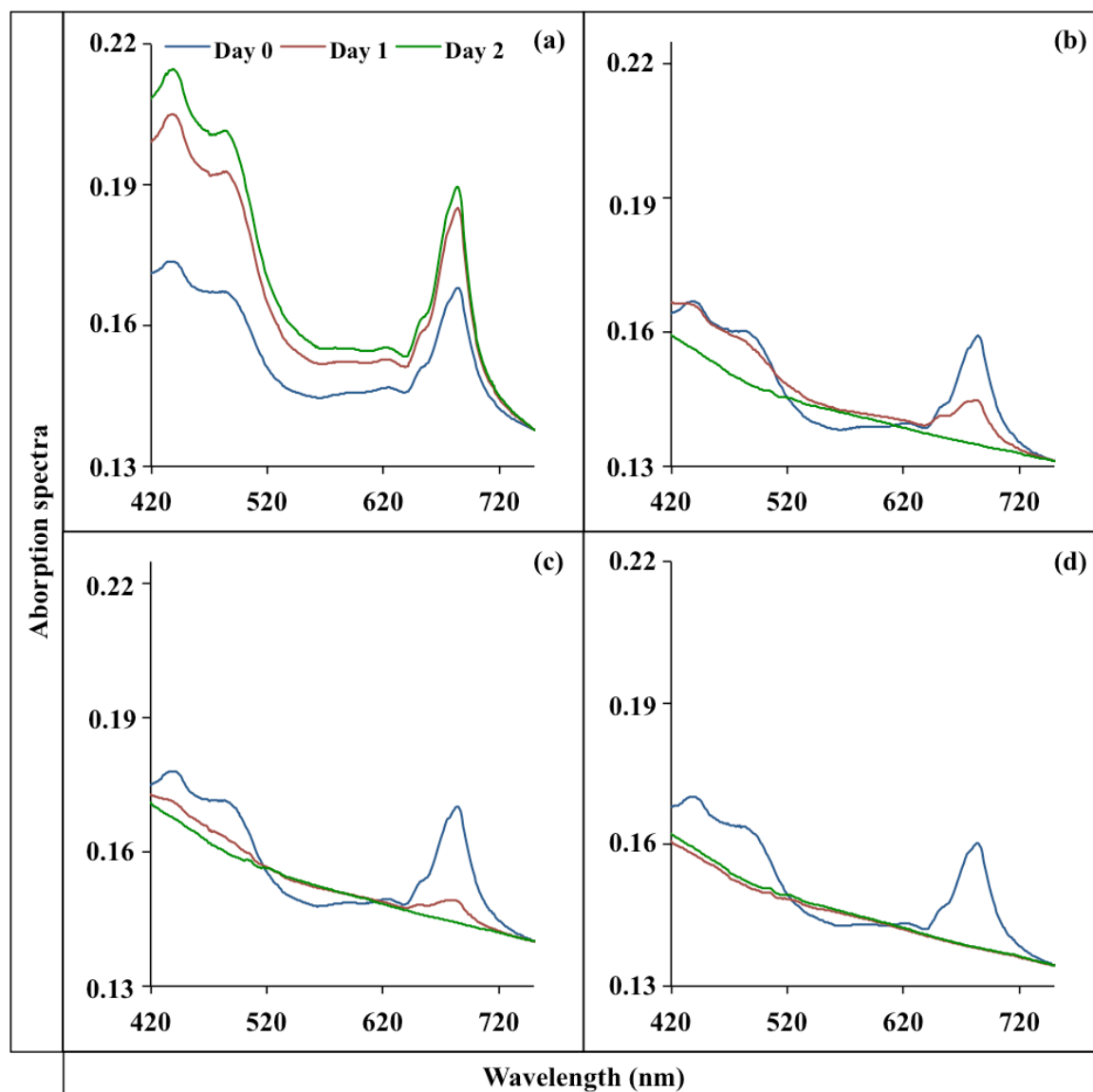


Fig. 2. Absorbance spectra of *Chlorella vulgaris* following (a) 0, (b) 2, (c) 10 and (d) 30 kJ m⁻² UV-C irradiations. Alga suspensions were maintained under culture condition.

3.4. Chlorophyll extraction

Chlorophylls from 30 kJ m⁻² irradiated algae was extracted with methanol and its degradation kinetics monitored for 14 hours. Results showed that chlorophyll *a* and *b* concentrations decreased until complete degradation (Fig. 4). After irradiation, chlorophyll *b* concentration was half that of chlorophyll *a*. However, 14 hours after UV-C treatment chlorophyll *b* concentration was twice that of chlorophyll *a*. Figure 4 also shows faster

chlorophyll *a* degradation. These results were confirmed by the calculation of both chlorophyll degradation constants. Indeed, chlorophyll *a* constant k with 0.148 h^{-1} ($R^2 = 0.97$) was higher than that of chlorophyll *b* (0.045 h^{-1} , $R^2 = 0.92$).

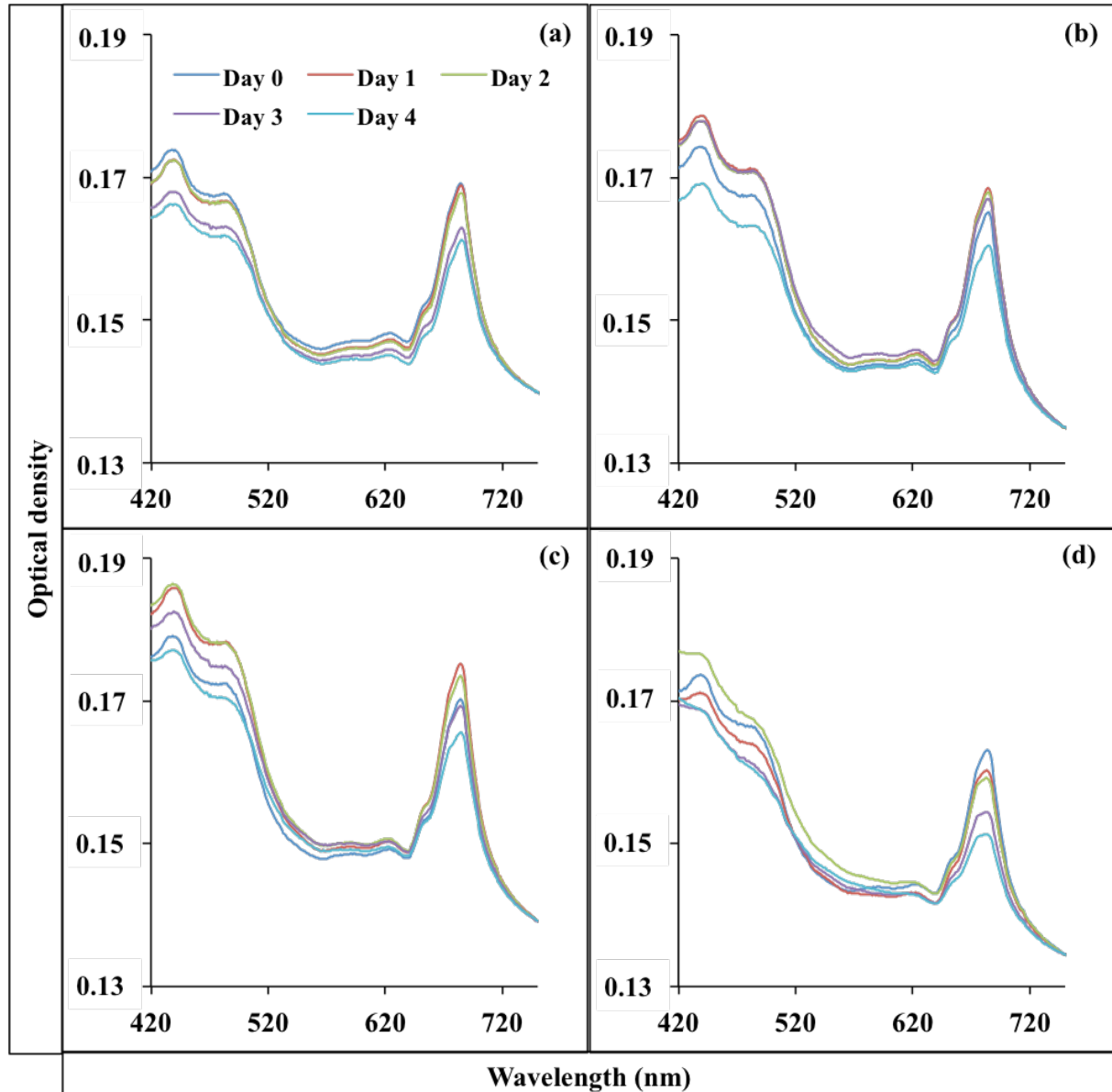


Fig. 3. Absorbance spectra of *Chlorella vulgaris* following (a) 0, (b) 2, (c) 10 and (d) 30 kJ m^{-2} UV-C irradiations. Alga suspensions were maintained in the darkness.

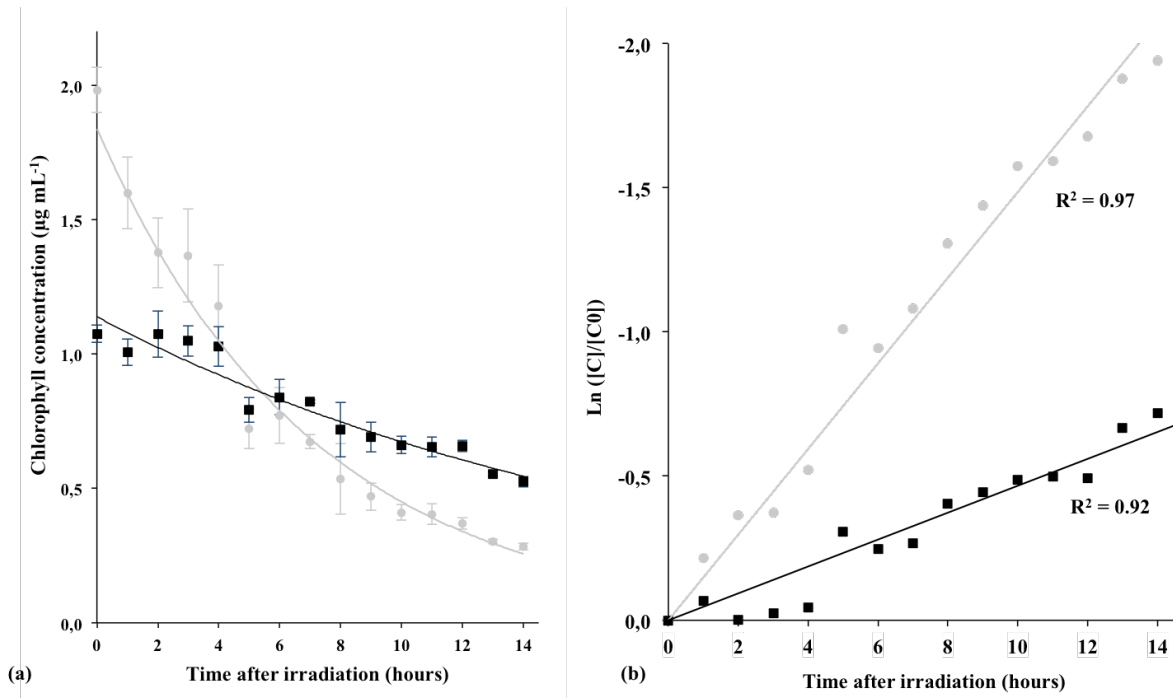


Fig. 4. The kinetic of chlorophyll *a* (•) and *b* (■) after 30 kJ m⁻² irradiation was carried out over 14 hours.

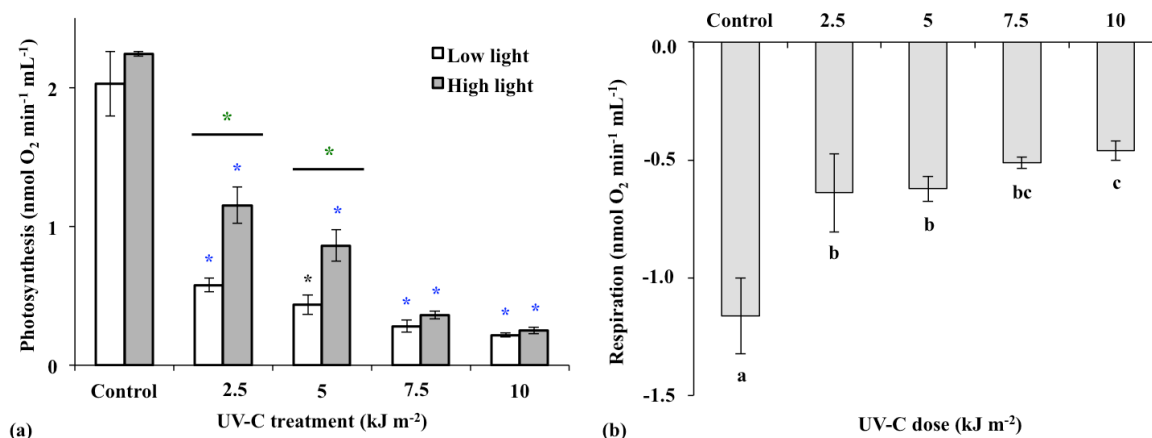
3.5. O₂ evolution rate and PSII activity

In order to demonstrate UV-C effects, both photosynthetic activity and dioxygen production were measured.

- Respiration and oxygen production

Whatever the VIS-light intensity results of O₂ production showed no difference between both controls (Fig. 5). However, a significant decrease in O₂ concentration (p-value < 0.05) was observed for all treatments after UV-C radiation. Moreover, both high and low irradiated samples (2.5 and 5 kJ m⁻²) were significantly different (p-value < 0.05). In fact, O₂ production was higher with high light intensity. However, no difference was observed for samples exposed to UV-C at 7.5 and 10 kJ m⁻² of.

Respiration measurements for all samples showed a significant decrease in O₂ consumption (p-value < 0.05) (Fig. 5). Thus, UV-C exposure time could be negatively correlated with *Chlorella vulgaris* O₂ consumption.



* : P-value < 0.05 (in comparison to the control), n = 5 ; * : P-value < 0.05 (comparison between low and high light), n = 5 ; Error bars correspond to the standard error.

Fig. 5. Evolution of *Chlorella vulgaris* photosynthesis (a) and respiration (b), before and after 2.5, 5, 7.5 and 10 kJ m⁻² UV-C exposition.

- Photosystem II physiological status

Results showed that quantum yield values decreased quickly after UV-C exposition with an EC₅₀ attaining 5 kJ m⁻² (Fig. 6). Furthermore, Fv/Fm values showed a dose-dependent response. In fact, the longer the treatment the more efficient the UV-C effect on algae PSII was. The results obtained after the treatment exhibited a logarithmic shape (R² = 0.98). The quantum yield values before irradiation ranged from 30 to 0.63 kJ m⁻² UV-C. It is noteworthy that over time and for the samples exposed to >2kJ m⁻², quantum yield values decreased to <0.1 four hours after irradiation.

The photochemical quenching coefficient ranging between 0 and 1 gives an estimation of the number of open reaction centers with the value of 1 reflecting a normal photosystem performance. The results showed that UV-C radiations led to an important decrease in

photochemical quenching values (Fig. 6). Moreover, UV-C treated samples exposed to >6 kJ m⁻² attained 0 after 4 hours.

NPQ ranged from 0 to 9, with 0 for healthy organisms. The results observed directly after treatments ≤ 10 kJ m⁻² showed a dose dependent response (Fig. 6). However, no evolution was observed over time. In contrast, for 20 and 30 kJ m⁻² NPQ increases every hour until attaining 5.4 and 8.9 kJ m⁻² respectively.

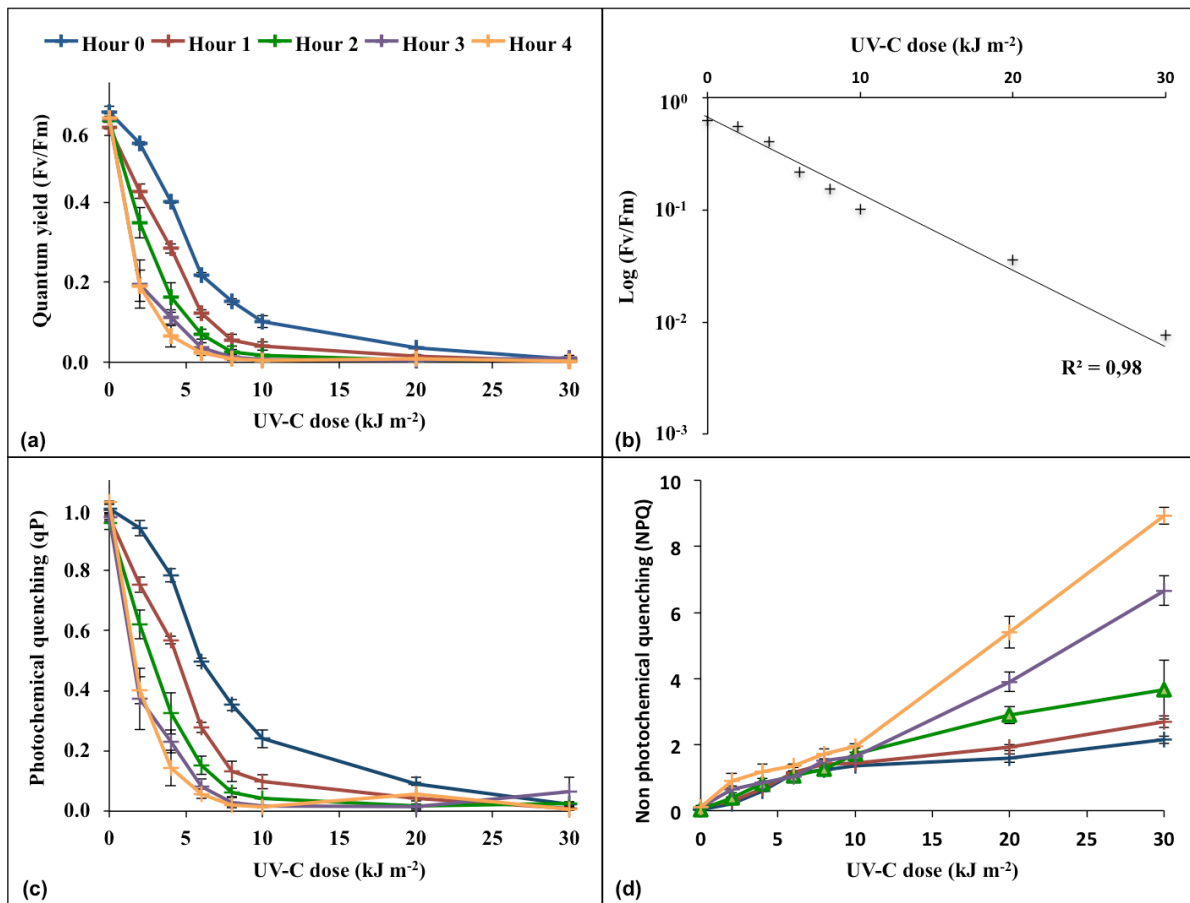


Fig. 6. Quantum yield (Fv/Fm) (a), photochemical quenching (qP) (c) and non-photochemical quenching (NPQ) (d) were monitored before and after UV-C irradiations (0, 2, 4, 6, 8, 10, 20 and 30 kJ m⁻²). Graphic (b) represents the quantum yield of *Chlorella vulgaris*, which was measured directly after the treatment and represented in logarithmic scale.

4. Discussion

The objective of this study was to investigate the effects of UV-C exposition on *C. vulgaris*, which is proliferating in the Moidons Cave. We monitored cell death, dioxygen evolution rate, chlorophyll degradation and photosystem II activities directly after irradiation and/or during a few hours or days following the treatment.

- *Chlorella vulgaris* tolerance to UV-C exposition

In our previous work (Borderie et al. 2014) we reported that the genus *Chlorella* was killed after a long UV-C exposition (150 to 300 kJ m⁻²). However, in this study, we used a lower UV-C exposition to refine *C. vulgaris* physiological responses to UV-C stress. In addition to cytometry results, monitoring of *C. vulgaris* culture showed that lower UV-C radiation (2 to 10 kJ m⁻²) resulted in death-delayed effects whereas algae irradiated at ≥ 20 kJ m⁻² were killed directly after exposition (Fig. 1). These results conformed to those of Moharikar et al. (2006) who also demonstrated a delayed cell death of the Chlorophyta *Chlamydomonas reinhardtii* at 1 – 100 J m⁻². Wang et al. (2015) indicated that the cyanobacteria *Microcystis aeruginosa* is able to grow only after low UV-C exposition (20 mJ cm⁻²).

The effects of UV radiation (UV-A, UV-B or UV-C) are highly nonspecific. For example, autotroph microorganisms are disturbed because UV-C targets DNA (Sinha et Hader 2002; Xue et al. 2005). Takeuchi et al (1996) reported that UV-radiations destroy the double bonds of unsaturated fatty acids, change the chemical properties of phosphor- and glycolipids and affect membrane integrity. In this sense, lipid injuries were also confirmed by Borderie et al. (2014) and Wang et al. (2015). Proteins are also a major target of UV-C (Neves-Petersen et al. 2012) which impair protein structure and enzyme activities such as those of Rubisco, ATP synthase and violaxanthin de-epoxidase (Nasibi and M'Kalantari

2005; Vass et al. 2005; Nawkar et al. 2013). Furthermore, mitochondria and chloroplasts produce reactive oxygen species (ROS) in response to UV-C radiation, acting downstream of the *radical induced cell death* gene (*AtRCD1*) thus making plants vulnerable to cell death (Nawkar et al. 2013).

On the other hand, tolerance mechanisms towards UV radiation can be seen among autotrophs. For example, during the period in which cyanobacteria thrived (3500 to 2800 Ma ago), no ozone layer blocked the shortwave UV radiation (UV-C and UV-B) suggesting that cyanobacteria or other early organisms developed certain resilience towards UV radiation-induced stress (Sanchez et al. 2014). Two decisive strategies are indeed used by organisms to face excessive levels of harmful UVR (Sanchez et al. 2014): either repairing or avoiding damages (Björn 2007) by means, for example, of mycosporine-like amino acids (Karsten et al. 2007). The genes involved in MAPK cascade can also confer tolerance against UV radiation (Nawkar et al. 2013). However, since UV-C exposition achieved in this study was quite high it had certainly generated irreversible damages to *Chlorella*.

- Respiration of *C. vulgaris*

Despite the absence of immediate effects on survival rates (0 to 10 kJ m⁻²), results showed that 2.5 kJ m⁻² was enough to significantly decrease respiration rates. However, several authors using lower UV intensities reported that respiration remained stable for some algae strains after UV-A and UV-B exposition (Aguilera et al. 1999). We infer that UV-C light is much more harmful than UV-A and UV-B. For instance, Bolige et al. (2005) reported that the Euglenophyta *Euglena gracilis* was thirteen times more sensible to UV-C than to UV-B. To justify the increase in respiration Aguilera et al. (1999) reported that phototrophic organisms attempt to guarantee the maintenance of basal metabolism while Mulley et al. (2001) attributed such an increase to enhanced residual respiration in *Chlamydomonas*

reinhardtii. However, the alternative oxidase pathway is inhibited following exposure to UVA, B and C and the increased oxygen uptake in UV-treated cells may not be due to true respiratory activity. According to these authors, the simultaneous increase in residual oxygen uptake may not be due to true respiratory activity but likely to an increased lipoxygenase activity. In the present study, however, even with the lowest UV intensity (2 kJ m^{-2}) the cells were extremely damaged preventing to assess the above processes.

- UV-C effect on photosynthesis

Both low ($340 \text{ } \mu\text{mol m}^{-2} \text{ s}^{-1}$) and high ($980 \text{ } \mu\text{mol m}^{-2} \text{ s}^{-1}$) exposition for the control impacted equally the photosynthetic activity. These results infer that the lighting used here was not a limiting factor. In fact, “low” light could represent a lower limit of PSII needs because high radiations did not stimulate photosynthesis and conversely, no photo-inhibition was observed with high light exposition. For instance, excessive light intensity (2400 to $3000 \text{ } \mu\text{mol m}^{-2} \text{ s}^{-1}$) has been shown to damage microalgae because of the overloaded photosystems, bleached pigments and broken photosystem II (Zhao et al. 2013; Cheirsilp and Torpee 2012). Beyond these values, photoinhibition defined as the light-dependent inactivation of photosystem II (PS II) reaction centers, can occur. However it may be restored *via* the degradation and synthesis of the D1 protein (Tyystjärvi and Aro 1996).

For irradiated algae, the question remains whether UV-C light acted in the same way as with an excess of VIS-light. Exposed to both low and high light, both 2.5 and 5 kJ m^{-2} UV-C treated samples exhibited different photosynthetic activities with high light enhancing significantly photosynthesis after UV-C treatment. Shelly et al. (2003) also demonstrated with the marine Chlorophyta *Dunaliella tertiolecta* that recovery after UV-B exposure increased with PAR up to $300 \text{ } \mu\text{mol}$ quanta, but no recovery was seen in the absence of PAR during the post UV-B exposure period. These findings indicate that the lack of light available for

photosynthesis likely depresses the repair mechanisms either directly or indirectly by affecting ATP synthesis (Shelly et al. 2003). However, no recovery was observed after higher UV-C radiations ($\geq 7.5 \text{ kJ m}^{-2}$) under high VIS-light exposition. We infer that these high radiations depressed any repair mechanisms able to overcome metabolism damages.

- Inactivation and destruction of PSII

A significant decrease in quantum yield (Fv/Fm) immediately after UV-C exposure was observed while chlorophyll degradation was delayed depending on light conditions (dark or light culture conditions). In fact, the quantum yield reached null values while it should approach 0.83 for higher plants (Maxwell and Johnson 2000) and ranges from 0.6 to 0.8 for micro-algae. These results indicated that UV-C drastically inactivated PSII leading to its destruction (Takeuchi et al. 1996; Sass et al. 1997, Wong et al. 2015).

While chlorophyll molecules still absorb photons light in excess is detrimental. For this reason, non photo-chemical quenching increased to reduce the excess excitation energy at the PSII and to avoid the formation of ROS in chloroplasts (Fernandez-Marin et al. 2010) by means of photoinhibition, including an active degradation of D1 protein and dissipation of zeaxanthin-driven thermal (Demming-Adam and Adams 1996; Krause and Jahns 2004). Moreover, increase in NPQ is associated with a decrease in photochemical quenching (qP), yet NPQ protective mechanisms failed to save algal cells from death.

- Delayed chlorophyll degradation

Our results showed that chlorophyll degradation did not occur immediately after UV-C exposition indicating that pigment degradation was not responsible of photosynthesis decrease. Moreover, chlorophyll destruction was slowed down and delayed for the samples maintained in darkness in contrast with enlightened samples. These results corroborate those

of Sztatelman et al. (2015) who studied the photosynthesis-related genes of *Arabidopsis thaliana*, its chlorophyll content and photosynthetic efficiency. For instance, both UV-B and UV-C are routinely used in the food industry to prevent vegetable yellowing during storage (Aiamla-or et al. 2010; Srilaong et al. 2011; Chairat et al. 2013) through inhibition of chlorophyllase, Mg-dechelataase and chlorophyll peroxidase involved in chlorophyll degradation pathways (Costa et al. 2006; Jiang et al. 2010; Aiamla-or et al. 2010). It is noteworthy, however, that UV-B and UV-C irradiation doses used in order to delay senescence in food industry are sublethal, *i.e.* much lower than those assayed in this study.

5. Conclusions

This study showed that *C. vulgaris* photochemical metabolism is strongly targeted by UV-C radiations at low UV-C radiations as reflected by the decline in respiration photosynthesis, quantum yield and photochemical quenching. Moreover, chlorophyll degradation was delayed and bleaching is light dependent. This finding highlights the need of exposing photosynthetic microorganisms to VIS-light to further optimize *in situ* treatments.

6. Acknowledgements

We thank the *Ministère de la Culture et de la Communication* (France), the *Laboratoire de Recherche des Monuments Historiques* (LRMH, Paris) and the Conseil Régional of Franche-Comté for their financial aid. We express our appreciation to the editor, Michael A. Borowitzka, and to the anonymous reviewers for helping to improve our paper.

7. References

Aguilera J, Karsten U, Lippert H, Vogele B, Philippe E, Hanelt D, Wiencke C (1999) Effects of solar radiation on growth, photosynthesis and respiration of marine macroalgae from the Arctic Mar Ecol Prog Ser 191:109-119.

Aiamla-or S, Kaewsuksaeng S, Shigyo M Yamauchi N (2010) Impact of UV-B irradiation on chlorophyll degradation and chlorophyll-degrading enzyme activities in stored broccoli (*Brassica oleracea* L. Italica Group) florets. Food Chem 120:645-651.

Aley T (1972) Control of unwanted plant growth in electrically lighted caves. Caves Karst J 14:33-35.

Bastian F, Alabouvette C, Saiz-Jimenez C (2009) The impact of arthropods on fungal community structure in Lascaux Cave. J Appl Microbiol 106:1456-62.

Björn LO (2007) Stratospheric ozone, ultraviolet radiation and cryptogams. Biol Conserv 135:326-333.

Bolige A, Kiyota M, Goto K (2005) Circadian rhythms of resistance to UV-C and UV-B radiation in *Euglena* as related to “escape from light” and “resistance to light.” J Photochem Photobiol B: Biol 81:43-54.

Borderie F, Alaoui-Sossé L, Raouf N, Bousta F, Oriol G, Riefel D, Aaloui-Sossé B (2011) UV-C irradiation as a tool to eradicate algae in caves. *Int Biodeterior Biodegrad* 65:579-584.

Borderie F, Tête N, Cailhol D, Alaoui-Sehmer L, Bousta F, Rieffel D, Aleya L, Alaoui-Sossé B (2014) Factors driving epilithic algal colonization in show caves and new insights into combating biofilm development with UV-C treatments. *Sci Total Environ* 484:43-52.

Borderie et al. 2015 (ESPR, cytométrie

Boston P (2006) To bleach or not to bleach: algae control in show caves. *In*: Hildreth-Werker V. & Werker J.C., editors. *Cave Conservation and Restoration*. Huntsville: National Speleological Society: 349-350.

Canaveras JC, Sanchez-Moral S, Soler V, Saiz-Jimenez C (2001) Microorganisms and microbially induced fabrics in cave walls. *Geomicrobiol J* 18:223-240.

Cennamo P, Marzano C, Ciniglia C, Pinto G, Cappelletti P, Caputo P, Pollio A (2012) A survey of the algal flora of anthropogenic caves of Campi Flegrei (Naples, Italy) archeological district. *J Cave Karst Stud* 74:243-250.

Chairat B, Nutthachai P, Varit S (2013) Effect of UV-C treatment on chlorophyll degradation, antioxidant enzyme activities and senescence in Chinese kale (*Brassica oleracea var . alboglabra*). *Int Food Res J* 20:623-628.

Cheirsilp B, Torpee S (2012) Enhanced growth and lipid production of microalgae under mixotrophic culture condition: effect of light intensity, glucose concentration and fed-batch cultivation. *Bioresour Technol* 110:510-516.

Costa L, Vicente AR, Civello PM, Chaves AR, Martínez GA (2006) UV-C treatment delays postharvest senescence in broccoli florets. *Postharvest Biol Tec* 39:204-210.

Demming-Adams B, Adams WW (1996) The role of xanthophyll cycle carotenoids in the protection of photosynthesis. *Trends Plant Sci* 1:21-26.

Elliott W (2006) Biological dos and don'ts for cave conservation and restoration – best management practices. In: Hildreth-Werker V. & Werker J.C., editors. *Cave Conservation and Restoration*. Huntsville: National Speleological Society: 33-42.

Elliott W (1997) A survey of ecologically disturbed areas in Carlsbad Cavern, New Mexico. Report to Carlsbad Caverns National Park, pp 10.

Faimon J, Stelcl J, Sas D (2006) Anthropogenic CO₂-flux into cave atmosphere and its environmental impact: A case study in the Císarská Cave (Moravian Karst, Czech Republic). *Sci Total Environ* 369:231-45.

Fernández-Marín B, Becerril JM, García-Plazaola JI (2010) Unraveling the roles of desiccation-induced xanthophyll cycle activity in darkness: a case study in *Lobaria pulmonaria*. *Planta* 231:1335-1342.

Gao Y, Cui Y, Xiong W, Li X, Wu Q (2009) Effect of UV-C on algal evolution and differences in growth rate, pigmentation and photosynthesis between prokaryotic and eukaryotic algae. *Photochem Photobiol* 85:774-782.

Grobbelaar JU (2000) Lithophytic algae: a major threat to the karst formation of show caves. *J Appl Phycol* 12:309-315.

Hildreth-Werker V, Werker J (2006) Cave restoration overview – why call it cave restoration? In: Hildreth- Werker V. & Werker J.C., editors. *Cave Conservation and Restoration*. Huntsville: National Speleological Society, 293-302.

Jiang T, Jahangir MM, Jiang Z, Lu X, Ying T (2010) Influence of UV-C treatment on

antioxidant capacity, antioxidant enzyme activity and texture of postharvest shiitake (*Lentinus edodes*) mushrooms during storage. *Postharvest Biol Technol* 56:209-215.

Karsten U, Karsten U, Lembcke S, Schumann R (2007) The effects of ultraviolet radiation on photosynthetic performance, growth and sunscreen compounds in aeroterrestrial biofilm algae isolated from building facades. *Planta* 225:991-100

Krause GH, Jahns P (2004) Non-photochemical energy dissipation determined by chlorophyll fluorescence quenching: characterization and function. In. *Chlorophyll a Fluorescence*, ed. Papageorgiou GC, and Govindjee G, Springer, Netherlands. pp. 463-495.

Kreslavski VD, Los DA, Allakhverdiev SI, Kuznetsov VV (2012) Signaling role of reactive oxygen species in plants under stress. *Russ J Plant Physiol* 59:141-154.

Kulandaivelu G, Noorudeen AM (1983) Comparative study of the action of ultraviolet-C and ultraviolet-B radiation on photosynthetic electron transport. *Physiol Plant* 58:389-94.

Lamprinou V, Danielidis DB, Pantazidou A, Oikonomou A, Economou-Amilli A (2014) The show cave of Diros vs . wild caves of Peloponnese , Greece - distribution patterns of Cyanobacteria. *Int J Speleol* 43:335-342.

Lichtenthaler HK, Wellburn AR (1983) Determinations of total carotenoids and chlorophylls *a* and *b* of leaf extracts in different solvents. 603rd Meeting Liverpool.

Maxwell K, Johnson GN (2000) Chlorophyll fluorescence - a practical guide, *J Exp Bot* 51:659-668.

Menetrez MY, Foarde KK, Dean TR, Betancourt DA (2010) The effectiveness of UV irradiation on vegetative bacteria and fungi surface contamination. *Chem Eng J* 157:443-450.

Mihajlovski A, Seyer A, Benamara D, Bousta H, Martino F, Di P (2014) An overview of techniques for the characterization and quantification of microbial colonization on stone monuments. *Ann Microbiol* doi : 10.1007/s13213-014-0956-2.

Moharikar S, D'Souza JS, Kulkarni AB, Rao BJ (2006) Apoptotic-like cell death pathway is induced in unicellular chlorophyte *Chlamydomonas Reinhardtii* (Chlorophyceae) cells following UV irradiation: detection and functional analyses. *J Phycol* 42:423-433.

Mulec J, Kosi G, Vrhovsek D (2008) Characterization of cave aerophytic algal communities and effects of irradiance levels on production of pigments. *J Cave Karst Stud* 70:3-12.

Mulec J, Kosi G (2009) Lampenflora algae and methods of growth control. *J Cave Karst Stud* 71:109-15.

Mulley D, Ghoshal D, Goyal A (2001) UV-A Inhibition of Alternative Respiration in Pea Leaves and an unicellular green alga *Chlamydomonas reinhardtii*. *Plant Biochem Biotechnol* 10:143-146.

Nasibi F, M'Kalantari KH (2005) The effects of UV-A, UV-B and UV- C on protein and ascorbate content, lipid peroxidation and biosynthesis of screening compounds in *Brassica napus*. *Iranian J Sci Technol Trans A* 29:39-48.

Nawkar GM, Maibam P, Park JH, Sahi VP (2013) UV-Induced Cell Death in Plants. *Int J Mol Sci* 8:1608-1628.

Neves-Petersen MT, Gajula GP, Petersen SB (2012) UV light effects on proteins: from photochemistry to nanomedicine. *Molecular Photochemistry - Various Aspects*, S. Saha, Ed., InTech, pp. 125-158.

Olson R (2002) Control of lampenflora in Mammoth Cave National Park. In: Hazslinsky, T.,

(Ed.), International Conference on Cave Lighting. Budapest: Hungarian Speleological Society: 131-133.

Piano E, Bona F, Falasco E, La Morgia V, Badino G, Isaia M (2015) Environmental drivers of phototrophic biofilms in an Alpine show cave (SW-Italian Alps). *Sci Total Environ* 536:1007-18.

Popović S, Simić GS, Stupar M, Unković N, Jovanović J, Grbić ML (2015) Cyanobacteria, algae and microfungi present in biofilm from Božana Cave (Serbia). *Int J Speleol* 44:141-149.

Ritz C, Baty F, Streibig JC, Gerhard D (2015) Dose-Response Analysis Using R. *PLOS ONE*, 10:12-0146021.

Sánchez FJ, Meeßen J, Ruiz C, Sancho LG, Ott S, Vilchez C, Horneck G, Sadowsky A, Torre R De (2014) UV-C tolerance of symbiotic *Trebouxia* sp. in the space-tested lichen species *Rhizocarpon geographicum* and *Circinaria gyrosa* : role of the hydration state and cortex / screening substances. *Int J Astrobiol* 13:1-18.

Sass L, Spetea C, Máté Z, Nagy F, Vass I (1997) Repair of UV-B induced damage of Photosystem II via de novo synthesis of D1 and D2 reaction centre subunits in *Synechocystis* sp. PCC 6803. *Photosynth Res* 54:55-62.

Sinha RP, Hader DP (2002) UV-induced DNA damage and repair: a review. *Photobio Sci* 1:225-236.

Shelly K, Heraud P, Beardall J (2003) Interactive effects of PAR and UV-B radiation on PSII electron transport in the marine alga *Dunaliella tertiolecta* (Chlorophyceae) *J Phycol* 39:509-512.

Sherwood AR, Presting GG (2007) Universal primers amplify a 23s rDNA plastid marker in

eukaryotic algae and cyanobacteria. *J. Phycol.* 43, 605–608.

Smith T, Olson R (2007) A taxonomic survey of lamp flora (Algae and Cyanobacteria) in electrically lit passages within Mammoth Cave National Park, Kentucky. *Int J Speleol* 36:105-114.

Srilaong V, Aiamlaor S, Soontornwat A, Shigyo M, Yamauchi N (2011) UV-B irradiation retards chlorophyll degradation in lime (*Citrus latifolia Tan.*) fruit. *Postharvest Biol Technol* 59:110-112.

Sztatelman O, Grzyb J, Gabryś H, Banaś AK (2015) The effect of UV-B on Arabidopsis leaves depends on light conditions after treatment. *BMC Plant Biol* p. 15-281.

Takeuchi Y, Murakami M, Nakajima N, Kondo N, Nikaido O (1996) Induction of repair and damage to DNA in cucumber cotyledons irradiated with UV-B. *Plant Cell Physiol* 37:181-187.

Tyystjärvi E, Aro E M (1996) The rate constant of photoinhibition, measured in lincomycin-treated leaves, is directly proportional to light intensity. *Proc Natl Acad Sci USA* 93:2213-2218.

Urzi C, De Leo F, Galletta M, Salamone P (2000) Efficiency of biocide in “in situ” and “in vitro” treatment. Study case of the “Template de Mudejar”, Conference: 9th International Congress on Deterioration and Conservation of Stone, At Venice, Italy, Volume: 1, pp. 9.

Vass I, Szilárd A, Sicora C (2005) Adverse effects of UV-B light on the structure and function of the photosynthetic apparatus. In. *Handbook of Photosynthesis*, ed. Pessaraki, M., Dekker, M., Inc., New York. pp. 931–949.

Wang B, Wang X, Hu Y, Chang M, Bi Y, Hu Z (2015) *Chemosphere* The combined effects of

UV-C radiation and H₂O₂ on *Microcystis aeruginosa*, a bloom-forming cyanobacterium. Chemosphere 141:34-43.

Wong CY, Teoh ML, Phang SM, Lim PE, Beardall J (2015) Interactive effects of temperature and UV radiation on photosynthesis of *Chlorella* strains from polar, temperate and tropical environments: differential impacts on damage and repair. PLoS ONE 10-10:0139469. doi:10.1371/journal.pone.0139469

Xue LG, Zhang Y, Zhang TG, An LZ, Wang XL (2005) Effects of enhanced ultraviolet-B radiation on algae and cyanobacteria. Crit Rev Microbiol 31:79-89.

Zhao Y, Wang J, Zhang H, Yan C, Zhang Y (2013) Effects of various LED light wavelengths and intensities on microalgae-based simultaneous biogas upgrading and digestate nutrient reduction process. Bioresour Technol 136:461-468.

Bleaching of biofilm forming algae induced by UV-C treatment: a preliminary study on chlorophyll degradation and its optimization for an application on cultural heritage

Stéphane Pfendler^{1*}, Thomas Munch¹, Faisal Bousta², Laurence Alaoui-Sosse¹, Lotfi Aleya¹ and Badr Alaoui-Sosse¹

¹ Laboratoire Chrono-Environnement – UMR 6249, Université de Bourgogne Franche-Comté
BESANCON

² Laboratoire de Recherche des Monuments Historiques (LRMH) – CRC-USR 3224,
Champs-Sur-Marne.

*Corresponding author

stephane.pfendler@univ-fcomte.fr;

Phone: + 33 (0) 3 81 66 65 98;

Fax: + 33 (0) 3 81 66 57 97

Abstract

Green microalgae colonizing stone surfaces represent a major problem for the conservation of heritage monuments since they lead to biodegradation and aesthetic issues. Previous studies in La Glacière show cave (France) have demonstrated that UV-C may have a strong effect on microalgae, thus leading to chlorophyll bleaching, which was increased when biofilms were maintained under VIS-light condition unlike to those maintained in the darkness. To understand the physiological mechanisms underlying this response and in order to optimize *in-situ* treatment, 30 kJ m⁻² UV-C exposure times were applied to Chlorophyta *Chlorella* sp. and chlorophyll degradation kinetics were then monitored. UV-C irradiation was enough to inhibit photosynthesis and to directly kill all algal cells. Results also showed that chlorophyll *a* was degraded faster than chlorophyll *b* and that 14 hours were necessary for complete degradation of all the present chlorophyll. In addition, our results highlighted the importance of visible light exposition after UVC-treatment which leading to chlorophyll bleaching. Irradiated algae cultivated in the dark were still green 5 days after treatment while cultivated samples in the light lost their green color after 14 hours. An efficient UV-C treatment applicable to show caves and other heritage monuments was proposed.

Keywords: *Chlorella*; UV-C; Viability; Gas exchange; Photosystem II; Bleaching

1. Introduction

Caves are particular ecosystems with a delicate balance between temperature, humidity, carbon dioxide concentration and nutrient contents (Brunet et al. 1985; Groth et al. 1999; Lefèvre 1974; Borderie et al. 2015). Nowadays, it is well known that caves were visited and used by mankind for tens of thousands of years, with the oldest traces of occupation dating back to 30,000 years BP (Before Present) (Valladas et al. 2005). Caves with paintings are therefore considered to be a part human culture and are thus included in different heritage protection programs (UNESCO 2015; Mauriac 2013). Since the early 20th century caves have aroused public interest because of discoveries in paleontology and the progressive development of tourism in European countries. Arrangements have been made to welcome visitors and the first cave visits broke the original balance in these ecosystems (Brunet et al. 1985; Borderie et al. 2014 a, b). Indeed, the release of CO₂ by visitors and installation of artificial lights (Borderie et al. 2016) along with the importation from the external environment of dust and soil containing various propagules has led to the proliferation of microalgae, cyanobacteria and even mosses or grass (Bastian et al. 2008; Lefèvre 1974; Borderie 2016). One famous example is the Lascaux Cave, where the development of green microalgae on its walls was first observed in the 1960s, a phenomenon called "Green Leprosy" (Lefèvre 1974). The presence of these microorganisms not only represents an aesthetic discomfort, with green patches affecting the viewing of paintings and geological formations, but also threatens the long-term conservation of these heritage sites. Indeed, the proliferation of microalgae is capable of causing a gradual erosion of stone materials by biochemical and/or biophysical mechanisms (Brunet et al. 1985, Borderie et al. 2014 a, b). In addition, it should be noted that this problem concerns not only cave environments, but also applies to the conservation of ancient artificial structures such as stone monuments, churches, crypts and even contemporary concrete structures (Bromblet 2010, Scatigno et al. 2016, Urzi

et al. 2016). Chemicals and water repellents have been used since the 1970s to overcome these developments (Lefèvre 1974; Moreau et al. 2008; Urzi and De Leo 2007; Bromblet 2010). Yet, seepage of these products into the surrounding environment and their percolation in water are inevitable, causing pollution of groundwater or underground streams (Borderie et al. 2015). In order to preserve the environment but also human health, the European Union has enacted stricter regulations concerning the use of biocidal products (regulation No 528; Borderie et al. 2015). It thus appears clear that new methods of surface treatment must be found to control the proliferation of these microorganisms. Over several decades, researchers have developed a new method of to eradicate pathogens in hospitals by UV-C irradiation at 254 nm (Rutala et al. 2010; Menetrez et al. 2010). This method also appears applicable to a wide range of microorganisms, such as bacteria in biofilm communities or certain species of mushrooms (Rutala et al. 2010; Menetrez et al. 2010). Moharikar et al. (2006) applied this treatment to kill the unicellular chlorophyte *Chlamydomonas reinhardtii*. More recently, Borderie et al. (2014 a, b), in agreement with the literature (Moharikar et al. 2006), have demonstrated that irradiation of *Chlorella* sp. by UV-C, induced fragmentation of nuclear DNA suggesting that this method would cause cell death by a mechanism similar to programmed cell death (PCD). This cell death was also accompanied by a bleaching of the algal biofilms or of cell suspensions after UV-C irradiation after a few hours and up to a few days, depending on the intensity. This gradual bleaching of algal cells after UV-C irradiation constitute a major strong point of the method as it induces an aesthetic improvement in addition to the eradication of microalga colony.

Borderie et al. (2011) have shown that after UV-C treatment coupled to VIS-light exposition, algae show a very significant reduction in colonization area and faster bleaching in comparison to a single UV-C treatment. Moreover, in our previous study (Pfendler et al., 2017b), we reported that irradiated biofilms bleached faster when they were exposed to VIS-

light than maintained in the darkness. In fact, VIS-light may have an important role in chlorophyll degradation (Pfendler et al., 2017b). Given that bleaching may be due to progressive denaturation, especially of chlorophylls *a* and *b*, which in green microalgae are more abundant than chlorophylls *c* and *d* which exist only in brown algae and cyanobacteria (Féret 2009), it becomes essential to answer the following questions: 1) What are the kinetics of chlorophyll *a* and *b* degradation? and (2) How to increase chlorophyll degradation rate to optimize the method?

To answer these questions, we used respectively the cell viability tests by FDA (Fluorescein di-acetate) assay, chlorophyll fluorescence measurements and ultraviolet-visible (UV-VIS) spectrophotometry. Experimentations were done using a model alga, *Chlorella* sp., which was identified by metabarcoding method as a biofilm-forming alga in several show caves (Pfendler et al., 2018).

2. Material and methods

2. 1. Cultivation of algae

Biofilms were sampled in the Moidons Cave (Jura, France) (Borderie et al., 2014). After culturing in Petri dishes with BG11 medium with 15% agar added, one colony of microalgae, identified as belonging to the taxonomic genus *Chlorella* sp., was isolated and purified. Algae cultures were maintained at 20°C and under 16 hours light per day (Sylvania © triphosphore, 54 W each = 270 W total, PAR = 268 $\mu\text{mol.m}^2.\text{s}^{-1}$).

For all the experiments in this study, the *Chlorella* sp. strain was cultured in a liquid BG11 medium and treatments were carried out on exponential growth phase cells in 5 replicates.

2. 2. UV-C treatments

Cell abundance of microalgae cultures was adjusted to 1.25×10^6 cells ml^{-1} . *Chlorella* sp. suspensions were then placed in glass Petri dishes (5 cm diameter) while a magnetic stirrer kept the suspension mixed during the 30 kJ m^{-2} of UV-C radiation (Philips lamps, 4 x 25 W each = 100 W total, $\lambda_{\text{max}} = 254$ nm). In order to avoid overheating by the UV-C lamps, an air conditioning system maintained the temperature at 20°C (+/- 1°C).

2. 3. Fluorescein di-acetate (FDA) assay

FDA stock solution ($\text{C}_{24}\text{H}_{11}\text{O}_7$, 97% pure, ACROS Organics) was prepared by dissolving FDA powder in acetone (99 %) to a concentration of 10 mg ml^{-1} and then stored at -20°C. A working solution was prepared by adding 40 μl of stock solution to 10 ml deionized water. After exposure to UV-C radiation, cells were harvested by centrifugation at 6 000 g for 5 min and washed with Phosphate-Buffered Saline (PBS). 400 μl of each washed cells in suspension were incubated with 300 μl of FDA solution for 15 min in the dark at room temperature. The fluorescence measurement was then carried out at 535 nm by flow cytometry (flow cytometer Accuri™ C6, $\lambda_{\text{excitation}} = 475$ nm). In order to confirm the FDA

assay, the algae suspensions were also cultured on solid BG11 medium under the previously described culture condition.

2. 4. *Quantum yield measurement*

Treated and non-treated *Chlorella* sp. suspensions (10 ml) were filtered through a cotton disk (1 cm diameter) with a vacuum pump. The discs were then placed for 30 min in the dark at room temperature. Following this, the quantum yield of microalgae was measured using a Mini-PAM (Walz ©, Germany).

2. 5. *Absorption of microalgae after UV-radiation*

Chlorella sp. suspensions were exposed to UV-radiations. Irradiated suspensions were then divided into two groups, the first cultivated under culture parameters (16 hours light per day, 20°C, PAR = 268 $\mu\text{mol m}^{-2} \text{s}^{-1}$) and the second in the dark. Spectra of control and treated cells were measured beforehand and once per day over 4 days with the spectrometer Analytikjena specord 205 (wavelengths between 350 nm and 750 nm).

2. 6. *Kinetic of chlorophyll degradation*

Following the UV-C irradiation (30 kJ m^{-2}), microalgae were cultivated under grow lamps until total chlorophyll degradation. A fraction of each culture was isolated before irradiation (control), and then every hour after irradiation for 14 hours.

In order to measure pigment absorption spectra by spectral scanning from 350 to 750 nm, samples were centrifuged at 6000 g for 5 minutes at 4°C (centrifuge 5415R Eppendorf™). To optimize the extraction, the obtained pellets were incubated overnight in 5 mL of methanol in the dark at 4°C. The samples were then milled for 5 min in a grinder with Fontainebleau sand and placed in the dark at 4°C for 1 hour. Supernatants were collected after centrifugation at 6000 g for 5 min at 4°C. Normalized sample concentration was obtained by adjusting the volume with methanol to 10 ml. Pigment extract absorption was analyzed with the spectrometer Analytikjena specord 205.

Calculations of chlorophyll *a* and *b* concentrations were then carried out using formulas established by Lichtenthaler and Wellburn (1983).

$$[\text{Chla}] = 15,65 \times A_{666} - 7,34 \times A_{653}$$

$$[\text{Chlb}] = 27,05 \times A_{653} - 11,21 \times A_{666}$$

2. 7. Statistical analysis

Statistical comparisons between values were performed with the R software (Version 3.2.5, R Core Team). Student and ANOVA tests were used for all statistical analyses. Significant difference threshold was set for p-value <0.05.

3. Results

3. 1. Effect of UV-C on *Chlorella* sp. viability

Following UV-C radiations, algae viability was measured by flow cytometry (Fig. 1a). With a highly significant difference, results show that 30 kJ.m^{-2} is enough to kill all algae cells. The algae were also cultured in solid BG11 medium but no development was observed, confirming that irradiated cells were deathly affected.

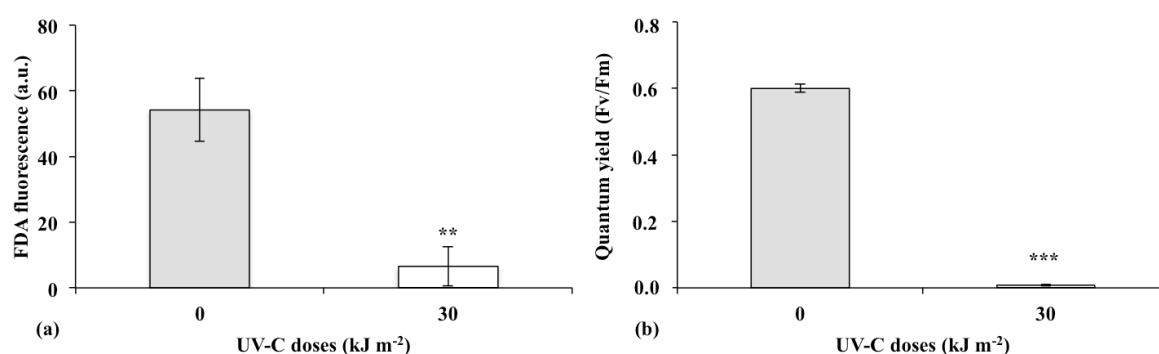


Fig. 1. Quantum yield (a) and FDA survival test (b) were performed on control algae and on 30 kJ m^{-2} treated algae suspensions.

3. 2. Quantum yield measurements

To understand whether algae photosynthesis was affected by UV-C radiation photosystem II (PSII) performance was tested (Fig. 1b) following irradiation. Results demonstrated that the algae quantum yield reached null values with a highly significant difference ($p\text{-value} < 0.001$).

3. 3. In vitro effect of VIS light

On the one hand, results from algae suspension cultured under light conditions show that UV-C induced chlorophyll degradation (Fig. 2a). In fact, all peaks corresponding to

chlorophyll *a* and *b*, which were present on the spectrum before the treatment, disappeared after day 1.

On the other hand, *Chlorella* sp. spectra cells cultured in the dark showed a slow degradation of chlorophyll *a* and *b*. Even after 5 days culture in the dark, chlorophyll peaks were still present, at half intensity in comparison to the control (Fig. 2b).

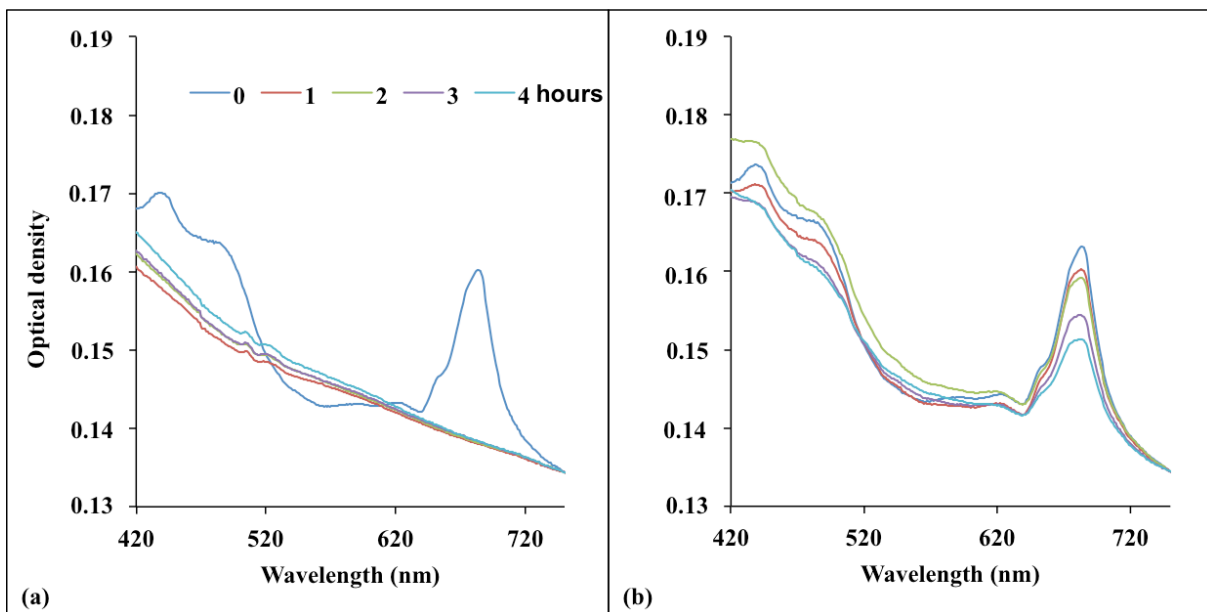


Fig. 2. Algae suspensions were irradiated with UV-C (30 kJ m^{-2}) and then cultivated under culture conditions (a) or in the dark. Suspensions were monitored with a spectrometer before treatment and every day for 4 days.

3. 4. Monitoring of chlorophyll degradation

Chlorophyll *a* and *b* were monitored until degradation was complete, estimated to be at 14 hours (Fig. 3). This degradation (Table 1) appeared progressive in time with a half degradation at 7 hours. However, results obtained directly after treatment showed a general increase in cell components. Other increases were observed during the 2nd and 8th hours in

both 350-400 nm and 520-605 nm regions. After 10 hours, both regions decreased until a linear curve was observed at 14 hours.

Table 1. Chlorophyll *a* peak (687 nm) intensity decreasing after 30 kJ m⁻² of UV-radiations.

| Time (hour) | Control | 0 | 2 | 7 | 10 | 14 |
|--------------------------------|---------|-----|----|----|----|----|
| Chlorophyll peak intensity (%) | 100 | 107 | 76 | 50 | 25 | 0 |

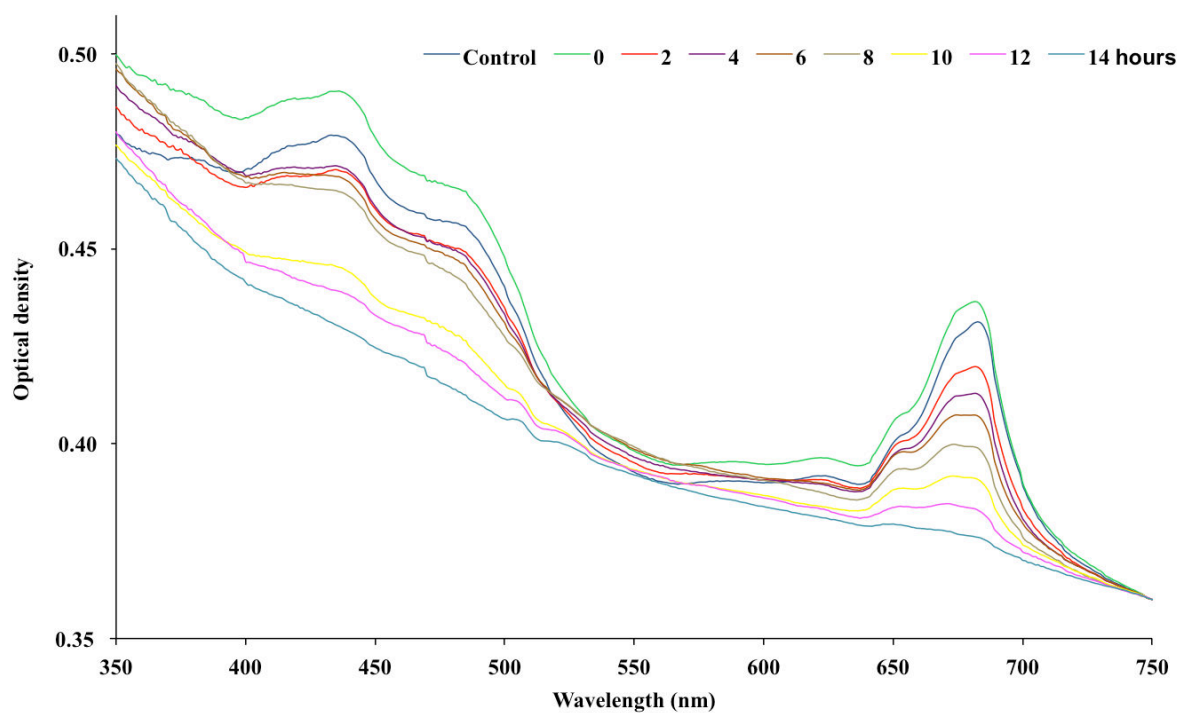


Fig. 3. Absorption of fresh algae suspension (control). Spectrum of *Chlorella* sp. suspension was measured directly following treatment and every 2 hours.

3. 4. 1. Chlorophyll extraction

Chlorophyll from previously irradiated algae was extracted with methanol and its kinetic degradation monitored for 14 hours. Results (Fig. 4) showed that the concentration of extracted chlorophyll *a* and *b* decreased until complete degradation.

As obtained in the previous experiment, an increase in the concentration of both chlorophylls was observed directly following treatment. Absorption values of the four chlorophyll *a* and *b* peaks were compared and statistically analyzed with the control, but no significant difference was found (Table 2).

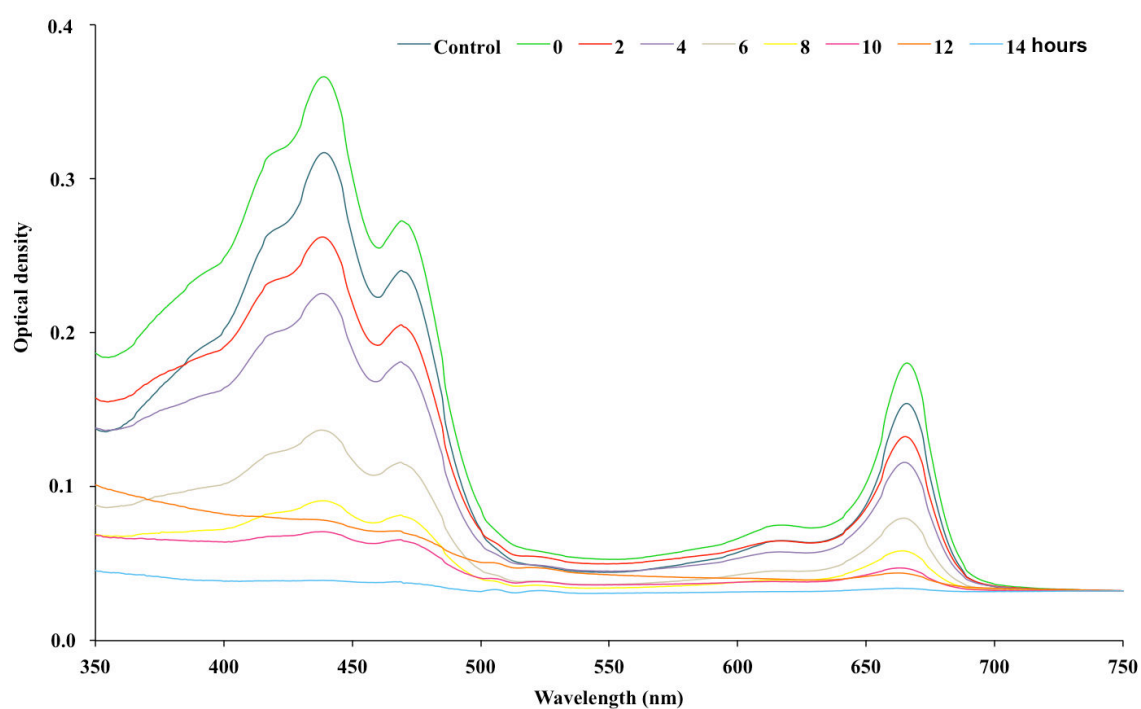


Fig. 4. UV-C-induced bleaching of pigment extract chlorophylls in methanol. Chlorophyll was measured before treatment, directly afterwards and every 2 hours until the chlorophyll complete disappearance.

Table 2. Optical density at 440, 666, 470 and 653 nm of chlorophyll pigments directly after UV-C radiations.

| Wavelength (nm) | Treatment | Optical density | P-value |
|-----------------|-------------------|-----------------|---------|
| 440 | Control | 0.32 ±0.045 | 0.39 |
| | After irradiation | 0.37 ±0.016 | |
| 666 | Control | 0.15 ±0.024 | 0.40 |
| | After irradiation | 0.18 ±0.007 | |
| 470 | Control | 0.24 ±0.030 | 0.37 |
| | After irradiation | 0.27 ±0.013 | |
| 653 | Control | 0.10 ±0.013 | 0.40 |
| | After irradiation | 0.11 ±0.004 | |

P-values were obtained with the Student test.

3. 4. 2. Degradation kinetic of chlorophyll *a* and *b*

Directly after irradiation, chlorophyll *b* was at half the concentration of chlorophyll *a* (Fig. 5a). However, 14 hours after UV-C treatment, chlorophyll *b* concentration was twice as high as chlorophyll *a*. Figure 4 also shows that chlorophyll *a* degradation was faster. These results were confirmed by calculation of both chlorophyll degradation constants (Fig. 5b). Indeed the constant k (0.148 h^{-1}) of chlorophyll *a* ($R^2 = 0.97$) was higher in comparison to chlorophyll *b* (0.045 h^{-1} , $R^2 = 0.92$) (Table 3).

Table 3. Correlation coefficients and kinetic parameters of chlorophyll *a* and *b*.

| Pigments | Equations | r^2 | $k \text{ (h}^{-1}\text{)}$ | R^2 |
|----------------------|-----------------------|-------|-----------------------------|-------|
| Chlorophyll <i>a</i> | $y = 1.84 e^{-0.14x}$ | 0.98 | 0.15 | 0.97 |
| Chlorophyll <i>b</i> | $y = 1.14 e^{-0.05x}$ | 0.94 | 0.05 | 0.92 |

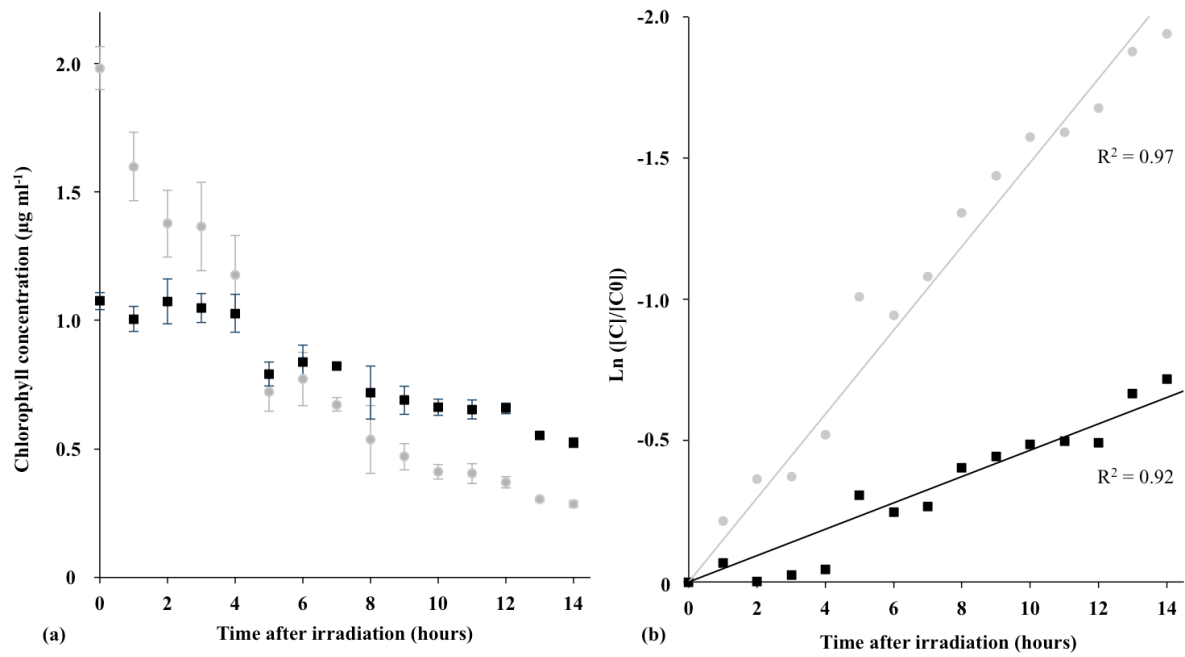


Fig. 5. The kinetic of chlorophyll *a* (●) and *b* (■) after 30 kJ m⁻² irradiation was carried out over 14 hours

4. Discussion

The mechanisms by which UV-A and UV-B radiation impact chlorophyll have been carefully explored (Zvezdanovic 2009), though much uncertainty remains as to those of UV-C which likely involve other chlorophyll bleaching mechanisms found in thylakoids. Given that UV-C comprises a promising and environmentally friendly means to combat algal biofilms (Pfundler et al., 2017b), our present investigation of the mechanisms of its irradiation effects on chlorophyll degradation in *Chlorella* sp. from show-cave samples may help to optimize its use in overcoming challenges faced by cave managers.

Effect of UV-C on Chlorella sp. metabolism and viability

The FDA survival test, which indicates esterase activity in cells, showed that 30 kJ m⁻² of UV-C (~39 min) applied to *Chlorella* sp. was enough to kill all the cells directly upon exposition. This exposure time was also sufficient to inhibit all chlorophyll fluorescence intensity as reported by Zvezdanovic et al. (2009). These results are confirmed by quantum yield values (Fig. 1b) indicating that PSII activity was definitively halted. This inhibition has been reported by many authors (Wang et al. 2015; Goa et al. 2009; Kulandaivelu and Noorudeen 1983) and is probably due to the damaged PSII D1 protein reaction center (Wang et al. 2015). In fact, the PSII complex is the most sensitive light component within the photosynthetic apparatus (Turcsanyi and Vass 2000; Zvezdanovic 2009, Kaucikas et al. 2017). Proteins are known to be a major target of UV-light which affects them by oxidation (Davies 2005; Tyystjärvi 2008). This degradation may be due directly by UV-irradiation or indirectly by reactive oxygen species (ROS) (Triantaphylidès et al. 2009; Wang et al. 2015) since the antioxidant enzymatic mechanisms protecting the cell (superoxide dismutase, peroxidases, etc.) are drastically reduced (Chairat et al. 2012). For instance, these authors showed an increase in respiration but also in the production of ethylene in *Brassica oleracea* after UV-C irradiation. It is known that ethylene is a phytohormone that induces the growth of

plants but can also induce senescence and thus cell death (Yordanova et al., 2010). This phytohormone is also produced in green microalgae (Maillard et al. 1993, Yordanova et al. 2010), and irradiation at low doses ($\leq 6 \text{ kJ m}^{-2}$) would lead to an increased production of ethylene thus causing the death of the algal cells, but is delayed, hence the longer time necessary to achieve cell bleaching at these doses. However, in this study the chlorophyll degradation rate was observed to be dependent on UV-C exposition time (data not shown) that was also reported by Borderie et al., 2014b.

Chlorophyll first-order kinetic degradation

Comparison of kinetics of *in situ* chlorophyll *a* degradation with that of chlorophyll *b* suggested that the bleaching mechanism of these molecules follows a first-order kinetic degradation, as indicated by the correlation coefficients of 97 and 93%, respectively. In addition, the chlorophyll *a* kinetic is faster than that of chlorophyll *b*. Indeed, while the chlorophyll degradation constant (k) is about 0.15 h^{-1} for chlorophyll *a*, for chlorophyll *b* it is only 0.05 h^{-1} , thus chlorophyll *b* may be degraded 3 times more slowly than chlorophyll *a* when the reaction took place *in-situ*. This difference has already been observed when these two molecules were degraded under the influence of heat (Erge et al., 2006) and may be explained by the chemical structures of the two compounds (Schwartz and Von Elbe, 1983).

Degradation kinetic difference induces a change in the chlorophyll *a* and *b* ratio which, in a tree leaf, ranges from 2:1 to 4:1 (Lee 2008; Lichtenthaler and Wellburn, 1983). However, these values may vary according to species, but also within the same species, depending on environmental conditions (light, temperature, nutrient concentrations, etc.). In this study a ratio of about 2:1 was obtained directly after UV-C irradiation of microalgae. Yet, chlorophyll *a* was degraded more rapidly than chlorophyll *b* and Chl *a/b* ratio decreased to 1:1 after 5½ hours of exposure to light; the ratio is then reversed as most of the chlorophyll was made up of chlorophyll *b*. The ratio Chl *a/b* then increased with time and is about 2:1

after 14 hours of exposure. This variation in ratio was associated with a change in the culture's color over time. Indeed, since chlorophyll *a* is responsible for the blue-green color of microalgae and chlorophyll *b* for yellow-green (Erge et al., 2006), a reversal of the ratio causes a change in the color of the cells, shifting from green to yellow before bleaching.

Inductive effect of UV-C irradiation on absorbance

In this study, monitoring of chlorophyll *a* and *b* *in situ* and *in vitro* using UV-VIS spectrophotometer revealed an increase in absorbance of these two molecules directly after irradiation. The results did not show a significant increase in the optical density after irradiation, though this had already been observed several times in the previous investigation (Kotani et al. 1999, Borderie et al., 2014a; Pfendler et al., 2017b) which confirmed this trend. Exposure to UV-C may therefore have an effect of increasing optical density. In fact, Costa et al. (2006), Chairat et al. (2013) and Pongpraset et al. (2011) have worked on broccolis, Chinese broccolis and banana's responses after UV-C treatment. All these studies have demonstrated that enzymatic activities significantly decrease in comparison to chlorophyll degradation. Further study should be done for a better understanding of this mechanism.

5. Conclusion

This study showed that 30 kJ m⁻² UV-C exposure times were enough to kill all algae immediately upon treatment. Chlorophyll *a* and *b* were heavily affected by this treatment, and first-order kinetic degradation followed. Though chlorophyll *a* showed a faster degradation in comparison to chlorophyll *b*, both chlorophylls were completely degraded within 14 hours of UV-C irradiation. These results also showed that VIS-light exposition after treatment contributed to faster chlorophyll degradation. In contrast, samples in the dark exhibited low and incomplete chlorophyll degradation, showing the importance of exposing biofilms to VIS-light after UV-C treatment. These results have led to confirm our previous observation in La Glacière show cave (Pfendler et al., 2017b) and to an optimization of the UV-C biofilm irradiation method in show caves or other heritage monuments. Meanwhile we are currently investigating UV-C damage caused to algae metabolism by low UV-C doses.

Acknowledgments

We are grateful to the owners of the Moidons Caves, Isabelle and François Gauthier, who kindly gave us access to the cave to collect samples. We also thank the *Ministère de la Culture et de la Communication* (France) and the *Laboratoire de Recherche des Monuments Historiques* (LRMH, Paris) for their financial support.

6. References

- Bastian F, Alabouvette C, Saiz-Jimenez C (2008) Bacteria and free-living amoeba in the Lascaux Cave. *Res Microbiol* 60:38-40
- Borderie F, Alaoui-Sossé L, Raouf N, Bousta F, Oriol G, Riefel D, Alaoui-Sossé B (2011) UV-C irradiation as a tool to eradicate algae in caves. *Int Biodeter Biodegr* 65:579–584
- Borderie F, Alaoui-Sehmer L, Bousta F, Alaoui-Sossé B, Aleya L (2014) Cellular and molecular damage caused by high UV-C irradiation of the cave-harvested green alga *Chlorella minutissima*: Implications for cave management. *Int Biodeter Biodegr* 93:118–130
- Borderie F, Tête N, Cailhol D, Alaoui-Sehmer L, Bousta F, Rieffel D, Aleya L, Alaoui-Sossé B (2014) Factors driving epilithic algal colonization in show caves and new insights into combating biofilm development with UV-C treatments. *Sci Total Environ* 484:43–52
- Borderie F, Alaoui-Sossé B, Aleya L (2015) Heritage materials and biofouling mitigation through UV-C irradiation in show caves: state-of-the-art practices and future challenges. *Environ Sci Pollut Res* 22:4144–4172
- Borderie F, Denis M, Barani A, Alaoui-Sossé B, Aleya L (2016) Microbial composition and ecological features of phototrophic biofilms proliferating in the Moidons Caves (France): investigation at the single-cell level. *Environ Sci Pollut Res* 23:12039–12049
- Bromblet P (2010) Guide “Guide Altération de la Pierre”. Association Medistone 32 p
- Brunet J, Vidal P, Vouvé J (1985) Conservation de l’Art Rupestre. CLT-85/WS/38 125 p
- Chairat B, Nutthachai P, Varit S (2012) Effect of UV-C treatment on chlorophyll degradation, antioxidant enzyme activities and senescence in Chinese kale (*Brassica oleracea* var. *alboglabra*). *Int Food Res J* 20:623–628

Chairat B, Nutthachai P, Varit S (2013) Effect of UV-C treatment on chlorophyll degradation, antioxidant enzyme activities and senescence in Chinese kale (*Brassica oleracea* var. *alboglabra*). *Int Food Res J* 20 :623–628

Costa L, Vicente AR, Civello PM, Chaves AR, Martínez GA (2006) UV-C treatment delays postharvest senescence in broccoli florets. *Postharvest Biol Tec* 39:204–210

Davies MJ (2005) The oxidative environment and protein damage. *Biochim Biophys Acta* 1703:93–109

Erge HS, Karadeniz F, Koca N, Soyer Y (2008) Effect of heat treatment on chlorophyll degradation and color loss in green peas. *GIDA* 33:225–233

Féret JB (2009) Apport de la modélisation pour l'estimation de la teneur en pigments foliaires par télédétection. Thèse de Doctorat de l'Université Pierre et Marie Curie p 6-20

Gao Y, Cui Y, Xiong W, Li X, Wu Q (2009) Effect of UV-C on algal evolution and differences in growth rate, pigmentation and photosynthesis between prokaryotic and eukaryotic algae. *Photochem Photobiol* 85:774–782

Groth I, Vettermann R, Schuetze B, Schumann P, Saiz-Jimenez C (1999) Actinomycetes in Karstic caves of northern Spain (Altamira and Tito Bustillo). *J Microbiol Meth* 36:115–122

Kaucikas M, Maghlaoui K, Barber J, Renger T, van Thor JJ (2017). Ultrafast infrared observation of exciton equilibration from oriented single crystals of photosystem II. *Nature Communications* doi:10.1038/NCOMMS13977

Kotani M, Yamauchi N, Ueda Y, Imahori Y, Chachin K (1999) Chlorophyll degradation in boiled broccoli florets during storage in the light. *Food Sci Technol Res* 5:35–38

Kulandaivelu G, Noorudeen AM (1983) Comparative study of the action of ultraviolet-C and ultraviolet-B radiation on photosynthetic electron transport. *Physiol Plant* 58:389–394

Lee RE (2008) *Phycology*. Cambridge University Press p.15

Lefèvre M (1974) La maladie verte de Lascaux. *Stud Conserv* 19:126–156

Lichtenthaler HK, Wellburn AR (1983) Determinations of total carotenoids and chlorophylls a and b of leaf extracts in different solvents. 603rd Meeting Liverpool

Maillard P, Thepenier C, Gudin C. (1993) Determination of an ethylene biosynthesis pathway in the unicellular green alga, *Haematococcus pluvialis*. Relationship between growth and ethylene production. *Journal of Applied Phycology* 5:93–98

Mauriac M (2013) Rapport sur l'état de conservation de la grotte au 31 janvier 2013. Dossier d'information pour le Centre du Patrimoine Mondial 19 p

Menetrez MY, Foarde KK, Dean TR, Betancourt DA (2010) The effectiveness of UV irradiation on vegetative bacteria and fungi surface contamination. *Chem Eng J* 157:443–450

Moharikar S, Souza JSD, Kulkarni AB, Rao BJ (2006) Apoptotic-cell death pathway is induced in unicellular chlorophyte *Chlamydomonas reinhardtii* (Chlorophyceae) cells following UV irradiation : detection and functional analyses. *J Phycol* 42:423–433

Moreau C, Fronteau G, Barbin V (2008) Water-repellent and biocide treatments : Assessment of the potential combinations. *J Cult Herit* 9:394–400

Pfendler S, Einhorn O, Bousta F, Khatyr A, Alaoui-Sossé L, Aleya L, Alaoui-Sossé B (2017a) UV-C as a means to combat biofilm proliferation on prehistoric paintings: evidence from laboratory experiments. *Environ Sci Pollut Res* 24:21601–21609

Pfendler S, Einhorn O, Karimi B, Bousta F, Caihol D, Alaoui-Sossé L, Alaoui-Sossé B, Aleya L (2017b) UV-C as an efficient means to combat biofilm formation in show caves : evidence from the La Glacière Cave (France) and laboratory experiments. *Environ Sci Pollut Res* doi : 10.1007/s11356-017-0143-7.

Pfendler S, Karimi B, Maron PA, Ciadamidaro L, Valot B, Bousta F, Alaoui-Sosse L, Alaoui-Sosse B, Aleya L (2018) Biofilm biodiversity in French and Swiss show caves using the metabarcoding approach: First data. *Sci Total Environ* 615:1207–1217

Pongprasert N, Sekozawa Y, Sugaya S, Gemma H (2011) A novel postharvest UV-C treatment to reduce chilling injury (membrane damage, browning and chlorophyll degradation) in banana peel. *Scientia Horticulturae* 130:73–77

Rutala WA, Gergen MF, Ascp MT, Weber DJ (2010) Room Decontamination with UV Radiation. *Infection Cont Hosp Ep* 31:6–10

Scatigno C, Moricca C, Tortolini Favero G (2016) The influence of environmental parameters in the biocolonization of the Mithraeum in the roman masonry of casa di Diana (Ostia Antica, Italy). *Environmental Sciences and Pollution Research* doi:10.1007/s11356-016-6548-x

Schwartz SJ, Von Helb JH (1983) Kinetics of Chlorophyll Degradation to Pyropheophytin in Vegetables. *J Food Sci* 48, 4 p

Triantaphylide C, Havaux M (2009) Singlet oxygen in plants : production, detoxification and signaling. *Trends in Plant Sci* 219–228

Turcsanyi E, Vass I (2000) Inhibition of photosynthetic electron transport by UV-A radiation targets the photosystem II complex. *Photochem Photobiol* 72:513–520

Tyystjärvi E (2008) Photoinhibition of Photosystem II and photodamage of the oxygen

evolving manganese cluster. *Coord Chem Rev* 252:361–376

Urzi C, De Leo F (2007) Evaluation of the efficiency of water-repellent and biocide compounds against microbial colonization of mortars. *Int Biodeter Biodegrad* 60:25–34

Urzi C, De Leo F, Krakova L, Pangallo D, Bruno L (2016) Effects of biocide treatments on the biofilm community in Domitilla's catacombs in Rome. *Sci Total Environ* 572:252-262

Valladas H, Tisnérat-Laborde N, Cacher H, Kaltnecker E, Arnold M, Oberlin C, Évin J (2005) Bilan des datations carbone 14 effectuées sur des charbons de bois de la grotte Chauvet. *Bulletin de la Société Préhistorique Française* 102:109–113

Wang B, Wang X, Hu Y, Chang M, Bi Y, Hu Z (2015) Chemosphere The combined effects of UV-C radiation and H₂O₂ on *Microcystis aeruginosa*, a bloom-forming cyanobacterium. *Chemosphere* 141:34–43

Yordanova ZP, Iakimova ET, Cristescu SM, Harren FJM, Kapchina-Toteva VM, Woltering EJ (2010) Involvement of ethylene and nitric oxide in cell death in mastoparan-treated unicellular alga *Chlamydomonas reinhardtii*. *Cell Biology International* 34:301–308

Zvezdanović J, Cvetić T, Veljović-Jovanović S, Marković D (2009) Chlorophyll bleaching by UV-irradiation in vitro and in situ: Absorption and fluorescence studies. *Radiat Phys Chem* 78:25–32

Effet des UV-C sur les champignons

Cette section de ce chapitre sera consacrée à l'étude préliminaire sur la survie des champignons suite à une exposition aux UV-C. Les cellules, les spores et les colonies des six souches fongiques préalablement échantillonnées, isolées, purifiées et identifiées (description dans la partie Matériel et Méthodes), ont été soumises au rayonnement ultra-violet.

I. Résultats de l'irradiation des six souches fongiques

Le traitement aux UV-C des suspensions fongiques, même avec la plus faible dose (2 kJ m^{-2}), a permis de tuer toutes les cellules fongiques des six souches testées. De même, les spores n'ont pas survécu, à l'exception celles de *Penicillium bilaiae*. Ces dernières sont capables de résister à des irradiations de 10 kJ m^{-2} , soit environ 13 minutes d'exposition. Cependant, tous les champignons irradiés, lorsqu'ils sont sous forme de colonie, survivent à des expositions de 30 kJ m^{-2} . De plus, ils sont capables de continuer leur croissance suite aux radiations. Cependant, il est à noter que leur vitesse de croissance est ralentie. En effet, dans le cas de *Rhizomucor* sp., la croissance de la colonie est légèrement ralentie après le traitement, puis reprend jusqu'à l'envahissement total de la boîte de Pétri (Fig. 1). Le champignon exposé aux UV-C avait envahi le milieu de culture en 6 jours, contre 5 jours pour le témoin.

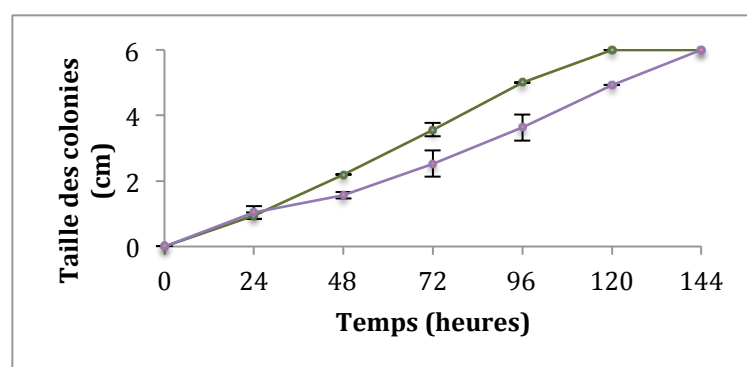


Figure 1 : Suivi de la croissance de *Rhizomucor* sp. en fonction du traitement : la courbe verte correspond au témoin non traité et la courbe violette au traitement par UV-C.

Dans le cas de *Rhizomucor* sp., les effets du traitement sont visibles sur la structure de la colonie par l'apparition de cernes. Afin de mieux les mettre en évidence, un nouveau lot de cette souche a été irradié à 2 reprises et à 2 jours d'intervalle. Sur la figure 2, on peut observer les cernes de la colonie correspondant aux traitements. Enfin, le dernier effet des UV-C est un net ralentissement de la vitesse de formation des spores.

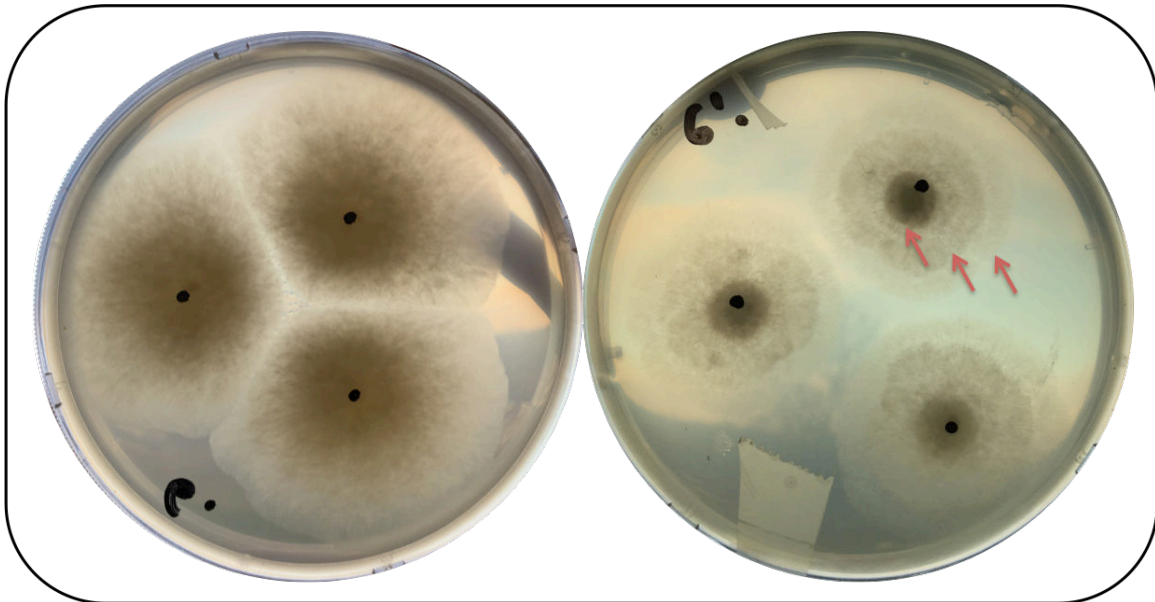


Figure 2 : Illustration d'une culture témoin (à gauche) et traitée aux UV-C (à droite) de *Rhizomucor* sp.. Les flèches rouges montrent les cernes formées suite aux traitements à la lumière UV - C.

Concernant les autres souches, leur vitesse de croissance est bien inférieure et l'envahissement complet des boîtes de Pétri n'a pas été observé. En effet, il s'agit de souches à croissance plus lente, et moins invasives. Les UV-C semblent légèrement ralentir leur vitesse de croissance (Fig. 3) ainsi que la formation des spores. Cependant après 11 jours de culture, les colonies traitées ont atteintes la même taille que les colonies non traitées.

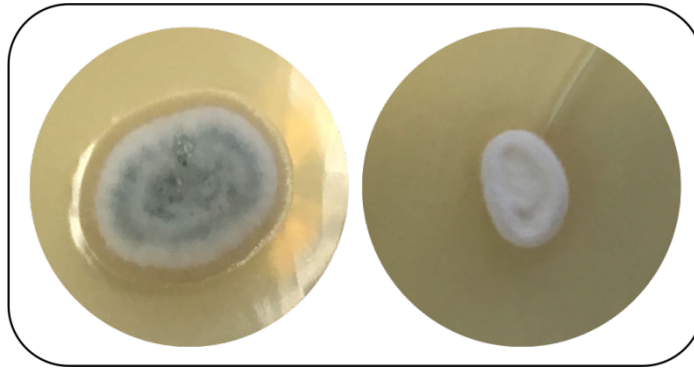


Figure 3: Les deux photos illustrent une souche de *Penicillium bilaiae*. La première photo correspond au témoin non traité dont la présence de spores bleues est visible. La seconde photo illustre la colonie qui a été précédemment irradiée aux UV-C. Sa taille est inférieure à celle du témoin et les spores ne se sont pas développées.

Seule la souche *Geomyces* sp. semble être considérablement atteinte au niveau de la structure de la colonie. En effet, la colonie blanche est devenue brun clair et sa structure semble s'être affaissée sur elle-même. Cependant, 3 jours après le traitement, la colonie s'est à nouveau développée.

Sur les six souches fongiquesensemencées sur bloc calcaire, seule la souche *Rhizomucor* sp. s'est développée suffisamment afin de pouvoir continuer l'expérience (Fig.4). La souche s'est développée rapidement et a atteint 1 cm de hauteur. Suite à la première irradiation, sa structure verticale s'est affaissée. Après le deuxième traitement, la colonie a perdu environ la moitié de son épaisseur. Après la troisième irradiation, une grande partie de la colonie a disparue. Enfin, une quatrième irradiation a permis la disparition totale de la colonie.

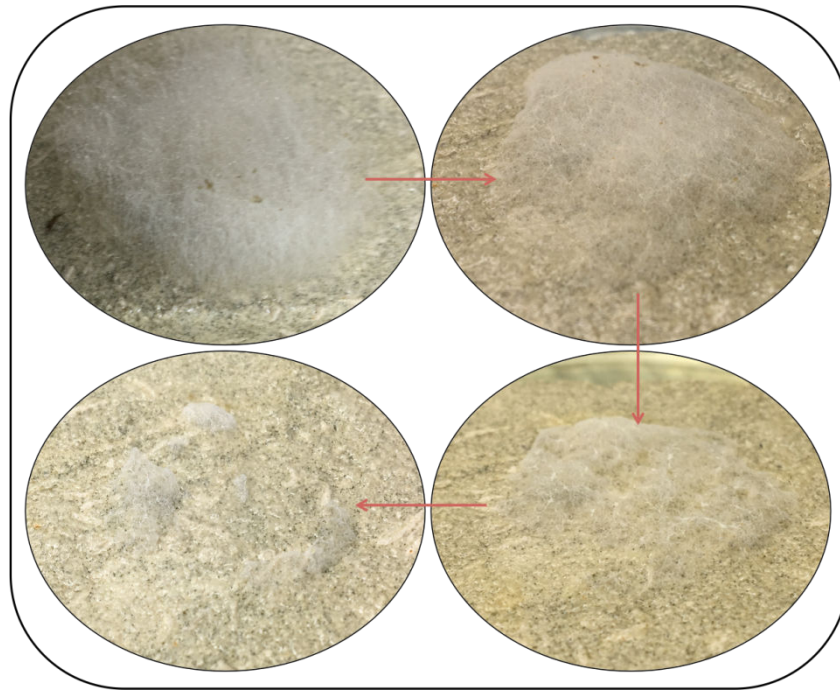


Figure 4: Illustration de développement fongique sur un bloc calcaire. La colonie a été exposée 4 fois à 555 kJ m^{-2} d'UV-C. Après chaque traitement, la taille et l'épaisseur de la colonie décroît jusqu'à sa disparition totale. Les photos correspondent à la colonie fongique avant le traitement, après la première, la deuxième et la troisième exposition aux UV-C.

II. Interprétation et discussion des résultats

L'effet des UV-C sur les spores de champignons microscopiques a été étudié à de nombreuses reprises, notamment dans le cadre d'étude sur les dispositifs de stérilisation de l'air ou de stérilisation de produits alimentaires (Valero *et al.*, 2007 ; Begum *et al.*, 2009 ; Pigeot *et al.*, 2013). Dans le cadre de cette thèse, les effets des UV-C ont été étudiés au niveau des spores, de la cellule et de la colonie.

Les résultats ont montré que les cellules fongiques sont sensibles aux radiations UV-C à la dose minimale testée (2 kJ m^{-2}) qui correspond à une exposition de 150 secondes. Cependant, les spores, qui sont un moyen efficace pour la dissémination des champignons dans l'environnement, sont capables de survivre à des conditions plus extrêmes (ex : UV, température, sécheresse, pression etc). C'est le cas des spores de *Penicillium bilaiae* qui ont résistées à une exposition aux UV-C de 10 kJ m^{-2} . Il est connu que certaines spores sont

capables de mieux résister aux UV-C, comme l'a montré Begum *et al.* (2009) en travaillant avec *Aspergillus niger*. Cette résistance aux UV-C peut être due à une grande quantité de pigments photoprotecteurs présente dans les spores, comme la mélanine, qui leur confèrent une résistance accrue face aux UV (Durrell et Shields, 1960 ; Bell et Wheeler, 1986). D'autre part, l'épaisseur de la paroi de spores peut également être un facteur de résistance (Begum *et al.*, 2009).

Le suivi de la croissance des colonies fongiques suite à une exposition aux UV-C a montré que les six champignons étudiés n'ont pas été affectés de manière létale. En effet, même si les colonies ont subi un arrêt temporaire de leur croissance, ils ont été capables de poursuivre leur développement. Cet arrêt temporaire de croissance est probablement expliqué par le développement même de la colonie. Celle-ci s'agrandit en augmentant son diamètre ; la périphérie de la colonie est donc composée de jeunes cellules et son épaisseur est faible. Les rayonnements UV-C a donc pu tuer ces cellules. Cependant, le centre de la colonie, composé d'une couche importante de filaments, n'a pas ou peu été affecté. Tout comme les biofilms algaux, les différentes couches de cellules supérieures confèrent une protection importante aux couches inférieures par effet d'ombrage (Borderie, 2014). Afin de détruire entièrement une colonie, il semble que plusieurs expositions aux UV-C soient nécessaires. Cette hypothèse a été confirmée par l'exposition successive de la souche *Rhizomucor* sp. se développant sur un bloc calcaire. En effet, après chaque exposition, les colonies semblent décroître en épaisseur et en diamètre jusqu'à leur disparition complète. Afin de confirmer ces premiers résultats, de nouveaux essais devront être effectués sur les six souches.

Synthèse du chapitre 2

L'étude des réponses physiologiques de la micro-algue *Chlorella* sp., présentée dans ce second chapitre, a permis de montrer que des faibles doses d'UV-C sont suffisantes pour induire une mortalité cellulaire des micro-algues utilisées.

En résumé :

- ✓ Même à de faibles doses (quelques minutes), la micro-algue ne peut pas survivre ;
- ✓ La dégradation de la chlorophylle est retardée et est entièrement dépendante d'une exposition à la lumière visible ;
- ✓ La respiration, la photosynthèse et le rendement quantique sont irrémédiablement affectés ;
- ✓ L'appareil photosynthétique de *Chlorella* sp. est significativement affecté par l'exposition aux UV-C et ce même à de faibles doses (2kJ m^{-2}) ;

De plus, cette étude a également permis de montrer que les champignons sont sensibles à un traitement UV-C.

En résumé :

- ✓ Mis en suspension, tous les champignons sont sensibles au rayonnement ultraviolet ;
- ✓ Les spores sont également affectées, mais certaine souche fongique présente plus de résistance que d'autre ; cela est dû à leur forte concentration en pigment photoprotecteur ;
- ✓ Les colonies fongiques cultivées en boîte de Pétri sont très résistantes aux UV-C, même à de très fortes doses, grâce à la forte épaisseur de la colonie ;
- ✓ Les colonies fongiques cultivées sur de la pierre calcaire s'avèrent moins résistantes, car elles sont moins denses ; leur éradication est possible après plusieurs traitements.

Ce travail a permis de montrer que les micro-algues et les champignons sont très sensibles aux UV-C. En outre, l'étude a permis d'optimiser le traitement. De futures recherches devront montrer les effets des UV-C sur les autres organismes colonisant les

biofilms et décrits dans le chapitre précédent. De plus, d'autres paramètres physiologiques pourront être étudiés, comme par exemple la résistance aux UV-C.

Ce travail a donc démontré que le traitement UV-C peut être efficace contre un large spectre d'organismes. Cependant, avant de pouvoir tester le traitement à l'intérieur d'une grotte, il est important de prouver l'innocuité des UV-C vis-à-vis des peintures préhistoriques.

Chapitre 3 : Étude en laboratoire de l'utilisation des UV-C comme moyen de traitement des biofilms colonisant les peintures préhistoriques

Après avoir démontré l'efficacité du traitement aux UV-C contre les micro-algues dans le chapitre précédent, il est important de se poser la question sur la faisabilité d'un tel traitement en condition *in situ*. En effet, les UV-C semblent être un moyen efficace pour éradiquer les micro-algues ; cependant il faut s'assurer que le rayonnement UV-C n'a pas d'effet délétère sur la matière minérale (dont les peintures rupestres) que colonisent les micro-organismes.

Ce chapitre, rédigé sous forme d'article scientifique et publié dans *Environmental Science and Pollution Research* présente les résultats obtenus suite à de longues irradiations sur différents pigments et liants utilisés durant la préhistoire.

Environ Sci Pollut Res
DOI 10.1007/s11356-017-9791-x



RESEARCH ARTICLE

UV-C as a means to combat biofilm proliferation on prehistoric paintings: evidence from laboratory experiments

Stéphane Pfendler¹ · Olympe Einhorn¹ · Faisal Bousta² · Abderrahim Khatyr³ · Laurence Alaoui-Sossé¹ · Lotfi Aleya¹ · Badr Alaoui-Sossé¹

Received: 25 April 2017 / Accepted: 19 July 2017
© Springer-Verlag GmbH Germany 2017

**UV-C as a means to combat biofilm proliferation on prehistoric paintings:
evidence from laboratory experiments**

Stéphane Pfendler ^a, Olympe Einhorn ^a, Faisal Boustia ^c, Abderrahim Khatyr^b, Laurence Alaoui-Sossé ^a, Lotfi Aleya ^{*a}, Badr Alaoui-Sossé ^a

^a Laboratoire Chrono-Environnement – UMR 6249, Université de Bourgogne Franche-Comté Besançon, France.

^b Institut UTINAM UMR CNRS 6213, Université de Franche-Comté, Besançon, France.

^c Laboratoire de Recherche des Monuments Historiques – USR 3224, Champs-Sur-Marne.

Abstract

A laboratory investigation of UV-C effects was conducted over a sixty-two hours period: a much higher dose than in classic UV-C treatment was applied to five pigments and two painting binders used by prehistoric humans. Colorimetric parameters were compared to a control to see if UV-C can change pigment and binder color. Infrared spectroscopy, scanning electron microscopy, inductively coupled plasma and X-ray crystallography were also carried out to confirm colorimetric measurement. In order to understand how microorganism may physically deteriorate paintings, limestone blocs were painted and monitored until their complete colonization by algae, cyanobacteria, fungi and/or mosses. The results show that UV-C has no effect on mineral compounds. Conversely, it is noteworthy that binder color changed under both UV-C light conditions as well as in visible light. Concerning painted blocs, a fast proliferation has been observed with deterioration of the paintings. These results show the high importance of treating biofilm as soon as possible. Moreover these findings may be a promising avenue inducing cave managers to use friendly UV-C light to treat contaminated cave paintings and also in the prevention of biodeterioration by lampenflora.

Keywords: UV-C; pigments; Binders; Laboratory; Prehistoric paintings; Lampenflora

I. Introduction

Subterranean sites have long interested both the academic world and the general public, with paleo-anthropological and archaeological discoveries, especially of prehistoric paintings, contributing heavily to their fascination. This prehistoric rock art from the upper Paleolithic between -40 000 and -10 000 BC (Chalmin 2003) constitutes the most unique feature of these sites, revealing a story of human occupation and activity in one of the world's most challenging environments.

Prehistoric cave art, along with speleothem formations, make these places major tourist attractions, though causing increases in temperature and carbon dioxide. Added to the use of high intensity artificial lighting used for tourist visits (Falasco et al. 2014; Borderie et al. 2015), these emerging environmental conditions promote the development of photosynthetic microorganisms such as algae and cyanobacteria (Popovic et al. 2015; Borderie et al. 2016) which in turn make organic matter and nitrogen bioavailable to heterotrophic fungi and bacteria (Hauer et al. 2015; Urzi et al. 2016).

The resulting photosynthetic biofilms thus become a major problem for curators causing not only esthetic problems (Ciferri 1999; Culter et al. 2013; Adhikary et al. 2015) but also, more dramatically, a deterioration of parietal paintings (Cuzman et al., 2010, Cutler et al. 2013; Adhikary et al. 2015) through the production of organic acid (Mulec 2005; McNamara et al. 2006; Albertano et al. 2012) or, mechanically, by growth within microfissures, which gain in volume provoking increased cracks in the paintings (Danin et Caneva 1990, Cennamo et al. 2016). For example, in the world famous ancient wall paintings of the Lascaux Cave (France) the development of algae on artworks estimated to be 17,300 years old led the authorities to an abrupt closure of the cave in the 1960s to limit the threat (Bastian et al. 2008). Moreover, the ceiling, walls and sediments were colonized by the fungus *Fusarium solani* in 2001 (Bastian et al. 2008).

Nowadays, cave managers use treatments such as high-pressure cleaners, bleach, or chemical compounds, which may degrade cave walls and mineral structures (Faimon et al. 2003; Mulec and Kosi 2009). In addition to being retentive and harmful to the environment, with a risk of contaminating the groundwater, their efficiencies are variable.

In order to protect natural heritage sites, new friendly environmental treatments have been investigated, especially the use of UV-C light (Borderie et al. 2014; Wang et al. 2015) which has shown itself to be efficient in the air and water treatment industries, but also in hospitals as a method of sterilization. UV-C light is also effective against algae and cyanobacteria in the laboratory and shows promising results in touristic caves (Borderie et al. 2011; Borderie et al. 2014). However, the potential effect of UV-C on parietal paintings and limestone cave walls has been poorly addressed due to: 1) the nature of pigments: prehistoric paints were made with natural pigments such as ochre, coal and manganese dioxide (Bikiaris et al. 1999; Arocena et al. 2008; Darchuk et al. 2011; Bonneau et al. 2012) and 2) the complexity of the binders that hold the pigments in the paint: certain organic compounds including blood, beeswax, animal fat and vegetable oils (Arocena et al. 2008; Prinsloo et al. 2008; Lofrumento et al. 2012).

We therefore investigated the effects of UV-C radiation on prehistoric pigments and binders. To determine whether some molecular or crystalline modifications appear after irradiation, measurements were taken with Fourier transform infrared spectroscopy (FTIR) and X-ray crystallography (XRD). Moreover, inductively coupled plasma mass spectrometry (ICP) and Scanning electron microscopy (SEM-EDX) were used to compare elemental pigment composition. FTIR, SEM-EDX and XRD methods have been previously used to study pigments and binders in prehistoric paintings (Zoppi et al. 2002; Mortimore et al. 2004). To monitor possible color changes, colorimetric parameters were assessed.

II. Materials and methods

1. *Effect of microorganism growth on paintings*

To ensure that microorganisms might growth on each pigment used in the composition of prehistoric paintings, but also to understand biofilm development, 2 g of pigments were mixed with 20 ml of water. The solution was painted onto limestone blocs. To simulate biofilm colonization in laboratory, blocs were placed on vermiculite to keep them moist but no inoculation has been carried out. The temperature (15°C), moisture (100%) and light (150 $\mu\text{mol m}^{-2} \text{s}^{-1}$, 16 hours per day) gave favorable conditions for microbial colonization by both photosynthetic and non-photosynthetic microorganisms. Seventy-three days after the beginning of the experiment, blocs were no longer moistened for one week so as to simulate cave dry periods.

2. *Preparation and irradiation of paints and binders*

In this study we tested five pigments and two binders used by prehistoric humans in caves (Fig. 1): coal, bone char, manganese dioxide, red ochre, yellow iron oxide, beeswax and lard. Colorimetric parameters, X-Ray Crystallography, inductively coupled plasma mass spectrometry (ICP), SEM-EDS and Fourier Transform Infrared Spectroscopy analysis were carried out on 8 g of each pigment and binder (Fig. 2, Fig. 3, Fig. 4). Pigments powder and binders were placed in glass Petri dishes (5 cm diameter). Samples were irradiated for sixty-two hours with 8 UV-C lamps (Philips, 25 W each = 200 W, $\lambda \text{ max} = 254 \text{ nm}$) corresponding to a dose of around 4 800 kJ m^{-2} . Several measurements were taken prior to treatment and 10 days after. During this 10-day time lapse, samples were stored under light conditions (150 $\mu\text{mol m}^{-2} \text{s}^{-1}$) 16 hours per day.

3. *Colorimetric measurement of pigments and binders*

Dry pigments and binders were used in order to avoid color change due to moisture. Colorimetric parameters were measured with a spectrophotometer (CM-600d KONICA MINOLTA, illuminant D65, SCI mode and 8 mm diameter target mask). Color measurements were analyzed according to the CIELAB color system. The dark-light scale (L^*) is associated with the lightness of the color and ranges from bottom (value: 0, black) to top (value: 100, white). The a^* and b^* scales are associated with changes in redness-greenness (positive a^* is red and negative a^* is green) and changes in yellowness-blueness (positive b^* is yellow and negative b^* is blue) (Borderie et al. 2014).

4. *Fourier transform infrared spectroscopy*

After grinding in a mortar about 2% by weight of each pigment in anhydrous KBr, the mixture was placed in a mechanic press to obtain a thin and translucent pastille. Then the spectra were measured with a Fourier transform infrared spectrometer (IRAffinity-1, Shimadzu) at room temperature.

Infrared spectra were measured with the Perkin-Elmer Spectrum 100-400 spectrometer. The samples were placed in the ATR bench diamond platinum (Single Reflexion Attenuated Total Reflectance) and smashed with a press, previously washed with ultrapure ethanol. In order to make a comparative study, a number of scans (30) was used for all samples.

5. *X-ray crystallography*

Pigment samples were crushed in a mortar with an agate pestle and placed in a mined glass slide. The diffractometer used was an automated Bruker D8 AdvanceLynxEye Detector (cobalt tube λ $K\alpha_1 \approx 1,789 \text{ \AA}$). The scan was 0 to $70^\circ 2\theta$, with a speed of about $0,005^\circ$ per second. The diffractograms obtained were traced on software Diffrac Plus Measure and interpreted using Diffrac Plus Eva.

6. *Inductively coupled plasma mass spectrometry (ICP)*

Chemical components in pigments were determined before and after UV-C treatment. Al, As, B, Ca, Cd, Co, Cr, Cu, Fe, Hg, K, Mg, Mn, Na, Ni, P, Pb, S, Sb, Se, Si, Sn, Sr, Ti and Zn were measured using ICP-AES after acid mineralization (1 ml HNO_3 and 2.5 ml HCl) of 0.25 mg in Digiprep Mineralizator. After adding ultra-pure water to 25 ml, samples were filtered (1 μ l). To assess the analytical quality, a standard reference material (Loamy Clay) was subjected to the same protocol. Chemical element concentrations are reported in Table 3.

7. *Scanning Electron Microscopy equipped with X-Ray microanalysis (SEM-EDX)*

The measurements were carried out by a JEOL 5510 microscope coupled to an SamX 30 mm² EDX module and equipped with a thermal emission gun. It was used for both imaging and EDS analysis, in high vacuum mode with an acceleration voltage of 24 kV, a spot size of 30 and a working distance of 21 mm. The powder is fixed on analytical carbon scotch and then covered with 20 nm of carbon by thermal sublimation.

8. *Statistical analysis*

All statistical analyses were performed using R.2.14 software (R Development Core Team, 2011) at the significant level of 0.05. An ANOVA statistic test was used for colorimetric measurements. All experiments were conducted with four replicates.

III. Results

1. Microorganism growth on paintings

Red ochre painting blocks maintained under culture conditions showed rapid colonization by micro-algae (predominance of unicellular green alga *Bracteacoccus* sp.), cyanobacteria (*Phormidium*) and fungi (*Verticillium*) (Fig. 1). After two weeks these different microorganism species formed colonies. Fifty-one days after the beginning of the experiments micro-algae and cyanobacteria invaded the entire painted bloc area. At day 73 (Fig. 1), dry colonies cracked and flaked from the bloc taking away a part of the pigment. After 3 months mosses began to grow and by the fourth month had completely invaded the painted limestone bloc. These mosses were identified as *Bryum argenteum*, *Bryum capilare* and *Barbula convolute* with the help of the “Mosses and Liverworts of Britain and Ireland” guidebook.

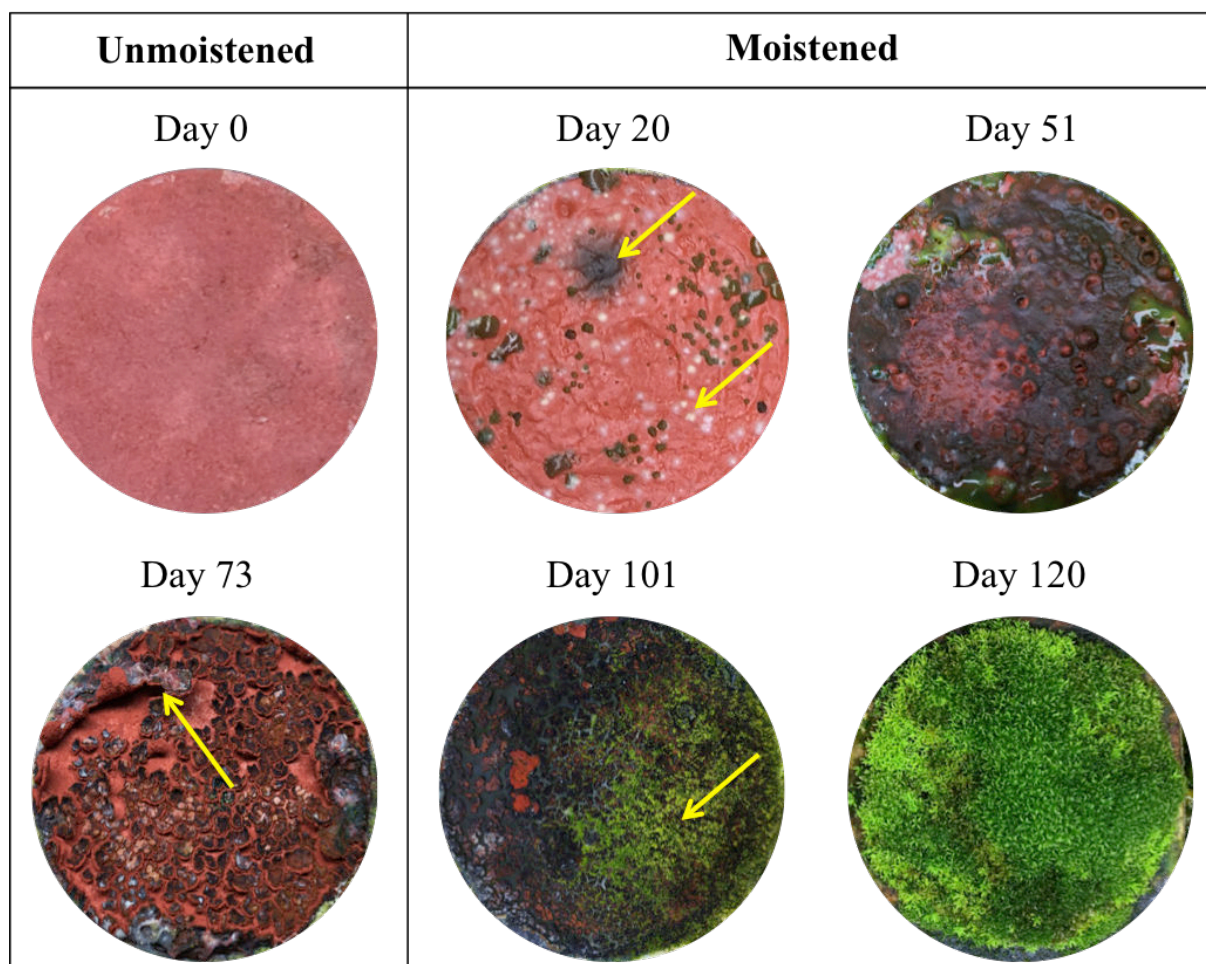


Fig. 1. Growth of algae, fungi and mosses on a limestone block previously painted with red ochre.

2. Monitoring of colorimetric parameters of pigments and binders

Pigments and binders were monitored with one of the CIELAB parameters, depending on their color (Table 1).

Colorimetric results show that the binder color changes after exposition to UV-C light. The lard color became significantly darker (L^*) after radiation (Fig. 2b), but no change was observed for the control (Table 1), while the beeswax showed a significant decrease in the yellow color (b^*) for both the control and UV-C irradiated samples (Fig. 2d).

As for pigment parameters, these were not statistically different in comparison to the control (Table 1). Figure 2a shows a^* parameters of red ochre. The data of the 4 other pigments are not shown, but the same non-significant difference between control and treated samples also appears.

Table 1. Statistical results (p-value) of colorimetric measurements.

| Treatments | Red ocher | Yellow iron | Manganese dioxide | Bone char | Coal | Beeswax | Lard |
|---------------------------------|-----------|-------------|-------------------|-----------|-------|---------|-------|
| Control | 0.39 | 0.27 | 0.70 | 0.10 | 0.69 | <0.05 | 0.32 |
| UV-C | 0.27 | 0.76 | 0.99 | 0.11 | 0.39 | <0.05 | <0.05 |
| Colorimetric measurement | a^* | b^* | L^* | L^* | L^* | b^* | L^* |

a^* : Green-red scale; b^* : Blue-yellow scale; L^* : Dark-light scale; P-value was obtained with an ANOVA test.

3. Fourier transform infrared spectroscopy

The study by infrared spectroscopy was realized to verify the effect of UV-C on molecules composing pigments and binders. The FTIR spectra obtained for all pigments show that all peaks, which were present before irradiation to UV-C, are present after (Fig. 3d). The only difference is around 2 300-2 400 cm^{-1} and this is due to the CO_2 present in the air and should not be taken into consideration. Results obtained for binders are similar: the curves can be superimposed and conserve all peaks before and after UV-C treatment (Fig. 2a, c).

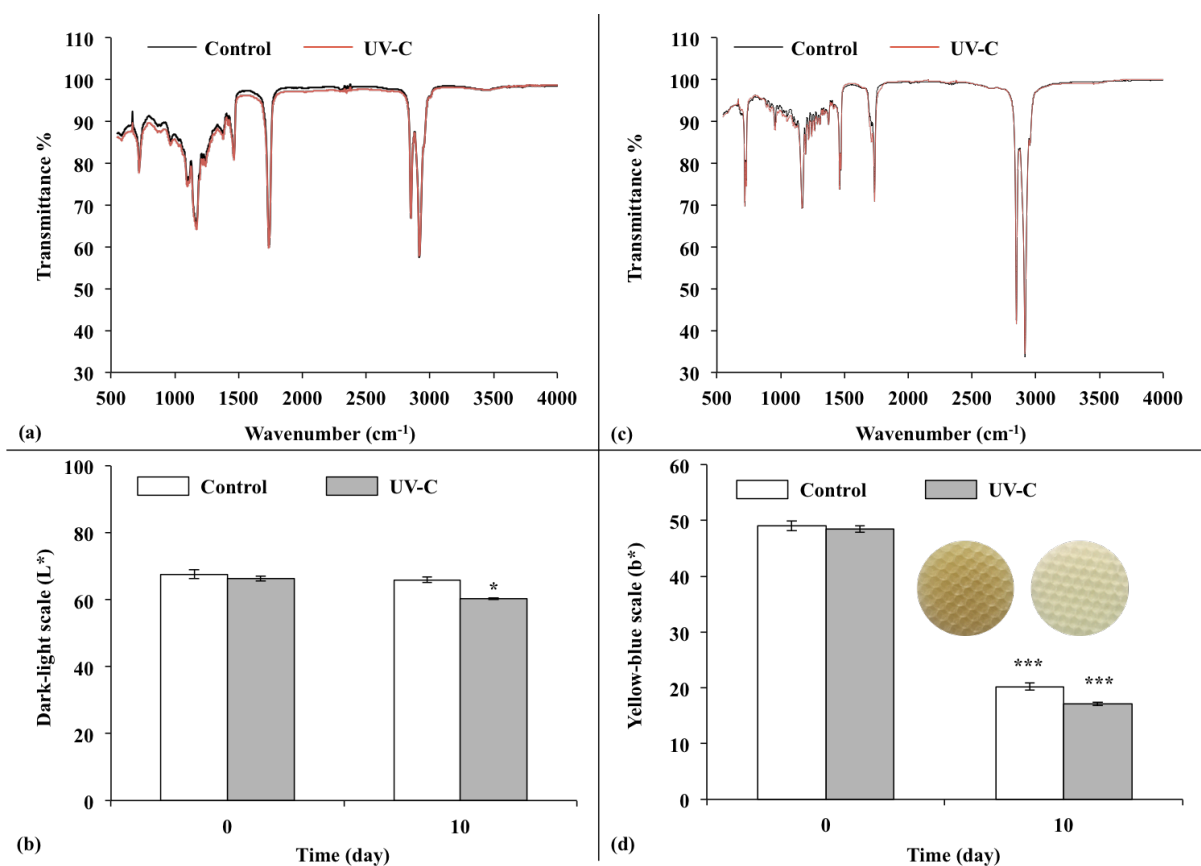


Fig. 2. Infra-red analysis of treated and untreated lard (a) and beeswax (c). Graphics (b) (lard) and (d) (beeswax) show results of colorimetric measurements of both treatments.

4. X-ray crystallography

X-ray crystallography revealed the crystalline composition of the pigments (Table 2) before and after UV-irradiation. Like infrared analysis, the X-ray crystallography graphics obtained for both UV-C exposed pigments and the control show no change in the characteristic peaks (Fig. 3c). Certain peaks corresponding to mineral elements sometimes appeared higher in the control than in the treated powder, a change attributable to a difference in concentrations. Results from UV-C treated pigments showed the same peaks in the same place with no peaks disappearing nor appearing. This suggests that no product has been degraded nor any by-product formed.

Table 2. Mineral composition of the five studied pigments.

| Pigment | Manganese dioxide | Bone char | Red ochre | Yellow iron oxide | Coal |
|-------------|----------------------|--------------------------|---------------------------------|---|----------|
| Composition | Hematite Jacobite | Quartz Hydroxyapatite | Quartz Kaolinite Graphite | Quartz Hematite Kaolinite Illite Goethite | Graphite |

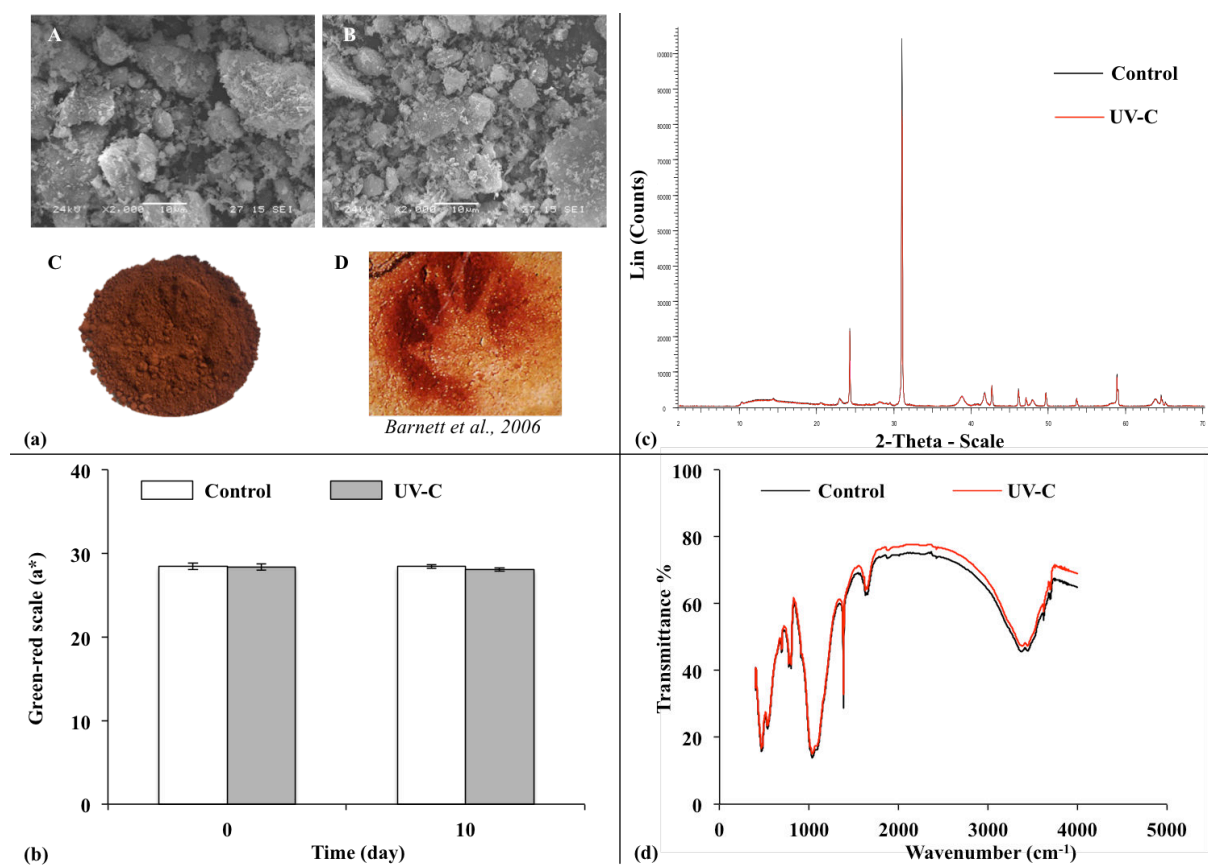


Fig. 3. (a) SEM picture of red ochre before (A) and after (B) UV-C radiations. The red powder (C) has been used by prehistoric human (D). Colorimetric measurements (b), DRX analysis (c), and infrared spectrometry (d) has been carried out before and after UV-C treatment.

5. ICP-MS

The five pigments were analyzed with ICP before and after UV-C irradiation to determine chemical element concentration. Results, reported in Table 3, showed that Fe was the element, which differed the most between both treated and untreated samples (-0.8%). However, this low difference was not significant.

Table 3. ICP results of red ochre pigment.

| Chemical elements | | Al | Ca | Fe | K | Mg | Na | P | S | Si | Ti | Zn |
|-------------------|---------|------|-----|------|-----|-----|-----|-----|-----|-----|-----|-----|
| Concentration (%) | Control | 27.1 | 0.5 | 66.9 | 2.9 | 0.5 | 0.3 | 1.2 | 0.1 | 0.1 | 0.1 | 0.1 |
| | UV-C | 27.7 | 0.5 | 66.1 | 3.2 | 0.4 | 0.3 | 1.1 | 0.1 | 0.1 | 0.1 | 0.1 |

6. Scanning Electron Microscopy equipped with X-Ray microanalysis

UV-C effect on pigments was tested by SEM analysis. Pictures of UV-C treated pigments showed no difference in mineral structure with the control (Fig. 3a). This result is corroborated by X-Ray microanalysis (Fig. 4). For instance concentration in O, Si, Fe, Al, K, Ti and P, as quantified in red ochre control, did not change significantly as compared with the treated pigment. The highest difference was observed for oxygen (+2.7%) and the lowest for phosphorus and titanium (+0.04 and -0.03 %, respectively).

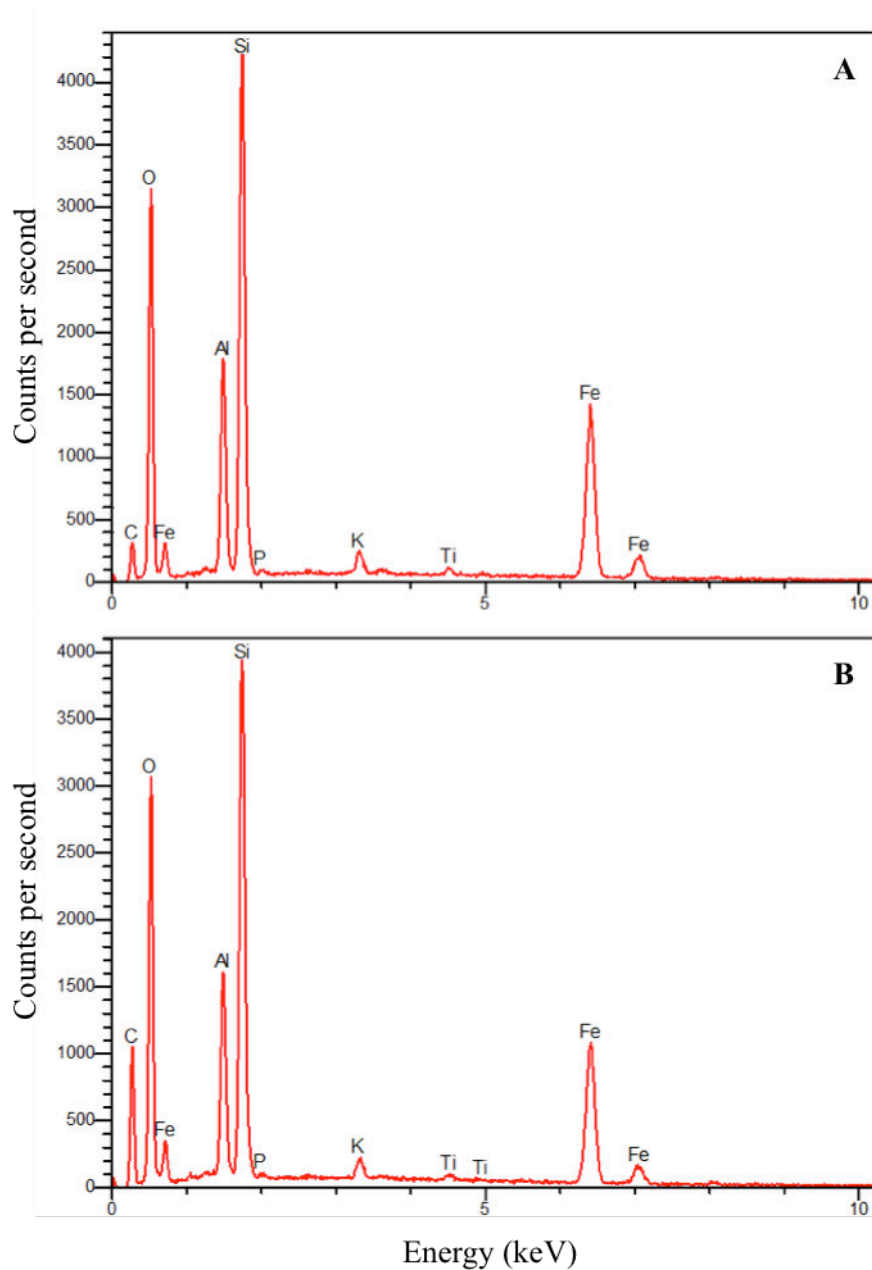


Fig. 4. X-Ray microanalysis on red ochre (A) before and (B) after UV-C radiations.

IV. Discussion

- Dynamics of microorganisms on painted limestone blocs

The results show that the assembly of microorganisms started with the proliferation of the pioneer unicellular green alga *Bracteacoccus* sp. This result is intriguing since a similar trend with massive development of *Bracteacoccus* sp. (Lefèvre 1974) after 12 years of tourist visits was also reported in the world's most famous cave, the Lascaux Cave (Dordogne, France). This colonization resulted in a threatening of the integrity of the unique and famous 17,000 year-old prehistoric paintings and ultimately leading to the cave being closed to the public in 1963. This strain may have originated from outside, via vectors such as visitors, air flows or some animals able to acclimate to low light and carbon dioxide conditions (Cigna 2000). Another pioneer unicellular green alga identified as *Chlorella minutissima* (Fott and Nováková) (Borderie et al. 2014) proliferated in the Moidons Caves giving rise to biofilm formation. The same occurred on our blocs as, over time, they became greenish due to the presence of organic pigments such as chlorophyll, giving rise to biofilm formation with the development of algae and cyanobacteria after only 2 weeks (Fig. 1). In this study, mosses, too, are capable of totally invading the paintings after 4 months. From a theoretical ecologist's perspective, our experiment simulates habitat-specific selectivity and random dispersal in building multi-specific assemblages (Hubbell 2001; Bell 2005). It becomes obvious that to counteract the 'green' disease responsible for aesthetic damage (Fig. 1) and biodegradation (Ciferri 1999; Cuzman et al. 2010; Adhikary et al. 2015), it is urgent to find an environmentally friendly treatment, one that will leave no trace of the pioneer unicellular green alga that induces biofilm formation on prehistoric paintings.

- Monitoring of colorimetric parameters of pigments and binders

The initial analysis undertaken in this study was via the monitoring of the colorimetric parameters of pigments and binders before and after UV-C treatment. In contrast to Athanassiou et al. (2000), we observed no change in any pigment; those authors, however, reported that the use of a UV-C laser caused a darkening of the pigment and an alteration in molecular composition proved by X-ray diffractometry. Chappé et al. (2003) found the same results with the use of a UV-C laser on medieval pigments (zinc white, red and white lead, brown ochre, cobalt blue). Laser use is known to induce a strong increase in temperature, causing damage to pigment structure, which we confirm in this study.

Binder colorimetric parameters tested in this study showed interesting results. Both lard and

beeswax show a decrease in color parameters of L^* and b^* , respectively (Fig. 1d). These results suggest the deleterious effect of UV light on organic compounds. In fact, UV-C can alter biological molecules, such as keratin, collagen and cellulose (Caneva et al. 2008). However, the beeswax control samples ($n=4$) show the same color change as the irradiated samples, meaning that, independently of light source, beeswax and especially carotenoid, responsible for the yellow color, are light sensitive. Nevertheless, and interestingly, infrared results show no differences between treated and non-treated samples. The color change observed on beeswax and lard is new and comprises the only argument against the use of UV-light. However, the presence of organic matter in prehistoric paintings is controversial (Chalmin 2003). We infer that organic compounds are not stable over several tens of thousands years. Pallipurath et al. (2015) also show that binders consisting of fats are not stable. Moreover, Couraud (1988) reported that presence of binders could not permit a good painting conservation and make them sensible to fungi. In fact, heterotrophic microorganisms might use these sources of organic matter for their own growth (Cennamo et al. 2016).

Concerning X-ray crystallography, infrared spectroscopy, ICP and scanning electron microscopy experiments, a change in the mineral components contained in pigments has been asserted when only one among the four techniques was used, never when these are used simultaneously. This was expected since theoretical UV-C energy is not powerful enough to break mineral-chemical bonds. These results were also corroborated by those of Gibeaux et al. (2014) and Borderie (2014), who conducted this experiment with lower UV-C intensities and time periods (16 hours at 45W maximum, and 13 hours at 100 W, respectively). In addition, Rifkin et al. (2015) showed that the red ochre, which has been used as a coloring agent in Africa for over 200,000 years and is still used by women of the Himba ethnic group in Namibia (Mcbrearty and Brooks 2000), inhibits the harmful effect of UV-radiations on their skin. In fact, red ochre absorbs, reflects or scatters UV-radiation (Rifkin et al. 2015).

V. Conclusion

Our approach shows that UV-C light can potentially be used as an environmentally friendly alternative to chemicals to combat biofilm contamination of prehistoric paintings. Microorganisms are killed by radiation while no change in pigment color nor in their chemical structure has been observed. Change in beeswax has been observed under UV-C light but also under VIS-light. However, many authors reported that organic matters are not stable in the time and that no binders could be detected in paintings. Our recent study showed that UV-C (553 KJ m⁻²) could be used with high efficiency against biofilms in tourist caves without prehistoric paintings and without recolonization during two years. Further studies must be conducted on some small part of original paintings to check definitively the safe use of UV-C on mineral pigments.

VI. Acknowledgements

This study is part of the PhD thesis of Stephane Pfendler. We thank the French Ministry of Culture and Communication and the *Laboratoire de Recherche des Monuments Historiques* (LRMH, Paris) for their financial contribution.-

VII. References

- Adhikary SP, Keshari N., Urzi C (2015) Cyanobacteria in biofilms on stone temples of Bhubaneswar, Eastern India. *Algo. Stud.* 147: 67-93.
- Albertano P (2012) *Cyanobacterial Biofilms in Monuments and Caves*. Springer, pp. 317–343.
- Arocena JM, Hall K, Meiklejohn I (2008) Minerals Provide Tints and Possible Binder/Extender in Pigments in San Rock Paintings (South Africa). *Geoarchaeology: An International Journal*, 23: 293-304.
- Athanassia A, Hilla AE, Fourriera T, Burgiob , Clarkb, RJH (2000) The effects of UV laser light radiation on artists' pigments. *J. Cult. Heritage* 1: 209-213.
- Bastian F, Jurado V, Novakova A, Alabouvette C, Saiz-Jimenez C (2010) The microbiology of Lascaux Cave. *Microbiologica*, 156: 644-652.
- Bell G (2005) The co-distribution of species in relation to the neutral theory of community ecology. *Ecology* 86, 1757–1770. Belehrádek, J., 1926. Influence of temperature on biological processes. *Nature* 118: 117–118.
- Bikiaris D, Sister D, Sotiropoulou S, Katsimbiri O, Pavlidou E, Moutsatsou AP, Chryssoulakis Y (1999) Ochre-differentiation through micro-Raman and micro-FTIR spectroscopies: application on wall paintings at Meteora and Mount Athos, Greece. *Spectroch. Acta A*. 56: 3-18.
- Bonneau A, Pearce DG, Pollard AM (2012) A multi-technique characterization and provenance study of the pigments used in San rock art, South Africa. *J. Archaeol. Sci.* 39: 287-294.
- Borderie F, Alaoui-Sehmer L, Raouf N, Bousta F, Oriol G, Rieffel D, Alaoui-Sosse B (2011) UV-C irradiation as a tool to eradicate algae in caves. *Int. Biodeter. Biodegr.* 65: 579-584.
- Borderie F (2014) *Utilisation du rayonnement UV-C comme méthode alternative aux produits chimiques dans la lutte et le contrôle de la prolifération des micro-organismes sur les matériaux du patrimoine*. Université de Franche-Comté, 312 pp.

Borderie F, Tête N, Cailhol D, Alaoui-Sehmer L, Bousta F, Rieffel D, Aleya L, Alaoui-Sossé B (2014) Factors driving epilithic algal colonization in show caves and new insights into combating biofilm development with UV-C treatments. *Sci. Total Environ.* 484: 43-52.

Borderie F, Alaoui-Sossé B, Aleya L (2015) Heritage materials and biofouling mitigation through UV-C irradiation in show caves: state-of-the-art practices and future challenges. *Environ. Sci. Pollut. Res.* 22: 4144–4172.

Borderie F, Denis M, Barani A, Alaoui-Sossé B, Aleya L (2016) Microbial composition and ecological features of phototrophic biofilms proliferating in the Moidons Caves (France) : investigation at the single-cell level. *Environ. Sci. Pollut. Res.* 23:12039–12049.

Caneva G, Nugari MP, Salvadori O (2008) *Plant Biology for Cultural Heritage. Biodeterioration and Concervation.* The Getty Conservation Institute.

Cennamo P, Montuori N, Trojsi G, Fatigati G, Moretti A (2016) Biofilms in churches built in grottoes. *Sci. Total Environ.* 543: 727-738.

Chalmin E (2003) *Caractérisation des oxydes de manganèse et usage des pigments noirs au paléolithique supérieur.* Université de Marne-la-Vallée, 382 pp.

Chappé M, Hildenhagen J, Dickmann K, Bredol M (2003) Laser irradiation of medieval pigments at IR, VIS and UV wavelengths. *J. Cult. Herit.* 3:264-270.

Ciferri O (1999) Microbial Degradation of Paintings. *Appl. Environ. Microb.* 65: 879–885.

Cigna AA, Burri E (2000) Development, management, and economy of show caves. *Int. J. Speleol.* p.1-17.

Couraud C (1988) Pigments utilisés en Préhistoire, provenance, préparation, mode d'utilisation. *L'anthropologie.* 92: 17-28.

Cutler N, Oliver AE, Viles H, Ahmad S, Whiteley AS (2013) The characterisation of eukaryotic microbial communities on sandstone buildings in Belfast, UK, using TRFLP and 454 pyrosequencing. *Int. Biodeter. Biodegr.* 82: 124–133.

Cutler NA, Viles HA, Ahmad S, McCabe S, Smith BJ (2013) Algal 'greening' and the conservation of stone heritage structures. *Sci. Total Environ.* 442: 152-164.

Cuzman OA, Ventura S, Sili C, Mascalchi C, Turchetti T, D'Acqui LP, Tiano P (2010) Biodiversity of phototrophic biofilms dwelling on monumental fountains. *Microb. Ecol.* 60, 81-95.

Danin A, Caneva G (1990) Deterioration of limestone walls in Jerusalem and marble monuments in Rome caused by cyanobacteria and Cyanophilous Lichens. *Int. Biodeterior.* 26: 397-417.

Darchuk L, Gatto Rotondo G, Swaenen M., Worobiec A, Tsybrii Z, Makarovska Y, Van Grieken R (2011) Composition of prehistoric rock-painting pigments from Egypt (Gilf Kébir area). *Spectrochim. Acta A* 83: 34-38.

Faimona J, Jindrich S, Kubesova S, Zimak J (2003) Environmentally acceptable effect of hydrogen peroxide on cave "lamp-flora", calcite speleothems and limestones. *Environ. Pollut.* 122: 417-422.

Falasco E, Ector L, Isaia M, Wetzel CE, Hoffmann L, Bona F (2014) Diatom flora in subterranean ecosystems : a review. *Int. J. Speleol.* 43: 231-251.

Gibeaux S, Tourron S, Bousta F (2014) Etude des effets du rayonnement UV-C sur la matière picturale dans le cadre d'une application en grotte ornée. *Laboratoire de Recherche des Monuments Historiques (LRMH) Rapport 1377A*, pp. 58.

Hauer T, Mühlsteinová R, Bohunická M, Kaštovský J, Mareš J (2015) Diversity of cyanobacteria on rock surfaces. *Biodivers. Conserv.* 24: 759-779.

Hubbell SP (2001) *The Unified Neutral Theory of Biodiversity*. Princeton University Press, Princeton, 448 pp.

Lefèvre M (1974) La maladie verte de Lascaux. *Stud. Conserv.* 19, 126-156.

Lofrumento C, Ricci M, Bachechi L, De Feo D, Castellucci EM (2012) The first spectroscopic analysis of Ethiopian prehistoric rock painting. *J. Raman Spectrosc.* 43, 809-816.

McBrearty S, Brooks AS (2000) The revolution that wasn't: a new interpretation of the origin of modern human behavior. *J. Human Evol.* 39: 453-563.

McNamara CJ, Perry TD, Barse KA, Hernandez-Duque G, Mitchell R (2006) Epilithic and endolithic bacterial communities in limestone from a Maya archaeological site. *Microbial. Ecol.* 51: 51-64.

Mortimore JL, Marshall LJR, Almond MJ, Hollins, Matthews W (2004) Analysis of red and yellow ochre samples from Clearwell Caves and Çatalhöyük by vibrational spectroscopy and other techniques. *Spectroch. Acta A* 60, 1179-1188.

Mulec J (2005) Algae in the karst caves of Slovenia. Dissertation thesis. Ljubljana : University of Ljubljana.

Mulec J, Kosi G (2009) Lampenflora algae and methods of growth control. *J. Cave Karst Stud.* 71: 109-115.

Pallipurath A, Skelton J, Bucklow S, Elliott S (2015) A chemometric study of ageing in lead-based paints. *Talanta* 144: 977–985.

Popović S, Simić GS, Stupar M, Unković N, Predojević D, Jovanović J, Grbić ML (2015) Cyanobacteria, algae and microfungi present in biofilm from Božana Cave (Serbia). *Int. J. Speleol.* 44: 141-149.

Prinsloo LC, Barnard W, Meiklejohn I, Hall K (2008) The first Raman spectroscopic study of San rock art in the Ukhahlamba Drakensberg Park, South Africa. *J. Raman Spectrosc.* 39:646-654.

Rifkin RF, Dayet L, Queffelec A, Summers B, Lategan M, d'Errico F (2015) Evaluating the Photoprotective Effects of Ochre on Human Skin by In Vivo SPF Assessment: Implications for Human Evolution, Adaptation and Dispersal. *PLoS ONE* 10 (9): e0136090.

Urzi C, De Leo F, Krakova L, Pangallo D, Bruno L (2016) Effects of biocide treatments on the biofilm community in Domitilla's catacombs in Rome. *Sci. Total Environ.* 572, 252- 262.

Wang B, Wang X, Hu Y, Chang M, Bi Y, Hu Z (2015) Chemosphere The combined effects of UV-C radiation and H₂O₂ on *Microcystis aeruginosa*, a bloom-forming cyanobacterium. Chemosphere 141, 34–43.

Zoppi A, Signorini GF, Lucarelli F, Bachechi L (2002) Characterisation of painting materials from Eritrea rock art sites with non-destructive spectroscopic techniques. J. Cult. Herit. 3: 299-308.

Synthèse du chapitre 3

Cette étude a été réalisée sur cinq pigments et deux liants et a permis de mettre en avant les différents résultats décrits ci-après.

En résumé :

- ✓ Les pigments inorganiques ne sont nullement affectés par UV-C ;
- ✓ Les liants organiques ont montré un changement de couleur suite à une irradiation aux UV-C. Cependant, leur couleur a également changé après une exposition à la lumière visible ;
- ✓ Les organismes semblent se développer préférentiellement sur les pigments en comparaison de la roche calcaire ;
- ✓ La colonisation du pigment est très rapide (15 jours) et après 120 jours le pigment est totalement colonisé par les mousses ;

D'autres études devront être menées sur le terrain afin de montrer définitivement l'innocuité des UV-C sur une partie d'une fresque. Le traitement par la lumière UV-C doit néanmoins être utilisé sur des peintures composées uniquement de pigments minéraux ; en effet, la matière organique est sensible au rayonnement UV-C.

Chapitre 4 : Traitement *in situ* des biofilms colonisant la pierre patrimoniale

Le premier chapitre de cette thèse a permis de comprendre la biodiversité des organismes se développant sous forme de biofilms sur les parois des grottes touristiques. Dans le second chapitre, le traitement UV-C a été proposé et testé en condition de laboratoire, montrant son efficacité contre les micro-algues vertes. Le troisième chapitre a permis d'être certain que le traitement proposé n'a pas d'effet secondaire indésirable sur le support colonisé par les micro-organismes.

Ayant montré son efficacité contre les micro-algues et son innocuité vis-à-vis du support minéral, le traitement UV-C est dans ce dernier chapitre appliqué en condition *in situ*.

Deux articles constituent ce quatrième chapitre :

- Le premier article, publié *Environmental Science and Pollution Research*, décrit le traitement UV-C sur tous les biofilms colonisant les parois de la grotte de la Glacière ainsi que le suivi colorimétrique des biofilms irradiés durant deux ans.
- Le second article permet de comparer le traitement UV-C à des traitements chimiques et allélopathiques dans l'église de Vicherey sur des biofilms algaux et cyanobactériens (en révision dans *Journal of Cultural Heritage*).

Ces deux articles apportent également des précisions sur la recolonisation des biofilms préalablement traités.

UV-C as an efficient means to combat biofilm formation in show caves: evidence from the La Glacière Cave (France) and laboratory experiments

Stéphane Pfendler ^a, Olympe Einhorn ^a, Battle Karimi^b, Faisl Bousta ^c, Didier Cailhol ^d, Laurence Alaoui-Sosse ^a, Badr Alaoui-Sosse ^a, Lotfi Aleya ^{a*}

^a Laboratoire Chrono-Environnement – UMR CNRS 6249, Université de Bourgogne Franche-Comté Besançon

^b Institut National de Recherche Agronomique (INRA), UMR1347 Agroécologie, BP 86510, F-21000 Dijon, France

^c Centre de Recherche sur la Conservation - Laboratoire de recherche des monuments historiques – USR 3224, Champs-Sur-Marne, Paris

^d Laboratoire Environnement, Dynamique et Territoires de Montagne (EDYTEM), UMRCNRS5204, Université de Savoie, F-73376 Le Bourg et du Lac, France

Environ Sci Pollut Res
DOI 10.1007/s11356-017-0143-7



RESEARCH ARTICLE

UV-C as an efficient means to combat biofilm formation in show caves: evidence from the La Glacière Cave (France) and laboratory experiments

Stéphane Pfendler¹ · Olympe Einhorn¹ · Battle Karimi² · Faisl Bousta³ ·
Didier Cailhol⁴ · Laurence Alaoui-Sosse¹ · Badr Alaoui-Sosse¹ · Lotfi Aleya¹

Received: 27 April 2017 / Accepted: 7 September 2017
© Springer-Verlag GmbH Germany 2017

Abstract

Ultra-violet C (UV-C) treatment is commonly used in sterilization processes in industry, laboratories and hospitals, showing its efficacy against microorganisms such as bacteria, algae or fungi. In this study, we have eradicated for the first time all proliferating biofilms present in a show cave (the La Glacière Cave, Chaux-lès-Passavant, France). Colorimetric measurements of irradiated biofilms were then monitored for 21 months. To understand the importance of exposition of algae to light just after UV-radiation, similar tests were carried out in laboratory conditions. Since UV-C can be deleterious for biofilm support, especially parietal painting, we investigated their effects on prehistoric pigment. Results showed complete eradication of cave biofilms with no algae proliferation observed after 21 months. Moreover, quantum yield results showed a decrease directly after UV-C treatment, indicating inhibition of algae photosynthesis. Furthermore, no changes in pigment color nor in chemical and crystalline properties has been demonstrated. The present findings demonstrate that the UV-C method can be considered environmentally friendly and the best alternative to chemicals. This inexpensive and easily implemented method is advantageous for cave owners and managers.

Key words: Algae; Caves; Conservation; UV-C irradiation; Bleaching effect

I. Introduction

Caves are oligotrophic habitats in which temperature and relative humidity are almost constant throughout the year (Borderie et al. 2015; Popovic et al. 2015). These ecosystems were long considered stable as they were subjected to few disturbances. In recent decades, however, they have begun to suffer from an important level of touristic activity, requiring the installation of artificial lights with high power lamps during most of the day. Due to the increased number of visits, carbon dioxide levels in cave atmospheres have risen (Faimon et al. 2006). The changes in illumination along with increased carbon dioxide has induced algal proliferation that has led to the development of structured complex multispecies biofilms (Faimon et al. 2006; Mulec and Kosi 2009; Popovic et al. 2015; Smith and Olson 2007; Piano et al. 2015; Borderie et al. 2016). This situation is of great concern to cave owners and managers who find themselves faced with a dual problem: the aesthetic impact of biofilms (Adhikary et al. 2015; Ciferri 1999; Cutler et al. 2013) and the bio-deterioration they induce to geological formations and historical cave paintings (Albertano 2012; Nugari et al. 2009). Indeed, many authors have used cultural methods (Vinogradova et al. 1998; Grobbelaar 2000; Cennamo et al. 2012) or genetic analysis (Cennamo et al. 2012; Hallmann et al. 2013) to describe wide diversity in metabolism and physiological pathways in interacting microorganisms in biofilms that include algae, bacteria and fungi biofilms, and whose physiological activity induces the degradation of colonized surfaces, particularly of limestone walls (Albertano 2012) and, more dramatically, may lead to the loss of prehistoric paintings (Mulec et al. 2008).

In an effort to counteract biofilm spread, cave managers have reduced lighting time and lamp power, thus reducing but never arresting algae proliferation. To retain the interest of tourists, caves have been treated with high-pressure cleaners (HPC) which may further spread algae cells via aerosol particles, resulting in additional algae seeding, or with chemical products that deteriorate limestone walls (Mulec and Kosi 2009) and that have been shown to be harmful to prehistoric paintings. It is also of note that some chemicals remain ineffective on some algae strains (Faimon et al. 2003). It has thus become urgent to apply environmentally friendly treatments. Previous studies (Borderie et al. 2011, 2014) applying UV-radiation partially and on only a few biofilms have demonstrated that photosynthetic biofilms may be partially eradicated with, however, a recolonization of the substrate after 16 months. It appears, therefore, that there is still a lack of, and a need for, a thorough study

integrating both entire biofilms and all biofilms colonizing cave walls, in order to produce reliable information on the efficiency of UV-C treatment in total biofilm eradication without recolonization. Such a protocol might be helpful in the goal of effective and environmentally friendly cave management.

Located in the central part of the Jura Mountains of eastern France, the show cave of La Glacière (Chaux-lès-Passavant, France) has long been the lowest-altitude ice cave in Western Europe. During the Little Ice Age, the cave's climate system was highly efficient in producing large quantities of ice (Poissenot 1586; Boissot 1686; Billerez 1712). With a single enormous entrance, the cave acted as a cold trap, provoking the accumulation at its bottom of a great volume of ice through both static and dynamic processes (Luetscher 2005). With the global warming of the 20th century, along with different environmental and climatic changes on the Vercel-Valdahon Plateau, the ice volume decreased to finally disappear 15 years ago. Non-exploitation of the forest above the cave has contributed to the decrease in ice production. Lumbering has fallen off drastically over the years. Consequently, trees have grown bigger; they now absorb more of the water which formerly streamed into the cave to contribute to the production of ice at the end of the winter and the beginning of spring. These conditions, along with an increased number of tourist visits in the second half of the 20th century which necessitated the installation of adapted lighting, induced the growth of green algae and cyanobacteria, with biofilms spreading through large sections of the cave and overlaying apparent fossils. We therefore hypothesized that an appropriate use of UV-C may remedy such developments on cave walls.

To further our study we monitored and compared the cave's two largest biofilms, one kept under artificial light and the other under sunlight. The application of UV-C to the biofilms allowed the feasibility of the method to be demonstrated and enabled evaluation of the recolonization kinetics *in situ* throughout twenty-one months. Moreover, to understand the results from *in situ* exposition and to optimize the UV-C treatment method, physiological (quantum yield = variable fluorescence / maximal fluorescence (F_v/F_m)), colorimetric (green-red values) parameters and chlorophyll spectrometry were measured daily in the laboratory on biofilms grown respectively on limestone blocks and on algae suspension. Finally, to ensure that no destruction or bleach of inscriptions and mineral paintings may be caused by UV-C treatment, manganese dioxide which is a pigment used by prehistoric humans was strongly irradiated in the laboratory.

II. Materials and methods

1. Study area

The La Glacière Cave (Fig. 1) is a well-known ice cave, 516 m a.s.l., located in the central part of the Jura Mountains in eastern France, on the Vercel-Valdahon Plateau. The plateau is a geologically complex area located within the Central Jura's thrust fault systems, just before the northern boundary of the Jura folding. In this part of the Central Plateau, the strike-slip faults—sinistral, mainly oriented north-south, and having many thrust-related folds and tear faults—disrupt the lateral continuity of the folds. In the La Grâce-Dieux-La Glacière area, the limestone is Bathonian with a Forest Marble facies. The Audeux River cuts the east-west structures. The river flows perpendicularly to the entrance of the La Glacière Cave, 300 m to the north.

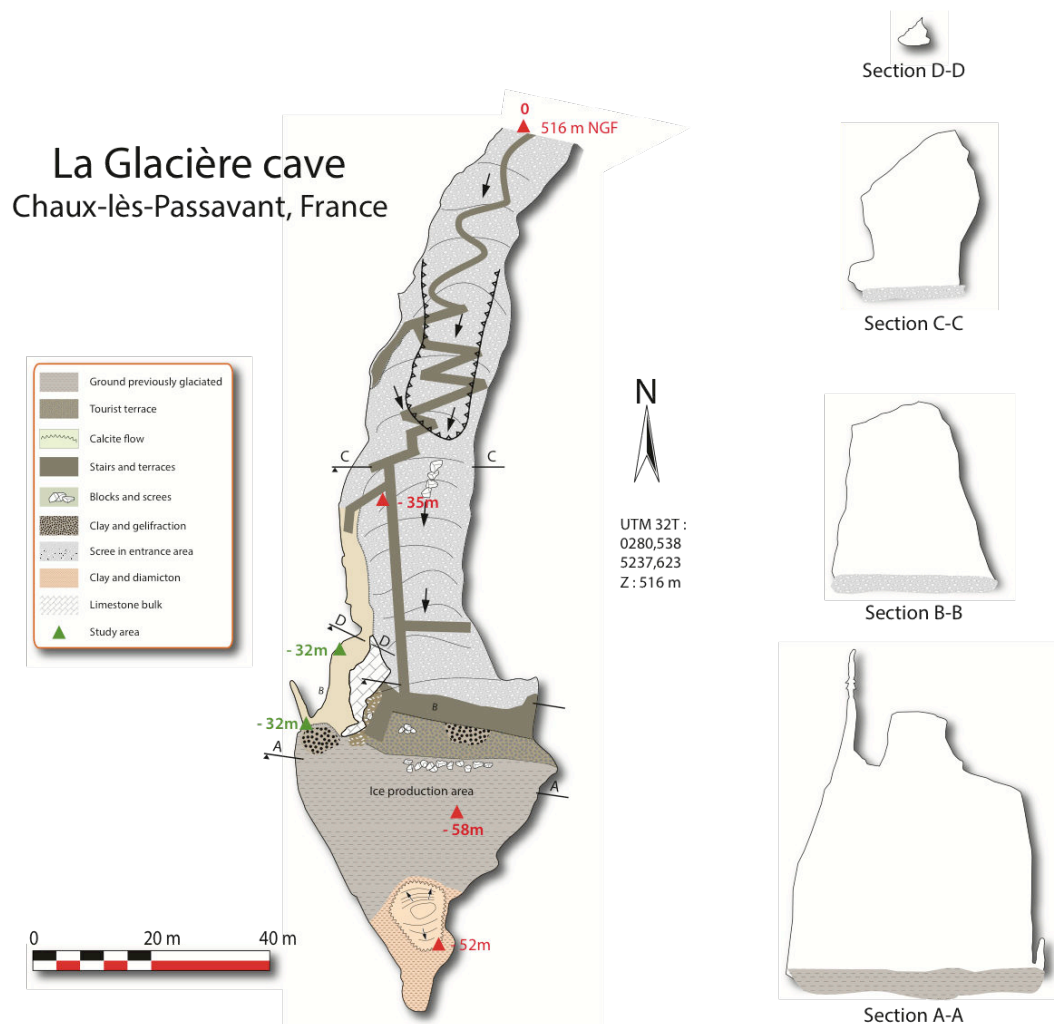


Fig. 1. Sections and plan of the Glacière cave (Doubs, France). The green triangles represent the location of both treated “Bio.int” and “Bio.ext” biofilms.

The La Glacière Cave is a huge collapsed room, 200 m long and 67 m deep. In the main chamber, a major strike-slip fault is observed. The dimensions of the main chamber are 48 m x 44 m and 52 m high. Many formations are observed: flow stones, stalactites in the ceiling and stalagmites at the southern end of the main chamber.

2. *Experiments in the cave*

Two biofilms were monitored over a period of 21 months. The first, called Bio.ext., was located 109 meters from the entrance, at a depth of 32 m, on the west wall and 2.7 m above the gallery floor. Indirectly exposed to sunlight, it was thus subjected to circadian diurnal light variations (photosynthetically active radiation (PAR) = $0.02 \mu\text{mol m}^{-2} \text{s}^{-1}$ at 12:00 in August). Its dimensions were approximately 6 m in length and 2 m in width, and in some parts its thickness reached approximately 0.5 cm. UV-C was applied to a delimited area of 1 m^2 of "Bio.ext."; colorimetric parameters were followed on 100 equidistant points (4 cm diameter) of this biofilm (Fig. 2). UV-C treatment consisted of 4 -12 hour-long exposures spread over two weeks (at T = 0, 2, 11 and 15 days). UV-C were provided by 16 UV-C lamps (Philips, 25 W each = 400 W, $\lambda \text{ max} = 254 \text{ nm}$, 553 kJ m^{-2}) installed 20 cm from the wall. In order to protect cave wildlife, UV-C box was hermetically sealed with black plastic to avoid UV-C dispersion around the treated area. Furthermore, UV-C radiation was targeted precisely onto the biofilm area, applied during the night.

The second biofilm, called "Bio.int.", was smaller (1.40 m long and 0.5 m wide, 0.7 m^2) and thinner ($<0.1 \text{ cm}$) than "Bio.ext.". "Bio.int." was located at the end of the phreatic gallery, arriving in the chimney linked with the western part of the main chamber, 127 m from the entrance and at -32 m depth. It developed at 2.9 m above the gallery floor, completely sheltered from sunlight yet directly exposed to an approximately 80 to 1500 W halogen projector (PAR = $61.49 \mu\text{mol m}^{-2} \text{s}^{-1}$). Daily exposure time to light depended on the flow of tourists (~ 4 hours per day). The entire surface of "Bio int." was UV-C treated as explained for "Bio ext." at T = 0, 5, 6 and 11 days. Colorimetric parameters were monitored on seventy points as previously described.

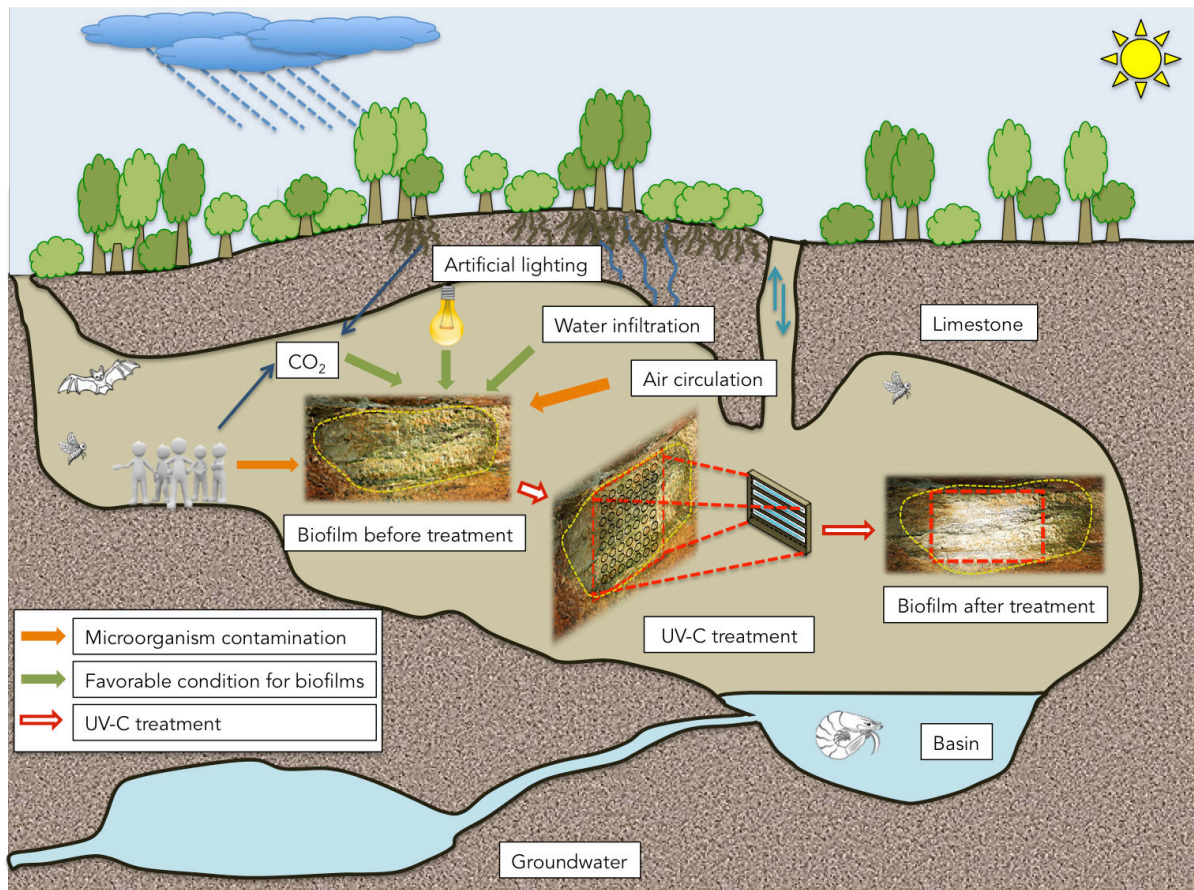


Fig. 2. Illustration of the cave showing (i) environmental parameters influencing biofilm proliferation and (ii) UV-C treatment on “Bio.ext.” with the measurement pattern.

For both biofilms, the colorimetric parameters were determined before the first UV-C treatment. These values constitute the control. Parameters were monitored according to cave owner availability and depending on tourist presence.

Temperature of the cave was monitored every 15 min close to both “Bio.ext” and “Bio.int” biofilms with the temperature sensors: Niphargus (from May to August 2016) and Reefnet (from August to December 2016) (Fig. 3). Temperature was calibrated in factory with a reference to improve its initial absolute accuracy from 0.5 °C to about 0.1 °C between 5 and 30 °C.

In order to confirm UV-C deleterious effect on microorganisms, “Bio.int.” and “Bio.ext.” biofilms were sampled before and after UV-C irradiation with sterile swab and then cultured on Petri dishes containing Blue-Green medium (BG11) added with 15 % pure agar. Agar plates were maintained 16 hours/day under artificial light ($150 \mu\text{mol m}^{-2} \text{s}^{-1}$) during 3 weeks. Then cultivable algae and cyanobacteria strains were identified with the microscope Olympus CX31.

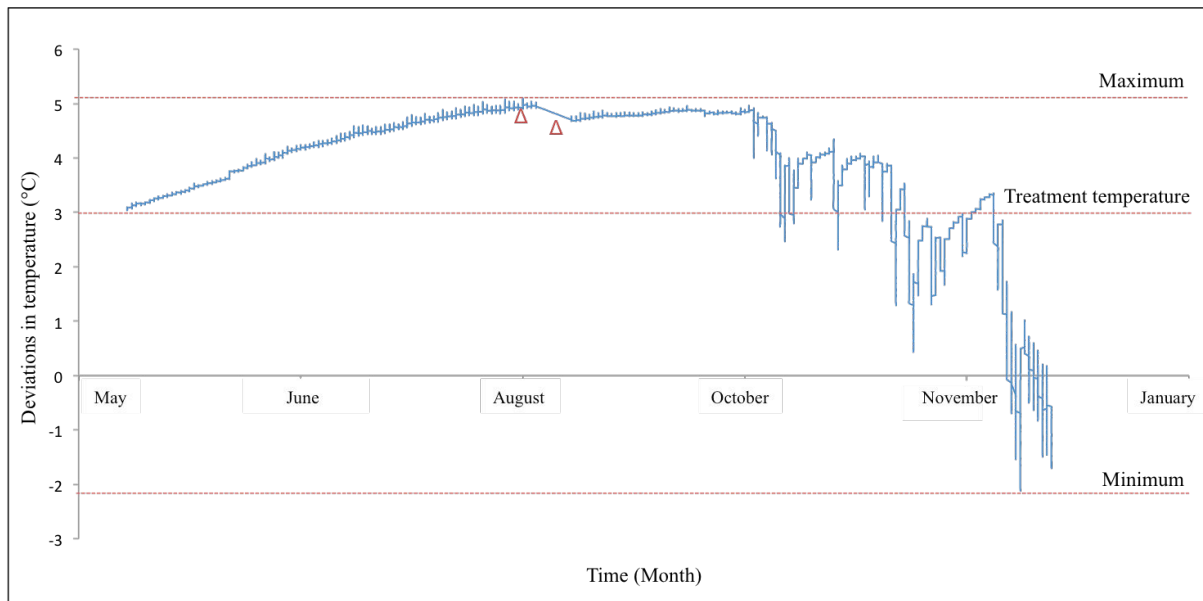


Fig. 3. Temperature inside La Glaciere show cave has been monitored during 7 months close to both “Bio.ext” and “Bio.int” biofilms with the temperature sensors: Niphargus (from May to August 2016) and Reefnet (from August to December 2016). Change of temperature device is shown with the red symbol “Δ”.

Fungal colonies growing on UV-C treated biofilm (Bio.ext.) were sampled, cultivated and purified on Malt Extract Agar medium (Sigma). DNA extractions were carried out by dissolving a small part of the colony in 100 μl Prepman Ultra solution (Applied Biosystems). Then, the suspensions were heated at 95 $^{\circ}\text{C}$ during 10 min. After centrifugation, 2.5 μl of supernatant of each sample were added into 250 μl ultra pure water. Polymerase Chain Reaction (PCR) reaction solutions were mixed as followed: 12.5 μl of DNA, 2 μl of forwards (Internal Transcribed Spacer 1 (ITS1)*f*: 5' -CTTGGTCATTTAGAGGAAGTAA- 3') and reverse primers (ITS2 *r*: 5' -GCTGCGTTCTTCATCGATGC- 3'), 25 μl of mastermix and 8.5 μl of ultra pure water. Afterward, DNA was amplified using following PCR steps:

denaturation at 95°C / 2 min, denaturation 95°C / 30 sec, hybridation 62°C / 30 sec, elongation 72°C / 1 min, (35 cycles at 57 °C) and final elongation 72°C / 10 min.

Then, 2 µl of ExoSAP[®] solution was added to 5 µl of amplified DNA (37°C / 15 min and 80°C / 15 min). Afterward, samples were amplified with fluorescent dideoxynucleotide (BigDyeTerminator 3.1, AppliedBiosystems) and purified with BigDye XTerminator (AppliedBiosystems). Finally, sequencing has been carried out with a 3130 DNA sequencer.

3. *Experiments under controlled conditions*

The laboratory experiments were conducted on a strain of *Chlorella* sp., a genus widely present in European caves and reported as dominant in a UV-C treated biofilms in the Moidons cave (Borderie et al. 2014) and previously sampled (Borderie et al. 2014) and isolated for measuring physiological response to UV-C. Cells were inoculated on limestone blocks, stored on vermiculite and moistened with BG11 medium (Sigma Aldrich) at 20 ml L⁻¹ concentration. They were then kept at 20°C, under artificial light (150 µmol m⁻² s⁻¹) for 16 hours per day at 50% moisture. Algal biofilms were allowed to develop over 2 weeks; the limestone blocks were then exposed for 39 minutes under 4 UV-C lamps (Philips, 25 W each = 100 W, λ max = 254 nm) corresponding to a dose of 30 kJ m⁻². This UV-C dose was previously calculated as the minimal exposure capable of killing all cells. After UV-C treatments, the blocks were stored on moistened vermiculite, 3 of them under artificial light (150 µmol photons m⁻² s⁻¹) and 3 others in the dark until day 21. At this date, they were transferred to the same light conditions (150 µmol photons m⁻² s⁻¹) as the other blocks and maintained there until the end of the experiment. Measurements of colorimetric parameters and quantum yield were taken just after irradiation (day 0) and at varying dates until day 24.

In order to understand the importance of exposing irradiated biofilms to VIS-light, *Chlorella* sp. suspension (optical density = 0.3) was irradiated in glass Petri dishes with 30 kJ m⁻² UV-C. Half of the samples were maintained in the dark and the other half under culture conditions (150 µmol m⁻² s⁻¹). Spectrometry analysis was carried out daily during one week with the spectrometer Analytikjena specord 205 (wavelengths between 350 nm and 750 nm).

4. *Measurements*

Biofilm color was determined using a spectrophotometer (CM-600d KONICA MINOLTA, illuminant D65, SCI mode and 8 mm diameter target mask) which measured the "a*" parameter on the green-red scale and the L* parameter on the dark-light scale. The dark-light scale (L*) is associated with the lightness of the color and moves from bottom (value: 0, black) to top (value: 100, white). The a* scale is associated with changes in redness-greenness (positive a* is red and negative a* is green). Both the L* and a* values were chosen for this study because they reflect the presence of a green biofilm (L* indicates darkening and a* greening) (Borderie et al., 2014). Measurements were taken daily for the following 21 days.

Quantum yield was measured using the photosynthesis yield analyzer mini-PAM (WALZ, Germany).

5. *UV-C treatment of pigment*

- Pigment preparation and treatment

Colorimetric parameters, X-Ray Crystallography and Fourier Transform Infrared Spectroscopy analysis were carried out on 8 g of manganese dioxide, a pigment used by prehistoric humans. Pigments powder and binders were placed in glass Petri dishes (5 cm diameter). Samples were then irradiated for 104 hours with 8 UV-C lamps (Philips, 25 W each = 200 W, λ max = 254 nm) corresponding to a dose of around 4 800 kJ m⁻².

- Colorimetric measurement of manganese dioxide

Colorimetric parameter L* was measured on dry pigments and binders (n=4) in order to avoid color change due to moisture with a spectrophotometer (see 2.5. *Measurements*).

- Fourier transform infrared spectroscopy

After grinding in a mortar about 2% of the weight of manganese dioxide in anhydrous KBr the mixture was placed in a mechanic press to obtain a thin and translucent pastille. The spectra were then measured at room temperature with a Fourier Transform Infrared Spectrometer (IRAffinity-1, Shimadzu). In order to make a comparative study, 30 scans were carried out.

- *X-ray crystallography*

Pigment sample was crushed in a mortar with an agate pestle and placed in a mined glass slide. The diffractometer used was an automated Bruker D8 AdvanceLynxEye Detector (cobalt tube λ $K\alpha_1 \approx 1,789 \text{ \AA}$). The scan was 0 to $70^\circ 2\theta$, with a speed of about $0,005^\circ$ per second. The diffractograms obtained were traced on software Diffrac Plus Measure and interpreted using Diffrac Plus Eva.

6. *Statistical analysis*

All statistical analyses were conducted using R.2.14 software (R Development Core Team, 2011) at a significant level of 0.05. Parametric statistics were used for in situ data results after verifying the normality (Shapiro test) and homogeneity of variances (Bartlett test of equality of variances). Parametric analysis (Anova) on colorimetric laboratory data and non-parametric analysis (Kruskal-Wallis) on quantum yield data has been used.

III. Results

1. *In situ* experiments

Following UV-C treatment the color parameters of the two biofilms in the La Glacière Cave were monitored for two years. Treatment effects were somewhat different for the two biofilms.

"Bio.ext.", the biofilm exposed to weak natural sunlight (Fig. 4, Fig. 5, Table 1), presented a rapid increase in the "a*" parameter which means that the green color faded immediately following the first UV-C exposures ($p\text{-value} < 0.001$). From there, a continuous and progressive fading of the green color, *i.e.* a continuous increase in the "a*" parameter was observed until the day 331. Concomitantly, the L* parameter increased, reaching a nearly constant value after 12 days ($L^* = 43$) corresponding to the brightness of the underlying rock.

In contrast, "Bio.int.", which was only exposed to artificial light (Fig. 4, Fig. 5), faded much more slowly since a significant modification in the color ("a*" parameter increase) was only detected on day 12, *i.e.* after the final irradiation event. Nevertheless, the biofilm brightness (L* parameter) was modified (after 4 days) as soon as the first UV-C exposure was achieved as it was also observed for "Bio.ext." and the values corresponding to those of the underlying rock persisted until the end of the experiment. From a human visual point of view the green color totally disappeared at day 51.

In addition to these findings, it is noteworthy that after the treatments no microorganisms sampled from the organic matter were able to grow on BG11 medium, whereas 7 strains of *Cyanobacteria* and *Chlorophyta* (Table 2) grew up before the treatment. Moreover, twenty-one months later no photosynthetic microorganisms nor fungi were observed for "Bio.int.". In contrast, two white small and thin fungal colonies (<0.5 cm diameter) were observed for "Bio.ext." one year after the first treatment and persisted over 2 months. These colonies corresponded to *Geomyces* sp.



Fig. 4. For 20 years ago, La Glacière show cave produced huge quantity of ice (A). Since global warming, positive temperatures were measured and no more ice was produced during the winter (B). In summer, plants (C) are able to growth between C-C section and cave entrance. “Bio.ext” (D) and “bio.int” (E) biofilms were eradicated by UV-C treatment and showed no proliferation (E), (G) after 21 months. “Bio.ext” showed a variety of color corresponding to different algae, cyanobacteria and mosses strains (F). After UV-C irradiation, all photosynthetic microorganisms showed a loss of their green color and an important amount of organic matter stayed on the treated cave wall (G).

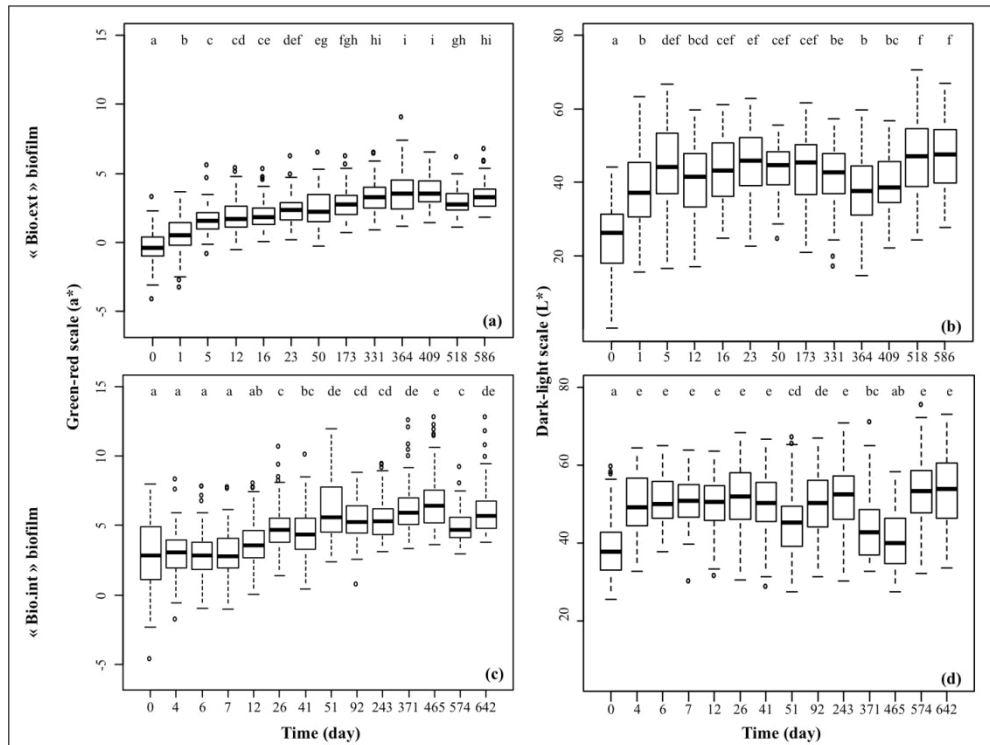


Fig. 5. Biofilm (“Bio.ext.” and “Bio.int.”) colorimetric measurement (green-red scale a* (a) (c), and dark-light scale L* (b) (d)) after 4 treatments of 12 hours. Statistical significant differences are represented with the letters “a” to “i”.

Table 1. Characteristics of the two biofilms and statistical results of colorimetric measurements.

| Biofilms | Colonization area (m ²) | PAR (μmol photons m ⁻² s ⁻¹) | Colorimetric parameters | p-value |
|----------|-------------------------------------|---|-------------------------|----------|
| Bio.ext | 0.7 | 0.02 | L* | 5.87E-06 |
| | | (sunlight at midday) | a* | 4.71E-04 |
| Bio.int | 1 | 0 | L* | 3.34E-02 |
| | | (without artificial light) | a* | 2.14E-04 |
| | | 61.49 | | |
| | | (with artificial light) | | |

Bio.ext: Biofilm exposed to low sunlight; Bio.int: Biofilm exposed to artificial light; PAR: Photosynthetically active radiation; L*: Dark-light scale; a*: green-red scale; P-value was obtained with Bartlett test.

Table 2. List of algae, cyanobacteria and mosses sampled on both biofilms and growing on Petri dishes.

| | |
|----------------------|--------------------------|
| Cyanobacteria | <i>Synechococcus</i> sp. |
| | <i>Cyanothece</i> sp. |
| Chlorophyceae | <i>Gloeocystis</i> sp. |
| | <i>Stichococcus</i> sp. |
| | <i>Scotiellopsis</i> sp. |
| | <i>Chlorella</i> sp. |
| | <i>Prasiolopsis</i> sp. |
| Bryophyta | <i>Syntrichia</i> sp. |
| | <i>Tetraphis</i> sp. |

2. Experiments under controlled conditions

- Colorimetric and physiological parameters

Samples maintained in the light after UV-C exposure showed a non-significant increase in the "a*" parameter the first day after exposure (Fig. 6, Table 3). Later it began to decrease, until day 9, while no green color had been observed since day 3. One week after UV-C exposure, the "a*" parameter was closer ($a^* = 0.03$) to the "a*" value for the limestone block ($a^* = 0.90$) than to the "a*" value for a fresh control biofilm culture ($a^* = -5.11$). After day 9 day, the "a*" parameter started to decrease slowly.

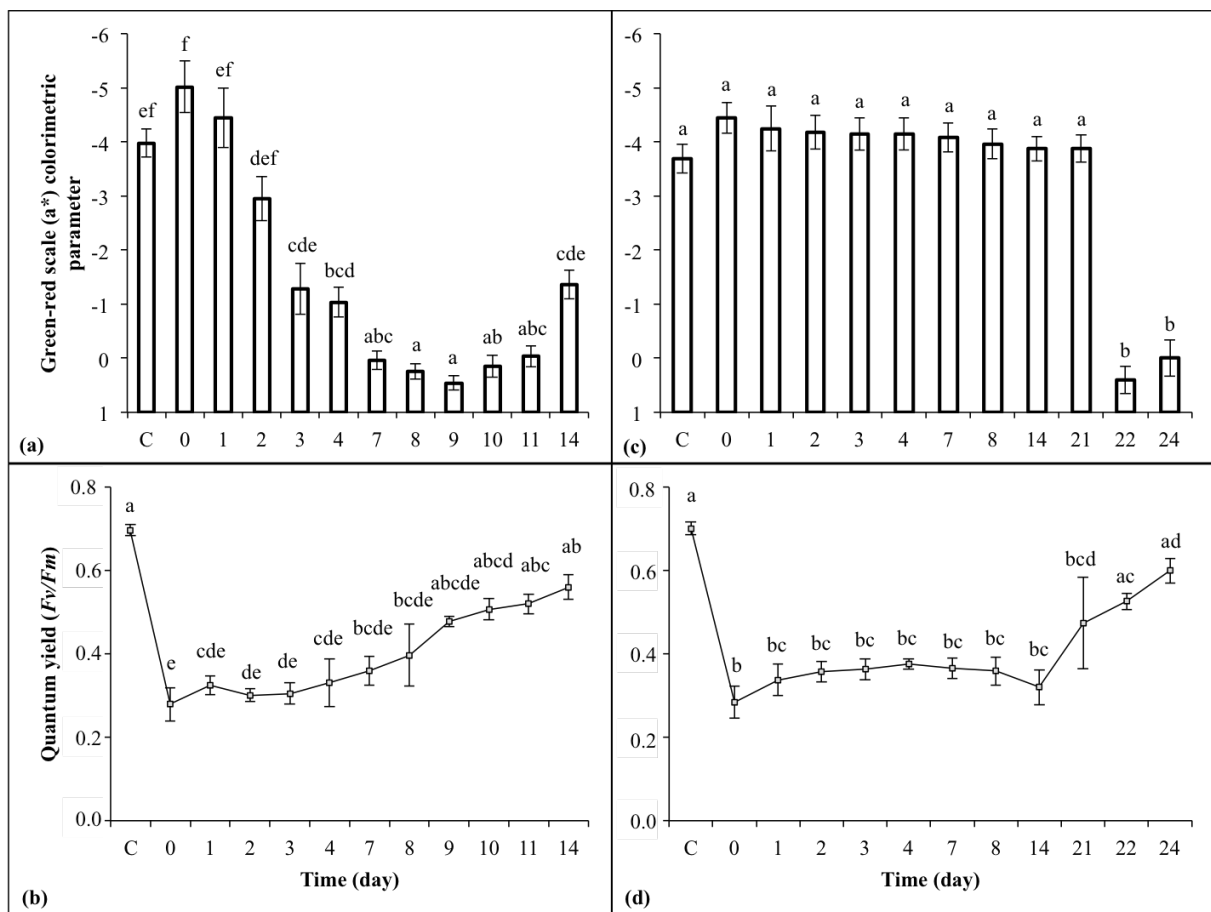


Fig. 6. Green colorimetric parameter (a^*) (a) and (b) quantum yield (F_v/F_m) of biofilms growing on limestone and treated with UV-C (30 kJ m^{-2}) maintained under light conditions throughout the experiment or in the dark. Green colorimetric parameter (a^*) (c) and (d) quantum yield of biofilm maintained in the dark for 21 days and previously treated with UV-C (30 kJ m^{-2}). They were then cultivated under light conditions.

For samples stored in the dark (Fig. 6), a similar non-significant increase in the "a*" parameter was observed just after exposition. After this first decrease in the "a*" parameter corresponding to an intensification of the green color, this parameter remained stable (no significant differences with day 0) until day 21. At this date, when the light was switched on, a drastic drop in the "a*" parameter value (80%) was observed, whereas for a human observer the green color disappeared in space of a few hours. At day 21 or only 24 hours after the return to light, the "a*" parameter presented a similar value to that recorded on day 9 for the sample maintained in the light after UV-C treatment. After that date, "a*" began a slow decline, indicating the beginning of recolonization of the block.

Concerning the maximum quantum yield, F_v/F_m , a drastic decrease (60% of the control value; $F_v/F_m = 0.697$ to 0.279) was observed immediately after UV-C treatment, whether on the sample exposed to the light or in the sample maintained in the dark. After that first drop, the F_v/F_m value evolved differently for the two samples. In the case of the sample exposed to light, the maximum quantum yield first stagnated and then began a gradual and significant increase as of day 7. At the end of the experiment, at day 14, its value (0.52) was significantly different from that noted just after UV-C treatment but also significantly different from the control value, suggesting a partial and gradual recovery. In contrast, for the dark-maintained sample, F_v/F_m remained stable at low values around 0.35 , similar to the value registered just after UV-C irradiation. At day 21, just after switching on the light, a very quick increase in the maximum quantum yield was observed. The F_v/F_m value changed from 0.33 to 0.60 over only 2 days, suggesting a partial but very quick recovery. At the end of the two experiments (in light and dark) the maximum quantum yields for the two samples were very close to each other, though they remained significantly smaller than the initial control value.

Table 3. Statistical results of colorimetric and quantum yield measurements.

| Light condition | Colorimetric parameter | p-value | Physiologic parameter | p-value |
|-------------------|------------------------|-----------|-----------------------|----------|
| Culture condition | a* | 2.15E-12 | Quantum yield | 3.23E-03 |
| Darkness | | 1.00 E-11 | (Fv/Fm) | 1.90E-02 |

a*: Green-red scale; P-value was obtained with an ANOVA test (colorimetric parameters) or a Kruskal-Wallis test (quantum yield).

- In vitro effects of VIS-light

Spectrometric results obtained on algae suspension treated by UV-C and maintained in the dark or under light conditions were correlated with previous colorimetric measurements. On the one hand, results from algae suspension cultured under light conditions show that UV-C induced chlorophyll degradation (Fig. 7). In fact, all peaks corresponding to chlorophyll *a* and *b*, which were present on the spectrum before the treatment, disappeared after 15 hours. On the other hand, *Chlorella* sp. spectra cells cultured in the dark show a slow degradation of chlorophyll *a* and *b*. Even after 5 days in the dark, chlorophyll peaks were still present.

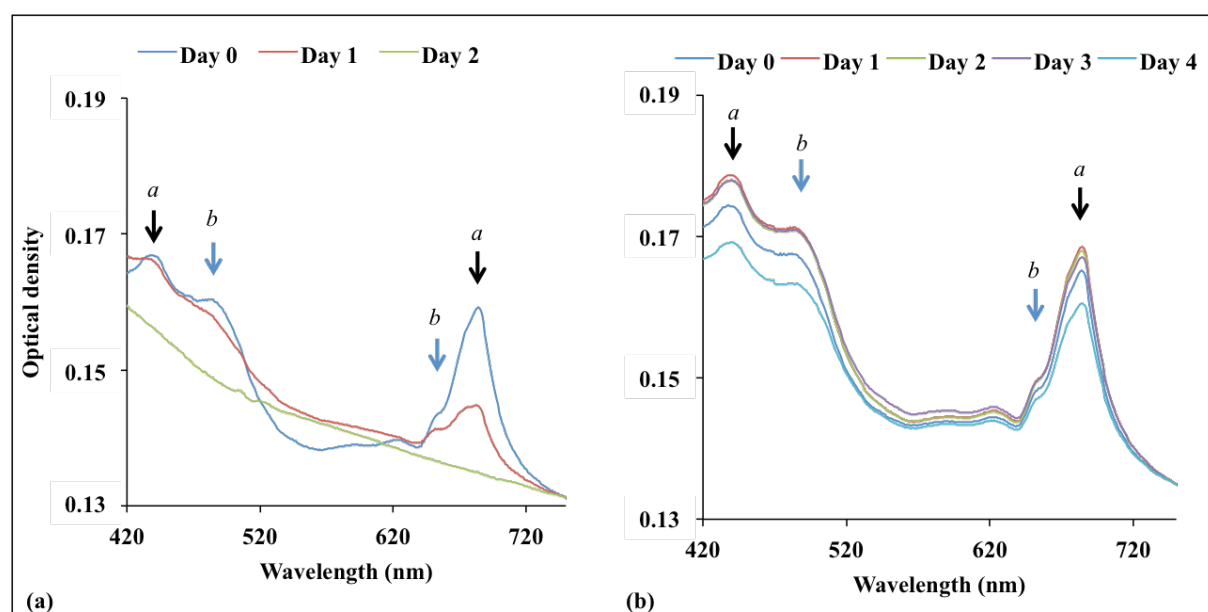


Fig. 7. Algal suspensions were irradiated with UV-C (30 kJ m^{-2}) and then cultivated under light conditions (a) or in the dark (b). Suspensions were monitored with a spectrometer before treatment and every day for 5 days.

- Monitoring of molecule, crystalline and color UV-C treated pigment

Manganese dioxide pigment was monitored with one of the CIELAB parameter (light-dark parameter, L^*). Furthermore, molecules composing the pigment were tested using infrared spectroscopy. Finally, crystalline composition was analyzed with X-ray crystallography before and after UV-C irradiations. None of these three methods revealed any change in manganese dioxide color, molecules or crystalline composition (Fig. 8). The curves conserved all peaks in IR and X-ray crystallography even if certain peaks appeared lower or higher between control and treated pigment, a change due only to a difference in concentration.

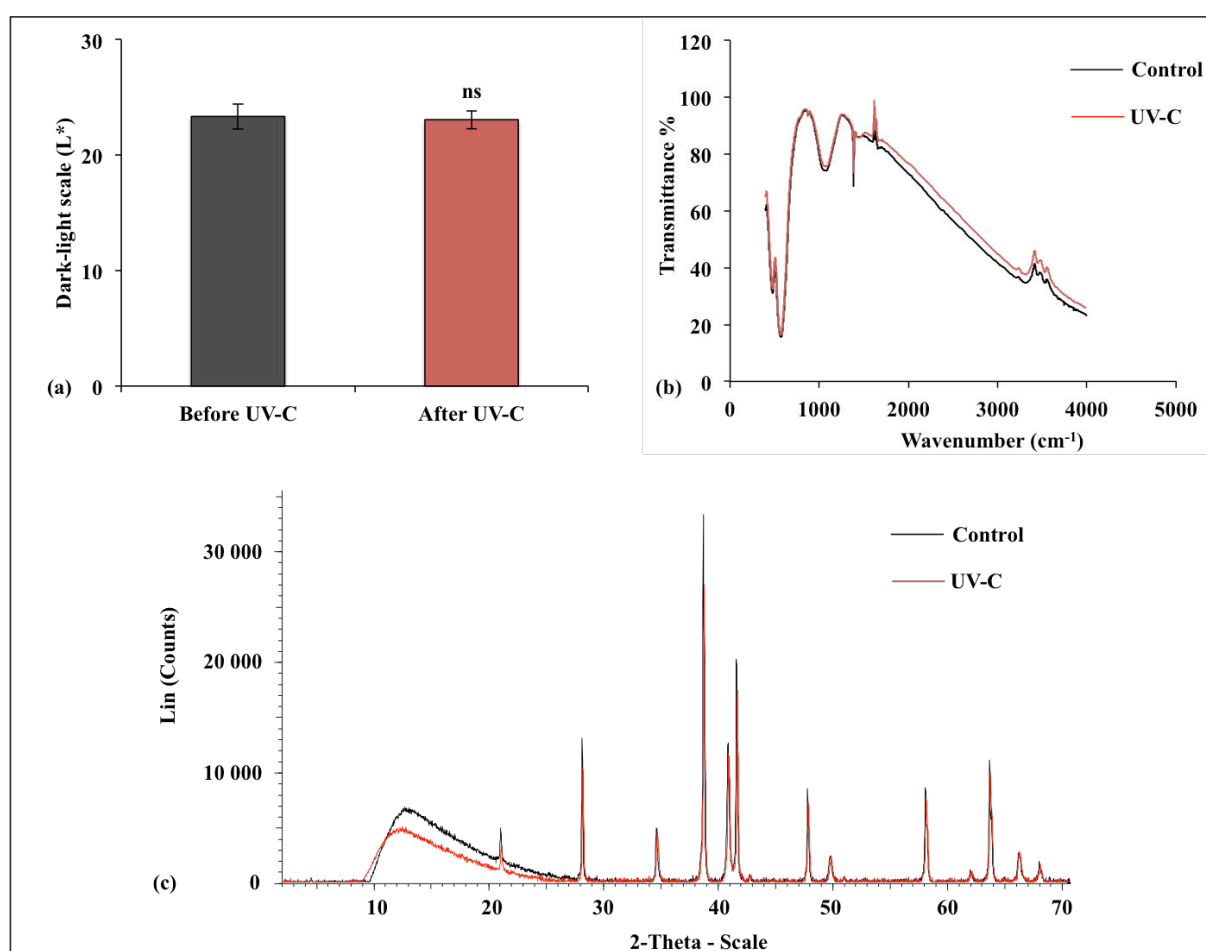


Fig. 8. Colorimetric measurements (a), infra-red analysis (b) and DRX analysis (c) has been carried out before and after UV-C treatment on manganese dioxide powder.

IV. Discussion

Caves are among the most extreme subterranean habitats; microorganisms inhabiting them must cope with harsh environmental conditions by forming biofilms (Borderie *et al.*, 2015). It becomes obvious that this adaptive strategy gives them a capacity to resist eradication. In this section, we discuss the application of UV-C to the epilithic biofilms and the recolonization kinetics *in situ*, and the physiological and colorimetric responses obtained in controlled laboratory experiments on biofilms growing on limestone blocks.

- *In situ* experiments

CIELAB color parameters (L^* and a^*) are a useful tool, which may be correlated with the chlorophyll a, carotenoid and phycocyanin contents of biofilm-forming microorganisms (Sanmartín *et al.*, 2010). Analogously, other authors have observed a good linear relationship between colorimetric measurements and the amount of cyanobacterial cells (Prieto *et al.*, 2004). Our results showed that only four expositions at 553 kJ m^{-2} over two weeks were enough to kill the microorganisms present in the biofilm and, consequently, to cause the green color to disappear from the biofilm and specifically from the microalgae. These results support those already obtained with our method but to a lesser extent than in another cave (Borderie *et al.* 2014). Moreover, this discoloration persisted for a longer time, since nearly twenty-one months later (642 and 586 days, respectively, for Bio.int. and Bio.ext.) no decrease in color parameters (a^* and L^*) were detected. These results are to be compared with those reported by Borderie *et al.* (2014) who observed a recolonization after nearly one year but who used a far lower UV-C exposure (180 kJ m^{-2}). Furthermore, this recolonization is probably due to the proximity of the treated biofilm to another non-treated biofilm. In addition, the discoloration occurred quickly, immediately after the first exposition for Bio.ext., for the biofilm which was exposed to weak but constant sun light throughout the day. It took place a little less quickly for Bio.int., after the fourth exposition, for the biofilm which was exposed only to the artificial and intermittent lighting inside the cave. At first glance, these results are even more surprising than for the outside biofilm Bio.ext. which bleaches more quickly and is thicker.

The non-ability of all algae and/or cyanobacteria forming the biofilm to growth on BG11 medium has been proved after the last irradiation, confirming that the treated wall was

effectively sterilized. However, the recolonization question is still open- if cave owners don't manage differently their cave, recolonization will occur.

In this study, we have shown that organic matter from dead microorganism remains on the support (Fig. 3) favoring the proliferation of opportunistic microorganisms such as fungi (Barberousse 2006). It is thus important to remove immediately the organic matter to prevent fungi development. In our study, however, the development of two small fungi colonies represented less than 2 cm² in comparison to the 1 m² suggesting that fungi grew on animal excrements, rather than on debris from algae and cyanobacteria. In fact, *Geomyces* sp. is well known as pathogenic fungi of bats (Kravchenko et al. 2015), which are present in the Glacière cave.

- UV-C treatment optimization

The experiments carried out under controlled conditions with a monospecific *C. vulgaris* biofilm grown on limestone blocks are in good accordance with the results observed in the cave. After UV-C exposure, the persistence of the green coloration was observed on blocks maintained in darkness. In fact, UV-B, like UV-C, are well known in the food industry for their ability to keep vegetables from yellowing during storage in darkness (Aiamla-or et al. 2010; Srilaong et al. 2011; Chairat et al. 2013). This may be explained by the fact that UV-B and UV-C exert an inhibitory effect on the enzymes chlorophyllase, Mg-dechelatase and chlorophyll peroxidase, involved in the chlorophyll degradation pathway (Costa et al. 2006; Jiang et al. 2010; Aiamla-or et al. 2010). However, the UV-B or UV-C irradiation dose used in order to delay senescence in food industry are sublethal, *i.e.* much lower than the dose used in this study. In our case, referring to a previous study (Borderie et al. 2014), we chose a dose sufficient to kill the cells within a few minutes or, at worst, in a few hours. UV-C is known as one of the most energetic and harmful photolytic agents. It has the potential for inducing DNA damage, even in very short exposures. Georgieva et al. (2015), using a dose similar to ours, reported significant nuclei damage to peas, barley and wheat. Moreover, these authors suggest that UV-C impact may depend on genome size. The greater the number of base pairs, the less significant the UV-C impact will be. With its small 46 Mb genome, *Chorella* may be severely impacted by UV-C exposure. Photosystem II (PS II) is another important target of UV-C, as discussed by Szilárd et al. (2007) who reported that UV-B absorption disrupts the structure of the Mn cluster from PS II, causing a structural and/or functional change that renders the entire complex inactive and leading to the production of reactive oxygen species.

Nevertheless, one or the other, and probably both phenomena have been implicated in the death of the algae.

The question remains, however, of the persistence of the green coloration on the dark-maintained blocks and suspensions and, in contrast, of its progressive disappearance over three days on blocks exposed to a weak light source. These observations are similar to those reported by Kotani et al. (1999) working on boiled broccoli florets. Chlorophyll is, by nature, photosensitive. Zvezdanovic et al. (2009) showed that under UV, chlorophyll undergoes destruction (bleaching) accompanied by fluorescent transient formation. According to these authors, the bleaching is governed by UV-photon energy input, as well as by different chlorophyll molecular organizations in different solvents (*in vitro*), and in thylakoids (*in situ*). However, in the boiled florets of broccoli, as well as in algae maintained in the dark, no bleaching was observed consecutively to the UV treatment, whereas the bleaching was significant for samples placed in the light. Moreover, in the case of algae maintained in the dark after exposition to lethal UV-C irradiation, discoloration begins only upon exposure to light. The light seems to interact with the already UV-C destabilized chlorophyll molecules and may be essential to the bleaching process. Kotani et al. (1999) have reported that the interaction of light with destabilized chlorophyll molecules gives rise to harmful oxygen-reactive species. Scavenging enzymes, whether in broccoli florets or in algae, do not remain functional after boiling, nor after UV-C exposure; they cannot be removed and therefore enhance the damage to chlorophyll and other cellular components (Kotani et al. 1999). The same phenomenon can explain the faster disappearance of "Bio.ext." in the La Glacière Cave even though it is thicker than "Bio.int."

The maximum quantum yield, F_v/F_m , was severely affected by the UV-C exposure and was vastly reduced as soon as the treatment ended. As reported by Szilárd et al. (2007) and by Takahashi and Badger (2011), PS II is one of the major targets of UV radiation. As mentioned previously, it is the Mn cluster of PS II which is mainly affected. Highly reactive singlet oxygen can always be produced at the PS II level, but also in the antenna (Krieger-Liszkay 2004). Thus, the drastic decrease of F_v/F_m was not surprising. Interestingly however, after the end of exposure, the maximum quantum yield of algae exposed to weak light began a slow but continuous increase and at day 9 that parameter was no longer significantly different from the control value prior to treatment. The same was observed in the case of the algae kept in the dark for 21 days and then exposed to the same weak light as the other samples. In this case, the recovery took place in only 24 hours. As reported by Allakhverdiev and Murata (2004) working on *Synechocystis* sp. and later supported by Takahashi and Badger (2011), the

rate of PS II repair depends on the presence of light, but is saturated at relatively weak light intensities. More recently, Mulo et al. (2012) working on *Chlamydomonas reinhardtii* showed that a correct splicing of the *pbsA* transcript could be achieved only under weak light intensities and this constituted the key step in the PS II reparation process. Our results are in agreement with these observations. In our case the weak light intensities promoted the recovery of PS II after UV-C exposure.

As previously stated, the UV-C treatment we applied was sufficient to cause the death of the algae in just a few hours. The explanation for this apparent contradiction lies in the structure of the biofilm itself. In fact, the biofilms on the blocks were composed of many layers of cells arranged upon each other. The cells of the upper layers which directly intercept the UV radiation are killed while the cells of the lower layers, protected by the shield formed by the overlying cells, survive. If the lower cells suffer from UV-C exposure at all, it is from sublethal doses. After treatment and as soon as they receive sufficient light, *i.e.* as soon as the pigments present in the upper layer cells have been destroyed, they undertake the PS II restoration process (if necessary) and are thus quickly able to resume photosynthesis. This is also why a new decrease in the "a*" parameter reflecting a greening was observed on both groups of limestone blocks at the end of the experiment, when they were exposed to weak light and when the green color of the overlying biofilm had disappeared.

- Effect of UV-C on prehistoric pigment

To ensure that UV-C could be applied without destruction or bleach in caves with prehistoric paintings, we applied a long UV-C exposition on manganese dioxide used by prehistoric human. In contrast to Athanassia et al. (2000) and Chappé et al. (2003) who reported a darkening of the pigment and an alteration in its molecular composition after UV-C laser use, we observed no change in the color nor in the molecule and crystalline structure of manganese dioxide using classic UV-C lamp. This difference may be explained by the fact that the use of laser induces a strong increase in temperature causing damage to pigment structure. These results were expected, given that theoretical UV-C energy is not powerful enough to break mineral-chemical bonds. These results were also corroborated by those of Gibeaux et al. (2014) who conducted this experiment with lower UV-C intensities and time periods (16 hours at 45W maximum).

V. Conclusions

Our results confirm that UV-C treatment is efficient on biofilms in caves since no microorganism recolonization was observed for 21 months. Microorganisms are killed by radiation while no change in manganese dioxide pigment color nor in its chemical structure has been observed. This study underscores the fundamental need for weak white light after UV-C exposure to induce a complete bleaching of dead cells. To counteract fungi proliferation we suggest the removal of organic matter debris by applying a vacuum on dry surfaces or by conventional methods to treat wet surfaces.

VI. Acknowledgements

This study is part of the PhD Thesis of Stephane Pfendler. First of all, we are grateful to the owners of the La Glacière Cave, Mr Roland Michel and Mr Roland Romain, who kindly gave us permission to access the cave and to carry out all our field experiments. We also thank the *Ministère de la Culture et de la Communication* (France) and the *Laboratoire de Recherche des Monuments Historiques* (LRMH, Paris) for their financial contribution. We also express our gratitude to Christophe Gauchon for his precious help in cave plan drawing. We express our appreciation to the editor, Dr. Philippe Garrigues, and to the anonymous reviewers for helping to improve our paper.

VII. References

- Adhikary SP, Keshari N, Urzi C (2015) Cyanobacteria in biofilms on stone temples of Bhubaneswar, Eastern India. *Algol. Stud.* 147, 67–93.
- Aiamla-or S, Kaewsuksaeng S, Shigyo M, Yamauchi N (2010) Impact of UV-B irradiation on chlorophyll degradation and chlorophyll-degrading enzyme activities in stored broccoli (*Brassica oleracea* L. Italica Group) florets. *Food Chem.* 120, 645–651.
- Albertano P (2012) Cyanobacterial Biofilms in Monuments and Caves. In: Whitton B.A. (Ed.) – Ecology of Cyanobacteria II: Their diversity in space and time. United Kingdom: 317-342.
- Allakhverdiev SI and Murata N (2004) Environmental stress inhibits the synthesis de novo of proteins involved in the photodamage–repair cycle of Photosystem II in *Synechocystis* sp. PCC 6803. *Biochim. Biophys. Acta.* 1657, 23– 32.
- Athanassia A, Hilla AE, Fourriera T, Burgiob L, Clarkb, RJH (2000) The effects of UV laser light radiation on artists’ pigments. *J. Cult. Heritage* 1: 209-213.
- Barberousse H (2006) Etude de la diversité des algues et des cyanobactéries colonisant les revêtements de façade en France et recherche des facteurs favorisant leur implantation. PhD thesis, pp 192.
- Billerez (1712) Description de la Glacière naturelle du Comté de Bourgogne. Mémoire de L’Académie pour 1712. pp . 21-24.
- Boissot (1686) Lettre à Monsieur Dodard. Mémoire de l’Académie pour 1686. pp. 4-5.
- Borderie F, Alaoui-Sossé L, Raouf N, Bousta F, Oriol G, Riefel D, Alaoui-Sossé B (2011) UV-C irradiation as a tool to eradicate algae in caves. *Int. Biodeterior. Biodegrad.* 65, 579–584.
- Borderie F, Tête N, Cailhol D, Alaoui-Sehmer L, Bousta F, Rieffel D, Aleya L, Alaoui-Sossé B (2014) Factors driving epilithic algal colonization in show caves and new insights into combating biofilm development with UV-C treatments. *Sci. Total Environ.* 484, 43-52.
- Borderie F, Alaoui-Sossé B, Aleya L (2015) Heritage materials and biofouling mitigation through UV-C irradiation in show caves: state-of-the-art practices and future challenges.

Environ. Sci. Pollut. Res. 22, 4144–4172.

Borderie F, Denis M, Barani A, Alaoui-Sossé B, Aleya L (2016) Microbial composition and ecological features of phototrophic biofilms proliferating in the Moidons Caves (France) : investigation at the single-cell level. Environ. Sci. Pollu. Res. 23, 12039–12049.

Cennamo P, Marzano C, Ciniglia C, Pinto G, Cappelletti P, Caputo P, Pollio A (2012) A survey of the algal flora of anthropogenic caves of Campi Flegrei (Naples, Italy) archeological district. J. Cave Karst Stud. 74, 243–250.

Chairat B, Nutthachai P, Varit S (2013) Effect of UV-C treatment on chlorophyll degradation, antioxidant enzyme activities and senescence in Chinese kale (*Brassica oleracea* var . *alboglabra*). Int. Food Res. J. 20, 623–628.

Chappé M, Hildenhagen J, Dickmann K, Bredol M (2003) Laser irradiation of medieval pigments at IR, VIS and UV wavelengths. J. Cult. Herit. 3:264–270.

Ciferri O (1999) Microbial Degradation of Paintings. Appl. Environ. Micro. 65, 879–885.

Costa L, Vicente AR, Civello PM, Chaves AR, Martínez GA (2006) UV-C treatment delays postharvest senescence in broccoli florets. Postharvest Biol Tec 39, 204–210.

Cutler NA, Viles HA, Ahmad S, McCabe S, Smith BJ (2013) Algal ‘greening’ and the conservation of stone heritage structures. Sci. Total Environ. 442, 152–64.

Faimon J, Stelcl J, Kubesová S, Zimák J (2003) Environmentally acceptable effect of hydrogen peroxide on cave “lampflora”, calcite speleothems and limestones. Environ. Pollut. 122, 417–22.

Faimon J, Stelcl J, Sas D (2006) Anthropogenic CO₂-flux into cave atmosphere and its environmental impact: A case study in the Císarská Cave (Moravian Karst, Czech Republic). Sci. Total Environ. 369, 231–45.

Georgieva M, Nikolova I, Bonchev G, Katerova Z, Todorova D (2015) A comparative analysis of membrane intactness and genome integrity in pea, barley, and wheat in response to UVC irradiation. Turk J. Bot. 39, 1008–1013.

Gibeaux S, Tourron S, Bousta F (2014) Etude des effets du rayonnement UV-C sur la matière

picturale dans le cadre d'une application en grotte ornée. Laboratoire de Recherche des Monuments Historiques (LRMH) Rapport 1377A, pp. 58.

Grobbelaar JU (2000) Lithophytic algae: a major threat to the karst formation of show caves. *J. Appl. Phycol.* 12, 309–315.

Hallmann C, Stannek L, Fritzlar D, Hause-reitner D, Friedl T, Hoppert M (2013) Molecular diversity of phototrophic biofilms on building stone. *Microbiol. Ecol.* 84, 355-372.

Jiang T, Jahangir MM, Jiang Z, Lu X, Ying T (2010) Influence of UV-C treatment on antioxidant capacity, antioxidant enzyme activity and texture of postharvest shiitake (*Lentinus edodes*) mushrooms during storage. *Postharvest Biol. Technol.* 56, 209–215.

Kotani M, Yamaushi N, Ueda Y, Imahori Y, Chachin K (1999) Chlorophyll degradation in boiled broccoli florets during storage in the light. *Food Sci. Technol. Res.* 5, 35–38.

Kravchenko KA, Vlashchenko AS, Prilutskii OV, Prilutskaya AS (2015) A Search for *Geomyces destructans*, a Dangerous Pathogen of Bats. *Ekol.* 46, 490–493.

Krieger-Liszkay A (2004) Singlet oxygen production in photosynthesis. *J. Exp. Bot.* 56, 337-356.

Luetscher M (2005) Processes in ice caves and their significance for paleoenvironmental reconstructions. Swiss Institute for Speleology and Karst Studies, La Chaux-de-Fonds, pp. 154.

Mulec J, Kosi G, Vrhovsek D (2008) Characterization of cave aerophytic algal communities and effects of irradiance levels on production of pigments. *J. Cave Karst Stud.* 70, 3–12.

Mulec J, Kosi G (2009) Lampenflora algae and methods of growth control. *J. Cave Karst Stud.* 71, 109–15.

Mulo P, Sakurai I, Aro EM (2012) Strategies for psbA. gene expression in cyanobacteria, green algae and higher plants: From transcription to PSII repair. *Biochim. Biophys. Acta.* 1817, 247–257.

Nugari MP, Pietrini AM, Caneva G, Imperi F, Visca P (2009) International Biodeterioration & Biodegradation Biodeterioration of mural paintings in a rocky habitat : The Crypt of the

Original Sin (Matera, Italy). *Int. Biodeterior. Biodegrad.* 63, 705–711.

Piano E, Bona F, Falasco E, La Morgia V, Badino G, Isaia M (2015) Environmental drivers of phototrophic biofilms in an Alpine show cave (SW-Italian Alps). *Sci. Total Environ.* 536, 1007–18.

Prieto B, Silva B, Lantes O (2004) Biofilm quantification on stone surfaces: comparison of various methods. *Sci. Total Environ.* 333, 1–7.

Poissenot B (1586) *Nouvelles Histoires Tragiques*. G. Bichon Paris. 474 p.

Popović S, Simić GS, Stupar M, Unković N, Jovanović J, Grbić ML (2015) Cyanobacteria, algae and microfungi present in biofilm from Božana Cave (Serbia). *Int. J. Speleol.* 44, 141–149.

Sanmartín P, Aira N, Devesa-Rey R, Silva B, Prieto B (2010) Relationship between color and pigment production in two stone biofilm-forming cyanobacteria (*Nostoc* sp. PCC 9104 and *Nostoc* sp. PCC 9025). *Biofouling* 26, 499–509.

Smith T, Olson R (2007) A taxonomic survey of lamp flora (algae and cyanobacteria) in electrically lit passages within Mammoth Cave National Park, Kentucky. *Int. J. Speleol.* 36, 105–114.

Srilaong V, Aiamla-or S, Soontornwat A, Shigyo M, Yamauchi N (2011) UV-B irradiation retards chlorophyll degradation in lime (*Citrus latifolia* Tan.) fruit. *Postharvest Biol. Technol.* 59, 110–112.

Szilárd A, Sass L, Deák Z, Vass I (2007) The sensitivity of photosystem II to damage by UV-B radiation depends on the oxidation state of the water-splitting complex. *Biochim. Biophys. Acta.* 1767, 876–882.

Takahashi S and Badger MR (2011) Photoprotection in plants: a new light on photosystem II damage. *Trends in Plant Sci.* 16, 53-50.

Vinogradova ON, Kovalenko OV, Wasser SP, Nevo E, Weinstein-Evron M (1998) Species diversity gradient to darkness stress in blue-green algae / cyanobacteria : a microscale test in a prehistoric cave, Mount Carmel, Israel . *Israel J. Plant. Sci.* 46, 229-238.

Zvezdanović J, Cvetić T, Veljović-Jovanović S, Marković D (2009) Chlorophyll bleaching by UV-irradiation *in vitro* and *in situ*: Absorption and fluorescence studies. *Radiat. Phys. Chem.* 78, 25–32.

**Comparison of biocides, allelopathic substances and UV-C as treatments
for biofilm proliferation on heritage monuments**

Stéphane Pfendler^a, Fabien Borderie^a, Faisal Boust^b, Laurence Alaoui-Sosse^a, Badr Alaoui-Sosse^a, Lotfi Aleya^{a*}

^a Laboratoire Chrono-Environnement – UMR 6249, Université de Bourgogne Franche-Comté.
16, route de Gray, 25 000 Besançon, France

^b Centre de Recherche sur la Conservation - Laboratoire de recherche des monuments
historiques – USR 3224, Champs-Sur-Marne, Paris

Abstract

UV-C and biocide treatments are frequently used to treat historical monuments contaminated by autotrophic biofilms. In this study, the authors compare for the first time the efficacy of these treatments against microorganisms such as cyanobacteria and algae proliferating in the Vicherey church (Vicherey, Vosges Department, France). To identify the most environmentally friendly and also efficient method, an allelopathic treatment was also tested. Colorimetric and physiological measurements of treated biofilms were thus monitored for 6 months. Fungi growing on necrotic matter from treated biofilms were sampled and sequenced. With biocides, results showed incomplete eradication of biofilms, even after two treatments. Biofilm color loss was delayed in comparison to UV-C treatment which appeared more efficient after just one treatment. Moreover, quantum yield (F_v/F_m) decreased immediately after UV-C treatment, indicating inhibition of algae and cyanobacteria photosynthesis. However, two species of fungi colonized the cyanobacteria biofilms treated with UV-C. Allelopathic treatment was not efficient on biofilm and showed no deleterious effect on photosynthesis. The present findings demonstrate that the UV-C method, coupled with a cleaning phase for necrotic organic matter, may be considered environmentally friendly and the best alternative to chemicals.

Key words: Biofilm, UV-C, Biocide, Allelopathic substances, Quantum yield

I. Introduction

For curators in charge of heritage monuments, the development of photosynthetic biofilms is a major threat [1]. Microbial communities excrete an exo-polysaccharide (EPS) matrix forming a biofilm that enables them to protect themselves and to share both nutrients [2] and water during dry periods [3,4]. Bacteria are often the first colonizers, followed by cyanobacteria and micro-algae when light is available [5,6,7,8]. In addition to their unsightly appearance [9,10,11] due to the presence of green, brown or black spots [12,13,14], autotrophic biofilms give rise to biodeterioration issues [15,16]. For example, through their metabolism, cyanobacteria and micro-algae produce organic acids [17] leading to degradation of monument rock substrate. Microorganisms may also colonize substrate pores and cracks resulting in mechanical biodegradation [14,18].

To remove biofilms, curators widely use chemical treatments before and after restoration [19]. However, some chemicals (e.g. sodium hypochlorite) remain ineffective or less effective on some algae strains [20] and may degrade certain walls and mineral structures (e.g. in natural caves) [5,20]. Also, resistance has been observed and has led to species selection [21]. In addition, it has been reported that some heterotrophic microorganisms may use chemicals as a carbon and nitrogen source [22] leading to a second microbial proliferation. Moreover, Urzi et al. [19] have also reported that chemicals become ineffective after a few years of treatment, followed by recolonization by all the species previously present. For instance, reported laboratory results showed that chemicals are not effective on all biofilm species [19]. Furthermore, *in-situ* treatment may act differently in comparison to laboratory results due to different environment parameters (e.g. moisture, temperature, e.g.).

New environmentally friendly treatments have been investigated, especially the use of UV-C light [23,24] which has proved efficient in the air and water treatment industries, but also in hospitals [25] as a method of sterilization. UV-C treatment has been used in a show cave in order to treat photosynthetic biofilms [1,26]. More recently, in the “La Glacière” show cave, all biofilms were irradiated with no re-colonization for two years [27].

Other environmentally friendly methods such allelopathic treatments are well known as inhibitors of autotrophic species [28], but are also used as fungicides or insecticides. In fact, these molecules are phenolic acids, flavonoids, terpenoids, or alkaloids [29] and most of

them are secondary metabolites [30] affecting photosynthetic parameters, such as photosystem II [31]. The studied Juglone molecule is produced by walnuts and inhibits plant growth around the tree [32]. Juglone solution is also known to kill some algae strains, e.g. *Micrasterias* and *Eudorina* [33]. Moreover, their efficiency has been proved on several green algal and diatom strains (e.g. *Chlorella pyrenoidosa*, *Scenedesmus quadricauda*, *Cyclotella meneghiniana*) [28]. Allelopathic interactions among phytoplankton species are regarded as one of the important factors contributing to phytoplankton species competition and succession [30]. These molecules may therefore be of interest to combat algae and cyanobacteria forming biofilms.

Many studies have reported the use of biocide molecules on biofilms of photosynthetic organisms [22,35] including algae or cyanobacteria [19,34]. Allelopathic treatment, which is considered a more environmentally friendly method in comparison to chemicals, has been studied several times for its effect on algal and cyanobacteria blooms [28,31,33]. Finally, UV-C irradiation efficiency has been demonstrated by Borderie et al. [1,26] on biofilms in both the laboratory and in show caves. However, as far as we know, a knowledge gap remains in comparing the effects of the three methods when used on photosynthetic biofilms proliferating on cultural heritage.

We thus compared, for the first time, the effects of the use of the three different methods: 1) three chemicals commonly used by the French Laboratory of Heritage Monuments, Paris, 2) a Juglone solution which contains an allelopathic molecule, and 3) UV-C irradiation. The methods were applied on two types of photosynthetic biofilms, the first composed mainly of cyanobacteria (black biofilm) and the second of green micro-algae (green biofilm). Biofilm bleaching was monitored with colorimetric parameters, while the microorganism's physiological status was assessed by quantum yield. In order to detect possible colonization by heterotrophic fungi, necrotic organic matter remaining on treated areas was examined after treatment.

II. Material and methods

1. Study area

The church of Vicherey is a heritage monument situated in Vicherey, in the Vosges Department (France). It is the former chapel of the local castle which was destroyed many centuries ago. Water infiltration has been observed on almost all of the building's walls. Due to algae and cyanobacteria development (Fig. 1), the naturally lighted inner part of the church turned green or black due to the development of microalgae and cyanobacteria, respectively. Interestingly, cyanobacteria biofilms were observed directly before the largest windows, the monument's section that has suffered the most from water infiltration. In contrast, green algae biofilm has proliferated, spreading throughout every lighted part of the church. Heavy biofilm proliferation in the church resulted in an aesthetic issue since the black biofilms were sticky and very difficult to clean. In addition, biodeterioration issues have been observed, mainly in cyanobacteria biofilms (Fig. 1). For the needs of this study, the most severely affected part of the church was chosen to test the different treatments for algae and cyanobacteria. The cyanobacteria-contaminated wall measured 4.83 m long and 1 m high. The studded sandstone floor, affected by micro-algae, was 4.83 m length and 0.80 m wide.

2. Biofilm treatment

- Chemical treatment

In order to remove biofilms from monuments, the French Research Laboratory of Historical Monuments (LRMH) recommends testing different chemicals on a limited part of the contaminated monument. The most efficient chemical should then be used to treat the totality of the biofilms. In this study, Biotin T[®] (diluted at 3%, composition: Didecyldimethylammonium chloride, Propan-2-ol, 2-octil-2h-isotiazol-3-one, formic acid), Oxi Antimousse Concentre Devor Mousse[®] (diluted at 10%, composition: quaternary ammonium cations, chloride, 2-n-Octyl-4-isothiazolin-3-one) and Net'toit professionnel[®] (diluted at 3%, composition: Alkyl-dimethyl-benzyl-ammonium-chloride) were tested (Fig. 2). As a complement to these treatments, 100 µM of Juglone previously dissolved in 1 ml of dimethyl-sulfoxide (DSMO) (q.s. 1 liter deionized water) was also used. Subsequently, biocides and allelopathic treatments were vigorously applied, to soak deeply biofilms, with a paintbrush once a day for two days, on app. 0.32 m² large areas on the floor and on app. 0.40 m² large areas of the cyanobacteria-contaminated wall.



Fig. 1. Illustration of Vicherey church (a) and its biodeterioration (b) due to biofilm proliferation. Wall with southern exposure and floor of the church were affected by microalgae and cyanobacteria (c), while north exposed wall was less invaded (d).

- UV- irradiation

UV-C treatment was applied using 8 UV-C lamps (Philips, 25 W each = 200 W, $\lambda_{\text{max}} = 254 \text{ nm}$) placed 20 cm from the biofilm. In order to protect the immediate environment, UV-C irradiation was targeted precisely onto the biofilm area while a dark cover protected the UV-C boxes. In contrast to the chemical treatment, a single radiation treatment was applied lasting 14 hours, corresponding to 646 kJ m^{-2} .

3. Colorimetric measurements

Forty-two and thirty-two equidistant areas ($\varnothing 4 \text{ cm}$) of cyanobacteria and algae biofilms were monitored, respectively. Colorimetric parameters and quantum yield ($F'v/F'm$) were measured prior to treatment, but also at 1 day, 2 days, 35 days and 180 days post-

treatment. Biofilm color was evaluated with a spectrophotometer (CM-600d KONICA MINOLTA, illuminant D65, SCI mode and 8 mm diameter target mask). Two parameters were thus measured: *i*) the parameter a^* , indicating the green-red scale, and *ii*) the parameter L^* , indicating the dark-light scale [1]. Due to the heterogeneous size of the biofilms on the measured area, only the 10 lowest a^* values and the 10 highest L^* values were selected, corresponding to the most heavily contaminated areas. To ensure that these values corresponded to contaminated areas, they were compared to biofilm pictures.

4. *Quantum yield measurements*

The relative quantum yield of PSII was calculated as $F'_v/F'_m = (F'_m - F'_o)/F'_m$, where F'_o is the minimal fluorescence of light-adapted biofilm, and F'_m is the maximal fluorescence during saturating light. Fluorescence measured with a modulated fluorometer (Mini-PAM, WALZ, Germany) using the saturation pulse method [36].

5. *Sanger sequencing*

Samples of fungal colonies were taken from a cyanobacterial biofilm previously treated with UV-C, cultivated and purified on Malt Extract Agar medium (Sigma). DNA was extracted by dissolving a small part of the colony in 100 μ l Prepman Ultra solution (Applied Biosystems). The suspensions were then heated at 95°C for 10 min. After centrifugation, 2.5 μ l of supernatant from each sample were added to 250 μ l ultrapure water. PCR reaction solutions were mixed as follows: 12.5 μ l of DNA, 2 μ l of forwards (ITS1 *f*: 5' - CTTGGTCATTTAGAGGAAGTAA- 3') and reverse primers (ITS2 *r*: 5' - GCTGCGTTCTTCATCGATGC- 3') [37], 25 μ l of mastermix and 8.5 μ l of ultrapure water. Afterwards, DNA was amplified using following PCR steps: denaturation at 95°C/2 min, denaturation 95°C/30 sec, hybridation 62°C/30 sec, elongation 72°C/1 min (35 cycles at 57°C) and final elongation 72°C / 10 min. Two μ l of ExoSAP[®] solution were added to 5 μ l of amplified DNA (37°C/15 min and 80°C/15 min). Afterwards, samples were amplified with fluorescent ddNTP (Big Dye Terminator 3.1, Applied Biosystems) and purified with Big Dye X Terminator (Applied Biosystems). Sequencing was finally done with a 3130 DNA sequencer.

6. *Statistical analysis*

Statistics were analyzed using R.2.14 software (R Development Core Team, 2011) at a significant level of 0.05. Multiple pairwise comparisons were used on colorimetric and quantum yield parameters taking into account the time and the type of treatment.

III. Results

1. Biofilm colorimetric and physiological monitoring

Colorimetric parameters and quantum yield were measured on the biofilms before and after both UV-C (Fig. 2) and chemical (Fig. 3) treatments. Biofilm color changes were assessed by means of the green-red scale (a^*) and light-dark (L^*) parameter. Differing results were obtained from UV-C, biocides and Juglone treatments.

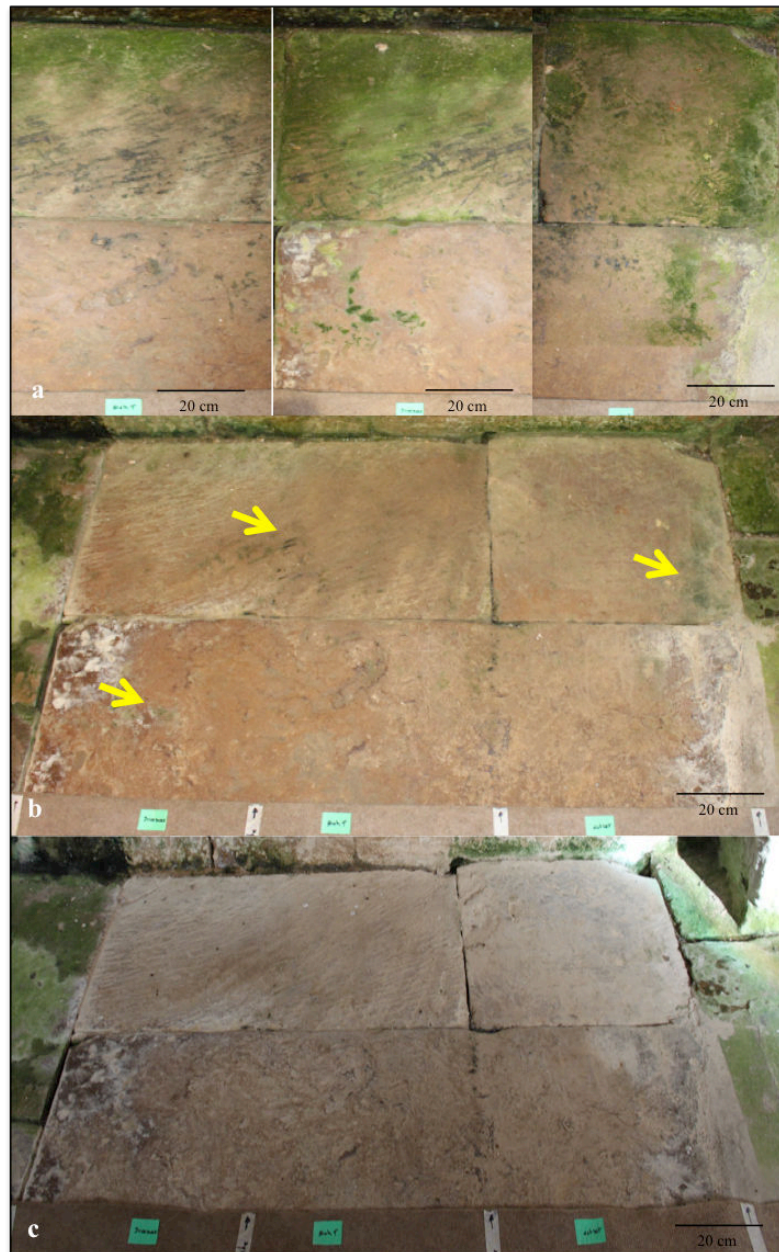


Fig. 2. (a) Biofilms on the floor of the Vicherey church: (a) before treatment, and (b) at 1 and 6 months after biocide treatments.

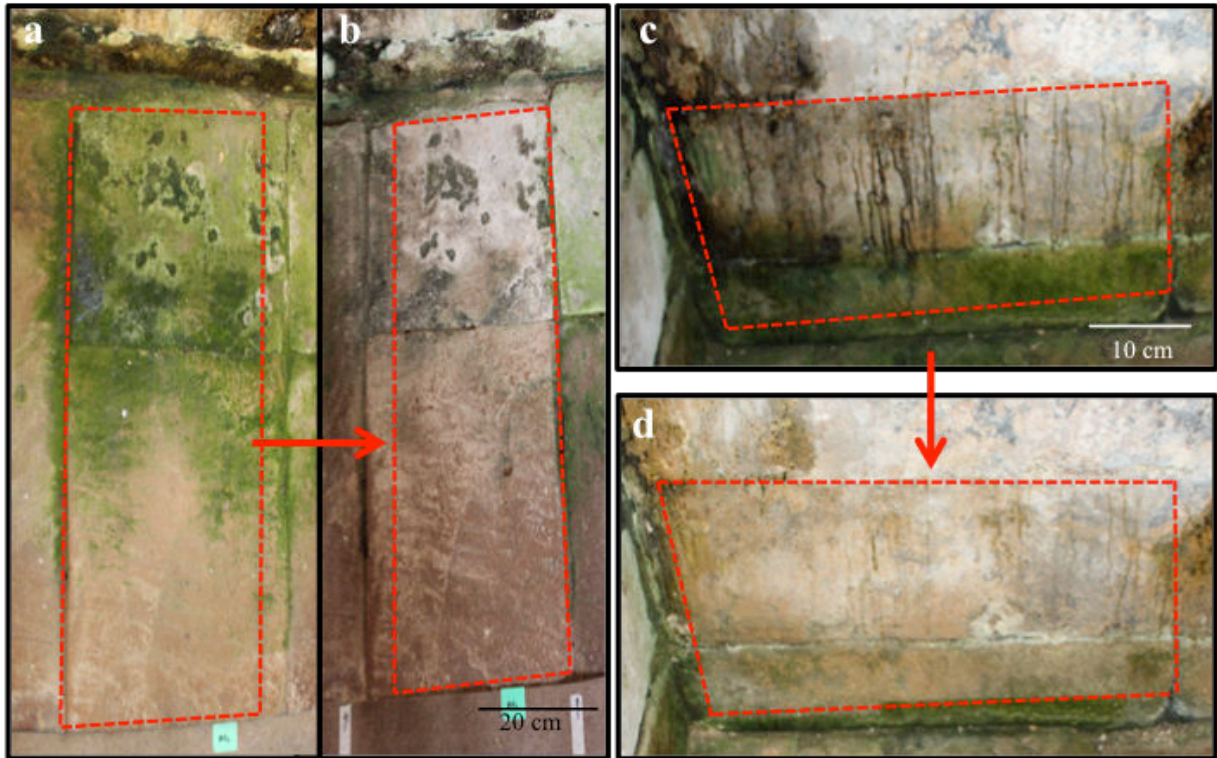


Fig. 3. Green (a) and black (c) biofilms growing on the floor and wall of Vicherey church, respectively. Both biofilms were treated with UV-C light (b, d). Pictures were taken one month after UV-C exposition.

- Monitoring of green and black biofilm color

This study showed that green and black biofilms, composed mainly of algae and cyanobacteria, respectively, showed different behaviors depending on treatment (Fig. 4). UV-C treatment appeared to affect the algae biofilm directly after irradiation. After the first day, data showed a significant difference in comparison to the situation at time zero (p -value < 0.01). In addition, the mean value was above 0, corresponding to the border color value, which separates green and red values. This discoloration continued until the last measurements at day 180. Unlike UV-C treatment, biocide solutions were not efficient at all the first two days (p -value > 0.05). A significant difference was observed at day 35 and showed that all measured areas lost their green color. Concerning Juglone treatment, the colorimetric measurement at days 1 and 2 exhibited very similar patterns in comparison to the control. However, after one and six months, the green color intensity increased to exceed even those measured initially, prior to treatment. Concerning the control no significant difference has been observed (p -value > 0.05).

The light-dark scale (L^*) colorimetric parameter for the black biofilm showed a quick and lasting significant increase after the treatment. In fact, the maximum effect was attained one day after irradiation. Unlike UV-C, the biocide treatment showed a progressive increase in the dark-light scale over the 6 months. Like the green biofilms, the black biofilms treated with Juglone were unaffected ($p\text{-value} > 0.05$). However, a significant increase in L^* values was observed 6 months after treatment ($p\text{-value} < 0.01$). For the control, a low, but however significant increase, has been observed after 35 days.

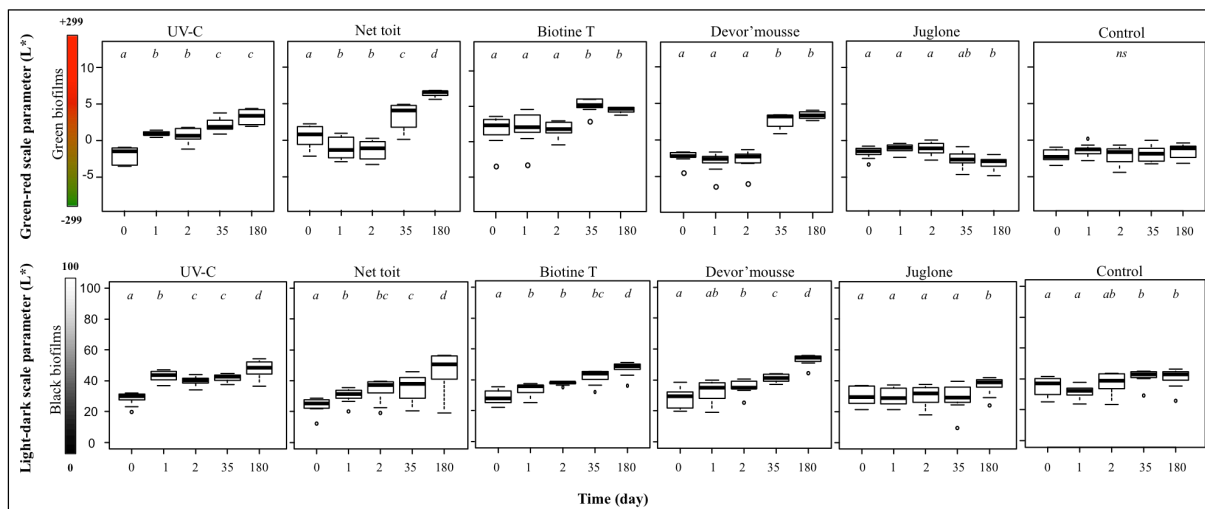


Fig. 4. Colorimetric parameters were monitored on all biofilms treated with biocides, allelopathic solution and UV-C. x-axis: time of day; y-axis: green–red scale and dark–light scale. The values *a*, *b*, *c*, *d* and *ns* correspond to statistically significant or non-significant differences.

- *Quantum yield measurements*

Quantum yield results (Fig. 5) of UV-C treated green biofilm showed a significant effect at day 1. Thirty-five days after irradiation, quantum yield values increased significantly in comparison to day 1 and 2, but did not reach healthy algae quantum yield values. Surprisingly, results at day 35 were not in accordance with colorimetric measurements. In fact, though the biofilm’s green color constantly declined, quantum yield values increased. At day 180, church moisture considerably decreased and biofilms were dry. Thus, quantum yield data were not taken into consideration for any treatment.

Net Toit solution produced a progressive but significant decrease in quantum yield until day 35 ($p\text{-value} < 0.01$). Biotine T and Devor’mousse showed better efficiency with quantum yield values close to 0, one and two days after treatment, while Juglone appeared to

have no effect and showed a significant increase (app. 0.1 point) at day 35. Finally, no significant difference has been observed for the control ($p\text{-value} > 0.05$).

UV-radiation strongly affected cyanobacteria PS II during the first month. In fact, values decreased quickly after treatment and remained stable for 35 days. Biocide solutions were also efficient, but less than UV-C, while both Juglone and the control showed no significant difference over the 35 days ($p\text{-value} > 0.05$).

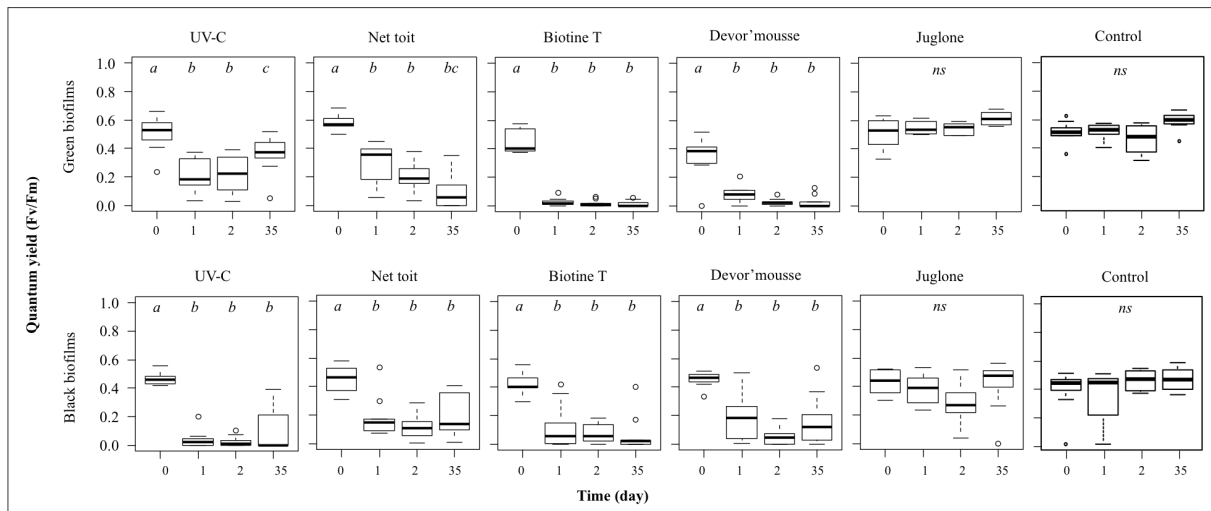


Fig. 5. Quantum yield was measured on all biofilms treated with biocides, allelopathic solution and UV-C. x-axis: time of day; y-axis: Quantum yield (F_v/F_m). The values a , b , c , d and ns correspond to statistically significant or non-significant differences.

2. Fungal colonization

A white cotton-like fungal colonization (0.4 m^2) was observed on UV-C treated cyanobacteria biofilm after six months (Fig. 6). Cultures obtained after sampling led to isolation of two different fungi species; microscopic observation (Olympus, CX31) showed that both were of the Ascomycota phylum. Both *Penicillium bilaiae* (identification at 99%) and *Engyodontium album* (identification at 100%) were identified from comparison of sequencing data to Genbank. Forward and reverse sequences length was from 250 to 300 pb.

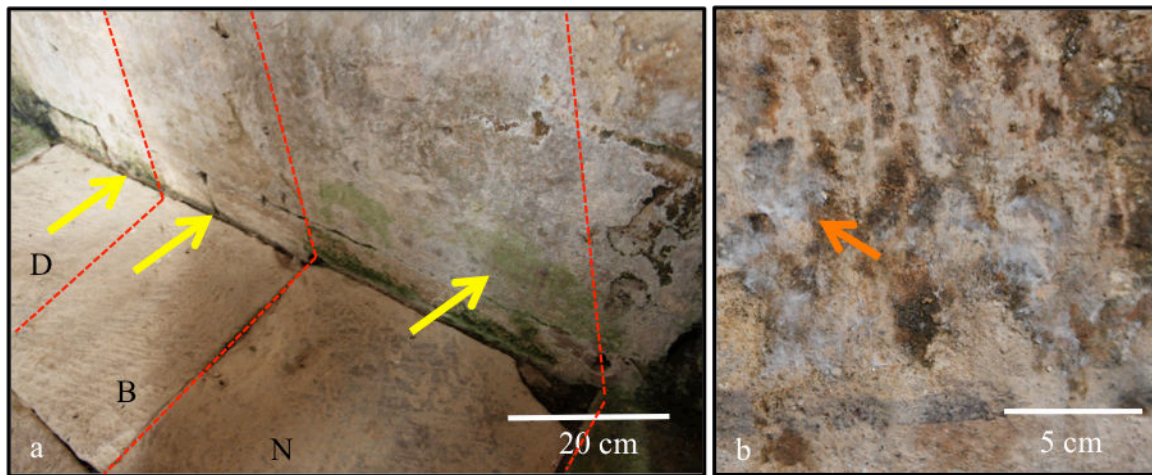


Fig. 6. Illustration (a) shows remaining green spot six months after Devor'mousse (D), Biotine T (B) and Net Toit (N) application. Black UV-C irradiated biofilm shows fungi colonization.

IV. Discussion

- *Biofilm colorimetric and physiological parameters*

Our results showed that one UV-C exposition at 646 kJ m^{-2} was enough to remove the green and black color from the biofilms. The treatment therefore degrades chlorophyll contained in both micro-algae and cyanobacteria. The present findings are supported by our previous results [1] obtained for biofilms growing in show caves. In our study, green biofilm was bleached directly following treatment, whereas for the biocide solutions discoloration took at least two days. The bleaching effect on algae chlorophyll continued for six months, whereas black biofilm appeared to show the maximum effect just after treatment. Furthermore, quantum yield results as well as the green and black color parameters showed a direct decrease following treatment. Several studies have reported that UV-radiation caused damage to photosynthesis [38,39,40], which might be deadly to cyanobacteria [23] and micro-algae [1]. Tyystjärvi et al. [41] reported that cyanobacteria PS II is highly sensitive to UV-irradiation due to the UV-C absorbance of their protein structure leading to molecular damage. Wang et al. [24] showed a significant effect on *Microcystis aeruginosa* suspension after a much lower irradiation (120 mJ cm^{-2}). Also, Ou et al. [23] reported a rapid decrease in quantum yield directly after irradiation and an increase a few days later on *Microcystis aeruginosa* suspension, while in our study it was observed after one month. These results showed that a second UV-C exposition would have helped to kill all microorganisms and to avoid a recolonization phenomenon. These findings might be due to multiple layers of cells arranged upon each other inside the biofilm and to the low penetration of UV radiation [42], resulting in the protection of the lower layer of cells while the upper strata are killed.

Both biocides and allelopathic solutions were vigorously applied with a paintbrush; thus all biofilm cell layers were treated. However, it is noteworthy that, contrary to UV-C treatment, some green spots remained on the treated area (Fig. 6). These results are probably due to the fact that some biocides have a strain-specific action [20] and/or that EPS protect the biofilm and microorganisms within [22].

Juglone is known as an allelopathic molecule able to disturb growth, photosynthesis and respiration in woody and herbaceous species [32]. Kessler [33] reported that Juglone was toxic to many algae species. Surprisingly, Juglone solution applied on biofilms showed no

promising results, neither in colorimetric nor on physiological parameters. These results might be explained by the fact that Juglone solution was not able to penetrate EPS, or because Juglone is not efficient on any of the algae species present in Vicherey church. In fact, some algae may persist (e.g. *Micrasterias* and *Eudorina*) [33]. Further laboratory experimentation will be necessary to find and test other allelopathic molecules. It has been previously demonstrated that they might be efficient on some heterotrophic organisms, e.g. ferulic acid on *Microcystisa eruginosa* [31] or stearic acid on *Chlorella pyrenoidosa* [28].

- Implementation of the treatments

Biocide solutions were mechanically applied with a paintbrush. It is noteworthy that these solutions must be applied carefully so as to avoid potential damage to wall paintings. Also, the chemicals used in this study persist in the environment and may be dangerous (corrosive, harmful, flammable) to human health [43,44,45], especially inside a monument. In addition to the human health risk, some chemicals are known to be a possible source of carbon and nitrogen for some microorganisms [22] (for some Gram-negative bacteria, for example). In this study some green spots remained even after two applications, thus demonstrating that chemicals did not succeed in killing all the microorganisms. Our results correlate with those of Meyer et al. [46] who reported that chemical formulations, effectiveness, and impacts on Lampenflora appear anecdotal and temporally limited. Finally, our results also show that biocide application leaves an unaesthetic white film on the floor.

Unlike biocides, UV-C irradiation did not mechanically degrade biofilm support and its action is targeted precisely. Implementation of this treatment is fast, cheap and its environmentally friendly aspect is a significant advantage. In addition, in comparison to chemicals, its efficiency was immediate. However, as a tool for biofilm treatment, UV-C light should be used carefully. Ultraviolet light may have an irreversible effect on organic matter present on biofilm support (e.g. paint containing organic binders). Some recent studies (unpublished data), though, have demonstrated that UV-C light has no deleterious effect on mineral pigments.

Following a treatment both quantum yield and colorimetric parameter measurements may be two excellent methods to monitor the growth of autotrophic organisms and bleaching respectively. In fact, a pulse amplitude modulated fluorimeter (PAM) has previously been used to monitor quantum yield of biofilm growing on speleothems in the Nerja Cave (Spain)

[47]. However, it is noteworthy that micro-algae are able to resist to desiccation [48] and during these periods, PS II activity is not measurable.

- *Fungal recolonization*

Algal residues are known to increase the natural organic matter that follow the death of cyanobacteria, creating a precursor to byproducts formed during disinfection [23,49]. In this study, we observed fungal proliferation which should be avoided as early as possible. In fact, *Engyodontium album*, a species known as a biodeterioration agent which has previously been found in wooden constructions [50], was sampled on a cyanobacteria biofilm. Some fungi may be resistant to UV-C thanks to pigments such as melanin [51]. Thus, UV-C treatment can be expected to play a role as an agent of selection and may lead to the proliferation of unwanted opportunistic and UV-resistant fungi. However, an “organic matter-cleaning” phase with a vacuum on dry surfaces, or with a curator’s conventional method on wet surfaces, can help to avoid heterotrophic fungal proliferation.

V. Conclusion

In this study, it has been reported that the use of UV-C is an excellent alternative to biocide treatments against algae and cyanobacteria biofilms. In fact, the removal of the black and green color of biofilms was much faster with UV-C in comparison to biotine T, Net Toit and Devor'mousse. Moreover, these three biocides were not completely efficient even after two treatments. In order to protect the immediate environment, the use of an environmentally friendly method, which is better or at least as efficient as chemicals, is more suitable. Further laboratory study should therefore be undertaken to find an efficient allelopathic treatment that can be used in addition to UV-C irradiation on certain areas where UV-C is not advisable (painting with organic binder, etc.).

Quantum yield measurement coupled with colorimetric monitoring may constitute a good combination to follow-up biofilm treatment. Both parameters may inform curators if any heterotrophic organisms remain post-treatment, which is not always possible by visual inspection. It is noteworthy that a cleaning phase of remaining organic matter is necessary to avoid heterotrophic microorganism proliferation such as fungi.

VI. Acknowledgements

First of all, we are grateful to Vicherey mayor, Mr Christian FRANCE, who kindly gave us access to the church and allowed us to carry out all our field experiments. We also thank the *Ministère de la Culture et de la Communication* (France), the *Laboratoire de Recherche des Monuments Historiques* (LRMH, Paris) and the Conseil Régional of Franche-Comté for their financial aid. We also express our gratitude to O. Einhorn for her help during field experiments and to Battle Karimi for improving statistical analysis. We express our appreciation to the editor, Dr. Tomasin, and to the anonymous reviewers for helping to improve our paper.

VII. References

- [1] F. Borderie, N. Tête, D. Cailhol, L. Alaoui-Sehmer, F. Bousta, D. Rieffel, L. Aleya, B. Alaoui-Sossé, Factors driving epilithic algal colonization in show caves and new insights into combating biofilm development with UV-C treatments, *Sci. Total Environ.* 484 (2014) 43-52.
- [2] A.A. Gorbushina, Life on the Rocks, *Environ. Microbiol.* 9 (2007) 1613–1631.
- [3] M.F. Macedo, A.Z. Miller, A. Dionísio, C. Saiz-Jimenez, Biodiversity of cyanobacteria and green algae on monuments in the Mediterranean Basin: an overview, *Microbiol.* 155 (2009) 3476-3490.
- [4] N. Keshari, S.P. Adhikary, Characterization of cyanobacteria isolated from biofilms on stone monuments at Santiniketan, India, *Biofouling*, 29 (2013) 525-536.
- [5] J. Mulec, G. Kosi, Lampenflora algae and methods of growth control, *J. Cave Karst Stud.* 71 (2009) 109–15.
- [6] V. Lamprinou, D.B. Danielidis, A. Pantazidou, A. Oikonomou, A. Economou-Amilli, The show cave of Diros vs. wild caves of Peloponnese, Greece - distribution patterns of Cyanobacteria, *Int. J. Speleol.* 43 (2014) 335–342.
- [7] S. Popović, G.S. Simić, M. Stupar, N. Unković, J. Jovanović, M.L. Grbić, Cyanobacteria, algae and microfungi present in biofilm from Božana Cave (Serbia), *Int. J. Speleol.* 44 (2015) 141–149.
- [8] F. Borderie, M. Denis, A. Barani, B. Alaoui-Sossé, L. Aleya, Microbial composition and ecological features of phototrophic biofilms proliferating in the Moidons Caves (France): investigation at the single-cell level, *Environ. Sci. Pollut. Res.* 23 (2016) 12039-12049.
- [9] S.P. Adhikary, N. Keshari, C. Urzi, Cyanobacteria in biofilms on stone temples of Bhubaneswar, Eastern India, *Algol. Stud.* 147 (2015) 67–93.
- [10] O. Ciferri, Microbial Degradation of Paintings, *Appl. Environ. Microbiol.* 65 (1999) 879–885.

- [11] N.A. Cutler, H.A. Viles, S. Ahmad, S. McCabe, B.J. Smith B, Algal ‘greening’ and the conservation of stone heritage structures, *Sci. Total Environ.* 442 (2013) 152–64.
- [12] L. Bruno, D. Billi, P. Albertano, C. Urzi, Genetic characterization of epilithic cyanobacteria and their associated bacteria, *Geomicrobiol. J.* 23 (2006) 293–299.
- [13] V. Lamprinou, D.B. Danielidis, A. Economou-Amilli, Distribution survey of Cyanobacteria in three Greek caves of Peloponnese, *Int. J. Speleol.* 41 (2012) 267–272.
- [14] A. Mihajlovski, A. Seyer, D. Benamara, H. Bousta, F. Martino, P. Di, An overview of techniques for the characterization and quantification of microbial colonization on stone monuments, *Microbiol.* 531 (2014) 289-303.
- [15] Albertano, P., 2012. Cyanobacterial biofilms in monuments and caves. In: Whitton, B.A. (Ed.), *Ecology of Cyanobacteria II: Their Diversity in Space and Time*. Springer, Netherlands, pp. 317-343.
- [16] M.P. Nugari, A.M. Pietrini, G. Caneva, F. Imperi, P. Visca, Biodeterioration of mural paintings in a rocky habitat: The Crypt of the Original Sin (Matera, Italy), *Int. Biodeter. Biodegr.* 63 (2009) 705-711.
- [17] L.M. Shields, L.W. Durell, Algae in relation to soil fertility, *Bot. Rev.* 30 (1964) 92–128.
- [18] J.J. Ortega-Calvo, M. Hernandez-Marine, C. Saiz-Jimenez, Biodeterioration of building materials by cyanobacteria and algae, *Int. Biodeter. Biodegr.* 28 (1991) 165–185.
- [19] C. Urzi, F. De Leo, M. Galletta, P. Salamone, Efficiency of biocide in “in situ” and “in vitro” treatment. Study case of the “Template de Mudejar”, Conference: 9th International Congress on Deterioration and Conservation of Stone, At Venice, Italy, Volume: 1, 2000, pp.9.
- [20] J. Faimon, J. Štelcl, S. Kubešová, J. Zimák, Environmentally acceptable effect of hydrogen peroxide on cave “lamp-flora”, calcite speleothems and limestones. *Environ. Pollut.* 122 (2003) 417–422.

- [21] F. Bastian, V. Jurado, A. Nováková, C. Alabouvette and C. Saiz-Jimenez, The microbiology of Lascaux Cave, *Microbiol.* 156 (2010) 644–652.
- [22] C. Urzi, F. De Leo, L. Krakova, D. Pangallo, L. Bruno, Effects of biocide treatments on the biofilm community in Domitilla's catacombs in Rome, *Sci. Total Environ.* 572 (2016) 252–262.
- [23] H. Ou, N. Gao, Y. Deng, J. Qiao, H. Wang, Immediate and long-term impacts of UV-C irradiation on photosynthetic capacity, survival and microcystin-LR release risk of *Microcystis aeruginosa*, *Water Res.* 46 (2012) 1241–1250.
- [24] B. Wang, X. Wang, Y. Hu, M. Chang, Y. Bi, Z. Hu, The combined effects of UV-C radiation and H₂O₂ on *Microcystis aeruginosa*, a bloom-forming cyanobacterium. *Chemosphere* 141 (2015) 34–43.
- [25] M.Y. Menetrez, K.K. Foarde, T.R. Dean, D.A. Betancourt, The effectiveness of UV irradiation on vegetative bacteria and fungi surface contamination, *Chem. Eng.* 157 (2010) 443-450.
- [26] F. Borderie, L. Alaoui-Sossé, N. Raouf, F. Bousta, G. Oriol, D. Riefel, B. Alaoui-Sossé, UV-C irradiation as a tool to eradicate algae in caves, *Int. Biodeter. Biodegr.* 65 (2011) 579–584.
- [27] S. Pfendler, O. Einhorn, B. Karimi, F. Bousta, D. Cailhol, L. Alaoui-Sosse, B. Alaoui-Sosse, L. Aleya, UV-C as an efficient means to combat biofilm formation in show caves: evidence from in situ and laboratory experiments, *Environ Sci. Pollut. Res.* (in revision).
- [28] S. Zuo, S. Zhou, L. Ye, Y. Ding, X. Jiang, Antialgal effects of five individual allelochemicals and their mixtures in low level pollution conditions, *Environ Sci. Pollut. Res.* 23 (2016) 15703–15711.
- [29] J. Leflaive, L. Ten-Hage, Algal and cyanobacterial secondary metabolites in freshwaters : a comparison of allelopathic compounds and toxins, *Freshwater Biol.* 52 (2007) 199–214.

- [30] G.O. Fistarol, C. Legrand, E. Selander, C. Hummert, W. Stolte, E. Granéli, Allelopathy in *Alexandrium* spp.: effect on a natural plankton community and on algal monocultures, *Aquat. Microb. Ecol.* 35 (2004) 45–56.
- [31] R. Wang, M. Hua, Y. Yu, M. Zhang, Q. Xian, D. Yin, Evaluating the effects of allelochemical ferulic acid on *Microcystis aeruginosa* by pulse-amplitude-modulated (PAM) fluorometry and flow cytometry, *Chemosphere* 147 (2016) 264–271.
- [32] A.M. Hejl, F.A. Einhellig, J.A. Rasmussen, Effects of juglone on growth, photosynthesis, and respiration, *J. Chem. Ecol.* 19 (1993) 559-68.
- [33] C.T. Kessler, Effect of juglone on freshwater algal growth, *J. Chem. Ecol.* 15 (1989) 2127-34.
- [34] C. Ascaso, J. Wierzchos, V. Souza-Egipsy, A. De Los Ríos, J.D. Rodrigues, In situ evaluation of the biodeteriorating action of microorganisms and the effects of biocides on carbonate rock of the Jeronimos Monastery (Lisbon), *Int. Biodeter. Biodegr.* 49 (2002) 1–12.
- [35] C. Urzi, F. De Leo, Evaluation of the efficiency of water-repellent and biocide compounds against microbial colonization of mortars, *Int. Biodeter. Biodegr.* 60 (2007) 25–34.
- [36] U. Schreiber, C. Klughammer, Wavelength-dependent photodamage to *Chlorella* investigated with a new type of multi-color PAM chlorophyll fluorometer, *Photosynt. Res.* 114 (2013) 165–177.
- [37] A. Durand, F. Maillard, J. Foulon, H.S. Gweon, B. Valot, M. Chalot, Environmental Metabarcoding Reveals Contrasting Belowground and Aboveground Fungal Communities from Poplar at a Hg Phytomanagement Site, *Microb. Ecol.* 2017, doi :10.1007/s00248-017-0984-0.
- [38] X.S. Liao, X. Wang, K.H. Zhao, M. Zhou, Photocatalytic inhibition of cyanobacterial growth using silver-doped TiO(2) under UV-C light, *J. Wuhan. Univ. Technol.* 24 (2009) 402-408.

- [39] J. Tandori, Z. Mate, P. Maroti, I. Vass, Resistance of reaction centers from *Rhodobacter sphaeroides* against UV-B radiation. Effects on protein structure and electron transport, *Photosynth. Res.* 50 (1996)171-179.
- [40] E. Turcsanyi, I. Vass, Inhibition of photosynthetic electron transport by UV-A radiation targets the photosystem II complex, *Photochem. Photobiol.* 72 (2000) 513-520.
- [41] E. Tyystjärvi, Photoinhibition of Photosystem II and photodamage of the oxygen evolving manganese cluster, *Coordin. Chem. Rev.* 252 (2008) 361–376.
- [42] N.K. Dhama, M.S. Reddy, A. Mukherjee, Application of calcifying bacteria for remediation of stones and cultural heritages, *Front. Microbiol.* 23 (2014) 15703-15711.
- [43] R. Kumar, A.V. Kumar, *Biodeterioration of Stones in Tropical Environments*, Los Angeles, CA: The Getty Conservation Institute, 1999.
- [44] O. Salvadori, *The Control of Biodeterioration*, Coalition No.6 (1), 2003, pp.16–20.
- [45] F. Cappitelli, C. Sorlini, From papyrus to compact disc: the microbial deterioration of documentary heritage, *Crit. Rev. Microbiol.* 31 (2005) 1–10.
- [46] E. Meyer, L.D. Seale, B. Permar, A. McClary, E. Meyer, The Effect of Chemical Treatments on Lampenflora and a Collembola Indicator Species at a Popular Tour Cave in California, USA, *Environ. Manage.* 59 (2017) 1034-1042.
- [47] F.L. Figueroa, F. Álvarez-gómez, Y. del Rosal, P.S.M. Celis-Plá, G. González, M. Hernández, N. Korbee, In situ photosynthetic yields of cave photoautotrophic biofilms using two different Pulse Amplitude Modulated fluorometers, *Algal Res.* 22 (2017)104–115.
- [48] U. Lüttge, B. Büdel, Resurrection kinetics of photosynthesis in desiccation-tolerant terrestrial green algae (*Chlorophyta*) on tree bark, *Plant Biol.* 12 (2009) 437–444.

- [49] R.K. Henderson, A. Baker, S.A. Parsons, B. Jefferson, Characterisation of algogenic organic matter extracted from cyanobacteria, green algae and diatoms, *Water Res.* 42 (2008) 3435-3445.
- [50] R. Ortiz, H. Navarrete, J. Navarrete, J. Navarrete, M. Párraga, I. Carrasco, E. De la Vega, M. Ortiz, P. Herrera, R.A. Blanchette, Deterioration, decay and identification of fungi isolated from wooden structures at the Humberstone and Santa Laura saltpeter works : A world heritage site in Chile, *Int. Biodeter. Biodegr.* 86 (2014) 309–316.
- [51] N. Singaravelan, I. Grishkan, A. Beharav, K. Wakamatsu, S. Ito, E. Nevo, Adaptive Melanin Response of the Soil Fungus *Aspergillus niger* to UV Radiation Stress at “Evolution Canyon”, Mount Carmel, Israel, *PLoS One* 3 (2008) 2–6.

Synthèse du chapitre 4

L'application des UV-C sur les biofilms proliférant dans la grotte de la Glacière et dans l'église de Vicherey ont démontré que le traitement est très efficace contre les biofilms.

En résumé :

- ✓ Les UV-C provoquent le bleaching des biofilms directement après l'irradiation;
- ✓ Le traitement a montré son efficacité dans le temps (plus de deux ans);
- ✓ Les UV-C permettent un bleaching des biofilms plus rapide que les produits chimiques;
- ✓ Les produits biocides ne sont pas entièrement efficaces; certaines zones traitées restent contaminées;
- ✓ Suite à l'application de tous les types de traitement, une étape d'élimination de la matière organique est nécessaire afin d'éviter une prolifération fongique;
- ✓ L'utilisation d'un fluorimètre et de la colorimétrie donne des informations précieuses lors du suivi du traitement des biofilms;

Ces deux études ont finalement montrées que le traitement UV-C est efficace sur différents types de biofilms. Cependant, il est à noter que l'épaisseur du biofilm est un facteur important dans le nombre de traitement à appliquer. Le même constat a été fait dans le Chapitre 2 concernant les colonies fongiques.

Afin d'optimiser la durée du traitement, l'utilisation des UV-C peut être faite dès les premiers signes de la prolifération d'un biofilm. En effet, un biofilm peu épais pourra être traité en quelques minutes, contre quelques heures pour les biofilms de forte épaisseur.

Dans de futures études, il serait intéressant de traiter également les mousses ; en effet, tout comme les micro-algues et les cyanobactéries, ces dernières colonisent très souvent les parois des grottes et leur éradication s'avère bien plus difficile.

Enfin, l'optimisation des UV-C box (plus légère, lampe LED plus puissante, utilisable dans des endroits difficiles d'accès) est un paramètre essentiel dans l'utilisation de la technique à plus grande échelle.

Discussion générale et perspectives

La thèse de Fabien Borderie (2014) a permis de poser les bases de l'étude sur « L'utilisation du rayonnement UV-C comme méthode alternative aux produits chimiques dans la lutte et le contrôle de la prolifération des micro-organismes sur les matériaux du patrimoine ». Le travail de recherche actuel a permis, quant à lui, d'approfondir les résultats précédemment obtenus sur la biodiversité des biofilms et sur la physiologie algale et fongique suite à une irradiation. De plus, cette thèse a permis de valider certains travaux préliminaires comme l'étude portant sur les effets des UV-C vis-à-vis des pigments préhistoriques mais également la faisabilité de l'utilisation des UV-C dans certains monuments historiques (grottes et églises).

I. La biodiversité des biofilms

Dans ce travail de recherche, la biodiversité des biofilms a été analysée par la technique de séquençage la plus moderne à ce jour: le séquençage haut débit (Pfundler et al., 2018). Cette technique permet de connaître la composition en organismes (bactéries, champignons, cyanobactérie, diatomées, micro-algues et mousses) des biofilms (Borderie, 2014), et apporte également une information semi-quantitative. D'après la littérature, il s'agit de la première étude aussi complète sur les biofilms dans le milieu karstique. Dans de futures études, les résultats obtenus avec ce type de technique pourront être corrélés avec les paramètres environnementaux afin de comprendre quels sont les facteurs (lumière, humidité, etc.) responsables de la spécificité d'un biofilm par rapport à un autre au sein d'une même grotte. D'autre part, des réseaux de cooccurrence apporteront une meilleure compréhension des interactions que tous les taxons peuvent avoir les uns avec les autres (Zappelini et al., 2015).

II. Les réponses physiologiques des micro-organismes

Au cours de ces travaux de recherche, plusieurs paramètres physiologiques ont été étudiés sur l'algues modèle *Chlorella* sp.. Toutes les données obtenues ont permis d'optimiser le traitement UV-C sur la micro-algue, notamment avec l'utilisation de la lumière visible suite au traitement. Les résultats ont également montré les effets des UV-C sur les réponses physiologiques (photosynthèse, respiration, rendement quantique, quenchings, dégradation de la chlorophylle). Ces expériences pourraient, dans de futurs travaux, être menées sur d'autres

souches de micro-algues ou de cyanobactéries. Enfin, d'autres expériences pourraient être menées, notamment sur l'augmentation de concentration des espèces réactives de l'oxygène (ROS) ou sur les produits de dégradation de la chlorophylle. Ces derniers devront être séparés et analysés notamment par chromatographie en phase liquide à haute performance (HPLC) ou chromatographie en phase gazeuse.

La résistance des micro-algues et des champignons cavernicoles face aux UV-C est une piste intéressante dans la poursuite des travaux. En effet, la mise en évidence des composés photo-protecteurs comme les Mycosporines-like amino acids (MMAs) ou la mélanine est envisageable par HPLC ou par spectrométrie Raman. Ces études sont d'autant plus nécessaires, qu'il a été montré au cours de cette thèse, que certaines souches de champignons noirs sont capables de résister plus de dix minutes à un rayonnement UV-C. En comparaison, la micro-algue *Chlorella* sp. ne peut survivre à une irradiation dépassant la minute.

III. L'effet des UV-C sur la matière picturale

L'innocuité des UV-C sur la matière inorganique, telle que les pigments utilisés à la préhistoire, a été démontrée au cours de cette thèse. Cependant, la matière organique utilisée comme liant a été altérée. L'utilisation des UV-C doit donc être utilisée sur des supports ou des peintures ne contenant pas de liants organiques. Afin de compléter ce travail, d'autres expériences peuvent être réalisées sur une plus grande variété de pigments et de liants, ainsi que sur des peintures. De plus, les expériences menées en laboratoire ont montré que les algues, les cyanobactéries et les mousses colonisent préférentiellement les pigments (préalablement déposés sur des blocs de tuf) par rapport au support calcaire. Cette préférence est encore plus significative sur certains types de pigments, comme l'oxyde de fer rouge, où un développement très rapide a été observé. Des études plus approfondies permettront de déterminer quels sont les éléments minéraux qui favorisent la croissance de ces organismes.

IV. Le traitement *in situ* des biofilms

Au cours de cette thèse, la grotte de la Glacière et l'église de Vicherey ont fait l'objet de traitements par les UV-C. Les résultats sont encourageants car aucune recolonisation n'a été observée deux ans après les traitements dans la grotte de la Glacière. De plus, l'utilisation de la lumière UV-C s'est montrée très efficace dans l'église de Vicherey contre les algues et les cyanobactéries, avec un bleaching instantané à contrario des résultats obtenus avec les biocides et une molécule allélopathique. Dans de futures expérimentations, l'irradiation avec la lumière UV-C pourra être testée sur les mousses qui sont également très présentes dans les grottes touristiques, et de surcroît, responsables de phénomènes de biodétérioration.

L'utilisation des UV-C semble être la méthode la plus écologique et la plus efficace dans le temps, connue à ce jour. Cependant, son utilisation est soumise à plusieurs contraintes :

- Le facteur temps : L'exposition des biofilms aux UV-C nécessite beaucoup plus de temps (quelques heures) que l'utilisation des produits chimiques (quelques minutes).
- La contrainte matérielle : Si l'on veut traiter de grande surface en une seule fois, le dispositif UV-C est relativement lourd, et son transport n'est pas des plus aisés dans les grottes. Dans l'attente de lampes LED suffisamment puissantes (actuellement limitées à 70 mW, 278 nm, par le constructeur LG), le poids des UV-C box restent une limite à la méthode dans les endroits les moins accessibles.
- Le courant électrique : Le dispositif nécessite une alimentation électrique ce qui contraint à tirer des rallonges sur plusieurs centaines de mètres dans les grottes.
- Les contraintes liées à la morphologie des grottes : Afin de palier à l'impossibilité de traiter certains biofilms du fait de leur inaccessibilité au sein des grottes, des travaux sur l'utilisation de solutions allélopathiques ou d'huiles essentielles, moins néfastes pour l'environnement, pourraient être entrepris.

- La matière organique résiduelle : Suite à un traitement avec la lumière UV-C, la matière organique reste sur le support. Dans les études menées à l'église de Vicherey, il a été montré que les champignons opportunistes peuvent s'y développer, causant un deuxième problème de prolifération microbienne. Afin d'y remédié, le traitement UV-C doit impérativement être suivi d'une étape de nettoyage de la matière organique résiduelle.

La cinétique de recolonisation

La cinétique de recolonisation de la roche, après un traitement aux UV-C, n'a pas été étudiée au cours de cette thèse. En effet, après le traitement de tous les biofilms dans la grotte de la Glacière, aucune recolonisation n'a été observée et ceci même après deux ans de suivi. Ce résultat est encourageant quant à l'efficacité de la technique. Cependant, il faut aussi prendre en compte que les basses températures de la grotte (entre -10 et 5 °C) ne permettent pas une recolonisation rapide des parois contrairement à d'autres grottes dont les températures sont plus favorables. Par conséquent, l'exposition aux UV-C de biofilms dans une grotte, dont les paramètres de températures sont plus favorables, seraient envisageable et devrait être suivi de prélèvements microbiologiques tous les mois jusqu'à l'établissement d'un nouveau biofilm. Les prélèvements pourraient alors être analysés par une méthode de type séquençage haut débit.

Le traitement effectué sur les biofilms se doit d'être efficace en tuant 100% des micro-organismes présents. De cette seule manière, il est possible obtenir une disparition des biofilms qui sera durable. Cependant, la recolonisation est inéluctable du fait de l'éclairage artificiel et du nombre important de touristes qui visitent les grottes. Le choix du traitement s'avère donc important selon que l'on veuille ou non *(i)* protéger l'environnement, *(ii)* avoir un effet durable du traitement *(iii)* ou que l'on ait des contraintes financières.

Conclusion générale

La biodiversité des biofilms

Au cours de cette thèse, les travaux entrepris ont permis de compléter et de valider plusieurs axes de recherche de l'étude précédemment menée par Borderie (2014). En effet, du point de vue de la biodiversité, les résultats des observations microscopiques et des mesures en cytométrie en flux ont été complétés, dans cette étude, par une analyse de séquençage haut débit. Les résultats obtenus ont montré que les bactéries, espèces pionnières, sont les principales colonisatrices des biofilms dans les grottes touristiques et sont divisées en deux groupes : les bactéries photosynthétiques et les non photosynthétiques. Les 442 genres de bactéries non photosynthétiques sont majoritaires en terme de nombre de genre présent, mais également en terme de proportion dans le biofilm. Les micro-algues, les diatomées et les mousses complètent la liste des autotrophes vivant au sein du biofilm. Les champignons (principalement des Ascomycètes) sont quant à eux présents uniquement dans la moitié des biofilms étudiés et sont uniquement présents dans les grottes non traitées à l'eau de javel ; leur rôle exact restant encore à déterminer.

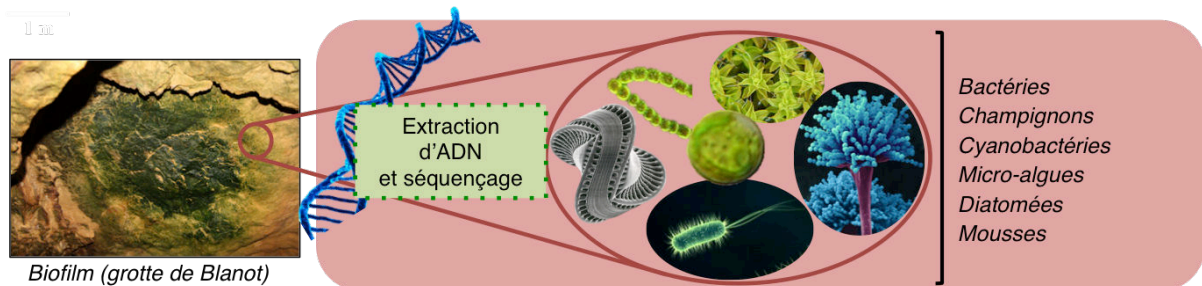


Figure 1: Représentation d'un biofilm et des principaux groupes taxonomiques le composant.

Les réponses physiologiques des micro-organismes

Dans l'étude sur la physiologie végétale, nous avons pu démontrer que le métabolisme de *Chlorella* sp. est fortement affecté par les radiations UV-C provoquant la mort cellulaire, même à de faible dose. En effet, des expositions à $2,5 \text{ kJ m}^{-2}$ sont suffisantes pour induire la mort des micro-algues. Cette mort cellulaire peut être expliquée en partie par la baisse observée de la respiration et la photosynthèse. Même si, après une irradiation de faible intensité, la photosynthèse peut être accrue avec une forte exposition à la lumière visible, les algues ne sont plus capables de maintenir un métabolisme permettant leur survie. De plus, l'inactivation et la destruction du photosystème II entraîne une augmentation du quenching non photochimique et la baisse du rendement quantique et du quenching photochimique. À cela s'ajoute la dégradation de la chlorophylle, qui est dépendante de l'intensité lumineuse reçue. Les résultats obtenus ont permis d'optimiser le traitement aux UV-C. En effet, en exposant les micro-algues à une forte intensité lumineuse (lumière visible) après un traitement aux UV-C, le processus de « bleaching » (ou blanchiment des pigments ; ex. : chlorophylle, caroténoïdes) est accéléré. Par exemple, une intensité de 30 kJ m^{-2} , suivie de 14 heures d'exposition à la lumière visible, permet d'obtenir un bleaching total. À une exposition plus faible (20 kJ m^{-2}), 25 heures de lumière visible seront nécessaires.

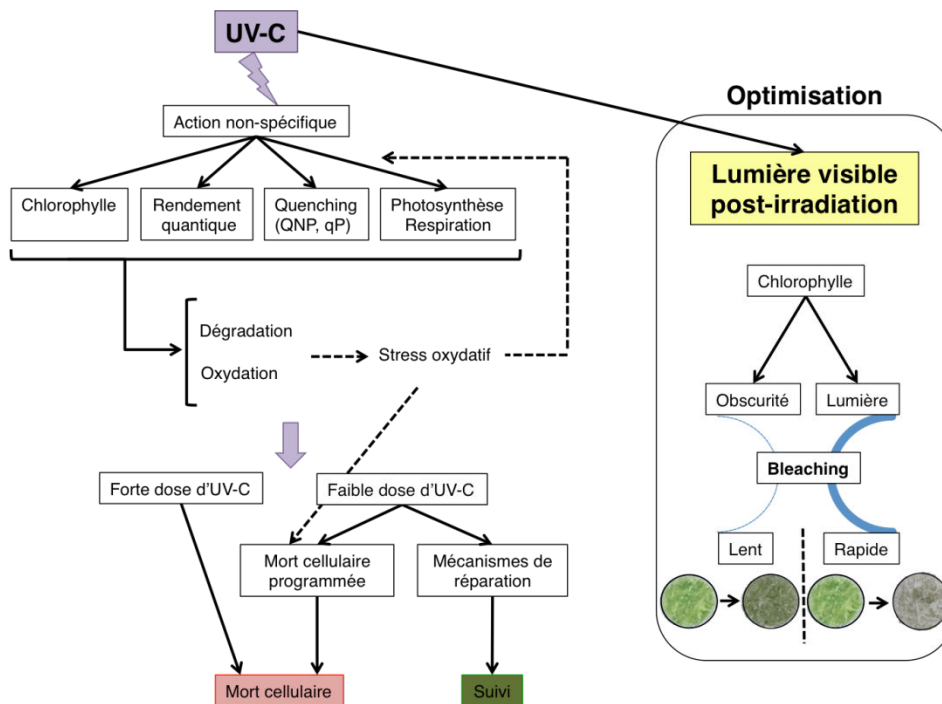


Figure 2: Synthèse non-exhaustive des effets des UV-C sur la micro-algues *Chlorella* sp..

L'effet des UV-C sur la matière picturale

L'utilisation des UV-C comme méthode de traitement des peintures pariétales colonisées par des micro-organismes est soumise à deux contraintes majeures. En effet, les pigments inorganiques ainsi que les liants organiques ne doivent pas être affectés par les radiations UV. Lors de cette étude, il a été démontré, par l'utilisation de six techniques différentes, que les UV-C n'ont aucun effet sur les pigments utilisés lors de la préhistoire. Cependant, les deux types de liants testés ont changé de couleurs après le traitement. Il est à noter que ce changement a également été observé sur les échantillons témoins maintenus à la lumière visible. L'utilisation des UV-C sur des peintures rupestres doit donc être réservée à des fresques qui ne contiennent pas de liants organiques, même si, aucune étude n'a pu démontrer la présence de liants organiques. En effet, la matière organique a probablement été dégradée au cours des millénaires ou a été polymérisée, la transformant progressivement en matière inorganique. Le principe de précaution doit donc s'appliquer en attendant la mise en place d'une irradiation UV-C sur une petite partie d'une fresque rupestre.

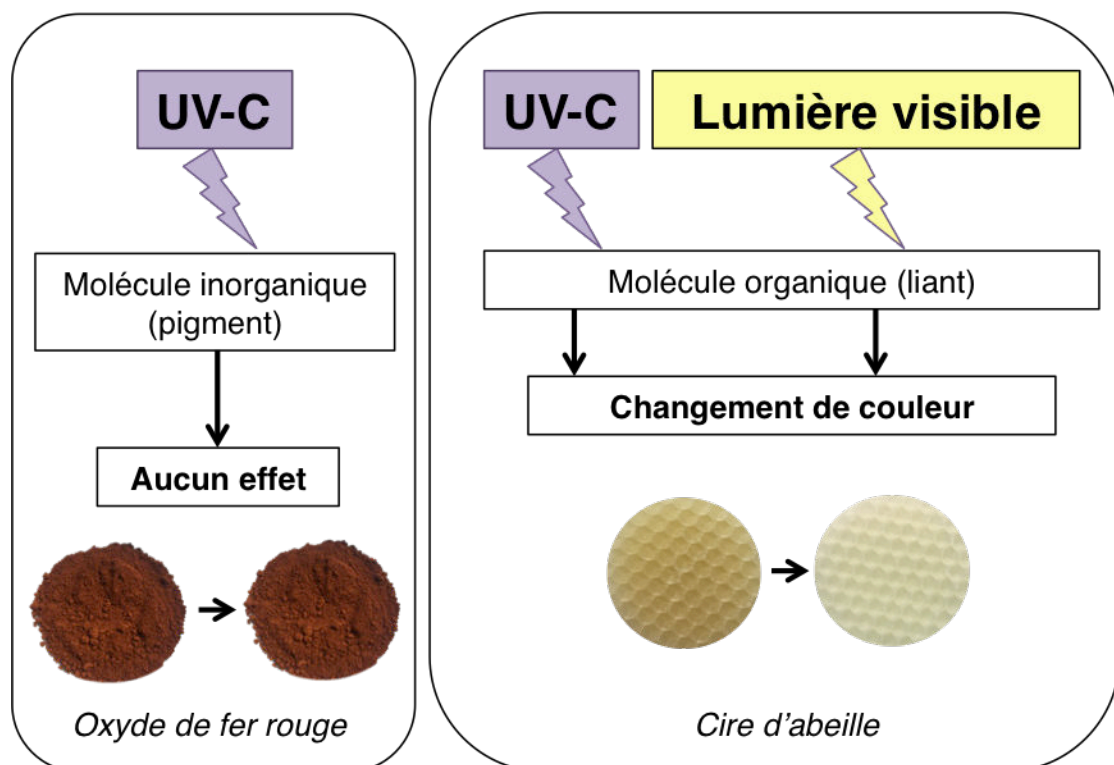


Figure 3: Effet des UV-C et de la lumière visible sur les pigments et les liants utilisés dans la réalisation de peintures rupestres.

Le traitement *in situ* des biofilms

Six groupes d'organismes sont responsables de la prolifération des biofilms dans les grottes touristiques et les monuments historiques (bactéries, champignons, cyanobactéries, micro-algues, diatomées et mousses). Le choix du traitement doit donc prendre en compte cette biodiversité et par conséquent être de large spectre. Cependant, les biocides, couramment utilisés, ne sont pas efficaces sur tous les types d'organismes recensés dans les biofilms, et leur efficacité est variable contrairement à des produits chimiques comme l'eau de javel ou le peroxyde d'hydrogène. Hors, ces derniers ont le désavantage d'être dangereux pour l'environnement et l'utilisateur. L'utilisation de la lumière UV-C comme méthode alternative semble être à ce jour la plus écologique et la plus efficace. Les différentes études sur le terrain (grotte et église) ont montré que les UV-C sont plus efficaces que les biocides et qu'aucune recolonisation n'a été observée pendant deux ans. Une question reste cependant en suspend : qu'elle serait l'effet des UV-C sur le support à long terme ?

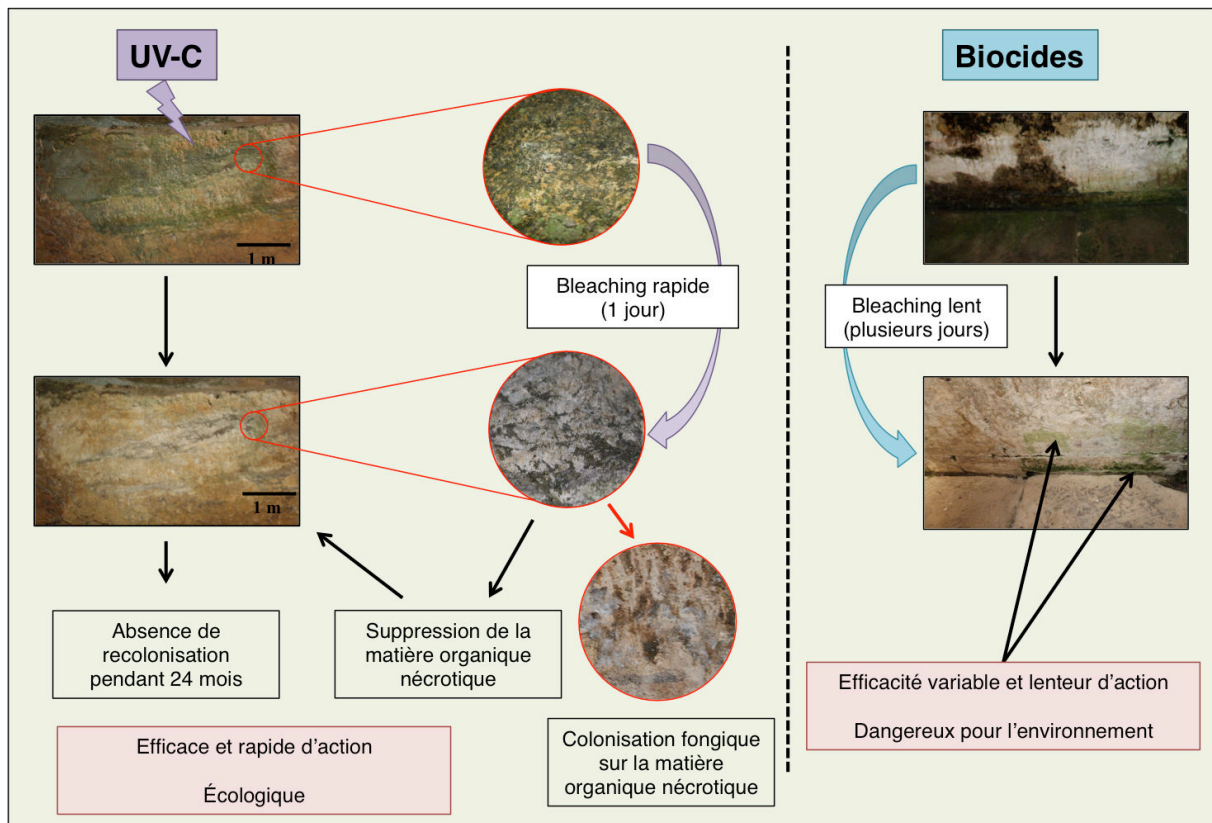


Figure 4: Schéma récapitulatif des traitements par la lumière UV-C et par les biocides.

Références

A

Abdelahad N (1989) On four Myxosarcina-like species (Cyanophyta) living in the Inferniglio cave (Italy). *Algological Studies, Archiv für Hydrobiologie, Supplement* 82(1) 54:3-14.

D'Agostino D, Beccarisi L, Camassa M, Febroriello F (2015) Microclimate and microbial characterization in the Zinzulusa show cave (South Italia) after switching to LED lighting. *Journal of Cave and Karst Studies*, p. 133–144.

Aley T (1972) Control of unwanted plant growth in electrically lighted caves. *Caves and Karst*, 14: 33-35.

Aley T, Aley C, Rhodes R (1985) Control of exotic plant growth in Carlsbad Caverns, New Mexico. *Proc. National Cave Management Symposium, Missouri Speleology*, 25: 159-171.

Aley T (2004) Tourist caves: algae and Lampenflora. In: Gunn J. (Ed.) - *Encyclopedia of Caves and Karst tropical Science*, New York: Fitzroy Dearborn, 1568-1570.

Asencio AD, Aboal M (2001) Biodeterioration of wall paintings in caves of Murcia (SE Spain) by epilithic and chasmoendolithic microalgae. *Algological Studies*, 103:131-142.

Argant A (1991) Carnivores quaternaires de Bourgogne. Thèse, Documents laboratoires de géologie de Lyon, Université Claude Bernard Lyon I, pp 278.

Athanassia A, Hilla AE, Fourriera T, Burgiob L, Clarkb RJH (2000) The effects of UV laser light radiation on artists' pigments. *Journal of Cultural Heritage* 1:209-213.

Aubert M, Brumm A, Ramli M, Sutikna T, Saptomo EW, Hakim B, Morwood MJ, Bergh GD, Van Den, Kinsley L, Dosseto A (2014) Pleistocene cave art from Sulawesi, Indonesia. *Nature*, 514:223–227.

Azua A (2010) Chilean Cave Cyanidium. *Red Algae in the Genomic Age*, pp.427-439.

B

Bahls L (1981) Diatoms of Lewis and Clark Caverns, Oregon. *Great Basin Naturalist*, 41:3-9.

Baker A, Genty D (1998) Environmental pressures on conserving cave speleothems: Effects of changing surface land use and increased cave tourism. *Journal of Environmental Management*, 53,165–175.

Baraibar MA, Ladouce R, Friguet B (2013) Proteomic quantification and identification of carbonylated proteins upon oxidative stress and during cellular aging. *Journal of Proteomics*, 92:63–70.

Barberousse H (2006) Étude de la biodiversité des algues et des cyanobactéries colonisant les revêtements de façade en France et recherche des facteurs favorisant leur implantation, Thèse du Muséum d'Histoire naturelle, pp 192.

Barnett JR, Miller S, Pearce E (2006) Colour and art : A brief history of pigments. 38:445-453.

Barriquand L, Barriquand J, Argant A, Floss H, Gallay A, Guérin, Guillot L, Jeannet M, Nykiel C, Quinif Y (2011) Le site des grottes d'Azé. *Quaternaire*, p.15-25.

Bartosch S, Mansch R, Knötzsch K, Bock E (2003) CTC staining and counting of actively respiring bacteria in natural stone using confocal laser scanning microscopy. *Journal of Microbiological Methods*, 52:75–84.

Bastian F, Alabouvette C, Saiz-jimenez C (2008) Bacteria and free-living amoeba in the Lascaux Cave. *Research in Microbiology*, 160:38–40.

Bastian F (2010) The microbiology of Lascaux Cave The microbiology of Lascaux Cave. *Microbiology*, 156:644–652.

- Beck L, Lebon M, Lahlil S, Grégoire S, Odin GP, Rousselière H, Castaing J, Duran A, Vignaud C, Reiche I, Lambert E, Salomon H, Genty D, Chiotti L, Nespoulet R, Plassard F, Menu M (2014) Analyse non destructive des pigments préhistoriques: de la grotte au laboratoire, Actes du colloque « Micro-analyses et datations de l'art préhistorique dans son contexte archéologique », p 63-74.
- Begum M, Hocking A, Miskelly D (2009) Inactivation of food spoilage fungi by ultra violet (UVC) irradiation. *International Journal of Food and Microbiology*, 129,74–77.
- Bell AA, Wheeler MH (1986) Biosynthesis and function of fungal melanin. *Annual Review of Phytopathology*, 24:411-451.
- Berdoulay M, Salvado JC (2009) Genetic characterization of microbial communities living at the surface of building stones. *Letter in Applied Microbiology* 49:311–316.
- Bolige A, Kiyota M, Goto K (2005) Circadian rhythms of resistance to UV-C and UV-B radiation in *Euglena* as related to « escape from light » and « resistance to light ». *Journal of Photochemistry and Photobiology B: Biology*, 81,43–54.
- Borderie F, Alaoui-Sossé L, Raouf N, Bousta F, Oriol G, Riefel D, Alaoui-Sossé B (2011) UV-C irradiation as a tool to eradicate algae in caves. *International Journal of Biodeterioration and Biodegradation*, 65:579–584.
- Borderie F, Tête N, Cailhol D, Alaoui-Sehmer L, Bousta F, Rieffel D, Aleya L, Alaoui-Sossé B (2014) Factors driving epilithic algal colonization in show caves and new insights into combating biofilm development with UV-C treatments. *Sciences of Total Environment*, 484:43-52.
- Borderie F, Alaoui-Sossé B, Aleya L (2015) Heritage materials and biofouling mitigation through UV-C irradiation in show caves: state-of-the-art practices and future challenges. *Environmental Sciences and Pollution Research*, 22:4144–4172.
- Borderie F, Denis M, Barani A, Alaoui-Sossé B, Aleya L (2016) Microbial composition and ecological features of phototrophic biofilms proliferating in the Moidons Caves (France) :

investigation at the single-cell level. *Environmental Sciences and Pollution Research* 23:12039–12049.

Boston P (2006) To bleach or not to bleach: algae control in show caves. In: Hildreth-Werker V and Werker JC, editors. *Cave Conservation and Restoration*. Huntsville: National Speleological Society, 349-350.

Bourges F, Genthon P, Genty D, Lorblanchet M, Mauduit E, D'Hulst D (2014) Conservation of prehistoric caves and stability of their inner climate: Lessons from Chauvet and other French caves. *Science of the Total Environment*, 493, 79–91.

Bruno L, Billi D, Albertano P, Urzi C (2006) Genetic characterization of epilithic cyanobacteria and their associated bacteria. *Geomicrobiology Journal*, 23:293–299.

Bruno L, Billi D, Bellezza S, Albertano P (2008) Cytomorphological and genetic characterization of troglolithic *Leptolyngbya* strains isolated from Roman hypogea. *Applied and Environmental Microbiology*, 73:608–617.

Buma A, Zemmeling H, Sjollema K, Gieskes W (1995) Effect of UV-B on cell characteristics of the marine diatom *Cyclotella* sp. In: Bauer H, Nolan C (Eds.), *The Effects of Environmental UV-B Radiation on Health and Ecosystems*. Eur. Comm.

C

Cañaveras JC, Sanchez-Moral S, Soler V, Saiz-Jimenez C (2001) Microorganisms and microbially induced fabrics in cave walls. *Geomicrobiology Journal*, 18: 223-240.

Caneva G, Nugari MP, Salvadori O (2008) *Plant Biology for Cultural Heritage: Biodeterioration and Conservation*. Getty Conservation Institute.

Cappitelli F, Sorlini C (2005) From papyrus to compact disc: the microbial deterioration of documentary heritage. *Critical Reviews in Microbiology*, 31:1–10.

- Caumartin V (1993) Evolution des idées en matière de corrosion et de conservation du milieu souterrain. Cent ans de spéléologie française. Fédération Française de Spéléologie, Spelunca Mémoire. n°17, Paris, 273-275.
- Cennamo P, Marzano C, Ciniglia C, Pinto G, Cappelletti P, Caputo P, Studies K (2012) A Survey of the algal flora of anthropogenic caves of Campi Flegrei (Naples, Italy). Archeological District, 243–250.
- Cennamo P, Montuori N, Trojsi G, Fatigati G, Moretti A (2016) Bio films in churches built in grottoes. Science of the Total Environment, 543, 727–738.
- Chalmin E (2003) Caractérisation des oxydes de manganèse et usage des pigments noirs au paléolithique supérieur. Université de Marne-la-Vallée, 382 pp.
- Champlot S, Berthelot C, Bennett EA, Grange T (2010) An Efficient Multistrategy DNA Decontamination Procedure of PCR Reagents for Hypersensitive PCR Applications, PLoS ONE, 28:5-9.
- Chappé M, Hildenhagen J, Dickmann K, Bredol M (2003) Laser irradiation of medieval pigments at IR, VIS and UV wavelengths. Journal of Cultural Heritage, 3:264-270.
- Choppy J (1984) Températures de l'air. In: Phénomènes karstiques, série 1.1, processus climatiques, 3ème partie, Spéléo-Club de Paris, pp. 1-73.
- Cigna AA (1967) An analytical study of air circulations in caves. International Journal of Speleology, pp. 41-54.
- Cigna AA (2012) Encyclopedia of Caves, Second Edition, Elsevier, pp. 963.
- Cigna AA (1993) Environmental management of tourist caves. Environmental Geology, 21:173-80.
- Cigna AA, Burri E (2000) Development management and 'Lampenflora' and economy of show caves. International Journal of Speleology, 29:1-27.

- Cigna AA (2011) The problem of Lampenflora in show caves. In: Bella P, Gazik P (Eds.), Proceedings of the 6th ISCA Congress. SNC of Slovak Republic, Slovak Caves Administration, pp. 201–205.
- Claus G (1962) Data on the ecology of the algae of Peace cave in Hungary. *Nova Hedwigia Zeitsch. Kryptogamenkunde*, 4:55-80.
- Couté A (1984) Contribution à l'étude cytologique, biologique et systématique de quelques algues dulçaquicoles peu connues. Thèse Doctorat d'état: Paris, pp. 260.
- Couté A (1985) Essai préliminaire de comparaison de deux Cyanophycées cavernicoles calcifiées: *Geitleria calcarea* Friedmann and *Scytonema julianum* Meneghini. *Archiv fur Hydrobiologie, Supplement 71(1-2) (Algological Studies 38-39)*: 91-98.
- Couté A, Chauveau O (1994) Algae: *Encyclopaedia Biospeologica I*. Juberthie C. & Decu V., editors. Société de Biospéologie: 371-380.
- Cutler NA, Oliver AE, Viles HA, Whiteley AS (2012) Non-destructive sampling of rock-dwelling microbial communities using sterile adhesive tape. *Journal of Microbiological Methods*, 91:391–398.
- Culver DC, Master LL, Christman MC, Iii H (2000) Obligate Cave Fauna of the 48 Contiguous United States, *Conservation Biology*, 14, 386–401.
- Culver DC, White WB (2005) *Encyclopedia of Caves*. Elsevier ed., pp. 654.
- Cuningham KI, DuChene HR, Spirakis CS (1993) Elemental sulfur in caves of the Guadalupe Mountains, New Mexico. New Mexico, Socorro: New Mexico Geological Society Guidebook 44th Field conference, Carlsbad region, New Mexico and West Texas, p. 129-136.
- Czerwik-Marcinkowska J, Mrozińska T (2009) Epilithic algae from caves of the Krakowsko-Czestochowska upland (Southern Poland). *Acta Societatis Botanicorum Poloniae*, 78: 301-309.

Czerwik-Marcinkowska J, Mrozińska T (2011) Algae and cyanobacteria in caves of the Polish jura. *Polish Botanical Journal*, 56: 203-243.

Czerwik-Marcinkowska (2013) Observations on aerophytic cyanobacteria and algae from ten caves in the Ojców National Park. *Acta Agrobotanica*, 66: 39- 52.

D

Dakal TC, Cameotra SS (2012) Microbially induced deterioration of architectural heritages: routes and mechanisms involved. *Environmental Sciences Europe*, 24:36.

Dhami NK, Reddy MS, Mukherjee A (2014) Application of calcifying bacteria for remediation of stones and cultural heritages. *Frontiers in Microbiology*, 26:5-304.

Danon A, Delorme V, Mailhac N, Gallois P (2000) Plant programmed cell death: a common way to die. *Plant Physiology and Biochemistry*, 38, 647–655.

Davis J, Rands D (1982) Lime incrusting *Hapalosiphon intricatus* (Cyanophyceae) and phosphate availability in a Florida cave. *Schweizerische Zeitschrift für Hydrologie*, 44:289-294.

Davies MJ, Truscott RJW (2001) Photo-oxidation of protein and its role in cataractogenesis. *Journal of Photochemistry and Photobiology B*, 63:114–125.

Davies MJ (2003) Singlet oxygen-mediated damage to proteins and its consequences. *Biochemistry and Biophysical Research Communications*, 305:761–770.

Davies MJ (2004) Reactive species formed on proteins exposed to singlet oxygen. *Photochemistry and Photobiological Sciences*, 3:17–25.

Dayner D, Johansen J (1991) Observations on the algal flora of Seneca Cavern, Seneca County, Ohio. *Ohio Journal of Science*, 91:118-121.

Dickson G, Kirk P (1976) Distribution of heterotrophic microorganisms in relation to detritivores in Virginia caves (with supplemental bibliography on cave mycology and microbiology). In: Roane M, Patterson R (Eds.). *Distributional history of the Southern Appalachians Part IV: Algae and Fungi*. University Press of Virginia, Charlottesville, Virginia, p. 205-226.

Dickinson BC, Chang CJ (2011) Chemistry and biology of reactive oxygen species in signaling or stress responses. *Natural Chemical Biology*, 7:504–511.

Dobat K (1970) Considérations sur la végétation cryptogamique des grottes du Jura Souabe (sud-ouest de l'Allemagne): *Annales de Spéologie*, v. 25, no. 4, p. 872–907.

Dragovich D, Grose J (1990) Impact of Tourists on Carbon Dioxide Levels at Jenolan Caves, Australia: an Examination of Microclimatic Constraints on Tourist Cave Management. *Geoforum*. Vol. 21. No. 1, pp111-120.

Dring MJ, Makarov V, Schoschina E, Lorenz M., Lüning K (1996) Influence of ultraviolet-radiation on chlorophyll fluorescence and growth in different life-history stages of three species of *Laminaria* (Phaeophyta). *Marine Biology*, 126,183–191.

Durrell LD, Shields LM (1960) Fungi isolated in culture from soil of the Nevada test site. *Mycologia*, 52, 636–641.

E

Edwards HGM, Newton EM, Russ J (2000) Raman spectroscopic analysis of pigments and substrata in prehistoric rock art. *Journal of molecular Structure*, 551, 245–256.

Elliott W (1997) A survey of ecologically disturbed areas in Carlsbad Cavern, New Mexico. Report to Carlsbad Caverns National Park.

Elliot W (2006) Biological dos and don'ts for cave conservation and restoration – best management practices. In: Hildreth-Werker V. & Werker J.C., editors. Cave Conservation and Restoration. Huntsville: National Speleological Society, 33-42.

F

Faimon J, Stelcl J, Kubesová S, Zimák J (2003) Environmentally acceptable effect of hydrogen peroxide on cave “lampflora”, calcite speleothems and limestones. *Environmental Pollution*, 122,417–22.

Franklin LA, Osmond CB, Larkum AWD (2003) Photoinhibition, UV-B and algal photosynthesis. In *Photosynthesis in Algae* (Edited by A. W. Larkum, S. E. Douglas and J. A. Raven), pp. 351–384.

Friedmann I (1955) Studies on cave-algae from Israel I. *Geitleria calcarea* n. gen. et n. sp. A new atmophytic lime-encrusting blue-green alga. *Botaniska Notiser*, 108:439-445.

G

Gao Y, Cui Y, Xiong W, Li X, Wu Q (2009) Effect of UV-C on Algal Evolution and Differences in Growth Rate, Pigmentation and Photosynthesis Between Prokaryotic and Eukaryotic Algae. *Photochemistry and Photobiology*, 774–782.

Gibeaux S, Tourron S, Bousta F (2014) Etude des effets du rayonnement UV-C sur la matière picturale dans le cadre d'une application en grotte ornée. *Laboratoire de Recherche des Monuments Historiques (LRMH) Rapport 1377A*, pp. 58.

Gillieson DS (2011) Management of caves. In: Van Beyen P. (Ed.) – *Karst Management*. Springer: 141-158.

Ginet R. Decou V. 1977. *Initiation à la biologie et à l'écologie souterraines*. Jean-Pierre Delarge, Paris, p. 319.

Gomes H, Rosina P, Holakooei P, Solomon T, Vaccaro C (2013) Identification of pigments used in rock art paintings in Gode Roriso-Ethiopia using Micro-Raman spectroscopy. *Journal of Archaeological Sciences*, 40:4073–4082.

Gorbushina AA (2007) Life on the Rocks. *Environmental Microbiology*, 9:1613-1631.

Gracanin M, Hawkins CL, Pattison DI, Davies MJ (2009) Singlet-oxygen- mediated amino acid and protein oxidation : Formation of tryptophan peroxides and decomposition products. *Free Radical Biology and Medicine*, 47:92–102.

Grobbelaar JU (2000) Lithophytic algae: a major threat to the karst formation of show caves. *Journal of Applied Phycology*, 12:309-315.

Gu JD (2003) Microbiological deterioration and degradation of synthetic polymeric materials: recent research advances. *International Biodeterioration and Biodegradation*, 52:69–91.

Guérin C (2009) Les grands herbivores pléistocènes des grottes d’Azé (Saône-et-Loire, France).

Gurnee J (1994) Management of some unusual features in the show caves in the United States. *International Journal of Speleology*, 23:13-17.

H

Hildreth-Werker V, Werker J (2006) Cave restoration overview – why call it cave restoration? *Cave Conservation and Restoration*. Huntsville: National Speleological Society: 293-302.

Hoffmann L, Darienko T (2005) Algal biodiversity on sandstone in Luxembourg. *Ferrantia*, 44:99–101.

Höhn A, König J, Grune T (2013) Protein oxidation in aging and the removal of oxidized proteins. *Journal of Proteomics*, 92:132–159.

Holzinger A, Lütz C, Karsten U, Wiencke C (2004) The effect of ultraviolet radiation on ultrastructure and photosynthesis in the red macroalgae *Palmaria palmata* and *Odonthalia dentata* from Arctic waters. *Plant Biology*, 6:568–577.

Hueck HJ (2001) The biodeterioration of materials—an appraisal. *International Biodeterioration and Biodegradation*, 48:5–11.

J

Jain M, Rivera S, Monclus EA, Synenki L, Zirk A, Eisenbart J, Feghali-Bostwick C, Mutlu GM, Budinger GRS, Chandel NS (2013) Mitochondrial reactive oxygen species regulate transforming growth factor- β signaling. *Journal of Biology and Chemistry*, 288:770–777.

Jaubert J, Verheyden S, Genty D, Soulier M, Cheng H, Blamart D, Burlet C, Camus H, Delaby S, Deldicque D, Edwards RL, Ferrier C (2016) Early Neanderthal constructions deep in Bruniquel Cave in southwestern France. *Nature*, 1–17.

Jezequel P, Wille G, Beny C, Delorme F, Jean-prost V, Cottier R, Breton J, Dure F, Desprie J (2011) Characterization and origin of black and red Magdalenian pigments from Grottes de la Garenne (Vallée moyenne de la Creuse-France): a mineralogical and geochemical approach of the study of prehistorical paintings. *Journal of Archaeological Sciences*, 38:1165–1172.

Jiang H, Qiu B (2011) Inhibition of photosynthesis by UV-B exposure and its repair in the bloom-forming cyanobacterium *Microcystis aeruginosa*. *Journal of Applied Phycology*, 23:691–696.

Juberthie C, Decou V (1994) *Encyclopaedia Biospeologica*. Société de Biospéologie, Moulis-Bucarest, p. 341-358.

Jurado V, Sanchez-Moral S, Saiz-Jimenez C (2008) Entomogenous fungi and the conservation of the cultural heritage. A review. *International Biodeterioration and Biodegradation*, 62:325–330.

K

Karentz D, Cleaver JE, Mitchell DL (1991) Cell survival characteristics and molecular responses of Antarctic phytoplankton to ultraviolet-B radiation. *Journal of Phycology* 27:326–341.

Keswick BH, Wang DS, Gerba CP (1982) The use of microorganisms as ground-water tracers: a review. *Groundwater*, 20:142-149.

Keshari N, Adhikary SP (2013) Characterization of cyanobacteria isolated from biofilms on stone monuments at Santiniketan, India. *Biofouling*, 29 (5): 525-536.

Kreslavskii V, Lyubimov V, Kotova L, Kotov A (2011) Effect of Common Bean Seedling Pretreatment with Chlorocholine Chloride on Photosystem II Tolerance to UV-B Radiation, Phytohormone Content, and Hydrogen Peroxide Content. *Russian Journal of Plant Physiology*, vol. 58, pp. 324–329.

Kulandaivelu G, Noorudeen AM (1983) Comparative study of the action of ultraviolet-C and ultraviolet-B radiation on photo-synthetic electron transport. *Physiological Plant*, 58:389-394.

Kumar R, Kumar AV (1999) *Biodeterioration of Stones in Tropical Environments*. Los Angeles, CA: The Getty Conservation Institute.

L

Lamprinou V, Danielidis DB, Economouamilli A (2012) Distribution survey of Cyanobacteria in three Greek caves of Peloponnese. *International Journal of Speleology*, 41:267–272.

Lamprinou V, Danielidis DB, Pantazidou A, Oikonomou A, Economouamilli A (2014) The show cave of Diros vs wild caves of Peloponnese, Greece - distribution patterns of Cyanobacteria. *International Journal of Speleology*, 43:335–342.

Liao XS, Wang X, Zhao KH, Zhou M (2009) Photocatalytic inhibition of cyanobacterial growth using silver-doped TiO₂ under UV-C light. *Journal of Wuhan University Technology*, 24:402-408.

Lisci M, Monte M, Pacini E (2003) Lichens and higher plants on stone: a review. *International Biodeterioration and Biodegradation*, 51:1-17.

Lismonde B (2002) *Climatologie du Monde Souterrain, Aérologie des systèmes karstiques*. CDS Isère.

Lüttge U, Büdel B (2010) Resurrection kinetics of photosynthesis in desiccation-tolerant terrestrial green algae (Chlorophyta) on tree bark. *Plant Biology* 12:437–444.

M

Macedo MF, Miller AZ, Dionísio A, Saiz-Jimenez C (2009) Biodiversity of cyanobacteria and green algae on monuments in the Mediterranean Basin: an overview. *Microbiology*, 155: 3476-3490.

Marnett LJ (1999) Lipid peroxidation-DNA damage by malondialdehyde. *Mutation Research*, 424:83–95.

- Martínez A, Asencio AD (2010) Distribution of cyanobacteria at the Gelada Cave (Spain) by physical parameters. *Journal of Cave and Karst Studies*, 72:11-20.
- May E, Zamarreño D, Hotchkiss S, Mitchell J, Inkpen R (2011) Bioremediation of Algal Contamination on Stone Biocolonization of Stone: Middle Missouri Plains Control and Preventive Village Sites Methods Proceedings from the MCI Workshop Series. pp 59-70.
- Meindl U, Lütz C (1996) Effects of UV irradiation on cell development and ultrastructure of the green alga *Micrasterias*. *Journal of Photochemistry and Photobiology B*, 36:285-292.
- Mihajlovski A, Seyer D, Benamara H., Boustia F, Di Martino P, (2014) An overview of techniques for the characterization and quantification of microbial colonization on stone monuments. *Microbiology*, 65:1243-1255.
- Monteux S (2013) Biospéologie, climatologie et phylobiogéographie dans le système du Rautély (Hérault, France). Mémoire de master1 Université de Montpellier 2. pp. 24.
- Mortimore JL, Marshall LR, Almond MJ, Hollins P, Matthews W (2004) Analysis of red and yellow ochre samples from Clearwell Caves and Çatalhöyük by vibrational spectroscopy and other techniques. *Spectrochimica Acta Part A*, 60:1179–1188.
- Mulec J, Kosi G, Vrhovsek D (2008) Characterization of cave aerophytic algal communities and effects of irradiance levels on production of pigments. *Journal of Cave Karst Studies*, 70:3–12.
- Mulec J, Kosi G (2009) Lampenflora algae and methods of growth control. *Journal of Cave Karst Studies*, 71:109–15.
- Mulec J (2014) Human impact on underground cultural and natural heritage sites , biological parameters of monitoring and remediation actions for insensitive surfaces : Case of Slovenian show caves. *Journal of Nature Conservation*, 22, 132–141.

N

Nawkar GM, Maibam P, Park JH, Sahi VP (2013) UV-Induced Cell Death in Plants. *International Journal of Molecular Sciences*, 8:1608–1628.

Neves-Petersen MT, Gajula GP, Petersen SB (2012) UV light effects on proteins: from photochemistry to nanomedicine. *Molecular Photochemistry, Various Aspects*, Saha S, Ed., pp. 125-158.

Northup DE, Carr DL, Crocker MT, Cunningham KI, Hawkins LK, Leonard P, Welbourn WC (1994) Biological investigations in Lechuguilla Cave, Carlsbad Caverns National Park, New Mexico. *Bulletin of the National Speleological Society*, 56:54-63.

Nugari MP, Pietrini AM, Caneva G, Imperi F, Visca P (2009) Biodeterioration of mural paintings in a rocky habitat: The Crypt of the Original Sin (Matera, Italy). *International Biodeterioration and Biodegradation* 63:705-711.

O

Olson R (2002) Control of lamp flora in Mammoth Cave National Park. In: Hazslinsky, T., (Ed.), *International Conference on Cave Lighting*, November 15-17, 2000. Budapest: Hungarian Speleological Society, 131-133.

Olson R (2006) Control of lamp ora in developed caves. In: Hildreth-Werker V. & Werker J.C., editors. *Cave Conservation and Restoration*. Huntsville: National Speleological Society: 343-348.

Orial G, Bousta F, François A, Warscheid T, Pallot Frossard I (2011) Managing biological activities in Lascaux : identification of microorganisms, monitoring and treatments. *Rapport du Ministère de la Culture, Éd. de la Maison des sciences de l'homme*, pp. 33.

Ortega-Calvo JJ, Hernandez-Marine M, Saiz-Jimenez C (1991) Biodeterioration of building materials by cyanobacteria and algae. *International Biodeterioration and Biodegradation* 28: 165–185.

Osmond CB (1994) What is photoinhibition? Some insights from comparisons of shade and sun plant. In *Photoinhibition of Photosynthesis, from the Molecular Mechanisms to the Field* (Edited by N. R. Baker and J. R. Bowyer), BIOS Scientific Publications, Oxford, pp. 1–24.

P

Pallipurath A, Skelton J, Bucklow S, Elliott S (2015) A chemometric study of ageing in lead-based paints. *Talanta*, 144:977–985.

Palmer AN, Palmer MV, Davis DG (1991) Geology and origin of Lechuguilla cave. In: Taylor M.R. (Ed.), *Lechuguilla-Jewel of the underground*, Speleoprojects, Basel, Switzerland, 22-31.

Perrichet A (1991) Développement de micro-organismes à la surface des bétons et enduits. *Sycodès Informations*, 11:19-24.

Pfendler S, Einhorn O, Bousta F, Khatyr A, Alaoui-Sossé L, Aleya L, Alaoui-Sossé B (2017) UV-C as a means to combat biofilm proliferation on prehistoric paintings : evidence from laboratory experiments. *Environmental Science and Pollution Research*. doi : 10.1007/s11356-017-9791-x.

Pfendler S, Einhorn O, Karimi B, Bousta F, Caihol D, Alaoui-Sossé L, Alaoui-Sossé B, Aleya L (2017) UV-C as an efficient means to combat biofilm formation in show caves : evidence from the La Glacière Cave (France) and laboratory experiments. *Environmental Science and Pollution Research*. Doi : 10.1007/s11356-017-0143-7.

Piano E, Bona F, Falasco E, La Morgia V, Badino G, Isaia M (2015) Environmental drivers of phototrophic biofilms in an Alpine show cave (SW-Italian Alps). *Sciences of the Total Environment*, 536:1007-18.

Pigeot-remy S, Real P, Simonet F, Hernandez C, Vallet C, Lazzaroni JC (2013) Applied Catalysis B: Environmental Inactivation of *Aspergillus niger* spores from indoor air by photocatalytic filters. *Applied Catalysis B : Environmental*, 167–173.

Popović S, Simić GS, Stupar M, Unković N, Jovanović J, Grbić ML (2015) Cyanobacteria, algae and microfungi present in biofilm from Božana Cave (Serbia). *International Journal of Speleology*, 44:141–149.

Prieto B, Silva B, Lantes O (2004) Biofilm quantification on stone surfaces: comparison comparison of various methods. *Sciences of the Total Environment*, 333:1–7.

Q

Qi-Wang MGY, He LY, Sheng XF (2011) Characterization of bacterial community inhabiting the surfaces of weathered bricks of Nanjing Ming city walls. *Sciences of the Total Environment*, 409:756–762.

R

Ray PD, Huang BW, Tsuji Y (2012) Reactive oxygen species (ROS) homeostasis and redox regulation in cellular signaling. *Cellular Signaling*, 24:981–990.

Ríos De Los A, Ascaso C (2005) Contributions of in situ microscopy to the current understanding of stone biodeterioration. *International Microbiology*, 8:181–188.

Ruspoli, M. (1986) *Lascaux: Un nouveau regard*. Paris: Bordas.

Rusterholtz KJ, Mallory LM (1994) Density, activity, and diversity of bacteria indigenous to a karstic aquifer. *Microbial Ecology*, 28:79-99.

S

Saiz-jimenez C, Cuezva S, Jurado V, Fernandez-cortes A, Porca E, Benavente D, Cañaveras JC, Sanchez-moral S (2011) Paleolithic Art in Peril : Policy and Science Collide at Altamira Cave. *Policy Forum*, 334, 42–43.

Salvadori O (2003). The control of biodeterioration. *Coalition*, 6:16–20.

Sandmann G, Kuhn S, Böger P (1998) Evaluation of structurally different carotenoids in *Escherichia coli* transformants as protectants against UV-B radiation. *Applied Environmental Microbiology*, 64:1972–1974.

Sebela S, Turk J (2014) Natural and anthropogenic influences on the year-round temperature dynamics of air and water in Postojna show cave, Slovenia. *Tourism Management*, 40:233-243.

Schaeffer T (2001) Effects of Light on Materials in Collections: Data on Photoflash and Related Sources. *Research in Conservation*. Los Angeles, CA: Getty Conservation Institute. pp 212.

Shields LM, Durell LW (1964) Algae in relation to soil fertility. *The Botanical Review*, 30:92–128.

Sinha RP, Hader DP (2002) UV-induced DNA damage and repair: a review. *Photochemical and Photobiological Sciences*, 1:225-236.

Slesak I, Libik M, Karpinska B, Karpinski S, Miszalski Z (2007) The role of hydrogen peroxide in regulation of plant metabolism and cellular signalling in response to environmental stresses. *Acta Biochimica Polonica*, 54:39–50.

Smith KC (1962) Dose dependent decrease in extractability of DNA from bacteria following irradiation with ultraviolet light or with visible light plus dye. *Biochemical and Biophysical Res. Commun.*, Vol. 8, No.3, (July), pp.157-163, ISSN: 0006-291X.

Smith T, Olson R (2007) A taxonomic survey of lamp flora (Algae and Cyanobacteria) in electrically lit passages within Mammoth Cave National Park, Kentucky. *International Journal of Speleology*, 36:105–114.

St. Clair L, Rushforth S (1976) The diatoms of Timpanogos Cave National Monument, Utah. *American Journal of Botany*, 63:49-59.

Sjöberg B (2013) Oxydation des protéines par les espèces réactives de l'oxygène: l'importance de l'environnement protéique. *Organic chemistry*, Université de Franche-Comté, France.

Sztatelman O, Grzyb J, Gabryś H, Banaś AK (2015) The effect of UV-B on Arabidopsis leaves depends on light conditions after treatment. *BMC Plant Biology*, p. 15-281.

T

Tandori J, Mate Z, Maroti P, Vass I (1996) Resistance of reaction centers from *Rhodobacter sphaeroides* against UV-B radiation. Effects on protein structure and electron transport. *Photosynthesis Research*, 50:171-179.

Tyystjärvi E (2008) Photoinhibition of Photosystem II and photodamage of the oxygen evolving manganese cluster. *Coordination Chemistry Reviews*, 252:361–376.

Turcsanyi E, Vass I (2000) Inhibition of photosynthetic electron transport by UV-A radiation targets the photosystem II complex. *Photochemical Photobiology*, 72:513-520.

V

Valero A, Begum M, Leong SL, Hocking AD, Ramos AJ, Sanchis V (2007) Effect of germicidal UVC light on fungi isolated from grapes and raisins. *Letters in Applied Microbiology*, 45:238–243.

Vanderwolf KJ, Malloch D, McAlpine DF, Forbes GJ (2013) A world review of fungi, yeasts, and slime molds in caves. *International Journal of Speleology*, 42:77-96.

Villar E, Bonet A, Díaz-Caneja B, Fernández PL, Gutiérrez I, Quindós LS, Solana JR, Soto J (1984) Ambient temperature variations in the hall paintings in Altamira cave due to the presence of visitors. *Cave Science*, 11:99–104.

Vinogradova ON, Nevo E, Wasser SP (2009) Algae of the Sefunim Cave (Israel): Species diversity affected by light, humidity and rock stresses. *International Journal on Algae*, 11:99-116.

W

Wang B, Wang X, Hu Y, Chang M, Bi Y, Hu Z (2015) Chemosphere The combined effects of UV-C radiation and H₂O₂ on *Microcystis aeruginosa*, a bloom-forming cyanobacterium. *Chemosphere*, 141:34–43.

Warscheid T, Braams J (2000) Biodeterioration of stone: a review. *International Biodeterioration and Biodegradation*, 46:343-368.

Wei Z, Cady CW, Brudvig GW, Hou HJM (2011) Photodamage of a Mn (III/IV)- oxo mixed-valence compound and photosystem II: evidence that a high-valent manganese species is responsible for UV-induced photodamage of the oxygen- evolving complex in photosystem II. *Journal of Photochemistry and Photobiology B: Biology*, 104:118-125.

Wilkinson F, Helman WP, Ross AB (1995) Rate constants for the decay and reactions of the lowest electronically excited state of molecular oxygen in solution : an expanded and revised compilation. *Journal of Physiological Chemistry*, 24:663-1021.

Woodall AA, Britton G, Jackson MJ (1997) Carotenoids and protection of phospholipids in solution or liposomes against oxidation by peroxy radicals: Relationship between carotenoid structure and protective ability. *Biochimical and Biophysical Acta*, 1336:575-586.

Wright A, Hawkins CL, Davies MJ (2003) Photo-oxidation of cells generates longlived intracellular protein peroxides. *Free Radical Biology and Medicine*, 34:637-647.

X

Xu S, Li J, Zhang X, Wei H, Cui L (2006) Effects of heat acclimation pretreatment on changes of membrane lipid peroxidation, antioxidant metabolites, and ultrastructure of chloroplasts in two cool-season turfgrass species under heat stress. *Environmental and Experimental Botany*, 56:274–285.

Xue LG, Zhang Y, Zhang TG, An LZ, Wang XL (2005) Effects of enhanced ultraviolet-B radiation on algae and cyanobacteria. *Critical Review in Microbiology*, 31:79-89.

Z

Zhang S, Jin Y (1996) Tourism resources on karst and caves in China. *Acta II Congress ISCA, Malaga*, p. 111-119.

Zucconi L, Gagliardi M, Isola D, Onofri S, Crocifissa Andarolo S, Pelosi C, Pogliani P, Selbmann L (2012) Biodeterioration agents dwelling in or on the wall paintings of the Holy Saviour's cave (Vallerano, Italy). *International Biodeterioration and Biodegradation*, 70:40-46.

Zvezdanović J, Cvetić T, Veljović-Jovanović S, Marković D (2009) Chlorophyll bleaching by UV-irradiation in vitro and in situ: Absorption and fluorescence studies. *Radiation Physics and Chemistry*, 78:25-32.

Annexes

Application Note

Metagenomics Service for Profiling Microbial Communities (16S rDNA & ITS)

Introduction

Amplicon deep-sequencing using next generation sequencing (NGS) technologies has become a powerful tool to study the diversity of microbial communities. By sequencing parts of the ribosomal

DNA (16S rDNA or ITS) derived from environmental samples NGS can generate unprecedented amounts of sequence data permitting rapid and profound analysis of microbial communities. However,

the processing and evaluation of NGS sequence data is a challenge due to the large amount of data generated.

Importance of Selecting the Appropriate Barcoding Locus

Metagenomic studies are commonly performed by analyzing amplicons from the 16S rDNA in prokaryotes or the internal transcribed spacer regions (ITS) in fungi (Figure 1). Both loci form a mosaic of highly conserved and hypervariable regions, the latter being used for phylogenetic classifications.

It is yet not possible to sequence amplicons spanning the entire 16S rDNA (~1.3 kb) or ITS regions because the read length of current NGS technologies is limited. Which parts of the 16S rDNA or ITS are best amplified for the profiling is still under debate, and varies depending on the study objectives, experimental design and type of sample. In general, if you aim to get a fine-scale taxonomic resolution, your objective should be to cover as many variable regions as possible in your PCR. The challenge of any profiling project is, however, to carefully balance the trade-off between the

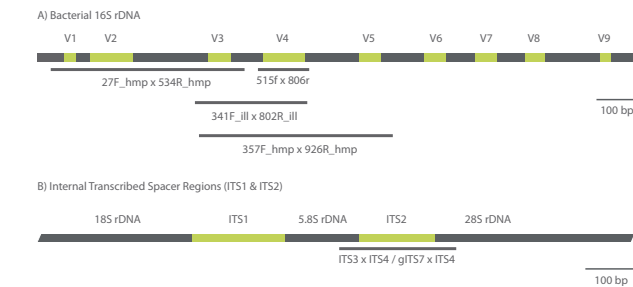


Figure 1. Overview of the ribosomal gene loci most often used for the analysis of microbial communities. **1A.** Structure of the 16S rDNA for bacterial species showing the 9 different variable regions (V1-V9) and common regions often used for community analysis. **1B.** Structure of the internal transcribed spacer regions (ITS) for fungi showing the two variable regions ITS1 and ITS2. Most often ITS2 is used for profiling fungal communities. Variable regions are green whereas conserved regions are grey.

taxonomic resolution and possible bias from PCR amplification resulting in an under-representation or loss of taxonomic entities [1] [2]. Often only a pilot

study will help to find the best primer set for a specific research question.

Microsynth Competences and Services

One of Microsynth's core competence areas is the profiling of microbial communities based on 16S rDNA analysis. Microsynth is able to offer its customers a full service covering the entire process from experimental design planning, DNA isolation, PCR amplification and sequencing up to a detailed bioinformatics analysis of the generated data (Figure 2).

DNA Isolation: Either the customer provides isolated DNA or outsources this critical step to Microsynth (>13 years of experience in DNA/RNA isolation from various and demanding matrices like plant material, food or stool).

PCR Amplification: The PCR amplification will follow a two-step PCR protocol using a state-of-the-art high-fidelity poly-

merase. This two-step PCR is applied in order to increase reproducibility and to improve the production of high-quality multiplex amplicon libraries. PCR products are purified, quantified with fluorescence spectroscopy using Picogreen and pooled in equimolar amounts.



NGS Sequencing: Sequencing is done using Illumina MiSeq sequencing technology. MiSeq allows high-throughput profiling at low costs with the advantage of long reads (up to 570 bp).

Bioinformatics Analyses: Depending on customer requirements Microsynth offers either a basic bioinformatics analysis package or an advanced bioinformatics analysis package. Both packages are based on the Qiime software [3]. The basic package provides taxonomic profiles and α -diversity measurements (i.e. diversity of organisms in one sample). The advanced package builds on the basic package and adds β -diversity measurements (i.e. diversity of organisms across samples). Guided by experimental parameters (e.g. different sample conditions like temperature, pH, etc.), the comparative analysis of the advanced package allows to test the experimental hypothesis.

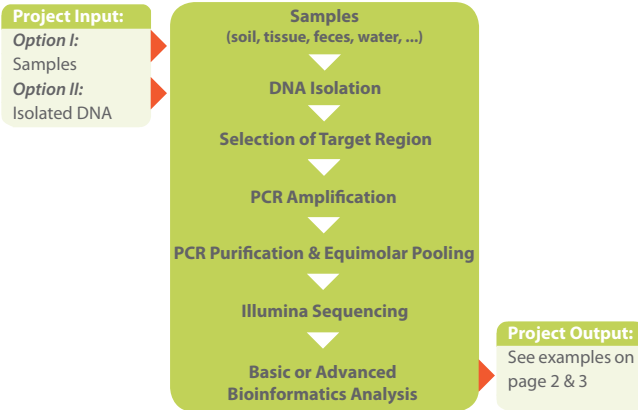


Figure 2. Typical steps in a profiling project. Depending on researcher needs Microsynth can deliver a one-stop service starting from DNA isolation and PCR amplification & sequencing right through to data analysis.

Microbial Profiling with Basic Bioinformatics Package

Data Processing: Input for further data analysis are demultiplexed, stitched (combining forward and reverse reads), quality filtered and Chimera cleaned fasta reads.

Data Enrichment: The Qiime software in

combination with a reference database is used to define operational taxonomic units (OTUs) and to assign each OTU to a taxonomic entity at different taxonomic levels (Figure 3). Output may serve as source for down-stream analysis done by

the customer.

α -Diversity: Chao1 and Shannon diversity measurements are calculated. Rarefaction analysis is also performed to estimate if sampling has been exhaustive (Figure 4).

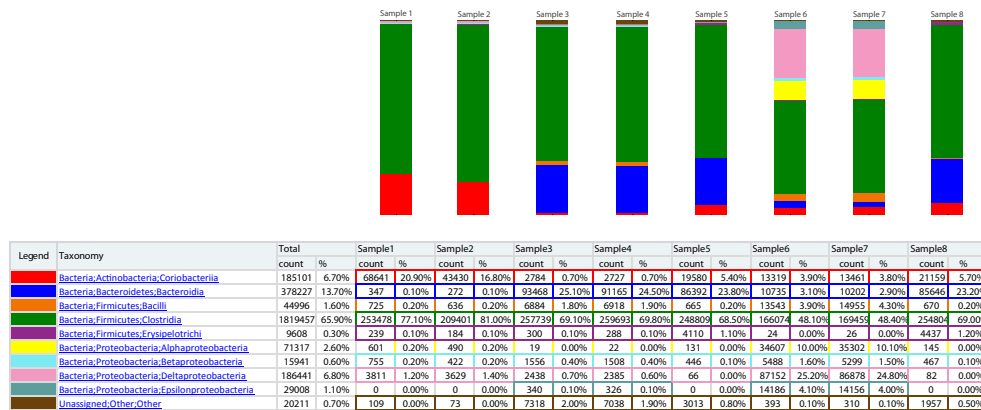


Figure 3. Example for an interactive HTML taxonomy plot on the Class level. The taxonomy is given for different taxonomic levels (phylum, class, order, family, genus, species).

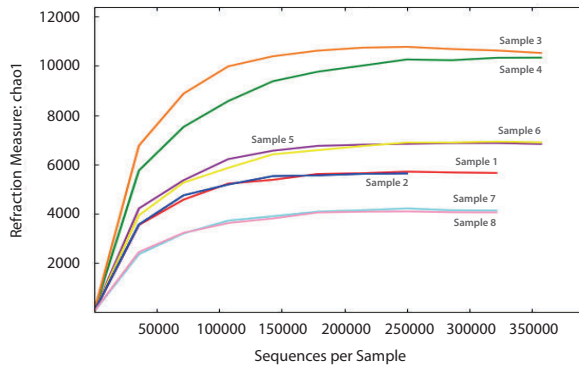


Figure 4: Rarefaction curves are calculated for each sample based on the OTU computations. Rarefaction curves help to estimate whether bacterial communities were sampled properly, i.e. enough sequence reads per sample where collected. Rarefaction curves are expected to reach a plateau if sampling has been exhaustive [4].

Microbial Profiling with Advanced Bioinformatics Package

The Advanced Bioinformatics Analysis includes the results of the basic analysis. In addition, the microbial community structures are compared against the environmental parameters provided by the customer in a phylogenetic context.

The OTU dataset obtained with the basic bioinformatics package serves as input for further analysis.

Data Enrichment: In a first step a phylo-

genetic tree is calculated for all OTUs in the dataset (UniFrac)[5]. The phylogenetic tree serves as basis for the comparative analysis and calculation of β -diversity.

β -Diversity: A qualitative overview of intersample diversity is obtained by means of principal coordinate analysis (PCoA, Figure 5A). In addition, significance of pairwise phylogenetic differences among communities is computed and

hierarchical UPGMA based clustering is performed (Figure 5B).

Comparative Analysis: A quantitative assessment is performed to test the experimental hypothesis which answers (i) whether the sample categories differ from each other and (ii) whether OTUs are differentially represented based on sample categories (e.g. different sample conditions).

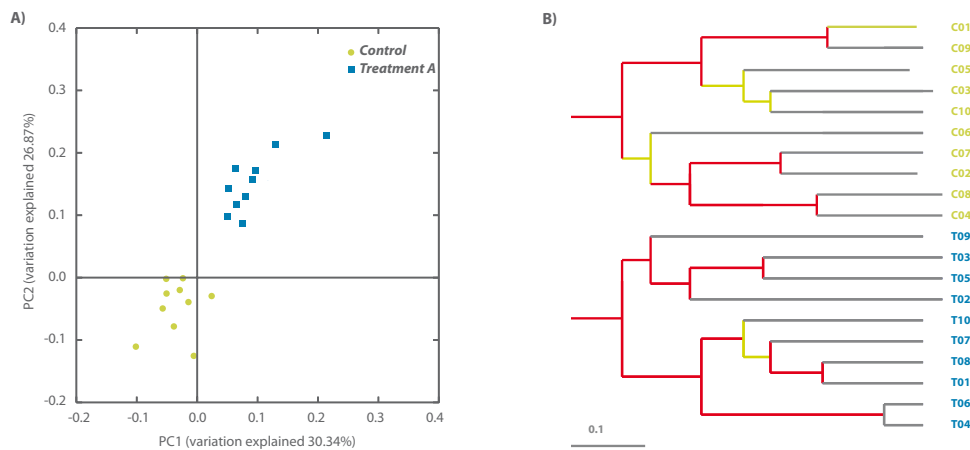


Figure 5. Example output of the comparative analyses (β -diversity). **5A.** 2D plot of a PCoA analysis based on the UniFrac distance matrix. PCoA reduces the dimensionality of a complex dataset and can be used to visualize the relationship of each sample to any other sample in the set. **5B.** UPGMA clustering based on the UniFrac distance matrix. UPGMA clustering discovers the hierarchical relationships that underlie the samples.



Primer Systems and Their Possible Effects on Profiling Results

| Primer Name | Sequence (5'-3') | Region | Size (bp) | Source |
|-------------|----------------------------|--------|-----------|----------|
| 515F | GTG CCA GCM GCC GCG GTA A | V4 | ~300 | EMP |
| 806r | GGA CTA CHV GGG TWT CTA AT | | | |
| 27F_hmp | AGA GTT TGA TCC TGG CTC AG | V123 | ~510 | HMP |
| 534R_hmp | ATT ACC GCG GCT GCT GG | | | |
| 357F_hmp | CCT ACG GGA GGC AGC AG | V345 | ~570 | HMP |
| 926R_hmp | CCG TCA ATT CMT TTR AGT | | | |
| 341F_ill | CCT ACG GGN GGC WGC AG | V34 | ~460 | Illumina |
| 802R_ill | GAC TAC HVG GGT ATCTAA TCC | | | |
| ITS3 | GCA TCG ATG AAG AAC GCA GC | ITS2 | ~300-400 | |
| ITS4 | TCC TCC GCT TAT TGA TAT GC | | | |
| gITS7 | GTG ART CAT CGA RTC TTT G | ITS2 | ~230-330 | |
| ITS4 | TCC TCC GCT TAT TGA TAT GC | | | |

Table 1. Summary of most common primer systems for profiling bacterial and fungal communities. Only template-specific sequences and its spanning variable parts are shown. These sequences combined with Illumina adaptor sequences are used in the Illumina Nextera 2-step protocol for the library preparation. EMP = Earth Microbiome Project (<http://www.earthmicrobiome.org/>); HMP = Human Microbiome Project (<http://www.hmpdacc.org/>).

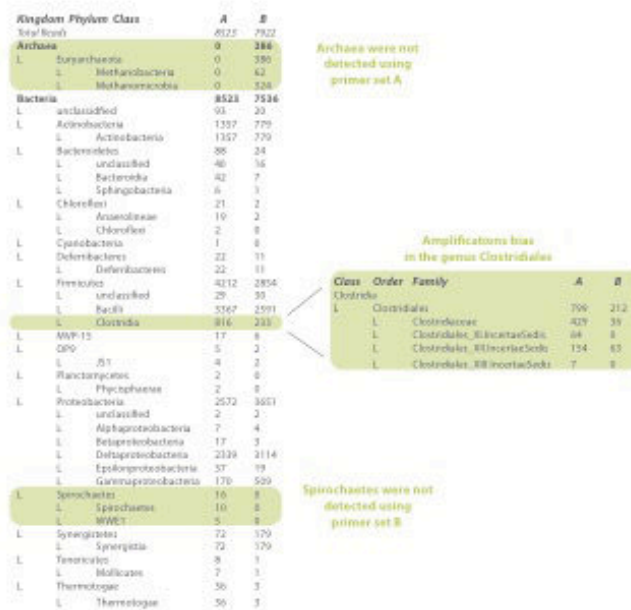


Figure 6. Analysis of the same environmental sample using different primer systems. In the first case (A) the V123 region was amplified using primers 9F & 534R (A) and in the second case the V345 region was amplified using primers 341F & 909R (B). This analysis clearly demonstrates that some of the taxa were not amplified using one of the primer sets, and also reveals differences in the amplification efficiency. For example the Archaea were detected using system B but not A. In contrast, the Spirochaetes were detected with primer system A but not B.

Literature

[1] Berry et al. (2011) Barcoded primers used in multiplex amplicon pyrosequencing bias amplification, *App Env Microb*, 77: 7846-7849.
 [2] Klindworth et al. (2013) Evaluation of general 16S ribosomal RNA gene PCR primers for classical and next-generation sequencing-based diversity studies, *Nucleic Acids Res* 41, e1.
 [3] Caporaso et al. (2010) Qiime allows analysis of high-throughput community sequencing data, *Nature Methods*, 7: 335-336.
 [4] Colwell, R.K. & Coddington, J.A. (1994) Estimating terrestrial biodiversity through extrapolation. *Philos T Roy Soc B*, 345: 101-118.
 [5] Lozupone, C. & Knight, R. (2005) UniFrac: a New Phylogenetic Method for Comparing Microbial Communities, *Appl Environ Microbiol*, 71: 8228-8235.



Intérêt du traitement par UV-C des communautés bactériennes, fongiques et des protistes autotrophes des biofilms colonisant la pierre patrimoniale : structure des peuplements, effets des UV-C sur la physiologie algale et innocuité du traitement vis à vis du support pictural.

Mots clés : Traitement, UV-C, *Chlorella* sp., Conservation, Séquençage, Pigments.

Dans le cadre de la conservation du patrimoine, les micro-organismes se développant sous forme de biofilm sont souvent considérés comme des agents entraînant des problèmes esthétiques et de détérioration du support colonisé. L'objectif général de cette thèse est l'utilisation de la lumière UV-C comme méthode de traitement des biofilms. Dans le but de comprendre la diversité des biofilms, les communautés bactériennes, fongiques et des protistes autotrophes ont été étudiées à l'aide d'une technique de séquençage haut débit. Puis, afin de comprendre les effets des UV-C sur les micro-algues (*Chlorella* sp.), des essais en laboratoire ont permis de caractériser les réponses physiologiques algales (mort cellulaire, dégradation de la chlorophylle, état de photosystème II, etc.) suite à

différents traitements aux UV-C. Tous les dommages observés au niveau cellulaire et moléculaire (dont la mort cellulaire et le « bleaching » de la chlorophylle) ont permis d'optimiser la méthode de traitement. Dans le but de s'assurer de l'innocuité du traitement aux UV-C sur le support des biofilms (peintures pariétales), des pigments et des liants, utilisés à la préhistoire, ont été fortement irradiés. Les résultats ont montré que les composés inorganiques sont insensibles aux UV-C au contraire des molécules organiques. Enfin, le traitement UV-C a démontré son efficacité dans une grotte touristique en permettant d'éradiquer tous les biofilms. De plus, aucune recolonisation n'a été observée deux ans après le traitement, démontrant que la lumière UV-C est le traitement le plus écologique à ce jour.

UV-C as an efficient means to combat biofilm formation in show caves

Key words: Treatment, UV-C, *Chlorella* sp., Conservation, Sequencing, Pigments.

Development of biofilm on monument heritage are often considered as agents leading to aesthetic issues and biodeterioration of their support. The aim of this study is the use of UV-C light as alternative treatment against Lampenflora. Bacterial, algal and fungal communities were studied using new generation sequencing approach. Following UV-C treatments, physiological responses of *Chlorella* sp. were studied in laboratory (cell death, chlorophyll degradation, photosystem II status, etc.). Damages at cellular and molecular levels (cell death, bleaching of the chlorophyll) were taken into consideration to optimize the UV-C treatment.

Then, to ensure the safety of UV-C for biofilms support (parietal paintings), several pigments and binders, used by prehistoric human, were highly irradiated. The results showed that UV-C radiations were not deleterious for inorganic compounds, while a color change was observed on organic binders. Finally, UV-C treatment has proven its effectiveness in La Glacière show cave by eradicating all biofilms. In addition, no recolonization was observed two years after treatment, showing that this treatment, which is the most environmental friendly to date, is effective over time.